Using multi-element comparisons to discriminate between natural and anthropogenic post-depositional additions in estuarine sediments

by

Fern Riva Beavis

A thesis submitted for the degree of Doctor of Philosophy at

The Australian National University

The Australian National University

Canberra

June, 2011

Declaration

The research presented in this thesis is my own original work. Due acknowledgement has been made in the text to all other material used. In all cases I am the principal author and contributor to the work presented. No part of this thesis has been submitted for any previous degree.

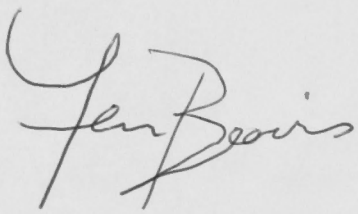

.....

Fern Riva Beavis

June, 2011

For my mentors, and greatest sources of inspiration, courage and wisdom:

Dr. S.G. Beavis

&

Prof. F.C. Beavis
(1924 – 2006)

Acknowledgements

As a third-generation geologist, I feel very fortunate and honoured to now be able to join the ranks of those before me, and contribute my piece of research to the scientific knowledge of this Earth. From my humble beginnings as a geologist, washing out my mother's scientific glassware for 2 cents a pop, to an undergraduate degree full of adventures and rock hunting trips, to undertaking my own research and presenting my PhD thesis, I am proud to be at this point in my career, and look forward to what the future holds as a professional in this wonderful field of geology.

A great many people have contributed to this journey over the past five years, providing me support, guidance and and wisdom.

My supervisory panel have been incredible mentors over the course of the last five years. First and foremost, David Ellis has provided me with wisdom, support, encouragement and belief in my abilities as a scientific researcher. By giving me countless opportunities to challenge myself as a researcher in the laboratory, field and in the broader scientific community through local and international conferences, he has given me the skills and confidence to embark on a career with enthusiasm and determination. I cannot express enough gratitude and appreciation for this. Andrew Christy has asked questions that have challenged me and forced me to take my thinking to another level, and in doing so has given me the confidence to ask those questions myself and explore exciting scientific tangents with no fear. Stephen Eggins and Sue Welch have been incredible sources of knowledge and encouragement, providing insight and ideas for the development of my research which have ensured the research fire has burned very brightly indeed! These four academics have mentored me to provide me with the skills to develop into an independent researcher, and for this I am so grateful.

There are a number of researchers, academics and staff who have provided me with invaluable training, support and assistance over the course of my PhD, and have been integral to my development as a scientist. Thank you to Ulrike Troitzsch for providing

me with a wealth of advice, training and assistance with sample preparation and analyses. Thank you to Linda McMorrow, Andy Christy, Stephen Eggins, David Ellis, Shane Paxton, Tony Phimphisane, John Vickers, Tony Eggleton, Frank Brink, Andrew Higgins, Charlotte Allen and Graham Mortimer for training and assistance with sample preparation, analyses and the development and implementation of scientific methods and analyses. Thank you to Richard Edwards for assistance with MapInfo. Many thanks also to ANSTO, in particular Henri Wong and Andrew Easton, for use of analytical equipment and training at AINSE laboratories.

Maree Coldrick, Brian Harrold and Nigel Craddy have been nothing short of wonderful over my entire university career, particularly over the last five years. Thank you to Brian Harrold not only for all assistance with all aspects of IT support, and consequently keeping me sane, but for the constant support and encouragement. Thank you to Nigel Craddy, for providing such wonderful support, encouragement, advice and assistance with field work and the production of sampling equipment, ensuring that every aspect of my sampling was a success.

Thank you to Maree Coldrick for providing me with endless support, motivation, encouragement and assistance in ensuring that my PhD has been a smooth and successful journey. Maree has, at many times, been my life buoy! Thank you also to Joy McDermid, who has also given invaluable assistance, support and encouragement. I cannot thank Maree, Brian, Nigel and Joy enough for all they have done for me.

Many thanks to Bega Valley Shire Council for their support of this project. Many thanks also to Mr Chris Boynton, Mr Ray Tynan and Mrs Chris Tynan for sharing invaluable local knowledge, and supporting the research being undertaken.

I have worked at several part-time jobs over the course of my studies. Many thanks to my work colleagues, John Beaton and the staff at The Academy of the Social Sciences in Australia, Nady and Luke Ferguson and Diana Zivkovich for supporting me throughout my PhD.

My comrades, my greatest motivators and my inspirations: thank you to Sarah Tynan, Luke Wallace and Al Usher for motivating me, understanding me, listening to me, and being on the same road as me. I have been truly blessed to have shared an often tough, yet always exciting road with such wonderful friends. Thank you to Matthew Stevens, Nick Tailby and Ned Summerhayes, whose excitement for adventure and all things geology has been intoxicating. I am truly blessed to have embarked on my career with these incredible friends by my side.

Thank you to my beautiful friend, Hannah Delaney, for supporting me, inspiring me, believing in me, always walking beside me, and never once doubting my abilities. Thank you to my wonderful housemates and beautiful friends, Ainslee Kells, Thomas Wallenius and Christian Downie, for their endless love and shared bottles of fine wine and pickles.

My fellow geologists, and dear friends: Jenna Roberts, Nicole Lenahan, Meryem Mojtahid, Michelle Ayling, Jennifer de Livera, Rebecca Hanrahan, Mick Hansby, Thomas Abraham-James, Alice Clement, Matt Crawford, Ailsa Robertson, Eugenie Finn, Elizabeth Henningham, Sophie Blix, Matthew Short, Catherine Coles, Charles Williams, Richard Edwards and Sam Tierney. Thank you for the constant stream of inspiring words, very large and very patient ears, constant support and plenty of laughter. Thank you for making the process not only a shared one, but a fun one too.

Thank you to my beautiful darling Adam, for being such a sparkle in my life, for loving me, supporting me and challenging me. Thank you to the magnificent Sumbak family, Rosemary, Katherine, Liam and Philippa for giving me such wonderful support, love and motivation!

Thank you to Francis Beavis, for giving me the love for geology, and Joan Beavis, for having so much belief in me. To my mother Sara, and my sisters, Amber and Summer: How proud and truly blessed I am to be one of the Beavis women! Thank you for walking along this entire journey with me, giving me advice, laughter and incredible love and support throughout my PhD and beyond. Thank you to Amber and Tom for

constantly cheering me along, and to Summer and Matt for making sure I was always aware of the big picture. And thank you so much to Sara, for being such an incredible mentor, for providing me with such wonderful advice and extraordinary wisdom, for being my greatest inspiration, and for being the scientist and person I aspire to be. Perhaps the best part of the last five years has been the opportunity to work so closely together on the subject we both adore the most. I look up to you all, and thank you so much for being so wonderfully beautiful!

Abstract

In most areas of the world, high population centres and heavy industry are located along river systems and provide a catchment wide source of heavy metal pollution along the length of the river system. These anthropogenically derived heavy metal pollutants enter the freshwater river systems and are transported downstream as part of the suspended sediment load. Such metals combine with the suspended sediment such that there is a higher concentration of heavy metals with the finer grained, clay-rich component of the transported sediment. In such cases, the ultimate depositional environment of contaminated sediments bears little relation to the distant source regions of anthropogenic pollution.

In an arid country like Australia, there are numerous coastal estuaries that are supplied with sediment transported down catchments that lack both industry and significant population centres. However such coastal estuaries are undergoing rapid population growth, even though in such regions the upstream catchment is notably lacking in population centres and industry. This provides an opportunity to study heavy metal additions and contamination in a post-depositional estuarine saline environment, in which relatively uncontaminated freshwater sediments are input into the system, mainly during seasonal flood events.

This study demonstrates that transported sediments, derived from upcatchment, undergo post depositional transformations across the freshwater- marine boundary. As a result of these terrigenous, biogenic, authigenic and anthropogenic changes, estuarine sediments do not necessarily reflect the original source composition.

Conservative elements, especially rare earth elements, were used to differentiate between original and post-depositional additions and transformations to the sediments of an estuarine system on the south coast of New South Wales, Australia, to show that metal contamination does not correlate wholly with sediment grain size, but also correlates with proximity to local townships surrounding part of an estuary. Metals such as Pb have been discriminated in terms of original, transported sediment compositions and local pollutant sources. Furthermore, analyses of baseline, spatial and temporal data

has generated a methodology and conceptual framework for assessing anomalies, even when concentrations are low within apparently 'pristine' settings.

This thesis identifies both natural and anthropogenic processes and contributions to estuarine sediments, and presents a methodology by which metal contamination of sediments and the potential future risks from remobilisation can be quantified.

Contents

List of Figures

List of Tables

Glossary

ABS: Australian Bureau of Statistics

AINSE: Australian Institute of Nuclear Science and Engineering

ANRA: Australian Natural Resources Atlas

ANSTO: Australian Nuclear Science and Technology Organisation

ANU: The Australian National University

ANZECC: Australian and New Zealand Environment Conservation Council

ARMCANZ: Agriculture and Resource Management Council of Australia and New Zealand

ASS: Acid Sulfate Soils

AVS: Acid Volatile Sulfur

BVSC: Bega Valley Shire Council

CCA: Copper Chrome Arsenate

CEC: Cation Exchange Capacity

CFCs: Chlorofluorocarbons

CRS: Chromium Reducible Sulfur

DDT: Dichlorodiphenyltrichloroethane, a synthetic pesticide

DLWC: Department of Land and Water Council

DNR: Department of Natural Resources

EC: Electrical Conductivity

EDS: Element Dispersive Spectrometer

EDXA: Energy-Dispersive X-ray Analyses

ENSO: El Nino Southern Oscillation

EPA: Environment Protection Agency

ESP: Exchangeable Sodium Percentage

ICOLL: Intermittently Closed and Open Lakes and Lagoons

IPO: Inter-decadal Pacific Oscillation

ISQG: International Sediment Quality Guidelines

LA-ICP-MS: Laser Ablation Inductively-Coupled Plasma Mass Spectrometry

LFB: Lachlan Fold Belt

LGM: Last Glacial Maximum

MC-ICP-MS: Multi Collector-Inductively Coupled Plasma Mass Spectrometry

MI: Methylene Iodide

NIST: National Institute of Standards and Technology

NZCC: New Zealand China Clay

OM: Organic Matter

PAAS: Post Archean Average Shale

PAHS: polycyclic Aromatic Hydrocarbons

PCBs: Polychlorinated Biphenyls, found in electrical equipment, lubricants paints and plasticisers

Ppb: Parts per billion

Ppm: Parts per million

REE: Rare Earth Elements

RSES: Research School of Earth Sciences

SEM: Scanning Electron Microscope

SOMER: State of the Marine Environment Report

SRCMA: Southern Rivers Catchment Management Authority

SRM: Standard Reference Material

TBE: Tetrabromoethane

TBT: Tributyl Tin

TRIS: Total Reduced Inorganic Sulfur

USGS: United States Geological Survey

XRD: X-Ray Diffraction

XRF: X-ray Fluorescence Spectrometer

Chapter One: Introduction and Objectives

1.1. Introduction

In many areas of the world, high population centres and heavy industry are located along river systems and provide a significant source of anthropogenically derived metal pollution to the river, its receiving body (for example, an estuary, lake or inlet) and associated sediments and organic material (Jones and Turki, 1997). Anthropogenically derived metal pollutants enter freshwater river systems and are transported downstream as part of the suspended sediment load and in solution. Such metals can combine with the suspended sediment such that there is a higher concentration of metals with the finer grained, clay-rich component of the transported sediment (Hirst, 1962; Crecelius *et al.*, 1991; Ip *et al.*, 2007). Estuaries consequently act as important sediment and pollutant sinks within the environment (Singh *et al.*, 1999; Acevedo-Figueroa *et al.*, 2006; Chau, 2006; Prasad and Ramanathan, 2008). Under these conditions, the ultimate depositional environment of contaminated sediments bears little relation to the distant source regions of anthropogenic pollution. The extent to which these systems are contaminated does not wholly rely on catchment input; instead, it relies on a number of point and diffuse sources, ranging from agricultural input, urban storm water outflow, and activities occurring within the estuary itself, such as boating, fishing and other recreational, commercial and industrial activities. In heavily populated regions, it is therefore difficult to distinguish between original source material and added components to the total sediment due to the associations of the pollutants with the suspended sediment load.

In an arid country such as Australia, there are numerous coastal estuaries that lack both industry and significant population centres up catchment. As a result, they have minimal pollutants derived from up catchment activities. However, such coastal estuaries are undergoing rapid population growth, even though the upstream catchment is notably lacking in population centres and industry. This provides an opportunity to study metal

additions through terrigenous, authigenic and biogenic processes as well as through anthropogenic contamination in a post-depositional estuarine saline environment, in which relatively uncontaminated freshwater sediments are input into the system, mainly during seasonal flood events. In order to do this, a distinction between natural and anthropogenic effects must be made. This study will compare freshwater terrigenous sediments with the sediments finally deposited in the saline estuary environment.

Estuaries act as a sink of transported material derived from a range of natural and anthropogenic sources, mobilised primarily via terrestrial transport and riverine and urban runoff. Estuarine sediments are therefore excellent environmental indicators of the surrounding catchment (Abrahim *et al.*, 2007). Transport via rivers, creeks and slopes in combination with inputs from urban stormwater drains, industry and agriculture provides a sediment mixture which reflects a variety of sources. Sediment analysis has thus been widely used as a tool to pinpoint pollutant inputs (Badri and Aston, 1985; Munksgaard *et al.,* 1998; Ip *et al*, 2004). However, the final sediment composition does not always reflect the original source material. Post-depositional geochemical changes can alter the total sediment composition via additions, subtractions and transformations of a suite of elements, nutrients and minerals by anthropogenic, terrestrial, biogenic and authigenic processes.

Future impacts on estuarine systems, driven by urbanization and increased anthropogenic fluxes into the estuary, have the potential to alter the physical and chemical characteristics of the sediment profiles. In particular, the accumulation and concentration of metals within the estuarine sediments have the potential to create an anomaly within an otherwise pristine environment. This could cause significant environmental effects if previously immobile metals and other pollutants become remobilized and are made bioavailable under certain conditions, such as pH dropping to more acidic levels (Gambrell *et al.*, 1991; Léonard, 1991; Kersten, 1988; Nowack *et al.*, 2001, Du Laing *et al.*, 2009) and metal solubility increasing due to acid sulfate soils or organic acids at depths below mangroves.

High metal concentrations within sediments are typically associated with those sediments which are fine-grained (high surface area), and have a higher capacity for cation exchange. Consequently, clay minerals and organic matter are often associated with higher metal concentrations in comparison to coarser grained particles such as sand and gravel. A range of conservative elements, especially rare earth elements (REE), are used here to show that metal contamination does not correlate wholly with sediment grain size, but also correlates with proximity to local townships surrounding part of an estuary. The behaviour of elements, such as the metals, can then clearly be discriminated in terms of original, transported sediment compositions and local pollutant sources in an estuary. This behaviour shows that metal pollution correlates with proximity to urban development, rather than with upstream contamination and transported sediment type. In many industrialized regions, metal pollution is derived from contaminated rivers that also carry sediment into an estuary (Southgate *et al.*, 1983; Douglas, 1985; Ridgway and Shimmield, 2002). In an Australian context, the source of metal pollution is directly attributable to local development within the vicinity of an estuary, as the river systems themselves are relatively pristine. It is therefore necessary to gather baseline geochemical data for such settings, in order to understand those geochemical additions to terrigenous sediments deposited in estuaries – namely authigenic, biogenic and anthropogenic factors.

Previous studies have discussed the composition of estuarine sediments as reflecting their up catchment sediment source (Brooke, 2003; Douglas *et al.*, 2005; Douglas *et al.*, 2006; Phillips and Slattery, 2006; Hancock and Caitcheon, 2010). This work will identify and interpret not only fluxes, but also a complex of transformations in which original source materials can evolve into quite discrete materials at the 'end' of the system. In addition, this work will provide a methodology by which sediments can be identified as original or transformed via authigenic, biogenic, anthropogenic or terrestrial sources and processes. This finding can then be taken and applied elsewhere, in larger, more polluted and complex systems as a way of defining the effects of geochemical post-deposition alterations affecting the sediment composition.

1.2. Aims and Objectives

Non-marine sediments transported into a marine environment can have chemical and mineralogical modifications due to changes in the associated water chemistry. In some cases (eg Jones et al., 2003) it has been assumed that no change occurs. Phyiscal mixing of diffeent chemical and physical weathering products will produce a chemical and mineralogical variation within a suite of estuary sediments that complicates single sample comparisons directly with a source rock. In addition, natural authigenic and biogenic changes can affect sediments once mixed and deposited in an estuary. How can anthropogenic changes be distinguished from these factors? This research aims to study these various factors and attempts to identify specific geochemical and mineralogical influences of each. This project will analyse the sediment geochemistry of the estuarine and freshwater components in order to satisfy the following aims:

- Discriminate between what is an original component in the bulk sediment, and what has been added post-deposition, via anthropogenic, authigenic, biogenic and terrestrial sources and processes.
- Use elements, such as the REE, to create sedimentary end member mixing relationships to determine what is natural and what is added and support this approach through the use of Sr and Pb isotope studies
- Determine the degree of influence of seawater modification on final results of elemental concentrations within the sediments.
- Characterise and determine the extent of uptake of elements from the seawater onto different clays
- Determine at what concentration an element may be defined as anomalous.

This study will identify both natural and anthropogenic inputs and processes and geochemically distinguish between the two. It will also develop scientific methods by which the levels of metal contaminants and their possible risk for remobilization in the future can be measured. This knowledge is important not only for coastal management, but also provides insight into the possible false identification of a heavy metal anomaly.

Furthermore, this thesis raises the following question: *Are human impacts on estuarine environments essentially creating anthropogenic metal anomalies as a result of accumulation in recently deposited regolith?* We can use this approach to define what is original and what is added to the sediment, which provides insight into sources of contaminants. We are able to define through this methodology that anomalies existing as a result of human activities are not confined to large concentrations of the element in question, but may also be anomalous even when present at relatively low levels.

By determining the geochemical processes occurring within the sediments and affecting associated elemental species post-deposition of the original transported sediment, isolated natural estuarine processes can be determined, independent of anthropogenic inputs and processes. The ability to distinguish between natural and anthropogenic metal concentrations within the sediments will allow us to define the geochemical pathways of metals within the system. Through the identification of naturally occurring processes post-deposition to the original sediment (such as the addition of Ca, Sr, S) as well as anthropogenically occurring sources and sinks, and quantifying the fluxes, transformations and accumulation of metals, this research will answer some key questions relevant to environmentally sensitive areas undergoing rapid and increasing change. The influence of urbanization and anthropogenic influences on the estuarine environment will be determined through the development of long-term projections for the pathways of metals within the system.

The principal aim of this project is therefore to show that transported regolith undergoes significant post-depositional geochemical changes that do not necessarily reflect the original source composition, specifically additions, subtractions and transformations affecting metals within the system. The outputs of the research will represent significant baseline data against which change can be measured, and that can also be used to inform planners and managers of risks and hazards within an estuary that have not been previously understood or identified.

1.3. Research Methods

Many studies have been undertaken on trace metal distribution in estuarine sediments throughout the world, with the majority of these studies concentrating on heavily polluted areas. The objectives of these studies are to describe trace metal concentration levels and identify the sources of the pollutants (Liaghati *et al.*, 2004). In an Australian context, a national Estuary Database is in place through OzCoasts (OzCoasts, 2007), which focuses on monitoring estuaries which range from pristine to highly modified conditions. Local council, State and National Governments have also monitored key coastal environmental concerns as identified by the Australian Government's State of the Marine Environment Report 2007 (SOMER). These concerns include, but are not limited to:

1. *Declining marine and coastal water/sediment quality, particularly as a result of inappropriate catchment land use practices, including:*
    - *Elevated nutrients and sediments from runoff sourced from land erosion, sewage and urban runoff.*
    - *Oil pollution sourced from urban runoff, the fuelling of vessels in ports and operational discharges.*
    - *Heavy metals, with particular problems in Lake Macquarie (NSW), Corio Bay (Vic), Derwent and Macquarie Estuaries (TAS) and Port Pirie (SA) (Zann, 2007).*
    - *Organochlorines sourced from herbicides and insecticides (sewage outfalls in Sydney, Homebush Bay, Port Phillip Bay sewage outfalls and Corio Bay).*
    - *Beach and ocean litter.*

2. *Loss of marine and coastal habitat.*
    - *Degradation of estuaries and coastal lakes due to eutrophication, sedimentation, acid sulfate soil runoff and groundwater discharge, coastal developments, pollution, loss of habitat and overfishing.*
    - *Declines in temperate seagrass due to elevated nutrients and sediments.*

- *Loss of mangrove and salt marsh habitats near urban areas due to reclamations, drainage and other developments.*
- *Unsustainable coastal development.*
- *Effects of trawling and overfishing on sea floor communities.*
- *Introduction of foreign species via ships' ballast waters and ships' hulls.*
- *Population increases of native species, such as crown-of-thorn starfishes in the tropical waters and the Drupella snail in Western Australian waters.*

3. *Unsustainable use of marine and coastal resources.*
    - *Decline in fish stocks due to overfishing.*
    - *Inappropriate fishing practices.*

4. *Lack of marine science policy and lack of long-term research and monitoring of the marine environment.*
    - *Lack of applied scientific knowledge on the marine environment.*
    - *Lack of scientific understanding of the functioning of marine ecosystems.*

5. *Lack of strategic, integrated planning in the marine and coastal environments.*
    - *Lack of non point-source pollution controls.*
    - *Insufficient representation of marine protected areas.*
    - *Indigenous issues*
    - *Social and cultural values of coast and sea.*

(Zann, 1995).

These environmental concerns are a response to degradation of some estuaries, coastal lake and bays throughout Australia. Major causes of environmental impacts are through elevated nutrients, sedimentation, pollution, coastal strip development and overfishing (DNR, 2008). Although a large number of estuaries in Australia are nearly-pristine (50%) or unmodified (22%) (ANRA, 2002), estuaries which are surrounded by concentrated urban development become the receiving bodies for sewage, urban runoff and industrial discharge, with localities that have been significantly modified including:

Wollongong, Port Kembla, Newcastle, and Sydney in NSW; Derwent River, Tamar River, Macquarie Harbour, and Burnie in Tasmania; and the Gippsland Lakes in Victoria (Zann, 1995).

These environmental concerns are not, however, restricted to high-industry, heavily-populated regions alone. Small population centres, with little or no industry are also at risk. In order to understand the impact of population growth on a coastal environment, this study will focus on the relatively pristine South Coast of New South Wales, specifically the Towamba Catchment, which includes Merimbula and Pambula.

The sampling of sediments in the estuaries and the catchment showed obvious spikes in concentrations of metals such as copper, lead, zinc, arsenic, chromium and tin, relative to proximity to urban development and agricultural modification. These patterns warranted further investigation, to determine the components of the sediments and geochemical processes which were influencing the concentration of metals in the sediments. This led to comparisons being made between conservative and non-conservative elements; the identification of anomalous concentrations with respect to proximity to anthropogenic influences; and an understanding, through *in situ* experiments, of the uptake behaviour of clay minerals within the estuarine water column.

This work forms the basis for predicting future environmental issues, caused by the accumulation and concentration of anthropogenically derived elements within the estuarine sediments. By determining which elements are being concentrated in the estuarine sediments by anthropogenic fluxes, instead of natural accumulations, we are able to provide a very important insight into the current state of the estuary, with consequences for future monitoring of the health of the estuary as populations increase.

Chapter Two: Study Site

2.1. Introduction

The south-eastern coastline of Australia is highly populated, with approximately 80% of the Australian population living within the eastern seaboard or along the coastal regions of the continent (ABS, 1996). Although capital cities, such as Sydney and Melbourne make up a large proportion of this total population, many regional centres also extend along the eastern coastline (Figure 2.1). These regions are likely to undergo significant population growth in the future, consequently causing major effects on the environment.

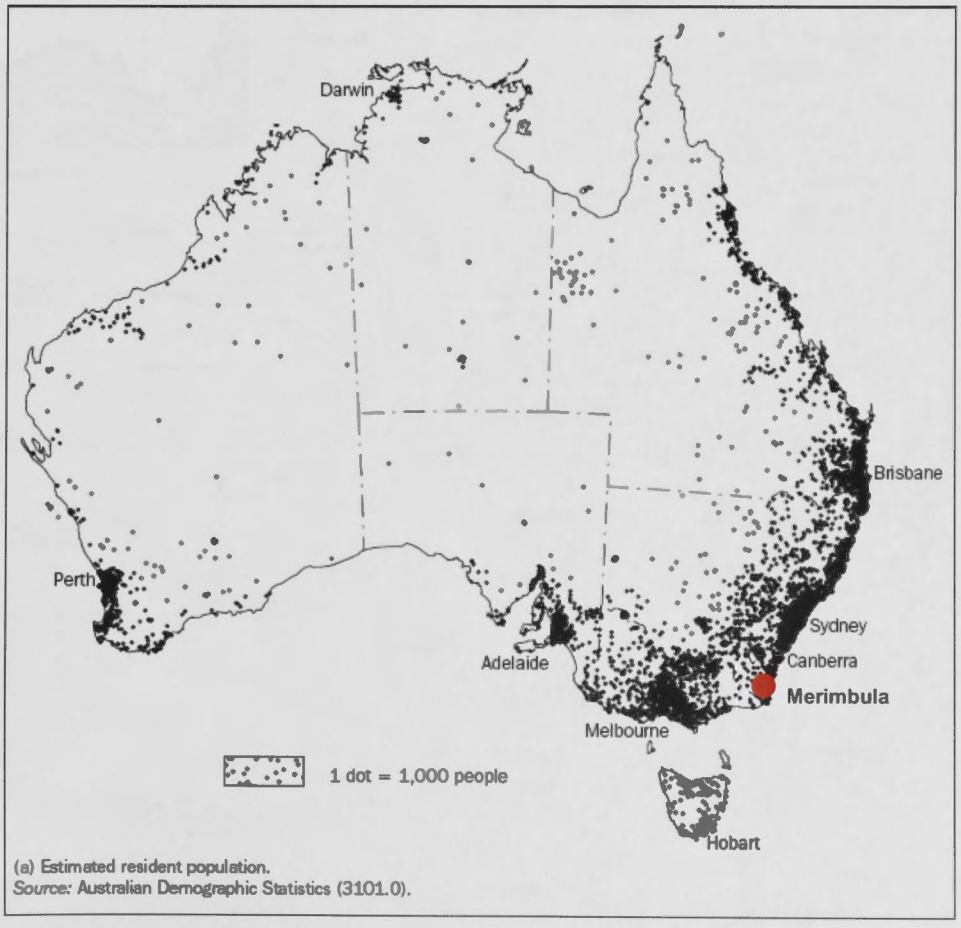

Figure 2.1. Estimated resident population of Australia and the location of the study site of Merimbula (ABS, 2008).

The study site for this research was concentrated within Merimbula Lake, Pambula Lake, Back Lagoon (36.895S, 149.923E) and their catchments. The lakes are in close proximity to the townships of Merimbula and Pambula, within the Sapphire Coast, a popular holiday area in southern New South Wales, approximately 455km south of Sydney (Figures 2.2a and 2.2b). The sampling undertaken for this project was determined based upon population density and land use of the estuaries, their immediate areas, and surrounding catchment; the pollution status of the lakes; and the use of the lakes by oyster farmers, which demands pristine levels to be maintained. These criteria were important in order for low concentrations of elements to be determined as a function of clay-sand and thus their variation with concentrations of major elements.

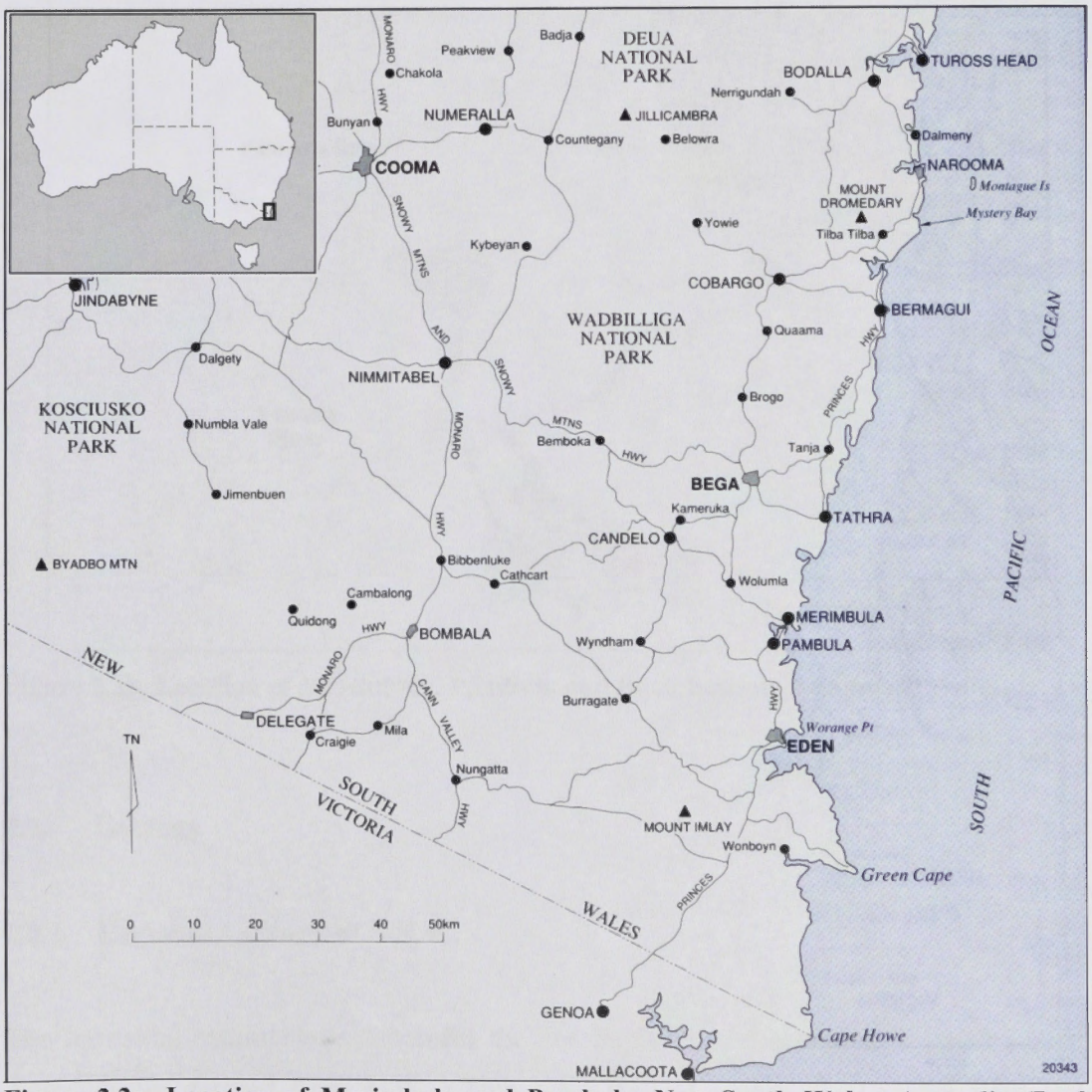

Figure 2.2a. Location of Merimbula and Pambula, New South Wales, Australia (Back Lagoon is immediately adjacent to Merimbula) (modified from Lewis *et al.*, 1994).

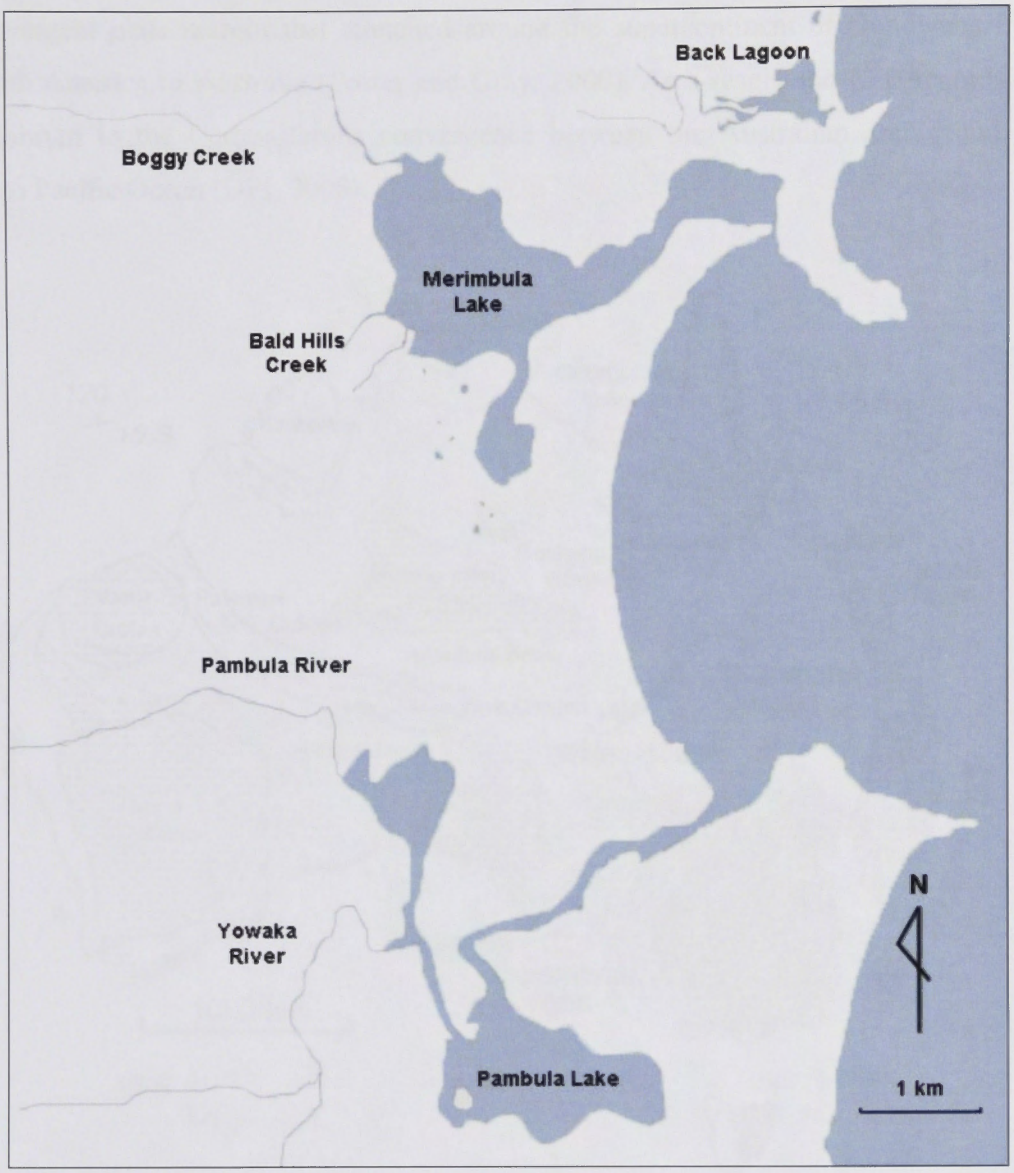

Figure 2.2b. Location of Merimbula, Pambula and Back Lagoon, New South Wales.

2.2. Geology

2.2.1. Regional Geology of N.S.W.

The terrestrial sediments which infill the coastal lakes and estuaries in south eastern Australia are derived from rocks which were formed within the Lachlan Fold Belt (LFB) (Figure 2.3). The LFB is a geological subdivision of eastern Australia which

formed in the Middle Palaeozoic (450 – 340 Ma), and was part of a Palaeozoic convergent plate margin that stretched around the supercontinent of Gondwana from South America to Australia (Foster and Gray, 2000). As a result, the LFB records the Cambrian to the Carboniferous convergence between the Australian craton and the proto Pacific Ocean (DPI, 2008).

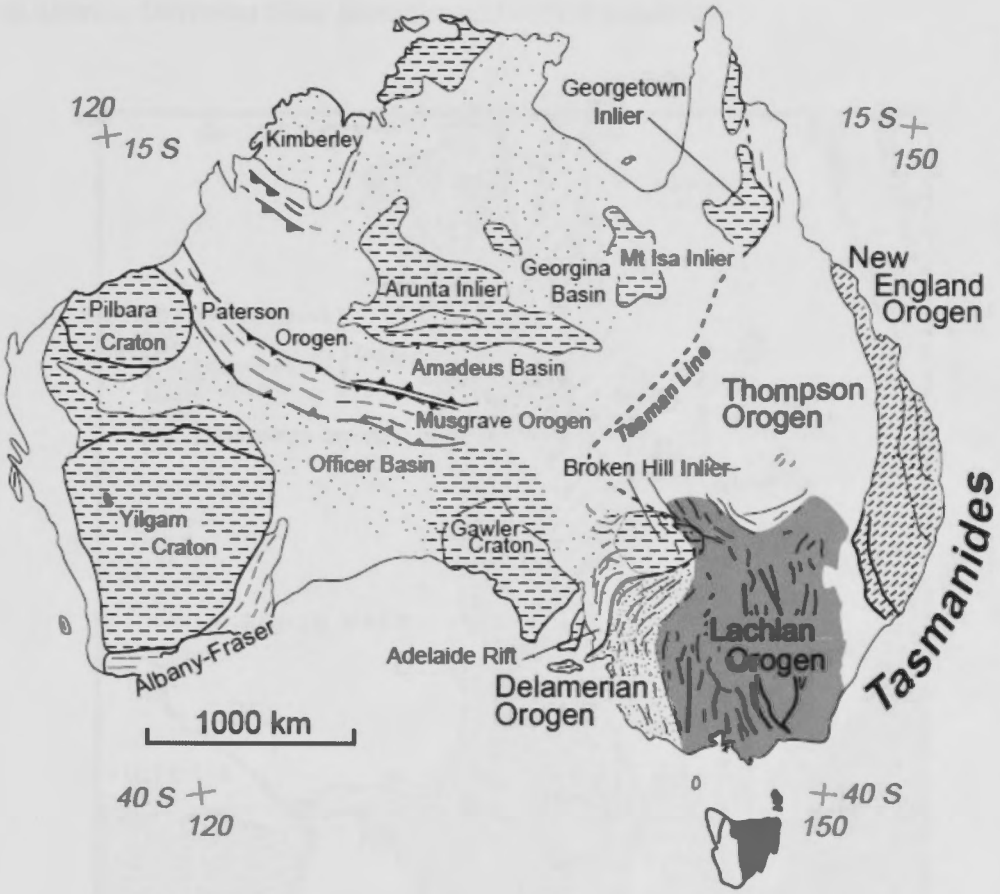

Figure 2.3: Map of major geological features of Australia showing the Lachlan Orogen (Lachlan Fold Belt) and other Orogenic belts of the Tasmanides (Foster and Gray, 2000).

The majority of New South Wales consists of the Palaeozoic Tasman Fold Belt System (Scheibner, 1978, 1987; Coney *et al.*, 1990). The successive cratonisation from west to east included the Early Palaeozoic Delamerian Orogen (550-470 Ma), the Middle Palaeozoic LFB (450-340 Ma) and the Late Palaeozoic to Early Mesozoic New England Orogen (310-210 Ma), with peak deformations of Late Cambrian – Early Ordovician, Late Ordovician – Silurian and Permian – Triassic ages, respectively (Schuchert, 1916;

Browne, 1947; Rutland, 1976; Crook, 1980; Foster and Gray, 2000; Gray and Foster, 2004). The major rock types in the LFB include quartz-rich turbidites, minor cherts, calc-alkaline volcanics, and large granitic plutons from the Lower Palaeozoic (545-365 Ma). These rocks overlie a mafic lower crust of oceanic affinity that is of very limited outcrop, as shown in Figure 2.4 (Fergusson and Fanning, 2002). The dominant outcrops forming the catchment of Merimbula-Pambula are the Ordovician turbidites together with Silurian-Devonian felsic plutonics and coeval volcanics.

Figure 2.4: Map of the Lachlan Fold Belt in south-eastern Australia with distribution of the Molong volcanic province and the Ordovician quartz turbidite succession. Northern subsurface continuation of the Molong volcanic province is shown by the extent of the magnetic anomaly. Ag, Adaminaby Group; BZ, Bendigo Zone; Gg, Girilambone Group; GZ, Girilambone Zone; SZ, Stawell Zone; MZ, Melbourne Zone; TZ, Tabberabbera Zone; Wg, Wagga Group; WOZ, Wagga–Omeo Zone (Fergusson and Fanning, 2002).

2.2.2. Regional geology of South Coast, N.S.W.

The geological history of the far south-eastern coastline (Bega-Mallacoota area) has its origins in the early Palaeozoic, with the accretion of the Mainland Terrane, which began with the deposition of the Adaminaby Group, a series of turbidite sandstones, siltstones and shales, with minor chert horizons (Lewis *et al.*, 1994) (Figure 2.5). The turbidites were most likely to have been laid down within a major submarine delta fan system.

During the late Silurian to early Devonian, the intrusion of granites within the Kosciuszko, Berridale, Murrumbidgee and Bega Batholiths occurred (Lewis *et al.*, 1994) (Figure 2.5). Later activity included strike-slip movement along the major transcurrent fault lines, with the Burragate Fault (approximately 10km north of Merimbula and trending NE) offsetting basement geology in the Merimbula-Pambula catchment.

By the Middle to Late Devonian, the area was likely to have been a land mass which was characterized by moderate relief and large lake systems and shallow seas along the eastern margin. During the Late Devonian, extensional tectonism occurred, along with rifting and bimodal volcanism, known as the Boyd Volcanic Complex (Lewis *et al.*, 1994). Besides the extensive basement of Ordovician-Silurian turbidites and Silurian-Devonian granites, the study area catchment also contains extensive outcrop of the Boyd Volcanic Complex, which unconformably overlies the LFB turbidites and intrusive granites (Fergusson *et al.*, 1979; Lewis *et al.*, 1994; Young, 2007). These are marine and non-marine sedimentary and igneous (volcanic and intrusive) rocks which extend from near the Victorian border to near Bermagui (Young, 2007, Figure 2.7). Subaerial, silicic volcanism also occurred along the eastern regions at Eden, Merimbula and Bunga Head. Basalt lava flows and clastic deposits developed as interbedded units (Lewis *et al.*, 1994). At Bunga Head and east of Eden, shallow marine or lake sediments including conglomerates, shales, sandstones and reworked volcanics were deposited. Intrusion of subvolcanic A-type granites was coeval with the silicic volcanism (Fergusson *et al.*, 1979; Collins *et al.*, 1992; Lewis *et al.*, 1994).

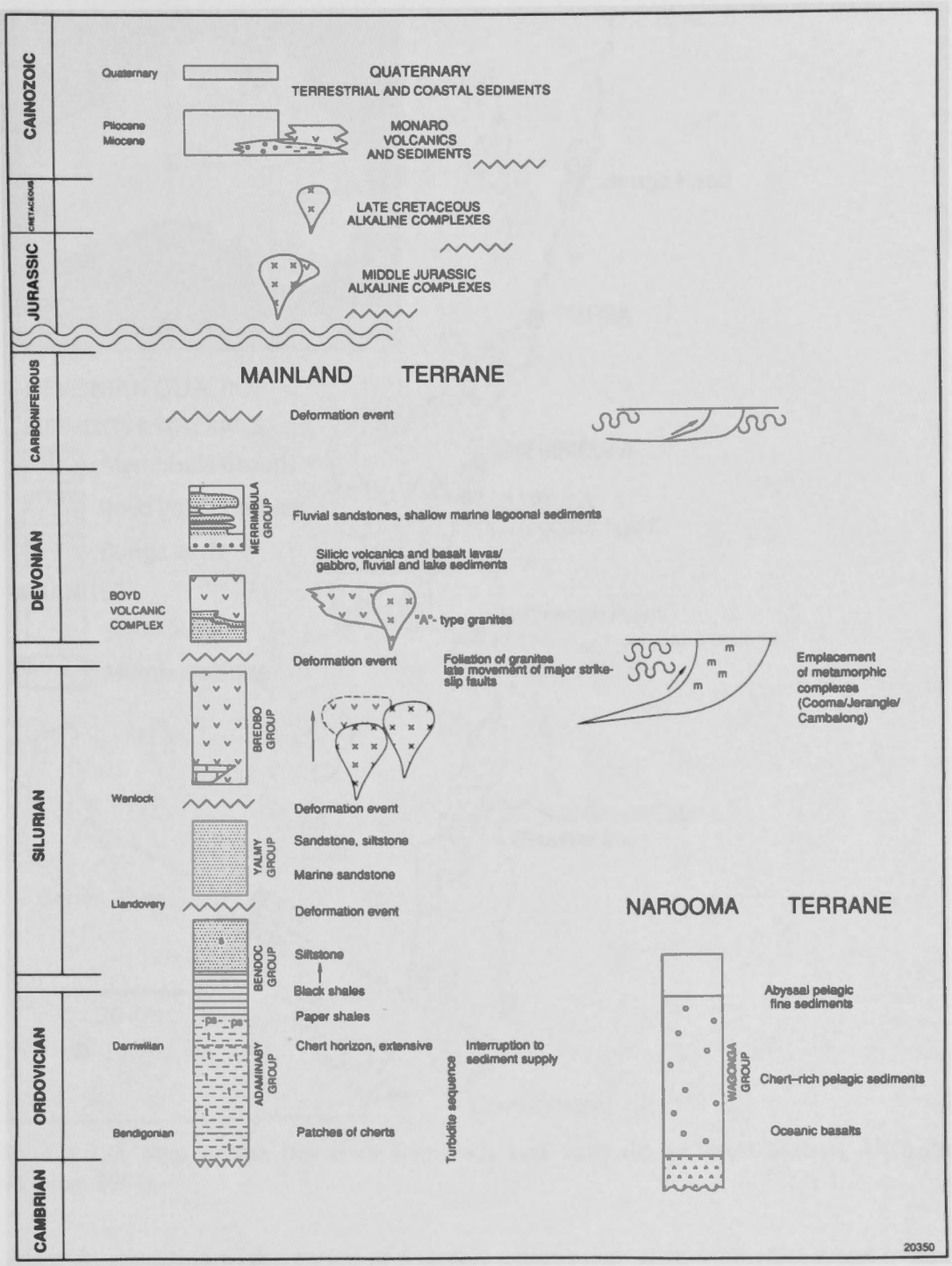

Figure 2.5: Geological history of Cooma-Bega-Eden area (Lewis *et al.*, 1994).

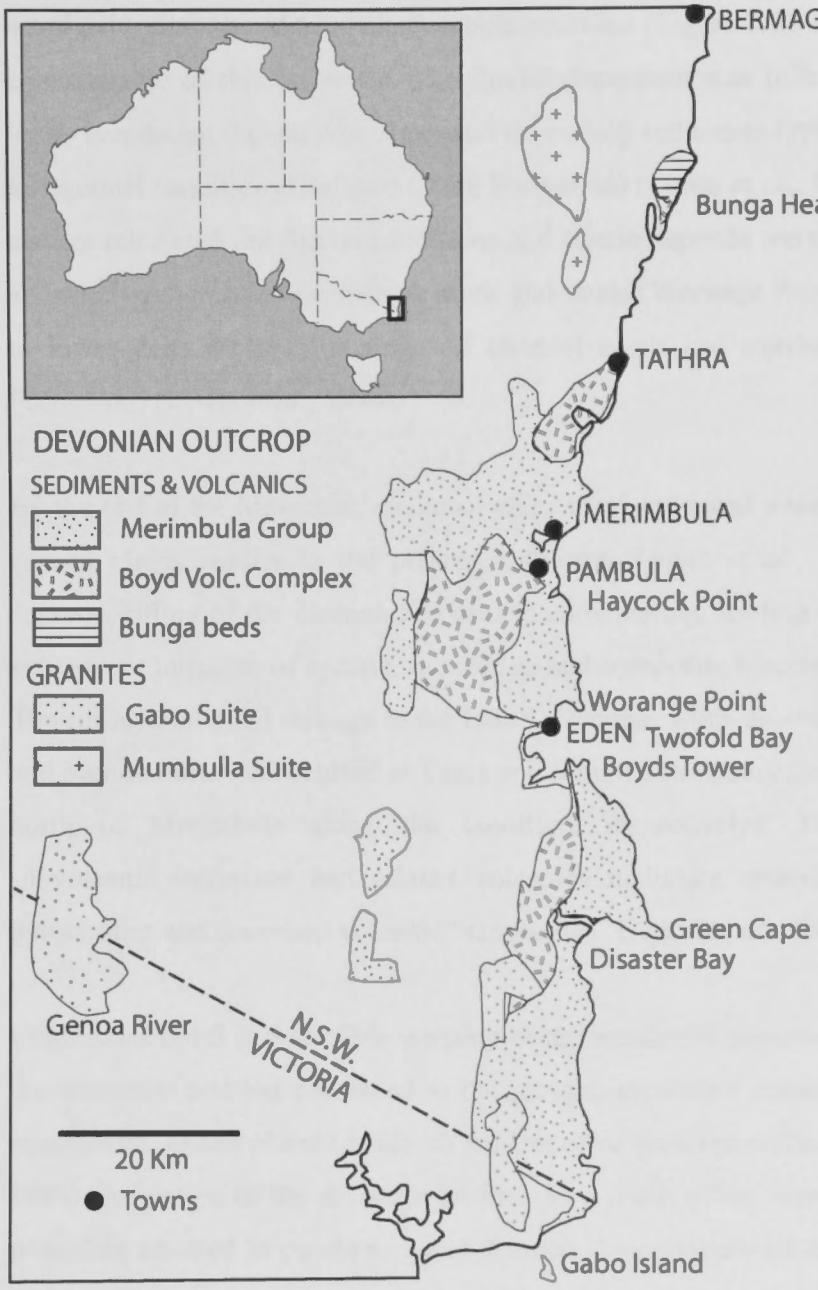

Figure 2.6: Map of the Devonian sediments and volcanics in south-eastern Australia (Young, 2007).

After the cessation of the period of volcanic activity, the area returned to a stable land mass with moderate relief, rift valleys, and shallow marine waters or extensive lake environments. A change in climate caused fluvial conditions to develop, depositing characteristic conglomerates, pebble sandstones, coarse sandstones and mudstones, which are known as the Twofold Bay Formation within the Merimbula Group. These are shown as the Devonian Merimbula Group in Figure 2.5 and form the very resistant

headlands along the Merimbula-Pambula coastline (Figure 2.6). Distinctive redbeds are characteristic of this sequence. The fluvial deposition was followed by a rise in sea-level, inundating the shallow areas and depositing sediments typical of shallow marine to lagoonal conditions (Bellbird Creek Formation) (Lewis *et al.*, 1994). Further eustatic change reinstated the fluvial conditions and clastic deposits were laid down, indicating an orderly progression from sheet sands and muds (Worange Point Formation) of a mid to lower delta facies to a series of channel sands and overbank muds (Ben Boyd Formation) (Lewis *et al.*, 1994).

By the end of the Mesozoic, erosional effects had produced a weathered peneplain and coastal plains similar to the present landform (Lewis *et al.*, 1994). In the Middle Jurassic, rifting of the Tasman Sea caused underplating, leading to heat generation and subsequent intrusion of syenite, monzonite and composite breccias (Lewis *et al.*, 1994). The rifting continued through to the Late Cretaceous when another period of monzonite and syenite intrusion occurred at Tanja and Mount Dromedary (located 30km and 65km north of Merimbula along the coastline, respectively). These rocks represent subvolcanic intrusives and related volcanics including andesitic lavas, crystal-rich pyroclastics and reworked volcanic "sandstones" (Lewis *et al.*, 1994).

Continuous uplift and possible warping of the weathered peneplain began at the end of the Mesozoic and has continued to the present, creating a coastal plain, a pronounced escarpment, inland plateau lands, as well as some drainage rearrangement (Lewis *et al.*, 1994). Alteration of the drainage systems as a result of the warping and tilting of the peneplain resulted in ponding, which formed large shallow lakes (Lewis *et al.*, 1994). These lake and associated fluviatile sediments are preserved underneath the blanket of extensive basalt lava flows that occurred during the Eocene to Oligocene, which erupted from numerous small vents aligned along north-south trending fracture zones. This sequence is based in the northern section of south eastern NSW, and is known as the Monaro Volcanics. These rocks consist of alkali basalt-basanite-nephelinite associations, which are spilt into an upper and lower series by extensive and thick dolerite-gabbro sill (Lewis *et al.*, 1994).

Clastic sediments of Tertiary age (Eocene to Pliocene) are present at many sites along the coastal plains as fluvial sheet-like deposits, which include cobble and pebble beds, coarse sands and clays, which have been transported due to increased sediments loads resulting from higher rainfall events (Lewis *et al.*, 1994). Quaternary deposits, which include valley fill, hill slope or alluvial fan deposits, aeolian deposits or residual soils cover a large region of the area. Along the coastline most of the sediments are products of processes currently occurring, or are associated with recent glacial and interglacial episodes. Deposit types include barrier sands, tidal deltas, estuarine muds and shelf sediments.

2.2.3. Local geology and geomorphology of the South Coast, N.S.W.

The basement geology of the Merimbula-Pambula catchment is mainly the Devonian Merimbula Group and the Boyd Volcanic Complex, together with Ordovician-Silurian turbidites and granites, and lower Tertiary-Cenozoic sediments which underlie much of the coastal estuaries and outcrop on prominent sea cliffs.

As noted above (Section 2.2.2), the late Devonian sedimentary sequences comprising predominantly fluvial deposits with a minor but significant amount of shallow marine sediments have been assigned to the Merimbula Group. The Merimbula Group outcrops along the South Coast of NSW (Taylor and Mayer, 1990), and extensively along the coastal ranges including the upland catchments of the study area.

Deposits of poorly consolidated sediments rest horizontally on the eroded surfaces of older Tertiary formations (Hall, 1969). The deposits are confined to areas along the coastline, with Cainozoic sediments outcropping discontinuously from the Victorian border to beyond Tuross Lake (located approximately 100km north of Merimbula along the coastline). These rocks are mainly ferrigenous conglomerate, quartz conglomerate, argillaceous sandstone, humic sandstone, clay, sand and gravel rarely exceeding 30m in thickness (Hall, 1969).

The coastal region is divided from the inland plateau regions by the Great Escarpment (Figure 2.7). The escarpment is an erosional feature, hundreds of metres high, which is retreating inland under the cumulative effects of rapidly eroding streams (Lewis *et al.*, 1994).

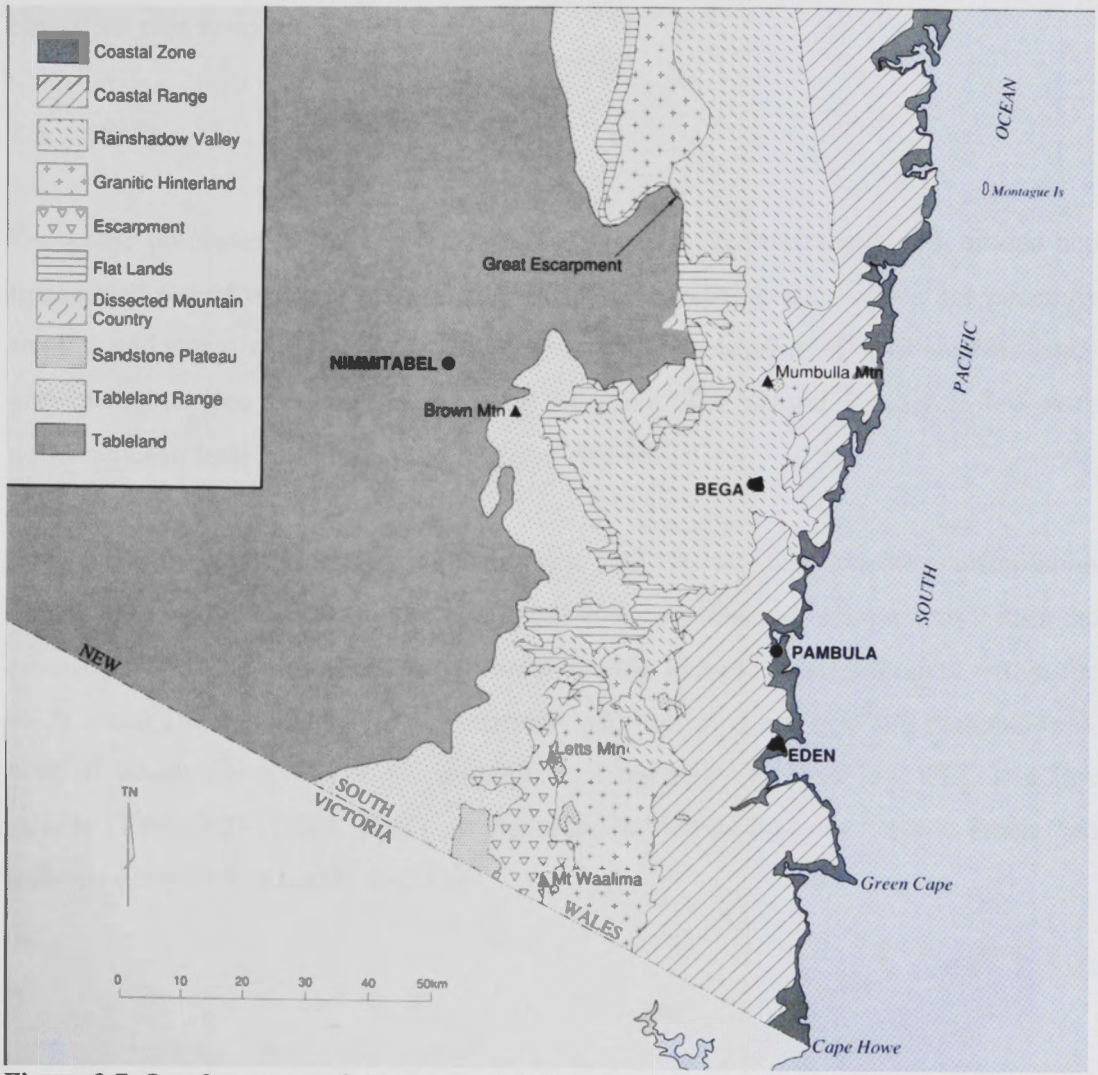

Figure 2.7: Land systems of the Bega – Mallacoota sheet area (modified from Keith and Saunders, 1990).

Inland there are granitic and metasedimentary hinterlands of low to moderate relief, 200-500m in elevation. Closer to the escarpment the country has a more dissected hilly landscape (300-1300m) high. The Devonian sediments (Merimbula Group) form several sandstone plateaus such as the main areas of the Wadbilliga, Nungatta and Mount Imlay National Parks.

Immediately west of the escarpment is a range of undulating or ridge country, mostly granite, marking the course of the Great Dividing Range. Inland from this range is a palaeo-plain - the Monaro Tableland - a low relief, low rainfall area of grassland or open woodland. This high plain country consists of a series of plateaus at different elevations plus residual hills.

2.3. Soils

Pedogenic processes in the study area have formed soils from weathered, eroded and transported parent material to form red and yellow podzolic soils which are generally shallow and stony, with numerous rock outcrops. The soils are acid, with shallow sandy grey/brown surface horizons over clay B horizons. The natural fertility is low with deficiencies in both phosphorus and nitrogen (Gibbs, 1978).

Soil landscape descriptions (Figure 2.8; Table 2.1) provide supplementary information on which to further develop an understanding of the sedimentary components within the estuarine system. Figure 2.8 indicates that a number of soil landscapes occur within the study area. The dominant soil landscapes include Yellow Pinch (yp) and Pambula (pa), both of which are acidic, sodic, erodible, and have low to very low CEC and low salinity (Table 2.2) (Tulau, 1997). In addition, Bald Hills (bh) and Yellow Pinch (yp) soils are dispersive to highly dispersive.

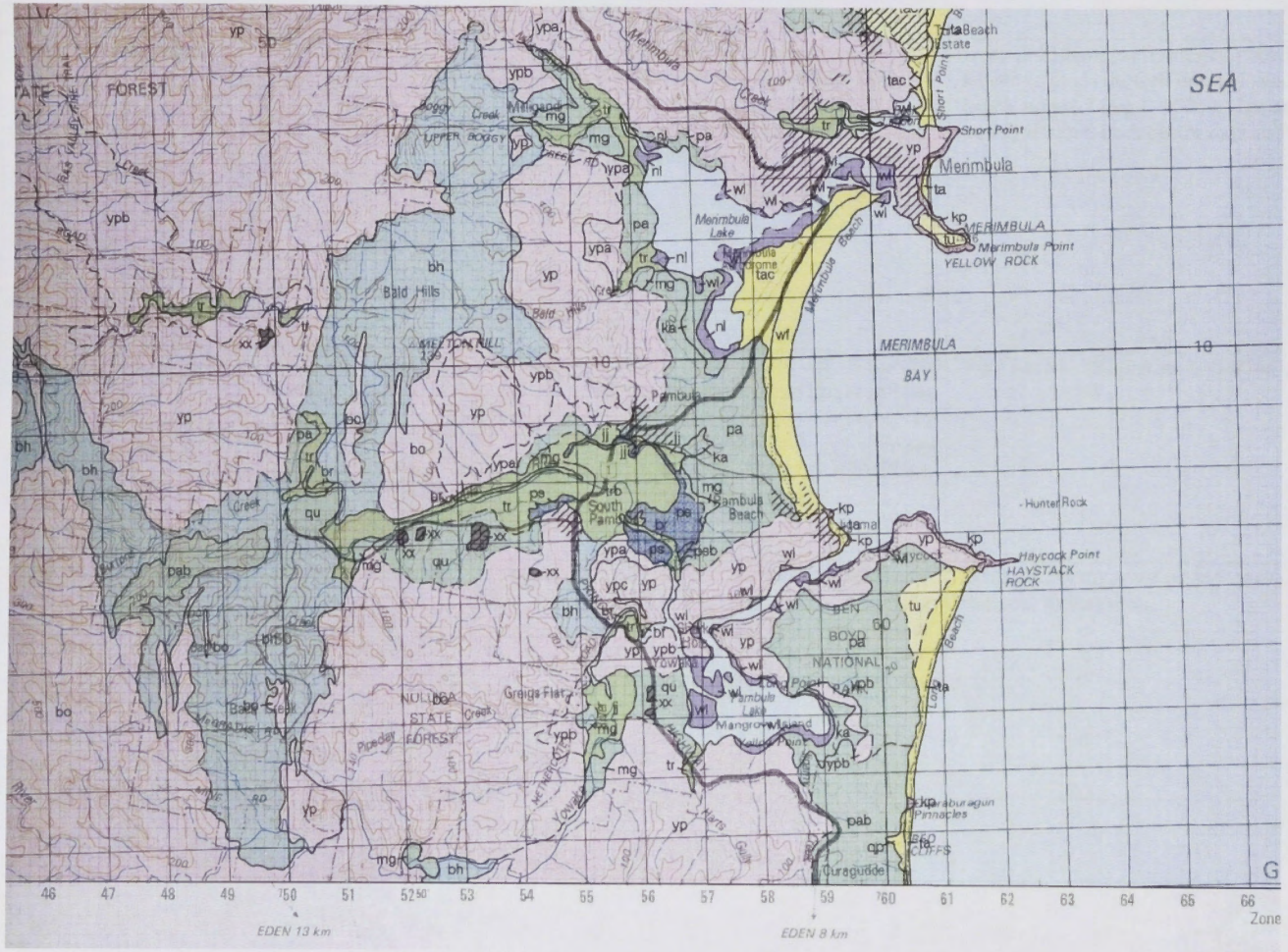

Figure 2.8: Soil landscape map (Tulau, 1997).

Landscape type	Classification	Area	Landscape	Soils	Limitations
Beach landscapes	tac – Tathra	6.5 km^2	Sand plains/beach ridges on Holocene aeolian sands. Local relief <5m, slopes < 5%, elev. 0-11m. Open forest, woodland and closed scrub.	Deep (>150cm), well drained podzols and siliceous sands on well drained sand plains and beach ridges. Deep (>150cm) imperfectly drained-poorly drained Podzols on flats and swales.	Highly permeable, non-cohesive, erodible, infertile soils with low available water holding capacity subject to seasonally high water tables (localized). Water (rain splash and sheet) erosion hazard, severe wind erosion hazard, and ground water pollution hazard.
	wf – Wallagoot fore dune	3.5 km^2	High fore dunes of Holocene aeolian sands. Fore dunes to 10m high and 75-300m wide, often with blowouts. Slopes moderately inclined (10-32%). Heath to sparse heath.	Very deep (>300cm), well drained siliceous sands.	Non-cohesive soils subject to mass movement (sand slumping) hazard and wind erosion hazard with groundwater pollution hazard and foundation hazard.
Estuarine landscapes	nl – Nelson Lagoon	2.5 km^2	Supratidal poorly drained fluvial delta to intertidal mudflats. Elevation <2m a.s.l; mangrove or swamp paperback low closed forest to low open woodland and salt marsh.	Deep (>150cm), very poorly drained alluvial soils and acid sulfate soils.	Acid, commonly sodic and saline, often potentially acid sulfate soils subject to severe flood hazard and permanently high water tables with groundwater hazard and pollution hazard.

	wl – Wapengo Lake	4.5 km^2	Flood-tide, supratidal and intertidal marine sand flats in Quaternary marine sediments. Elevation <1m a.s.l. Mangrove to salt marsh.	Very deep (>300cm), very poorly drained estuarine sands over deep clayey sand on supratidal and intertidal sites.	Non-cohesive, sodic, saline sands which may be potential acid sulfate materials, subject to severe flood hazard with water logging, permanently high water tables, water (wave) erosion hazard, ground water pollution hazard and foundation hazard.
Residual landscapes:	pa – Pambula	38 km^2	Undulating rises to rolling low hills on Tertiary sediments. Local relief 0-40m; slopes gently inclined (>10%). Elevation 0-49m. Partially cleared open-forest with heathland in exposed sites.	Moderately deep (50-150cm) to deep (>150cm), moderately well-drained to well-drained lateritic Soloths or moderately well-drained to imperfectly drained yellow Soloths over deeply weathered Tertiary sediments on crests, summits surfaces, slopes and flats. Moderately deep to deep, poorly drained Brown clays in drainage lines.	Infertile. Hard setting, acid, often non-cohesive (pal) erodible soils subject to water (sheet) erosion hazard with seasonally high water tables (localized in drainage lines).
	mg – Milligandi	3.5 km^2	Level to gently undulating terraces on Quaternary alluvium. Local relief 0-15m; slopes gently inclined (<3%). Elevation 5-30m. Cleared.	Moderately deep (50-150cm), moderately well-drained Yellow Podzolic Soils on terraces.	Infertile soils.
	ka – Kalaru	4 km^2	Gently undulating plain to undulating rises on Tertiary sediments. Local relief <15m; slopes very gently inclined (<3%). Elevation 0-20m. Partially cleared tall open-forest to closed-shrub land in poorly drained sites.	Moderately deep (50-150cm) to deep (>150cm), imperfectly drained yellow Soloths over deeply weathered bedrock on moderately well-drained sites. Moderately deep (50-150cm) to deep (>150cm), poorly drained gleyed Soloths over deeply weathered bedrock in poorly drained sites.	Acid, infertile soils with aluminium toxicity potential subject to waterlogging and permanently high watertables (localized), seasonal waterlogging (localized), water (sheet) erosion hazard and foundation hazard.

Alluvial landscapes:	tr – Towamba River	40.5 km^2	Narrow, high energy floodplains of coarse Quaternary alluvium. Elevation 0-200m; predominantly cleared tall open-forest.	Deep (>150cm), well-drained Alluvial soils.	Soils subject to flood hazard, high run-on, water (stream bank) erosion hazard, groundwater pollution hazard and foundation hazard.
Erosional landscapes:	yp-Yellow Pinch	186.5 km^2	Rolling to steep hills on sandstone, siltstone and conglomerate. Local relief 140-240m; slopes moderately inclined to steep (25-35%). Elevation 0-774m. Open-forest on crests and slopes, tall open-forest to closed-forest in sheltered sites. Bedrock outcrop generally <2%; >29% locally.	Moderately deep (50-150cm), moderately well-drained to imperfectly drained yellow Soloths and Yellow Podzolic Soils on crests to midslopes on sandstones and conglomerates, siltstones and mudstones. Shallow (<50cm), well-drained Lithosols on sites with resistant rock strata. Deep (>150cm), well-drained to imperfectly drained yellow Soloths and Yellow Podzolic Soils, Earthy Sands or Brown Earths on colluvial slopes.	Shallow soils (localized), non-cohesive soils with minor bedrock outcrop on steep slopes (localized), subject to mass movement hazard (localized) and minor to moderately severe water (sheet) erosion hazard.
	ypa-variant ypa	5 km^2	Deeper or less rocky soils on undulating low hills.		
	ypb-variant ypb	10 km^2	Rolling low hills.		
Transferral Landscapes:	bh – Bald Hills	35 km^2	Rolling hills on basalts. Local relief 80-160m; slopes moderately inclined (10-32%) and convex. Elevation 20-319m. Bedrock outcrop 20-50% on some ridges. Cleared.	Moderately deep (50-150cm), moderately well-drained Chocolate Soils and reddish Chocolate Soils on crests to midslopes. Moderately deep (50-150cm), imperfectly to poorly-drained Chernozems in drainage lines.	Non-cohesive (self-mulching) soils subject to seasonal waterlogging (localized, drainage lines).

Table 2.1: Soil landscape descriptions for the Merimbula-Pambula area (Tulau, 1997).

Soil landscape	% clay (whole sample)	Dispersion (%)	pH 1:5	EC (µS/cm)	CEC meq/100g	ESP (%)	Exchangeable cations (meq/100g)				
							Ca	Mg	K	Na	Al
Milligandi (mg1)	9	43	4.9	70	7.4	3	5.9	0.9	0.5	0.2	0.1
Milligandi (mg2)	9	77	5.4	30	3.4	6	2.3	0.3	0.1	0.2	nd
Milligandi (mg3)	33	28	5.6	50	10.3	4	7.7	3	0.2	0.4	0.2
Pambula (pa1)	4	0	3.5	40	3.3	9	0.9	0.5	0.1	0.3	0.7
Pambula (pa3)	24	8	3.8	70	3.7	22	0.3	1.0	0.2	0.4	1.3
Pambula (pa4)	13	0	4.4	90	1.7	18	nd	0.3	0.1	0.3	0.8
Bald Hills (bh1)	19	6	4.8	50	21.7	2	11.5	7.6	0.4	0.5	0.2
Bald Hills (bh2)	28	19	5.7	30	32.6	2	9.7	22	0.1	0.8	0.2
Yellow Pinch (yp1)	3	29	3.8	50	6.8	6	2.4	1.4	0.4	0.4	0.5
Yellow Pinch (yp2)	9	59	4.5	30	3.7	11	0.2	0.9	0.2	0.4	0.4
Yellow Pinch (yp3)	31	37	4.1	30	8.4	6	0.2	3.9	0.18	0.45	2.8

Table 2.2: Soil properties for representative samples of each soil landscape in the study area (Tulau, 1997).

2.4. Climate

The climate of south-eastern Australia is subject to a number of major controls:

(a) The westerly airstream encircling the Southern Hemisphere about these latitudes,

(b) The influence of depressions off the east coast,

(c) The occasional intrusion of moist tropical air masses from northern Australia, and

(d) The episodic influences over the long-term of the El Nino Southern Oscillation (ENSO) and Inter-decadal Pacific Oscillation (IPO).

These controls result in the South Coast of NSW having a mild, temperate climate with fairly uniform rainfall. The average maximum temperature for Merimbula is 20.6°C, and the average minimum temperature is 9.6 °C. The annual mean rainfall for

Merimbula is 830mm, with a summer dominance. The winter rains are commonly prolonged but relatively light. Summer and autumn months are drier, especially inland, but along the coast the effects of offshore depressions have more impact. Intrusion of moist air from northern Australia can cause an increase in rainfall and thunderstorm activity. In winter and spring there is a regime of episodic depressions and frontal disturbances from the west and south-west.

There is a noticeable rain shadow effect out of the Alps on the Monaro tablelands and in the Bega and Towamba valleys (Figure 2.9). There are also orographic effects which are associated with higher rainfall occurring along the coastal ranges as moist maritime air rising along the Great Escarpment is cooled and condenses to form precipitation.

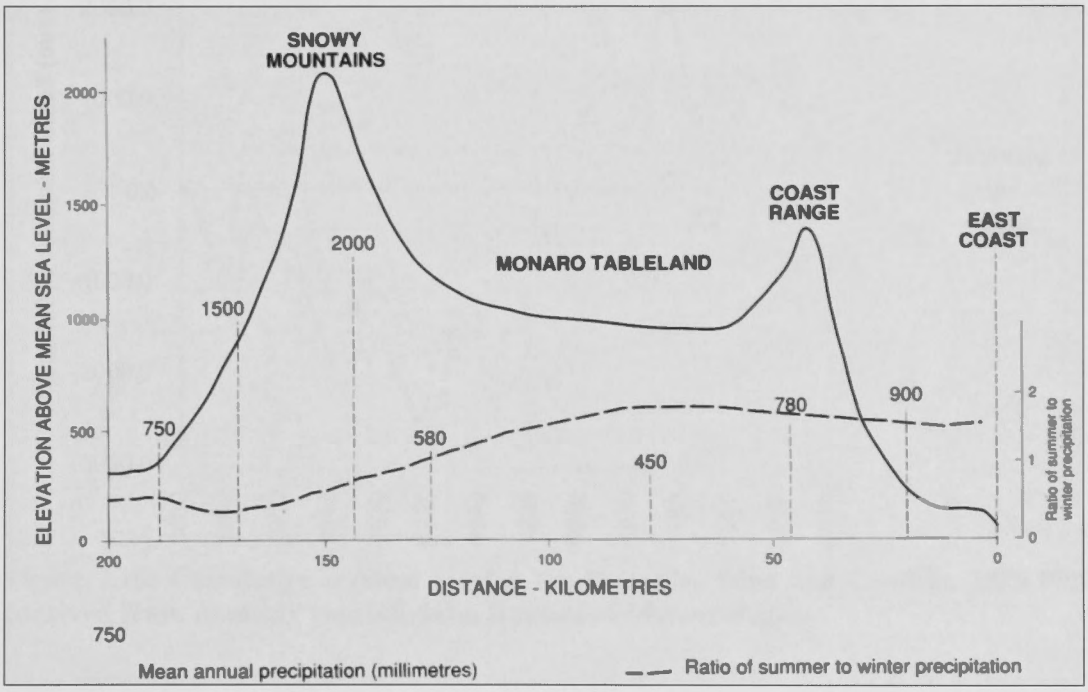

Figure 2.9: Rainfall variation (west-east) along latitude 36°30'. Bega-Mallacoota sheet area (modified from Brown and Millner, 1989 *in* Lewis *et al.*, 1994).

Analysis of long term rainfall indicates a number of trends. A plot of the cumulative residual rainfall indicates an approximately one hundred year cycle in which the first half of the 20th century was drier and the 2nd half was wetter than average (Figure 2.10).

This pattern of alternating drought dominated and flood dominated regimes has been identified along other locations of the eastern seaboard of Australia (Erskine and Warner, 1988). This long term pattern is also evident when annual data are plotted with the 40th and 60th percentiles illustrating the range for 'average' conditions (Figure 2.11).

As a consequence of the climatic conditions of the region, freshwater recharge of the estuaries is episodic, and generally not strong enough to flush the systems. As a result, there is a long term residence time of the sediments in the deep basins of the lakes.

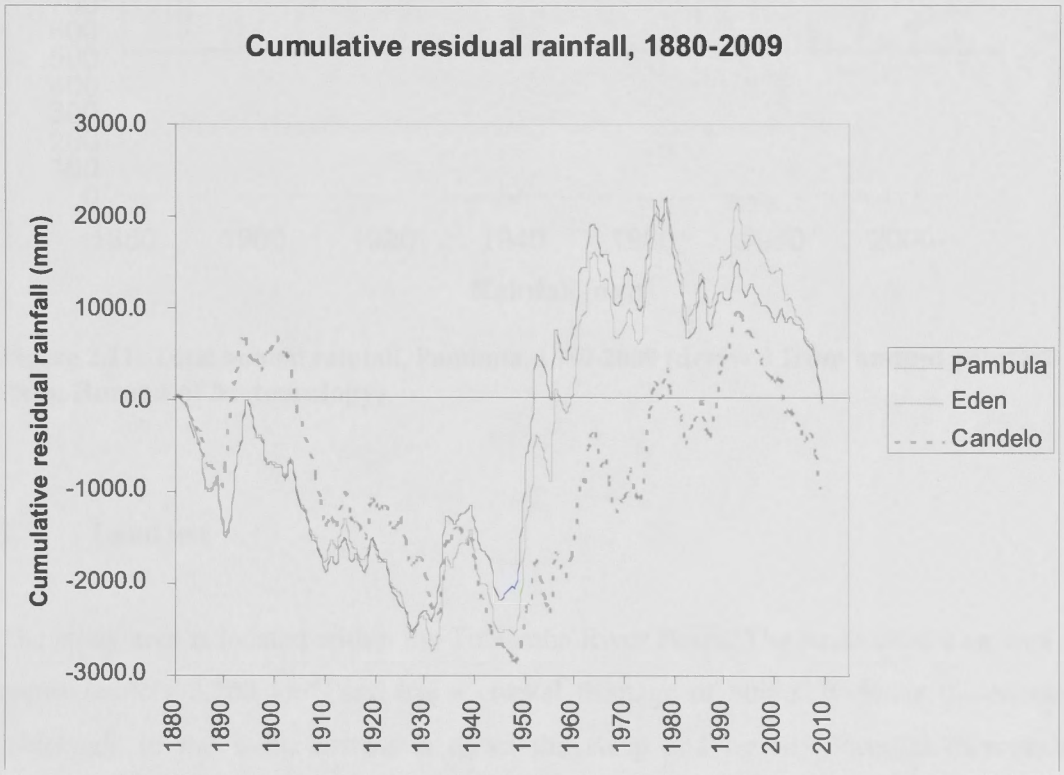

Figure 2.10: Cumulative residual rainfall for Pambula, Eden and Candelo, 1880-2009 (derived from monthly rainfall data, Bureau of Meteorology).

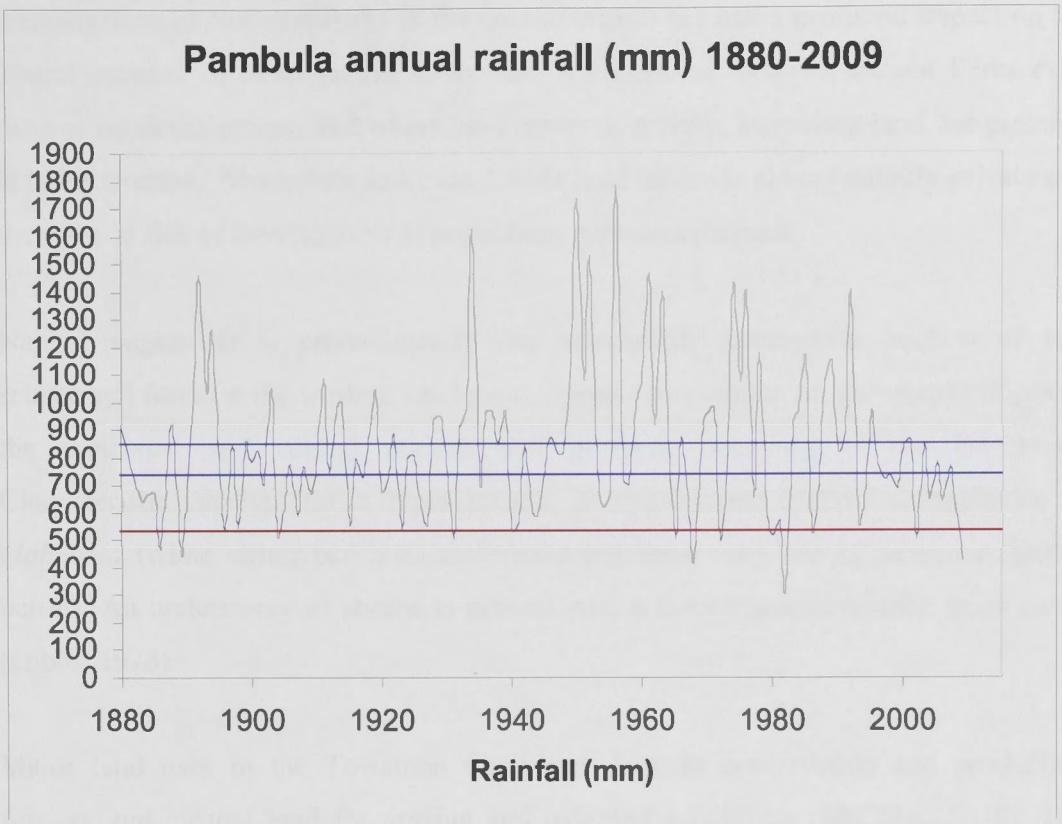

Figure 2.11: Total annual rainfall, Pambula, 1880-2009 (derived from annual rainfall data, Bureau of Meteorology)

2.5. Land use

The study area is located within the Towamba River Basin. The basin covers an area of approximately 2,200 km^2, and has a coastal frontage of 80km. It drains the Monaro tablelands in the west, eastwards down the steep and heavily forested escarpment slopes, through foothills and valleys where a combination of forests and cleared land for grazing and farming dominate, to rich agricultural land in the floodplains (SRCMA, 2010). The elevation of the catchment varies from sea level to approximately 450m in the far northwest corner (Gibbs, 1978). Land tenure comprises private land, State forest and National Estate. A chain of National Parks extends along the coastal ranges; with isolated parks also being present along the coastline (including Mount Imlay (40 km^2), Nalbaugh (40 km^2) and on the coast south of Eden, the Ben Boyd National Park (94 km^2) and the Nungatta National Park area). These parks plus numerous nature reserves constitute a major form of land tenure and usage within the catchment. The

promulgation of National Parks in the coastal region has had a profound impact on the spatial patterns of development in the last few decades. Where National Parks exist there is no development, and where land tenure is private, increasing land use pressure is being exerted. Merimbula Lake catchment land tenure is almost entirely private and therefore at risk of development as population pressures increase.

Natural vegetation is predominantly dry sclerophyll forest with pockets of wet sclerophyll forest in the western catchment. Forest areas remain on the steeper slopes of the northwest and central regions and northern boundary of the catchment. Characteristic eucalypt forest types include *E. muelleriana* (yellow stringybark), *E. globoidea* (white stringybark), *E. sieberiana* (silvertop ash) and *E. fastigata* (brown barrel). An understorey of shrubs is present with a discontinuous tussock grass cover (Gibbs, 1978).

Major land uses in the Towamba Catchment include conservation and production forestry and cleared land for grazing and irrigated agriculture (SRCMA, 2010). The major forms of agricultural land usage on the coastal fringe are crops, dairy and beef cattle grazing, dairy farming and viticulture, with a large proportion of this land being irrigated for dairy production (SRCMA, 2010). As a result, there is a high level of dependence of this productivity on continued access to water from the rivers for pasture irrigation. Much of the economy is linked to the productivity of the dairy industry, with the Bega Cheese Factory a major commercial operation in North Bega.

There is a long history of Aboriginal occupation on the Far South Coast, which is defined by strong associations with the natural heritage of the catchments and coastal areas (SRCMA, 2010). For example, two large Aboriginal shell middens are located in the surrounds of Merimbula Lake (Bell and Edwards, 1980) and are numerous along the Pambula River.

An increasing land use on the Far South Coast is for rural residential and coastal settlement as the population continues to grow (SRCMA, 2010). The township of Merimbula has a population of 3851 (2006 Census, ABS), which increases threefold in

the peak summer season (BVSC, 2008) due to the strong drawcard of tourism to the area. During peaks in populations, the greatest concern is overloading of the sewerage system, resulting in overflows into the Lake, as well as increased pollutant loads entering the lake via storm water drains (ABS, 2006).

The combined population of Merimbula, Tura Beach, Pambula and Pambula Beach is expected to increase by at least 4000 people (+/- 25%) by the year 2026 (BVSC, 2008). The population projection is estimated to include a largely older population in the retirement age group. This is significant for a number of reasons, namely the need to maintain the recreational and aesthetic qualities of Merimbula Lake. In addition, a higher permanent population means a higher anthropogenic loading on the lake. Land tenure and land use, as well as changing population dynamics will play some role in the condition of environments at the bottom of the catchment, including estuaries, and this is reflected in their current status which varies from pristine to modified (Figure 2.12).

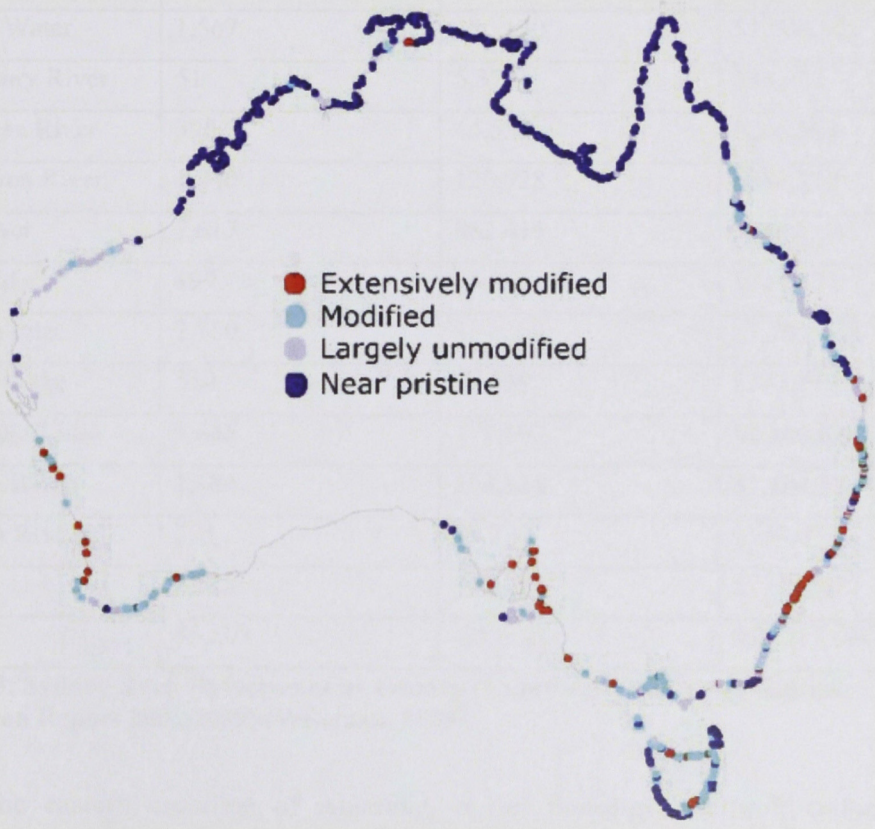

Figure 2.12: The condition of Australia's estuaries (ANRA, 2007).

As a consequence of these current conditions, Merimbula Lake and Pambula Lake are two of the most utilised recreational fishing and oyster farming estuaries of the region (Table 2.3). The Far South Coast's shellfish industry is undergoing continuous growth, with its contribution to the NSW aquaculture industry becoming increasingly significant. Much of this success is dependent on continued high standards of water quality delivered from the surrounding catchments (SRCMA, 2010).

Estuary		**Total**	
	Bags	**Dozens**	**Value ($)**
Nambucca River	839	91,573	$599,124
Macleay River	333	40,673	$206,940
Hastings River	2,189	266,497	$1,368,377
Camden Haven	1,508	161,580	$1,113,394
Manning River	1,158	125,930	$832,725
Wallis Lake	23,146	2,773,842	$14,822,211
Port Stephens	5,461	600,240	$3,890,172
Brisbane Water	1,567	186,130	$1,006,805
Hawkesbury River	51	5,375	$38,063
Shoalhaven River	390	44,535	$266,903
Crookhaven River	1,040	120,928	$689,210
Clyde River	7,617	882,415	$5,068,435
Tuross Lake	499	55,875	$344,529
Wagonga Inlet	2,780	334,259	$1,767,468
Wapengo Lake	510	58,039	$343,773
Merimbula Lake	**1,646**	**179,605**	**$1,186,033**
Pambula River	**1,684**	**198,126**	**$1,104,538**
Wonboyn River	765	84,270	$544,073
*Others	2,928	329,394	$2,024,279
Totals	56,109	6,539,286	$37,217,054

Table 2.3: Sydney Rock Oyster sales by estuary in southern NSW (Aquaculture Production Report 2008/2009) (Wiseman, 2009).

Along the eastern coastline of Australia, oyster farming is a multi-million dollar industry (Wiseman, 2009). Oysters are filter feeders, with each individual oyster

capable of filtering up to 60 litres of water per day. In order for the industry to operate successfully, the water body must remain pristine. Of greatest concern to the oyster industry with respect to the quality of the water, is the input of anthropogenic contaminants to the water body. With 77% of Australia's total population living within 50km of the coast (ABS, 2006), and this figure increasing at a rapid rate, maintaining the quality of coastal water bodies is becoming increasingly difficult. This is a result of anthropogenic pollutants being added to lakes, estuaries and lagoons, which ultimately generates a sink and potential source of pollutants within the sediments.

Oysters are exceptional bio-indicators of water quality because, as filter feeders, they can accumulate pollutants and heavy metals in their flesh and shells, providing an indication of the level of pollutants present within estuarine systems (Boening, 1999; Valdez Domingos *et al.*, 2007). Thus aquaculture in the estuaries requires the water quality to be maintained at rigorous standards. Merimbula Lake is also used for commercial activities including fishing, boating and tourism, and recreational activities such as boating, fishing, prawning and swimming; while Pambula Lake is used for commercial aquaculture, and recreational activities such as boating, fishing, prawning and swimming.

2.6. Estuarine form and processes

Coastal regions represent a dynamic interface between marine and terrestrial systems. They are also an expression of both past and present processes which ultimately define the form of specific coastal features, such as estuaries.

2.6.1. Sea level change

Sea level change has a profound impact on coastal morphology and sedimentology. Over geologic time, a number of cycles of eustatic sea level change have occurred in the study region (Figure 2.13), but the most important in terms of defining the shape of the coastal landscape occurred after the Last Glacial Maximum (LGM), when sea level rose rapidly from approximately -120m at 20000 cal BP (Ferland *et al.*, 1995; Sloss, 2006)

(Figure 2.13). The Holocene sea level highstand of +1.0-1.5m was attained ~7000 cal yr BP, and fell to its present height after 2000 yr BP (Lewis *et al.*, 2008). Oscillations of sea level may have occurred twice in this period, around 4600 and 2800 yr BP (Lewis *et al.*, 2008).

The effects of sea level changes on the geomorphology of the coastal system caused the coastal zone to be displaced seaward onto the continental shelf during the glacial periods, causing rivers to cut to new base levels. During the interglacial periods of high sea level, bedrock ridges, river valleys and lowlands were drowned, forming coastal features, such as estuaries, which were then infilled with both terrestrial and marine sediments (Hall, 1969; Roy *et al.*, 2001). Environments which were formerly marine were therefore gradually transformed to terrestrial environments. This cut and fill cycle has been repeated many times in geological history, with many of the coastal valleys containing remnants of interglacial deposits, as well as those deposited during the Holocene period (the last 10,000 years) (Roy *et al.*, 2001). During oscillations of sea level, these features were reworked and extended (Hall, 1969). The most recent phase of estuarine sedimentation occurred towards the end of the Post-Glacial Marine Transgression, between 7,000 and 8,000 years ago (Roy and Thom, 1981; Roy, 1984; Roy *et al.*, 2001).

The most prominent features of New South Wales coastal morphology have been influenced by this Holocene eustatic rise in sea-level, which caused drowning of the lower reaches and the formation of onshore sand barriers. The morphological features arising from these changes in sea level are identified in the coastal estuaries, lakes and lagoons along the south coast of NSW, with Merimbula and Pambula being prime examples.

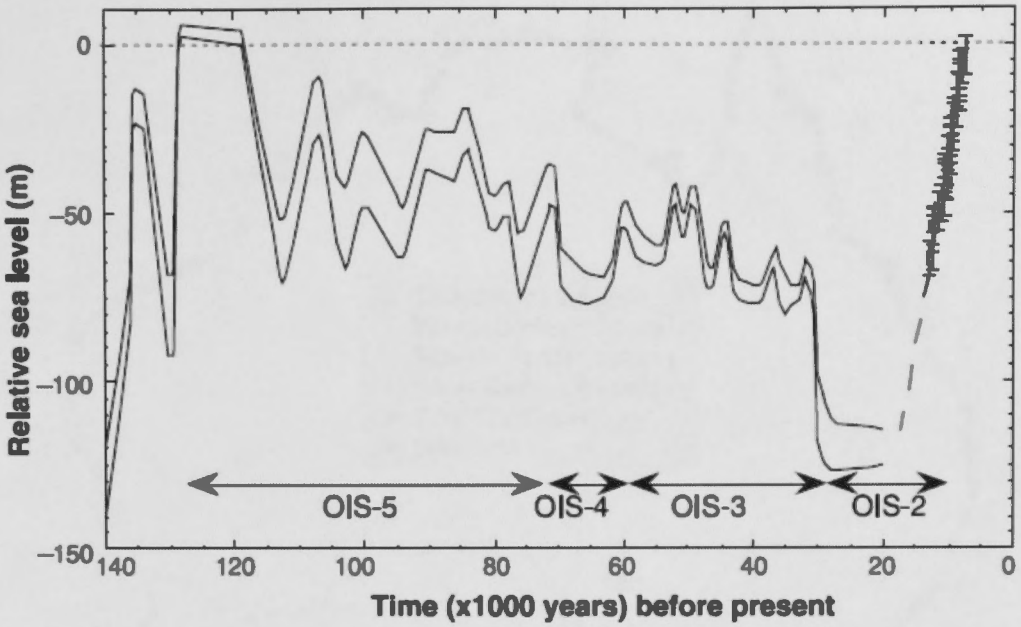

Figure 2.13: Relative sea level at Huon Peninsula, Papua New Guinea, for the past 140000 years. The fluctuations are the result of the glacial cycle-induced changes in continental-based ice volumes. Upper and lower limits are shown for the pre-LGM part of the record (before about 25,000 years ago), and mean sea level estimates with error bars are shown for the post-LGM record. The timing and duration of the major oxygen isotope stages is shown (Lambeck and Chappell, 2001).

2.6.2. Estuarine classification and morphology

The coastline of Australia comprises wave- and tide-dominated shelf environments (Harris *et al.*, 2002; OzCoasts, 2010) within which there are 974 estuaries and lagoons (Turner *et al.* 2006). The south-east coast of Australia, characterised by a low tidal range, is largely dominated by wave-dominated estuaries (42%), coastal lagoons/strandplain creeks (35%) and wave-dominated deltas (10%) (OzCoasts, 2010) (Figure 2.14).

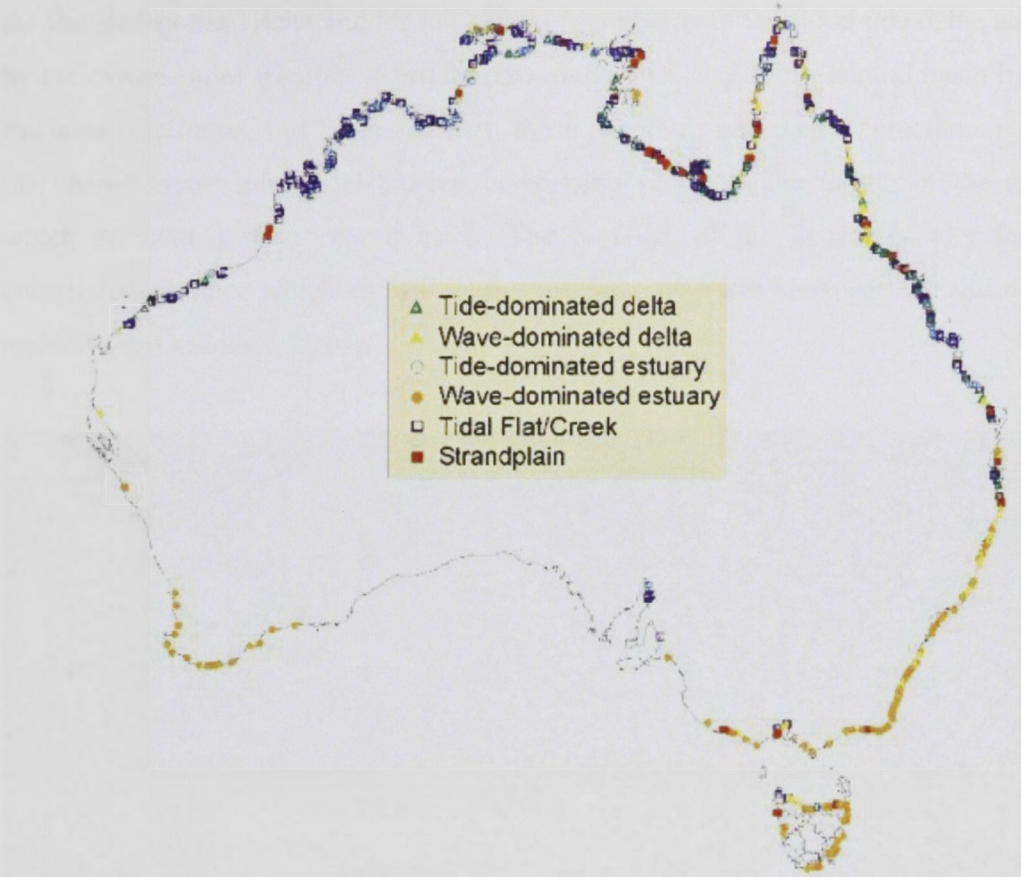

Figure 2.14: Spatial distribution of tide and wave dominated estuaries in Australia (ANRA, 2007).

Wave-dominated estuaries, specifically, form on those coastlines which are exposed and have small tidal influences (Roy *et al*, 2001). Examples include Clarence River (NSW) (Figure 2.15), Gippsland Lakes (VIC), Hunter River (NSW), Lake Illawarra (NSW), Margaret River (WA), Merimbula Lake (NSW) (Figure 2.16), and Pambula Lake (NSW). Wave-dominated estuaries are formed from a coastal bedrock embayment which has undergone partial infilling by sediments derived from up catchment and marine sources. Waves are the primary force shaping the overall geomorphology of these systems (OzCoasts, 2010).

The distribution of estuarine particulate matter is dependent on a number of physical processes, including water circulation patterns, gravitational settling, and sediment deposition and resuspension (Chester, 1990). Within such estuaries, these factors drive the estuarine evolutionary process through the simultaneous seaward progradation of

the fluvial bay-head delta and the landward progradation of the flood tide delta, and also by the expansion of fringing intertidal flats, due to infilling of the central basin by finer fractions (OzCoasts, 2010). In addition, these processes and their interactions produce the characteristic supra-tidal barrier, comprising sands, at the mouth of the estuary which encloses a wide central basin. The presence of the barrier usually forms a constricted entrance which allows for the exchange of water between the central basin and the sea (OzCoasts, 2010).

Figure 2.15: Clarence River, NSW – an example of a wave-dominated estuary where there is a small tidal influence

Figure 2.16: Merimbula Lake, NSW. A wave-dominated estuary with a township concentrated on the seaward side of the study area.

Wave-dominated estuaries are distinguished by relatively high wave energy at the mouth, compared to tidal energy. This wave energy is dissipated in the central basin, resulting in a relatively low energy estuarine environment (OzCoasts, 2010). The geomorphology of an estuary plays an important role in where 'sinks' occur, with hydrodynamic conditions controlling grain-size distribution (Sarkar *et al.,* 2004). The conditions in these estuaries result in sand beaches and channel sands from high energy environments; and muddy basins as a result of low energy environments. Consequently, sediments in wave-dominated estuaries range in distribution from fine to coarse sands in the barrier and tidal inlet deposits; fine organic muds and sandy muds in the central basin; to coarse, unsorted gravels, sands and muds of terrigenous origin in the fluvial bayhead delta (OzCoasts, 2010).

Key features of wave-dominated estuaries can be summarised as (OzCoasts, 2010):

1. *A diverse range of marine and brackish, subtidal, intertidal and supratidal estuarine habitats.*
2. *Narrow entrances which limit marine flushing, resulting in only a small proportion of the estuarine water volume being exchanged during each tidal cycle.*
3. *River flow rates that can be episodically high, with consequent event-based high flushing capacity.*
4. *Low turbidity of the water column, with the exception of extreme events (for example in response to extreme storms or winds).*
5. *A central basin that acts as an efficient 'trap' or sink for terrigenous sediments, organic material and associated pollutants.*
6. *Long residence time of water, which is conducive to the trapping and processing of terrigenous solutes*

The physical morphology of an estuary is very important in determining the flow paths and rates of water and sediments in the system. The placement and flow rates of a major channel with respect to slower moving waters for instance, plays an important role in the flushing rate of the sediments and water. Similarly, anthropogenic constructions such as bridges, dredging and altered entrances will also impact on the overall morphology of the system. Estuarine morphology is largely determined by the relative influence of wave, tide, and river power (Boyd *et al.*, 1992; OzCoasts, 2010). Having an understanding of estuarine morphology when classifying sediments is useful as it takes into account the extent of the physical dispersion of inputted sediments.

The physical transport of solid matter by moving water leads to a geochemical fractionation based on size and specific gravity as gradient lessens, hydraulic energy drops, and sedimentation takes place (Siegel, 2002). The fractionation is evident in the sand size fraction of water-borne sediment where heavy minerals are deposited as a function of their specific gravity. The fine-grained clay fraction containing the heavy metals component may also show directional flow signatures, based upon current flow patterns (Dalrymple, 2007). Consequently, the sediments in wave-dominated estuaries

range from fine to coarse sands in the tidal inlet and barrier deposits; fine muds, sandy muds and accumulated organic matter in areas of seagrass growth, flanking environments (mangroves, salt marshes and tidal flats) and the deeper central basin; and coarse, unsorted gravels, sands and muds of terrigenous origin in the fluvial bayhead delta (OzCoasts, 2010). Furthermore, in nearshore sediments, chemical composition is primarily determined by sedimentological parameters such as grain size, mineralogical composition, and calcium carbonate and organic carbon contents (Cha *et al.*, 2007).

2.7. Merimbula and Pambula Estuaries

2.7.1. Merimbula Lake

The immediate catchment of Merimbula Lake (149.922°E, 36.896°S) has an area of 26 km^2. The perimeter of the Lake is 17.89km; with the waterway itself encompassing an area of 4.89 km^2 (Figure 2.17).

Figure 2.17: Merimbula Lake showing Front Lake in the foreground, Golf Lake in the left background and Top Lake in the right background (OzCoasts, 2005).

Merimbula Lake is an inlet/lake system, consisting of a natural entrance, an inlet channel, and a substantial marine flood delta (Front Lake) that is prograding and depositing into a large, medium depth (3-4 metres) basin (Top Lake), and a much smaller southern shallow (0.3m) basin (Golf Lake) (DLWC, 2004) (Figures 2.17 and 2.18).

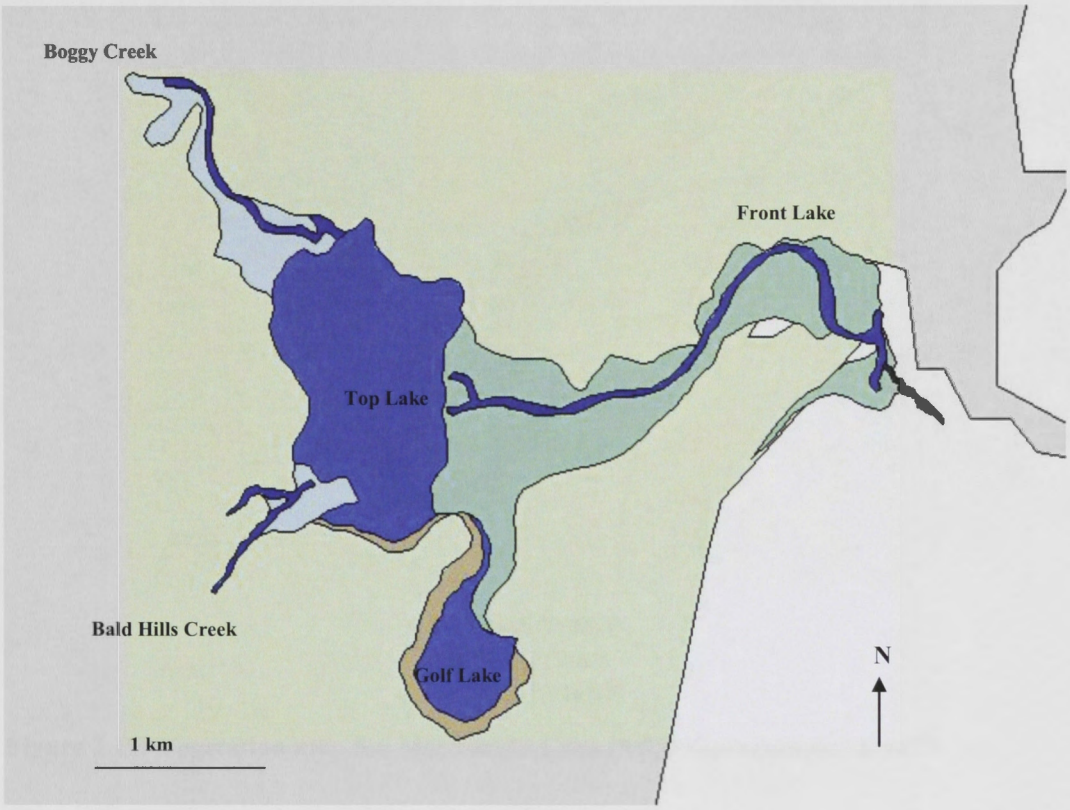

Figure 2.18: Merimbula Estuary (BVSC, 2001), see text for description.

The entrance is open and formed naturally along the northern side. Although the entrance width is narrow (0.10km), there is no record of the entrance ever having been closed, and bar depths (1.4 m at low tide) have remained relatively unchanged since first European settlement (DLWC, 2004). The major basin (Top Lake) has a rocky shoreline, while the small basin (Golf Lake) has a mangrove and sand based shoreline (DLWC, 2004). The vegetation is primarily seagrass (2.297 km^2) followed by salt marsh (0.629 km^2) and mangroves (0.377 km^2) (DLWC, 2004) (Figure 2.19).

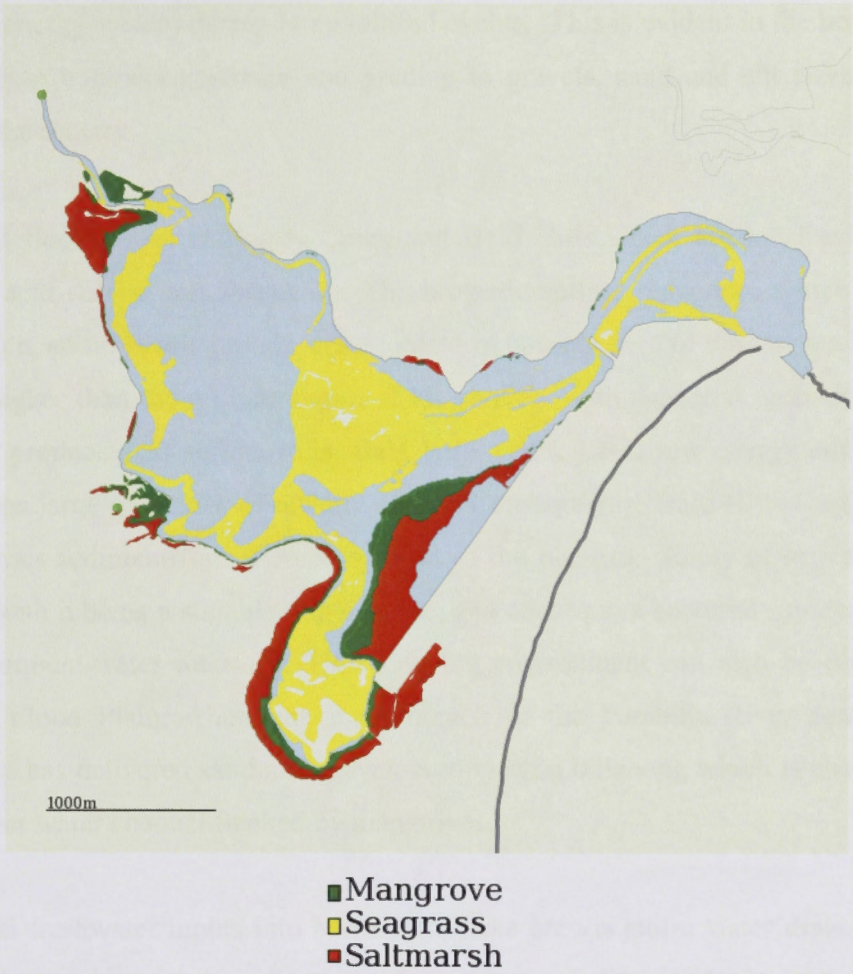

Figure 2.19: Vegetation map for Merimbula Lake (NSW Government, 2006/7).

Merimbula Lake is a wave-dominated estuary, with high sediment trapping efficiency, naturally low turbidity and salt wedge/partially mixed circulation (OzEstuaries, 2005). The estuary is also tidal, which supports a range of subtidal, intertidal, supratidal, marine and brackish estuarine habitats. The tidal period is semi-diurnal (tidal cycles of 12 hours, with two high tides and two low tides of approximately the same height each day). Merimbula Lake features one of the best developed ebb tidal deltas along the NSW coast, forming as a result of wave protection afforded by Merimbula Point (DLWC, 2004).

Freshwater enters the Top Lake through two small creeks, Boggy Creek in the north, and Bald Hills Creek further south. Although both Boggy Creek and Bald Hills Creek

are generally low energy tidal creeks, field observations indicate that Boggy Creek can be a high energy system during large rainfall events. This is evident in the bed material ranging from boulders upstream and grading to gravels, sand and silt sized particles closer to the estuary.

The small flood plains at Boggy Creek and Bald Hills Creek are localised sites for potential acid sulfate soil formation. The biogenic sulfate reduction, which produces organic rich, sulfur bearing muds, are a long term consequence of the last sea level high (~1-2m higher than today) (see Figure 2.13, above). With subaerial weathering, these sites will produce acid sulfate soils. Bald Hills Creek has a low energy environment, which traps large quantities of organic matter. Consequently, Bald Hills Creek is a site for sulfurous sediment formation as a result of the plentiful supply of organic matter, together with it being a suitable trapping site, and consequent bacterial sulfate reduction at the sediment-water interface. This reducing environment can also be observed at Pambula Flood Plain, where the main branch of the Pambula River south of the racecourse has delivered sand and gravel, cutting off a billabong which is characterised by a deeper water channel flanked by mangroves.

Additional freshwater inputs into Merimbula Lake are via storm water drains, and hill slope drainage. Alluvial deposits occur along the stream lines and in tidal areas on the perimeter of the lake (Gibbs, 1978).

The basin of Merimbula Lake at Top Lake is largely defined by the western shoreline and, to the east, the limit of the prograding flood delta (see Figures 2.17 and 2.18 above). It is within this basin that deep water (3-4m) conditions enable fine clays and organic matter to settle out as deltaic and bed sediments. The principal sites for deposition of silt/clay, therefore, are low energy areas within the creeks, as isolated backwaters, and the deep lake. By contrast, the principal deposition sites for medium to coarse physical weathering products, transported down catchment, are the creeks and associated prograding fluvial bay-head deltas extending into the lake (Figure 2.18). Mixing will occur under high energy conditions (for example in response to floods), but

generally the depositional environments of for coarse and fine materials are quite discrete.

The lake has been classified as being in a modified condition, with the major influences being rural residential land use (OzCoasts, 2007). Merimbula town centre (population 3,851; ABS Census, 2006) is situated north of the lake. The urban area comprises 2.1km^2 (DLWC, 2004). The point sources of contaminants into the system are minimal, and include stormwater outlets; a Sewage Treatment Plant (STP), which is situated to the south of the lake; Merimbula airport which runs along the edge of the shoreline of the small southern lake (Gold Lake); and, contaminated sites from earlier settlement. Contaminants are also derived from diffuse sources across the lower catchment in response to urbanization and rural residential development in the immediate lake environment. The Princes Highway crosses the inlet by a 250m long causeway and short bridge. The causeway was constructed in 1909, and although it altered the hydraulic regime of the system, records show that the lower estuary channel and shoal patterns were unchanged. This suggests that the overall impact of the construction was not overly significant (DLWC, 2004). However, the causeway and natural training walls have caused significant modification to the tidal regime in the Top Lake.

The flood delta near the mouth of Merimbula estuary is partially exposed with each low tide and as a result, is a higher energy environment. Seagrass needs to be permanently under water, hence the distribution of seagrasses is indicative of the extent of subaerial exposure of the flood delta during low tides. In those areas of the flood delta which are periodically exposed during low tide, the sediments are oxidised and the accumulation of organic matter is limited. However, with depth into the surface layer of the sediment, the effect of anaerobic, sulfate reducing bacteria is evident and the sand is a grey-black colour. Organisms which excavate through this grey sand form burrows which rapidly oxidise to yellow sand. This sedimentary environment is dominantly sand with only a minor clay component. By contrast, in deeper waters on the flood delta, the permanent presence of seagrasses is associated with trapping and build up of organic matter.

In the inter-tidal zone where mangroves exist, the exposed roots act as a trap for drifting organic material, and a significant build up of organic material in the sediments occurs. This is of minor importance in the Front Lake at Merimbula as most mangroves have been removed to improve property views (Figure 2.20). However, this is an important process in Top Lake, Pambula Lake and Golf Lake (Figure 2.21).

Figure 2.20: Foreshore of Front Lake of Merimbula estuary showing the absence of mangroves (Merimbula Information Centre, 2011).

Figure 2.21: Organic material trapped by mangrove pneumatophores (sub-aerial roots)

2.7.2. Back Lagoon

Back Lagoon (149.929°E, 36.883°S) is a shallow lagoon which has been substantially infilled with arkosic gravels, alluvial muds, and beach sands (Figure 2.22). The lagoon is very small, with a perimeter of 5.82km, and a water area of 0.41km^2. The lagoon is classified as modified, as a result of urban land use and associated modification to the estuary ecology through impacts on water quality. Back Lagoon is an ICOLL (Intermittently Closed and Open Lakes and Lagoons), a system which is closed most of the time with little tidal influence, resulting in mangroves being absent from this system. Although the lagoon is intermittently closed, when it is open the system acts as a wave-dominated estuary. The freshwater supply to the lagoon is Merimbula Creek in the western extremity of the water body. Merimbula Township adjoins the lagoon to the south.

Figure 2.22: Back Lagoon (note that barrier has been breached in this image due to large rainfall event) (OzCoasts, 2005).

2.7.3. Pambula Lake

Pambula Lake (149.916°E, 36.948°S) has a catchment area of 275 km^2. The perimeter of the lake is 26 km, with a waterway area of 2.9 km^2 (Figure 2.23).

Figure 2.23: Entrance to Pambula River and Lake (central basin can be seen in the background) (OzCoasts, 2005).

Pambula Lake is a wave-dominated inlet/lake system, comprising an open and untrained entrance, forming a channel which leads to a deep and relatively shoal free inlet, resulting in a large estuarine tidal response. There is a relatively constant tidal range throughout the inlet and lake, with the lake range slightly exceeding that of the inlet (DNR, 2009). The lake is shallow close to the shoreline (and consequently has been utilised extensively for oyster leases), and deepens rapidly towards the centre. The lake is vegetated along the perimeter by patchy mangrove (0.45 km^2) and salt marsh (0.19 km^2) cover. Patchy seagrass in the central basin and the channel covers an area of 0.706 km^2 (Figure 2.24).

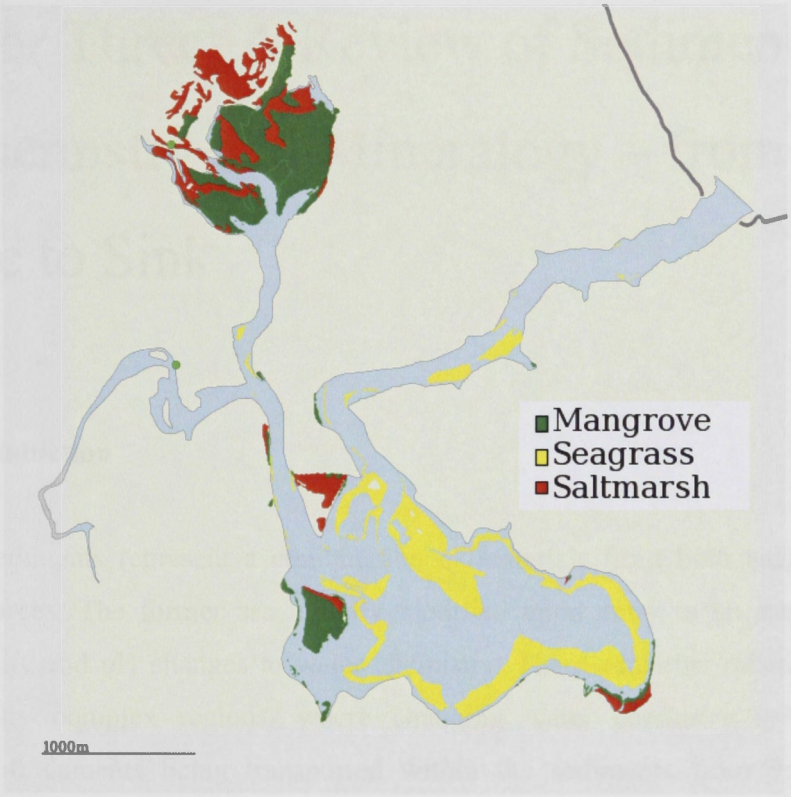

Figure 2.24: Vegetation distribution of Pambula Lake (NSW Government, 2006/7).

The lake receives freshwater inputs from the Yowaka and Pambula Rivers. The tidal limits for the rivers are approximately 10km upstream (DNR, 2009). Both Pambula Lake and Yowaka River are recreational fishing havens (DNR, 2009).

Pambula Lake is a largely unmodified estuary, with modification being from agricultural land use, oyster farming and rural residential properties (OzCoasts, 2010). In contrast to Merimbula Lake and Back Lagoon, Pambula Lake is located on the perimeter of a National Park, with the southern shoreline of the estuary being located within the Ben Boyd National Park (DNR, 2009).

Chapter Three: A Review of Sediment Geochemistry and Mineralogy – from Source to Sink

3.1. Introduction

Estuarine sediments represent a combination of materials from both terrigenous and marines sources. The former are initially modified upon entry to an estuary due to abrupt salinity and pH changes to water chemistry. These estuarine mixing zones are geochemically complex regions, where changing water chemistry influences the behaviour of elements being transported within the sediments from the terrestrial freshwater environment to the marine environment (Sholkovitz, 1976; Duinker *et al.*, 1985; Butcher *et al.*, 1992; Chester, 2003; Fan *et al.*, 2008; Waeles *et al.*, 2008). These sediments are then further modified by post-depositional authigenic, biogenic and anthropogenic factors within an estuary. The geochemistry of the transported sediment thus undergoes change from the riverine source to the estuarine sink, with modifications occurring from the time freshwater sediments enter the saline environment of an estuary, to settlement, mixing with marine beach sands and post-burial.

Estuarine particulate matter as a whole can be classified as:

a. **River transported particulates** – crustal weathering products (clay minerals, quartz), precipitated oxyhydroxides (principally those of iron and manganese), terrestrial organic components (plant remnants, humic substances) and pollutants (fly ash, sewage, etc).
b. **Atmospherically transported particulates** – aeolian dust, soils, crustal weathering products and pollutants such as fly ash, leaded petrol emissions (prior to 2002).

c. **Ocean-transported particulates** – biogenic components of marine origin (skeletal debris, organic matter) and inorganic components (originating in coastal sediments or formed in the marine water column).

d. **Estuarine-generated particulates** – inorganic and organic flocculants and precipitates, living and non-living particulate organic matter. Flocculation, precipitation and the biological production of organic matter are especially important in the formation of estuarine particulates (Salomons and Förstner, 1984; Chester, 1990).

Elements of natural and anthropogenic origin are transported by rivers and transferred to the coastal marine system through estuaries, where elements are distributed between dissolved and solid phases (Censi *et al.*, 2006). Their ultimate fate and bioavailability are strongly dependent on particle chemistry and competition between surface and dissolved forms (Censi *et al.*, 2006). Estuaries can therefore be described as being reactors in which processes occurring at the interface between the dissolved phase and suspended particulate matter constitute an important function in the trace element geochemical cycle (Censi *et al.*, 2006).

The terrestrial weathering products and organic matter are transported down river systems and deposited in the marine environment of the estuary, where they undergo mixing with marine sands and are influenced by changing geochemical, physical and biological conditions and processes. This process produces a significant binary mixing array in terms of sediment geochemistry, from an SiO_2-poor, Al_2O_3-rich clay sediment to an SiO_2-rich, Al_2O_3-poor quartz sediment. The transportation and ultimate fate of freshwater and marine sediments are dependent on a number of chemical and physical factors, including: an increase in ionic strength of the water from the freshwater environment to the marine environment. This is due to changing concentrations of cations and anions present, variations in pH and EC, and in the reduction-oxidation potential of the sediments and porewaters, concentrations of complexing ligands, nutrients, organic matter, and particulate matter (Chester, 1990; Acevedo-Figueroa *et al.*, 2006), all of which lead to geochemical processes which influence the sediments such as adsorption, complexation, precipitation, cation exchange and speciation. Clay

minerals are particularly susceptible to significant compositional changes in response to subtle changes in conditions (Guggenheim and Koster Van Groos, 2001). Physical controls which influence the depositional behaviour of sediments include estuarine morphology, river flow rate, river suspended load, sediment grain-size, vegetation distribution, and tidal fluctuations and circulation (Uncles, 2002).

The variations to the geochemistry of the sediments and water are subject to natural variability due to seasonal and tidal cycles. Upon deposition within an estuary a number of geochemical and mineralogical changes can occur to sediments due to natural authigenic and biogenic processes. Furthermore, the addition of anthropogenic contaminants to the sediments is also likely to cause significant geochemical changes in the sediment and water column. The final composition of the total sediment is therefore dependent on a number of pathways and processes. The modifications to a terrigenous flux are by no means uniform throughout the entire area of an estuary, nor with depth within the sedimentary column. For instance, those areas which are able to trap organic matter below tidal limits may develop reducing conditions in surface sediments. Yet close by, the same terrigenous detrital sediments, which in contrast are exposed daily to the atmosphere at low tide, are kept at more oxidizing conditions and thus have contrasting biogenic and authigenic processes occurring.

Although the components of a marine sediment are often classified according to their origin (Goldberg, 1963; Li and Schoonmaker, 2005), the mixing of the primary sedimentary end-members with post-depositional additions and changes to the geochemistry from terrestrial, biogenic, authigenic and anthropogenic components, alters the original sediment significantly. As a result, the final composition of the estuarine sediment may not reflect the original source material. An understanding of the components of the original terrestrial sediments, the post-depositional marine sediments, and the complex geochemical processes which occur in the estuarine mixing zone provide a valuable insight into the behaviour of estuarine sediments in response to both natural and anthropogenic processes. Sageman and Lyons (2005) presented a conceptual model for the origin of mixed detrital-biogenic facies relating the three major inputs to the processes that control them – namely terrigenous, biogenic and

authigenic processes (Figure 3.1, Sageman and Lyons, 2005). This thesis will look at these inputs, and also post-depositional anthropogenic processes.

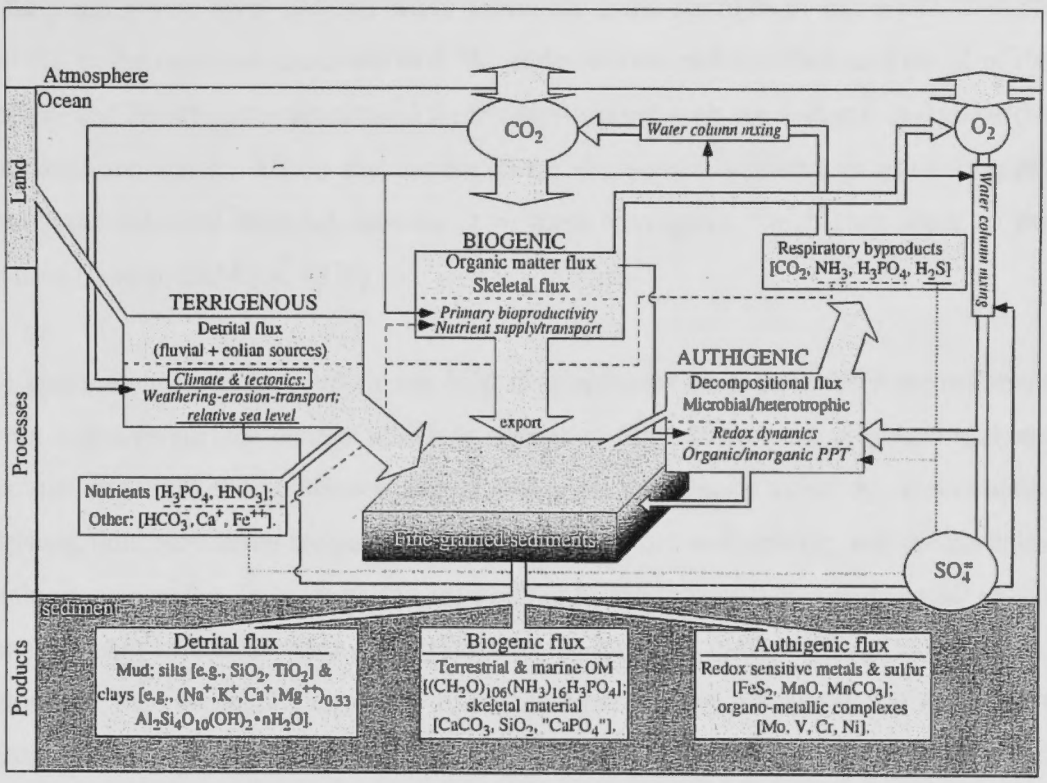

Figure 3.1 Conceptual model for the origin of mixed detrital-biogenic facies as a function of the major inputs (terrigenous, biogenic and authigenic) that control them. The model identifies the controlling factors (italicised), fluxes of key components of sedimentation and biogeochemical cycling (wide - medium arrows), and the relationships between these factors and processes (narrow arrows). Note that major nutrient fluxes and major authigenic fluxes are shown by thin dashed and dotted arrows respectively. (Sageman and Lyons, 2005)

3.2. Sediment geochemistry

The parameters discussed above are subject to strong variability in the estuarine environment as a result of a variety of dissolved to particulate transformations which are produced in the mixing zone (Chester, 1990). These transformations occur by a variety of physical, chemical and biological processes including: sorption at the surfaces of suspended particles, complexation, precipitation, flocculation and uptake by biota

(Chester, 1990; Siegel, 2002). These processes may occur amongst soluble phases, suspended and bottom sediments and biota (OzCoasts, 2010).

At the point where river and sea water meet, the ionic strength of the water changes from 0M in the river end-members to 0.7M in the marine end-member, as a result of the calcium- and bicarbonate- dominated river water mixing with the sodium- and chloride-dominated sea water. Within the mixing zone, the sudden gradient in ionic strength destabilizes colloidal material, causing it to form aggregates which then settle to the substrate (Burton and Liss, 1976).

Fine-grained clay particles which are held in suspension in a freshwater environment have a negative surface charge which is only partially balanced by adsorbed cations. This net negative charge causes the particles to repel each other by electrostatic repulsion, thus preventing the particles from forming flocs and sinking, and the particles remain in suspension. In more saline environments, the repulsive forces decrease as the cations present in the seawater are attracted to the negative surface charge of the clays, neutralising the charge, and allowing for adjacent particles in solution to destabilise and aggregate. This increase in ionic strength of the water causes both organic and inorganic components (river transported clay mineral suspensions, colloidal species of iron and dissolved organics such as humic materials) and trace elements associated with fine-grained suspended matter to be removed by flocculation (Chester, 1990; Baeyens *et al*, 1998). Coarser particles entering an estuary retain their individual sizes, and their depositional behaviour is governed largely by hydrodynamic factors (Burton and Liss, 1976).

Flocculation occurs more rapidly when particles collide, such collisions being increased by particle movement and higher concentrations of particulate material (Burton and Liss, 1976). Sedimentation due to flocculation is therefore often localized to the low-salinity region in estuaries. However, the aggregation of particles may also take place through biological mediation, where filter-feeding organisms produce faecal pellets (Chester, 1990).

At the mixing zone of fresh and saltwater, physico-chemical longitudinal gradients also form as a result of salinity, pH and temperature changes. These affect the processes controlling the removal of trace elements from the dissolved phase, by adsorption, precipitation and co-precipitation of solutes (Baeyens *et al.*, 1998). Adsorption is the principal process which occurs, due to metal cations having strong affinities for Fe- and Mn-oxyhydroxides, particulate organic matter, and clay minerals (Elder, 1988). The formation of precipitates on the surfaces of minerals due to the removal of manganese, iron and other metals from solution during estuarine mixing, are some of the most important estuarine precipitation processes (Chester, 1990). Iron and manganese are very important in marine geochemical processes as their various oxide and hydroxide species act as scavengers for a number of other metals. The processes which control the two elements are, however, different.

Dissolved iron in aerated river water is mainly present as hydrous Fe^{3+} oxides, which are stabilised in colloidal dispersion by high-molecular-weight humic acids (Chester, 1990). This is important as humic material is affected by speciation changes during the mixing of freshwater and marine water, where changes in pH, ionic strength and redox potential occur (Kretzschmar and Schäfer, 2005). The dominant pathway for iron removal from solution to the particulate state is therefore the flocculation of mixed iron-oxide-humate colloids of fluvial origin. This occurs by electrostatic and chemical destabilization during estuarine mixing as a result of the neutralisation of colloid charges by marine cations (Chester, 1990). The coagulative removal of iron therefore takes place at low salinities.

Manganese is another redox-sensitive element which is biogeochemically active in the aqueous environment, and readily undergoes transformation between the dissolved and particulate phases in response to physicochemical changes (Chester, 1990) (Figure 3.1). Manganese is therefore regarded as being a non-conservative element. Dissolved manganese supplied from rivers is in the reduced state, Mn^{2+}, which can undergo oxidative conversion to particulate Mn^{4+} as the physico-chemical parameters change on the mixing of fresh and marine waters (Chester, 1990). This process is pH dependent, and will proceed faster in the presence of a particulate phase which is able to adsorb the

Mn (II) (i.e. in the presence of a turbidity maximum). In the estuarine environment, it is therefore the redox-driven processes involving the dissolved to particulate reactions that influence the chemistry of manganese. These processes also occur after deposition of Mn (IV) particulates in the bottom sediments. Many sediments are reducing at depth so that the Mn (IV) solids can become reduced during diagenesis, therefore releasing Mn (II) into the interstitial waters (Chester, 1990). The bacterial utilization of this metal as an electron acceptor releases Mn ions to pore water solution that are then transported upward by diffusion and reincorporated into the sediment, favouring the enrichment of Mn in the upper sediments (Froelich *et al.*, 1979). When upper sediments are reduced, dissolved Mn will migrate upwards, and be released into the overlying water column. Alternatively, when upper sediments are oxidised, much of the dissolved manganese will be reprecipitated as Mn (IV) hydrous oxides. Profiles of dissolved manganese in estuarine surface waters are controlled by the fluvial input of dissolved Mn (II), the oxidative conversion of the dissolved Mn (II) to particulate Mn (IV), and the reduction and resolubilisation of Mn (IV) in either the water column or the sediment compartments (Chester, 1990).

Other important parameters which determine the chemical forms of elements when introduced to an estuarine environment include soil/sediment textural heterogeneity (grain size), soil/sediment matrix composition (e.g. mineralogy, organic matter content), fluid or particle interaction with interstitial or overlying waters, and organism activity (including bacterial processes) (Siegel, 2002). Under certain conditions, colloid-facilitated transport can become the major transport mechanism of strongly sorbing trace metals in soils and aquifers (Kretzschmar and Schafer, 2005). Mobile colloids affect the transport, bioavailability and natural cycling of trace metals in lakes, rivers and estuaries (Kretzschmar and Schafer, 2005). The chemical composition of marine sediments therefore reflects the source of the particulate material, the reactions occurring between dissolved and particulate phases, and the post-depositional changes which may lead to diagenetic reactions or precipitation in the sediments (Calvert and Pederson, 1993; Cha *et al.*, 2007). Consequently, an understanding of sediment geochemistry can be very useful as a tracer for environmental changes induced by

natural and anthropogenic sources (Leblanc *et al.*, 2000; Borrego *et al.*, 2004; Garcia *et al.*, 2004; Lopez-Gonzalez *et al.*, 2006).

3.2.1. Terrestrial end-member: clays, gravels and sands

The fine-grained silts, sands and gravels in south eastern Australian rivers are a mixture of the crustal weathering products quartz, feldspar, micas, clay minerals and heavy minerals, precipitated iron and manganese oxyhydroxides, terrestrial organic components (plant remain and humic material), and a variety of pollutants (e.g. fly ash and sewage) (Chester, 1990). These are transported downstream, generally under conditions of neutral to slightly acidic pH (~4-6) and low salinity (5-10‰), to the marine zone of higher pH (7.5-8.4) and higher salinity (35‰) levels. The pH of seawater remains constant as a result of the buffering capacities of carbonate in the water; however, pH can fall below 5.0 due to pyrite oxidation or exceed 8.0 due to the presence of shell fragments (Cox and Preda, 2005). Such variables in the system which are responsible for changes in pH have consequences for the stabilities of elemental phases which may be present in the sediment. Under conditions of low pH, the solubility of metal hydroxides increases as pH decreases, the adsorption capacity of solid surfaces decreases and H^+ ions compete with metals for coordination sites on organic molecules (Elder, 1988).

Contamination of river sediments can change drastically depending on the extent of residential, commercial, industrial and agricultural development along the river system itself, and its surrounding catchment. The material mobilised in the suspended sediment load of the river water, such as clays, iron hydroxides and organic matter, are very important in terms of the transportation of pollutants into the estuarine environment and ocean, as it these fine grained sediments which have the greatest capacity to adsorb metals and other anthropogenic contaminants. Accumulation of heavy metals within the sediment is generally site specific, with concentration correlating with clay and organic rich particles. Valsami-Jones (2000) states that the most important ways in which minerals control the flux of pollutants are the following:

a) *High solubility of a pollutant host (e.g. carbonate minerals) which will result in the release of the pollutant;*
b) *Low solubility of a pollutant host, which is desirable in order to reduce the availability of a pollutant (e.g. sparingly soluble phosphates);*
c) *Large surface area which is important since release or uptake is often surface controlled. For example, Fe oxyhydroxides, often poorly crystalline phases, forming very small crystallites and possessing, as a consequence, exceptionally high surface areas;*
d) *Layered crystal structure, a property that, together with high surface areas, characterizes clay minerals. This structure of clay minerals gives them a unique ability to intercalate pollutants between layers; and*
e) *Open structure, a property characteristic of zeolites, which may act as molecular sieves and trap a range of pollutants.*

3.2.2. Marine end-member: beach sands

In the marine environment, nearshore sediments are composed of a mixture of gravels, sands, silts and muds which are derived from:

a) Terrigenous, lithogenous and arkosic constituents derived from river-transported land erosion, atmospherically driven dusts, submarine volcanoes, and underwater weathering (where the solid phase undergoes no major change during its residence in the sea water), and particles formed both *in situ* biologically or inorganically weathering of rock from the ocean, land/ocean or from volcanic eruptions.
b) Biogeneous components comprising planktic and benthic organisms, and biogenic apatite.
c) The hydrogenous, authigenic component encompassing phases formed by inorganic precipitation from seawater (Chester, 1990; Li and Schoonmaker, 2005; Cha *et al*, 2007).

The chemical composition of nearshore sediments are primarily controlled by sedimentological parameters such as grain size, mineralogy and concentration of

calcium carbonate and organic carbon (Cho *et al.*, 1999; Cha *et al.*, 2007). These sediments, which are readily known as beach sands, have a wide variety of grain sizes, with the fine grained material being found in low energy environments, and the coarser material being found in high energy environments.

3.3. Sediment mixing relationships

NSW estuarine sediments in this study are principally a physical mixture between two end members:

1. Terrestrial clays, sands and gravels continually being deposited by freshwater river systems and atmospherically driven dusts;
2. Marine carbonate-quartz beach sands sourced from the oceans and particles formed in situ biologically (e.g. skeletal debris, organic matter) or inorganically (e.g. those particles originating in coastal sediments or formed in the marine water column) (Chester, 1990).

In the absence of further additions from anthropogenic, biogenic or authigenic sources, and reactivity as a result of changing ionic strength from freshwater to saline waters, the binary mixing of these two end members should show a linear relationship between the concentrations of elements in each of these sediments. For instance, an increasing gradient of beach sand concentrations would trend seaward, and the inverse for the gradient towards land. If the distribution and concentration of a component within the sediments is controlled only by physical mixing processes, then a range of sediment samples taken from throughout the system will theoretically fall on a straight line, and the components are known as being conservative or non-reactive (Chester, 1990). In contrast, when a component is added to, or depleted from an estuarine sediment, in the dissolved state its concentrations will deviate from this mixing line, and its behaviour is termed non-conservative, or reactive (Chester, 1990). This is particularly interesting in obtaining information as to the timing of the addition of the elements, as it allows one to ascertain whether the element is part of the original, detrital or beach sand component, or whether it has been added after deposition of the original sediments. In an area free

from contaminants from mining, heavy industry or effluent, this is likely to be from local point and diffuse anthropogenic sources, biogenic additions and *in situ* authigenic precipitates.

This mixing relationship is valuable in that it enables identification of components due to non-end member sources, of authigenic, biogenic and anthropogenic origins. By creating a theoretical mixing relationship of a known conservative component, and then imposing upon this a range of samples of unknown sources, we are able to distinguish between several sources based upon the conservative and non-conservative behaviour of the element.

There are some elements whose behaviour remains conservative under all estuarine conditions, including the major dissolved constituents which contribute to the salinity of seawater - Na^{+}, K^{+}, Ca^{2+} and SO^{2-}_{4} (Chester, 1990), Mg^{2+} (de Villiers and Nelson, 1997); and sediments - Li^{+} (Green-Ruiz and Páez-Osuna, 2001), Al^{3+} (Green-Ruiz and Páez-Osuna, 2001; Machado *et al.*, 2008), Fe^{2+} (Förstner and Wittmann, 1979; Cortesao and Vale, 1995; Schiff and Weisberg, 1999; Ruiz, 2001) and the REE (Munksgaard *et al.*, 2003; Lawrence *et al.*, 2006).

Elements which behave conservatively are characterised by constant concentrations irrespective of changing geochemical conditions, and display very little interaction with biological cycles. In the estuarine environment, the REE, Y, Sc and Th in particular, behave in a conservative manner due to very low concentrations of the elements in natural waters, and a short residence time in the oceans. As a result, these elements are transferred quantitatively during erosion and sedimentation from the parent rock into clastic sediments (Taylor and McLennan, 1995; Taylor and McLennan, 2009). Other elements, such as Zr, Hf and Sn have similar properties, but the fate of these elements in clastic sediments is dominated by heavy minerals such as zircon and cassiterite, which are readily segregated in geological processes (Taylor and McLennan, 2009).

The REE are not readily fractionated in sedimentary processes (except that Ce^{3+} may be oxidized to Ce^{4+} and separated as insoluble phosphate in marine environments, or less

frequently as the hydroxide in terrestrial environments) (Taylor and McLennan, 2009). The distribution of the REE in sediments is therefore a valuable tool in the characterization of the origin of the sediments and their sedimentation processes (Gouveia *et al.*, 1993; Prasad and Ramanathan, 2008). In contrast, non-conservative behaviour of elements varies considerably in the estuarine zone, as a result of the chemical compound in which it is present, variations in ionic strength of the seawater, and biological activity. As a result, non-conservative behaviour can result in removal from solution, addition to solution or a combination of both (Chester, 1990).

Sediment mixing relationships can therefore be used to ascertain whether an element has been added post-deposition or whether it is an original component, whether it has undergone estuarine reactivity, or whether it has been added or removed from the sediments. In order to relate this to the complex geochemical nature of estuaries, and to determine additions, removals and transformations occurring to elements within the sediments, conservative elements must be used. That is, elements which do not undergo geochemical transformations within the mixing zone.

3.4. Post-depositional modifications

In addition to the two primary sedimentary end-members, a number of post-depositional additions, transformations and alterations to the sediment may occur as a result of inputs from terrestrial, biogenic, authigenic and anthropogenic sources.

Additions and transformations to the sediments through biogenic processes include the bioturbation and reworking of sediments; bioaccumulation and subsequent concentrations of elements within the sediments; modifications via bacterial processes; addition of bacteria, and subsequent transformations; addition of biogenic silica; addition of calcium and strontium, and nutrients such as carbon, nitrogen and phosphorus. Bioturbation and reworking of the sediments generally occurs in the top 20-30 cm of the sediment, allowing the sediments to become reoxidised. Biogenic flux is an important contributor to the overall chemical composition of fine grained sediments. Photosynthetic production of organic matter and associated skeletal material

defines the second major input to fine-grained, mixed siliclastic-biogenic sediments (Sageman and Lyons, 2005). This sedimentary organic carbon has two major sources: terrestrial and marine. 65% of the total terrestrial flux is present as recalcitrant organic matter (OM) and can be incorporated into marine sediments (Sageman and Lyons, 2005). Much of this material is transported as sorbed phases on mineral surfaces, which can be shed in the nearshore zone and replaced by marine OM. Marine C_{org} is more labile, providing the dominant substrate for microbial decomposers (Sageman and Lyons, 2005).

Authigenic material is precipitated at or near the sediment-water interface as a consequence of Eh-pH-controlled organic and inorganic reactions (Sageman and Lyons, 2005). These estuarine generated particulates include inorganic and organic flocculants and precipitates and both living and non-living particulate organic matter. Of the processes occurring within the estuarine system which lead to the formation of estuarine material, flocculation, precipitation and the biological production of organic matter are the most important (Chester, 1990). Elements which increase in concentration in sediments post-deposition may be derived directly from the sea water, as well as through the remobilization and precipitation of elements derived from terrigenous inputs. These post-depositional authigenic processes may include the modification of pre-existing minerals; formation of new minerals such as sulfides; addition of elements through adsorption to minerals such as clays and iron hydroxides (such as phosphorus); the creation of redox boundaries; and the formation of anoxic sediments.

Anthropogenic inputs into coastal environments range from physical, biological and chemical additions and transformations and may be derived from both point and non-point sources. Anthropogenic influences may include, but are not limited to, the addition or removal of vegetation and sediments; inputs of material recreational impacts such as fishing and boating; addition of organic matter and nutrients; and, additions of organic and inorganic contaminants, heavy metals and nutrients from riverine flow, sewage, stormwater, urban, industrial, commercial and agricultural runoff. The movements of such additions into a coastal environment affect the sediment-composition significantly. Following the deposition and burial of sediments and their

associated contaminants in an estuarine environment, metals may be influenced by physical, chemical and biological processes which may cause mixing, remobilization and ultimately the reworking of the metals back into the water column. These processes may be natural, such as the presence of acid sulfate soils, mangroves, erosion and bioturbation, and/or anthropogenic such as dredging and clearing of land (Lee and Cundy, 2001).

The most common classifications of environmental impacts by anthropogenic activities may be made on the basis of the activity or source of the pollutant; the type of pollutant; and the classification and level of impact on the environment (Scoullus, 2003).

The major types of pollutants in sediments include nutrients (phosphorus and nitrogen), organics (oil and grease), halogenated hydrocarbons and persistent organics from pesticides (DDT and PCBs), polycyclic aromatic hydrocarbons (PAHS, petroleum products), tributyl tin (TBT), pharmaceutical drugs, radionuclides, chlorofluorocarbons (CFCs) and metals (Andrews *et al.*, 2004; EPA, 2010). Anthropogenic activities are particularly responsible for concentrations of metal contaminants entering estuarine systems. In estuarine environments, where the presence of carbonates buffers the pH, metals are likely to remain immobile in the sediments. These anthropogenic inputs are both adding exotic chemicals to the environment (as new substances synthesized and manufactured by industry), and changing natural cycles by the addition or subtraction of existing chemicals by normal cyclical and/or human induced effects (Andrews *et al.*, 2004).

Trace metal accumulation in estuarine sediments is a function of the physical and chemical conditions in the sediments such as particle size, organic matter content, salinity, pH and redox potential (Salomons and Förstner, 1984). The fixation of metals onto the sediments are not necessarily permanent, and can be remobilised into the water column as a result of changes occurring in the environment, such as variations in pH, redox potential, and the presence of organic chelators (Förstner, 1987).

According to Salomons and Förstner (1984), trace elements exist in the estuarine environment in a number of different geochemical forms:

1. *Oxidation type (iron- and manganese-oxides or native sulfur precipitated by oxidation of reducing solutions and usually caused by water emergence at the surface or a flow of reducing water out of a swamp);*
2. *Reducing type (U, V, Cu, Se and Ag precipitated as metals or lower-valency oxides by reducing of oxidizing waters and usually caused by an encounter with organic matter or a mixing with reducing water or gases);*
3. *Reducing sulfide type (Fe, Cu, Ag, Zn, Pb, Hg, Ni, Co, As and Mo are precipitated as sulfides by reduction of oxidizing waters, usually by the action of sulfate-reducing bacteria) (U, V and Se may also be precipitated and the causes are the same as for the reducing type, but they require the presence of dissolved sulfate)*
4. *Sulfate-carbonate type (Ba, Sr and Ca precipitated by increased sulfate or carbonate as a result of the mixing of waters, the oxidation of sulfide, or passage into carbonate rock);*
5. *Alkaline type (Ca, Mg, Sr, Mn, Fe, Cu, Zn, Pb, Cd and other elements precipitated by increased pH, usually caused by the interaction of acid waters with carbonates or silicate rocks, or its mixing with alkaline waters);*
6. *Adsorptive type (adsorption or coprecipitation of ions on accumulations of Fe-Mn-oxides, clays and organic materials) (the cations of transition metals and those with high valence tend to be more strongly adsorbed than anions and low valency cations).*

Metals are held in deposited sediments in a number of different sites. Firstly, metals are substituted in the mineral lattices (often referred to as the residual phase metals), which in uncontaminated sediments is the most important site quantitatively. Secondly, trace metals from both natural and anthropogenic sources are associated with particle surfaces; hence there is often a significant correlation between trace metal content and grain size or surface area, which is in turn related to sedimentary mineralogy. Metals in detrital minerals (such as feldspar and quartz) are incorporated within the crystalline

structure, usually in trace amounts. Metals can be incorporated in sediments via adsorption to carbonates, clays, hydrated oxides of Fe/Mn and humate; co-precipitation of Fe/Mn oxides; complexation by organic matter; and solid solution within the crystalline structure of minerals (Carman *et al.*, 2007).

The slight alkalinity changes from the freshwater to the saltwater environment results in the formation and precipitation of hydroxides, carbonates, sulfides and phosphates of metals (Förstner, 1979). Co-precipitation of Fe/Mn oxides, cation exchange, complexation by organic matter, and the incorporation of the metals within the crystalline structure of minerals (Förstner and Wittman, 1981; Salomons and Förstner, 1984) are also important pathways which create accumulations within the sediments, particularly in mud flat and mangrove environments (Lee and Cundy, 2001). Organic substances play an important role in the transfer of metals between dissolved and solid phases, especially through the process of flocculation (Förstner, 1979). Alternatively, desorption from particle surfaces, and the breakdown of organics, may result in the addition of metal components to the dissolved phase. Consequently, the sediment compartment represents the most concentrated physical pool of metals in aquatic environments, with more than 90% of the heavy metal load in aquatic systems being bound to suspended particulate matter and sediments (Rodríguez-Barroso, 2009).

Depending on the physico-chemical conditions (such as pH and O_2), sediments can act either as a pollutant sink or source, particularly when disturbance of the sediment causes a change in the sediments from anoxic to oxic conditions (Vdović *et al.*, 2006). The hydrous oxides of Al, Fe/Mn (especially redox-sensitive Fe/Mn hydroxides and oxides under oxidizing conditions) constitute significant sinks of heavy metals in the aquatic environment (Förstner, 1979). Oxygen deficiencies in the bottom sediments may lead to the dissolution of hydrous iron and manganese oxides and to a release of coprecipitated heavy metals (Förstner, 1979). Thus, accumulations of hydrous Fe/Mn oxides can act as a major heavy metal source. This change in the physico-chemical conditions also changes the behaviour of the metals (Åström, 1998; Standring *et al.*, 2002; Davranche *et al.*, 2003; Vdović *et al.*, 2006). For instance, contaminated sediments have the potential to release the metals into the overlying water, causing readsorption to other

sediments and/or organic fractions due to natural and anthropogenic processes such as bioturbation and dredging (Acevedo-Figueroa *et al.*, 2006). Dissolved organic matter may form complexes with metals and thus increase metal solubility, altering the distribution between oxidized and reduced forms of metals. This may influence the extent to which metals are adsorbed on suspended matter, and affect the stability of metal containing colloids (Singer, 1977).

Metal solubility can vary significantly with depth in the sediment profile as a result of historical changes and changing sediment geochemistry. The redox boundary in the sedimentary column is extremely important in terms of metal stability (Chester, 1990), as the redox conditions and the decay processes affecting the organic matter control the cycling of Fe and Mn, which in turn cause changes to concentrations and associations of heavy metals (Marchand *et al.*, 2006) (Figure 3.2). Oxidized conditions generally favour metal insolubility while reducing conditions favour metal solubility or mobility (Miao *et al.*, 2006). Many trace elements have multiple valence states, and under anoxic conditions the reduced forms are more readily complexed with organic acids, taken into solid solution by authigenic sulfides or precipitated as insoluble oxyhydroxides (Algeo and Maynard, 2004). Redox sensitive trace metals including Cu, Ni, Pb, Zn, Mo, Se, Cd, are among the most widely used indicators of redox conditions (Harrington *et al.*, 1998; Morford and Emerson, 1999; Miao *et al.*, 2006).

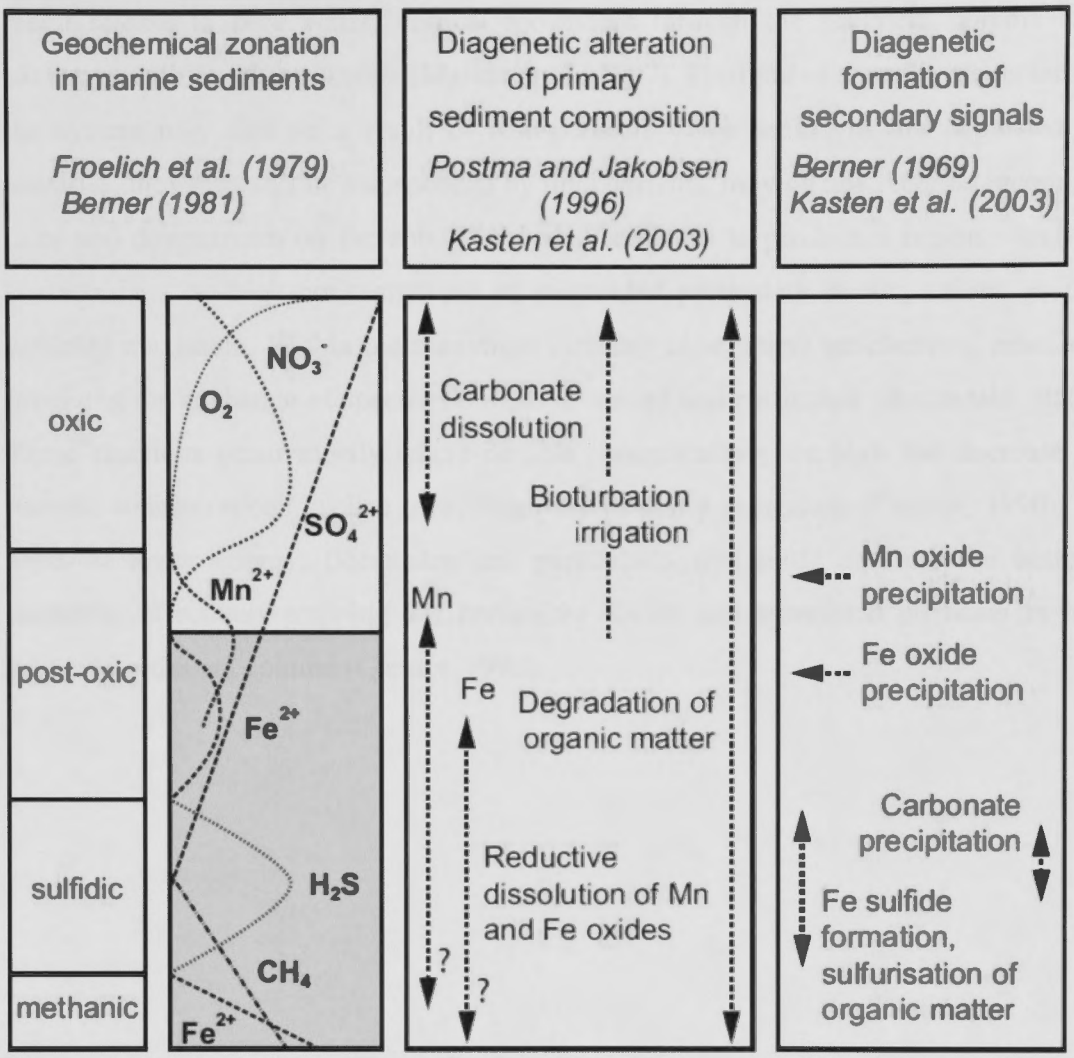

Figure 3.2: Schematic representation of geochemical zonation in marine sediments, diagenetic alteration and diagenetic formation (redrawn from van der Land *et al.* 2011, sourced from Kasten *et al.*, 2003).

Changes in pH, Eh, EC, organic matter content, or redox potential of the sediment and pore waters, instigated by natural or anthropogenic processes such as bioturbation and dredging, may also affect the remobilization of these metals (Acevedo-Figueroa *et al.*, 2006). The risk of disturbing acid sulfate soils (ASS) also has a high probability of metal remobilisation (Bierwirth and Brodie, 2005). Although these geochemical processes are subject to natural variability due to seasonal and tidal cycles, the addition of anthropogenic contaminant fluxes into the sediments is also likely to cause significant geochemical changes in the sediment and water column. This has the potential to remobilize previously immobile metals within the sediments. Post-depositional mobilization of some trace metals may occur in sediment, resulting in trace

metal release to pore water, vertical movement through the sediment column and exchange with overlying waters (Marins *et al.*, 1997). Flushing of these elements out of the system may also be a result of resuspension. Once sediments are deposited in estuaries, they may still be resuspended by tidal currents, moving upstream on incoming tides and downstream on the ebb. The overall effect is to produce a region which is characterized by high concentrations of suspended particulate matter, known as the turbidity maximum. Within the maximum turbidity zone, many geochemical reactions involving the exchange of species between dissolved and particulate phases take place. These reactions occur mostly where particle concentrations are high and decrease as particle concentrations decline away from the turbidity maximum (Chester, 1990). In areas of lower energy, flocculates and particulates will settle out into the bottom substrate, effectively trapping the particulate matter and associated elements in the estuarine sediment column (Chester, 1990).

Chapter Four: Sediments of Merimbula and Pambula Lakes, New South Wales, Australia

4.1. Introduction

The following chapter outlines the methodologies undertaken and includes a detailed description of the sediments collected and analysed from Merimbula and Pambula Lakes and their catchment. All data tables may be found in Appendix 2 as Tables A.1-A.10.

4.2. Methods

4.2.1. Field Methods

In order to define the geochemistry of the sediments of Merimbula Lake, Pambula Lake, Back Lagoon and their catchments, a range of marine and freshwater sediment samples were collected from the top 5cm of surface sediment as grab samples; and up to 1 metre depth by coring. A total of 17 freshwater sediment samples were collected from input creeks, dams, ponds and floodplains, while a total of 110 marine sediment samples were collected from the three estuary basins, mudflats, beaches and mangroves (Figure 4.1). In addition, gastropods and bivalves from the Front Lake at Merimbula were collected for analysis.

All surface sediment samples were collected using a plastic spade, then sealed in plastic bags and refrigerated until analysed. Marine surface sediment samples were collected at low tide from exposed sand and mud flats using a PVC scoop. In those parts of the estuary where sediments were not exposed by tidal changes, weighted PVC scoop

buckets were lowered from a boat, at various water depths to collect surface samples from the bottom of lakes and creeks. Samples were collected both adjacent to the small town centre of Merimbula, located near the entrance of the estuary, and elsewhere in the estuary that was not surrounded by urban development (Figure 4.1). pH, EC and Eh were measured in the field using an Orion Meter. Six cores were obtained from a number of exposed tidal flat locations within Merimbula Lake using a PVC corer.

4.2.2. Analytical methods - bulk geochemistry of sediment samples

Unless otherwise indicated, all analytical data was obtained using equipment at the Research School of Earth Sciences (RSES), at the Australian National University (ANU).

127 sediment and rock samples were crushed and milled to obtain the whole rock and trace element compositions. The samples were oven dried overnight at 40°C, crushed in a mortar and pestle, and then passed through a 500μm sieve. An aliquot of 2g was milled in a micronising mill with ethanol for 10 minutes, and then oven dried overnight at 40°C. Whole-rock major elements were analysed using a PW2400 wavelength-dispersive X-ray fluorescence (XRF) spectrometer, and whole-rock and individual mineral trace elements were analysed by laser ablation inductively-coupled plasma mass spectrometry (LA-ICP-MS) by the methods outlined by Spandler *et al.*, (2003) and Gingele *et al.*, (2007).

Major elements Na, Mg, Al, Si, P, S, K, Ca, Ti, Mn, Fe, F and Cl were determined by XRF with a Phillips (now PANalytical) PW2400 wavelength-dispersive X-ray fluorescence spectrometer. Lithium borate discs were prepared by fusion of 0.27g of dried sample powder and 1.72g of "12-22" eutectic lithium metaborate-lithium tetraborate at 1010 °C for 10 minutes in a rocker furnace. The major elements were calibrated against a set of 28 international standard rock powders. The lithium borate discs were then mounted in epoxy blocks and analysed for trace elements by LA-ICP-MS. These trace elements were determined on glasses made from rock powders fused with lithium borate flux (1: 3 mass ratio).

The LA ICP-MS employs an ArF^+ (193 nm) excimer laser and a Hewlett Packard Agilent 7500 ICP-MS. Laser sampling was performed in an Ar-He atmosphere using a spot size between 80 and 100 μm. The counting time was 20 seconds for the background and 60 seconds for sample analyses. The external standard for calibration was NIST 612 glass, using the standard reference values of Pearce *et al.*, (1997).

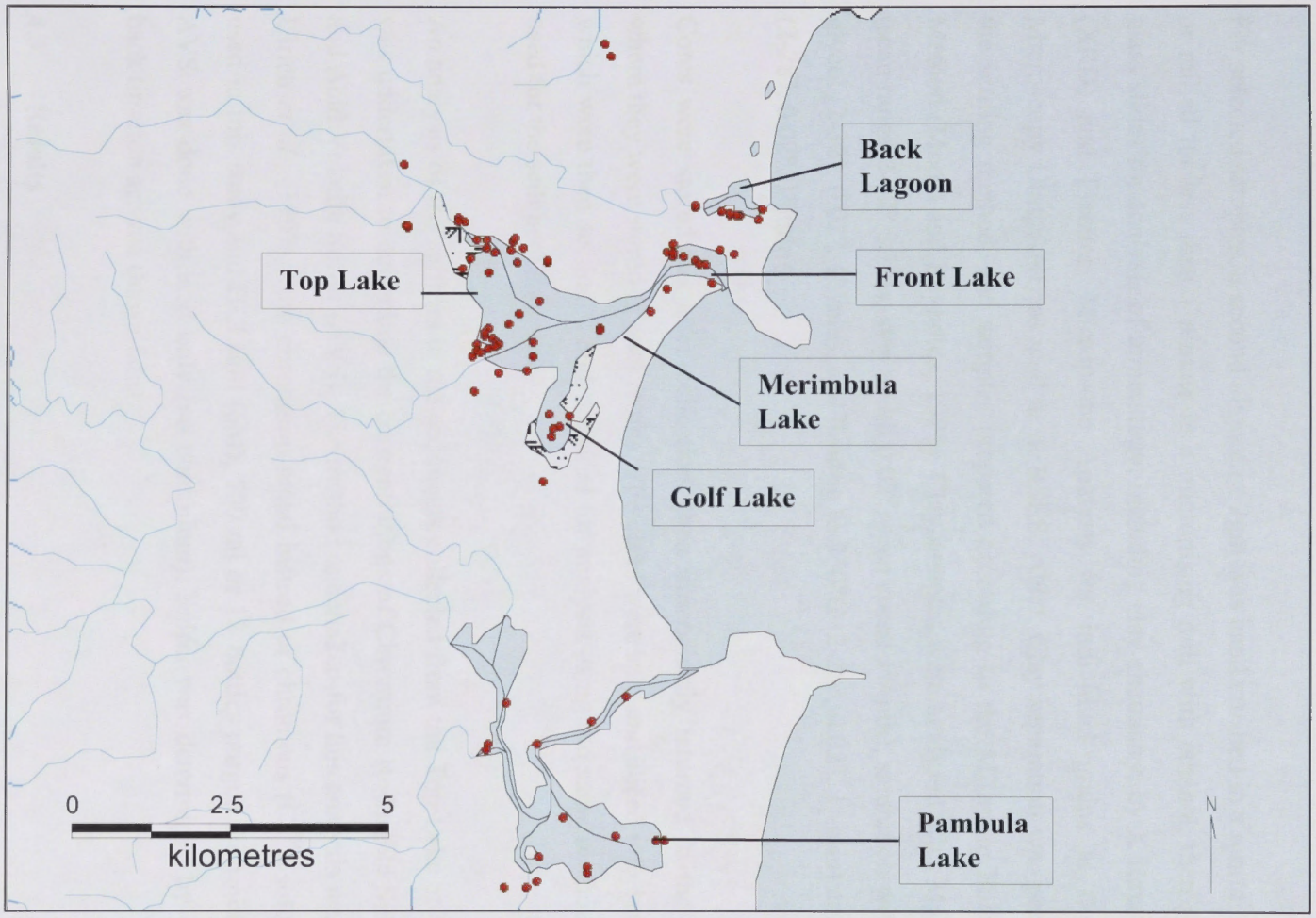

Figure 4.1: Location of surface sediment samples (for a more detailed map, see Appendix 1).

The NIST 612 glass was analysed every 10–15 samples to correct for instrument drift. Si was employed as the internal standard, employing the SiO_2 concentration previously measured by XRF (Eggins, 2003).

For selected samples, a second aliquot of 2gm was hand crushed in a mortar and pestle, or milled for less than 1 minute in a micronising mill with ethanol, then packed into glass slides for analysis of mineralogy, including clay chemistry, by X-Ray Diffraction (XRD) and Electron Microprobe Analysis for individual grains at the Electron Microscopy Unit, ANU as well as at RSES, ANU. Clay separation was performed by the settling method, and samples prepared according to the Millipore Filter Transfer Method (Moore and Reynolds, 1997). Clay samples were analysed after Mg-saturation (scan range 2-42° 2theta, step width 0.02°, scan speed 1°/min), saturation with ethylene glycol (2-32°, 0.02°, 1°/min), and heating to 350°C (2-28°, 0.02°, 1°/min) and to 550°C (2-28°, 0.02°, 1°/min).

Cores were stored flat after collection, then immediately returned to the laboratory where they were stored in cool rooms. The cores were split and sliced into 1cm aliquots, which were then sectioned and prepared for analysis using the same methodologies as used for the sediment samples.

An analysis of the sulfides in the sediments collected from the Top Lake at Merimbula was undertaken to determine the concentrations of Chromium Reducible Sulfur (CRS) and Acid Volatile Sulfur (AVS). The method undertaken for this analysis was based on Ulrich *et al.*, (1997), with chromium metal instead of chromous (Cr^{2+}) solution being used in this study and HCl acid (6M), 500 ml or 1L bottles purged with nitrogen. The AVS was done with acid only (no chromium). Sulfur was determined by iodometric back titration against thiosulfate.

4.3. Results

A total of 127 sediment and rock samples were collected from Merimbula Lake, Pambula Lake, Back Lagoon and a range of freshwater sites within the catchment and

analysed. This data has been readjusted to 100 wt% in order to avoid errors with unanalyzed H_2O^+, H_2O^- and organic matter in the samples.

The bulk rock geochemistry reports total iron as Fe_2O_3. This merely reflects the analytical method using XRF. The natural samples contain both ferrous and ferric iron, with the oxidised beach sands containing Fe^{3+} and the organic and sulfur-rich muds containing Fe^{2+}, but these have not been determined individually. Thus in all plots, iron is represented as Fe_2O_3, but this does not mean all iron is Fe_2O_3. The same applies for sulfur. Total sulfur is reported as an oxide (SO_3), however, in the samples sulfur is likely to be present in both oxidised and reduced forms (sulfate and sulfide).

4.3.1. Sediment description

The sediments present in Merimbula Lake, Pambula Lake and Back Lagoon represent a mixture of carbonate-quartz-rich beach sands grading landward into clay-rich (smectite, chlorite, illite, and kaolinite) and organic-rich, fine grained terrestrial sediments. Grain size of the sediments sampled ranged from <200μm to 2.00mm. The sediments present in the estuary are a representative mixture of terrestrial and marine inputs. Terrestrial sediments are transported down creeks into the estuarine environment, while beach sands grade from the ocean into the estuarine basins. As a result of the sources of sedimentary inputs, the greatest influence on the geochemistry of the sediments, post-deposition into the system, is the addition of elements (including calcium, iron, sodium and sulfur) directly from the seawater through authigenic and biogenic processes. The biological addition of shells to the sediments in the form of calcium carbonate greatly affects the bulk geochemistry of the sediments. The pH of the water in the estuary showed minimal variation (7.35 – 8.37) from brackish to saline water, where it is buffered by the presence of carbonate. Bioturbation and reworking of the sediments can cause isolated oxidation of the sediments, which may be observed in the precipitation of Fe-oxyhydroxides along worm burrows in the sediments.

The following lithological sediment types were collected, each providing information on the sedimentary end members for physical mixing within the estuary:

1. Clay/silt sampled from the freshwater creeks and rivers upstream of the estuaries;
2. Terrigenous sand/gravels of arkosic composition from the freshwater creeks and rivers and where they discharge into estuaries forming bay head deltas;
3. Mature beach sand;
4. Organic rich silt/clay.

Freshwater inputs

A number of freshwater sediment samples were obtained from creeks, dams and ponds throughout the catchment in order to determine baseline/background concentrations of selected elements to compare with saltwater samples. A rock sample was also taken from a Devonian Merimbula Formation red mudstone outcrop. Sediment samples were obtained from farmlands, creeks, dams, and areas cleared for residential development. The samples ranged from fine grained clays that had settled out from suspension, gravels, fluvial deposits, bed rock and organic rich sediments from collection dams. Grain size of the sediments ranged from <200μm to 4.0mm. The sandy-gravels are found deposited in the deltas at the input creeks, and also in Back Lagoon. These sediments are indicative samples of the weathered bedrock sourced from upstream in the catchment.

The terrigenous sands and gravels are poorly-sorted gravel-sand-clay mixtures, which are composed of a mixture of rounded to sub-rounded quartz and feldspar dominated grains. The organic-free silts and clays are sourced from the upland catchment, (which is small, extending only some 20 kilometres upstream in each case), and are principally transported into the estuary during high rainfall events, where they are deposited in the deeper basin of the top lake, trapped amongst mangrove roots and other aquatic vegetation, and in the input creeks. Once deposited in the estuary, post-depositional sulfur and organic material are added to the composition. These muds grade into clayey/silty-sands in the delta connecting the top lake to the front lake. The organic inputs are from degrading terrestrial and marine-sourced plant and animal material and nutrients such as phosphorus and nitrogen from sewage and agricultural inputs. The silts

and clays are very fine, organic-free sediments, which are composed of a mixture of the clays smectite, chlorite, illite, and kaolinite. The geochemistry of the sediment samples is outlined below and the data are located in Appendix 2 (Table A.1).

The freshwater sediment data may be used as baseline measurements of element concentrations of sediment samples *prior* to any post-depositional geochemical changes resulting from incorporation into the marine environment. This dataset has been used as a guide to pre-anthropogenic inputs.

Merimbula Lake – Front Lake

Mature carbonate-quartz beach sands form the back dunes and beaches and have been deposited in the Front Lake and channel at Merimbula, dominating the seaward side of the estuary. They are transported by wave and tidal movements landward, forming a prograding delta into the estuary as a tide dominated flat, connecting the Top Lake to the Front Lake. These medium to fine grained beach sands have little to no fines present and are mainly well rounded quartz grains together with minor carbonate shell fragments and accessory minerals. They are relatively well sorted, not including the addition of very large shell fragments. Coatings of iron oxyhydroxides and organic matter are responsible for some of the variation in colour of the individual sand grains, ranging from clear, to yellow to orange.

The Front Lake of Merimbula Lake estuary is strongly influenced by tidal energy. The landward progradation of the beach sand means it is the dominant sedimentary component in the central region of the Front Lake. The presence of seagrasses and mangroves in the Front Lake increase the fine-grained sediment trapping efficiency, concentrating the fine-grained sediments and organic-rich material in areas where seagrasses and mangroves dominate, or where water movement is restricted. Bioturbation then mixes this organic clay and silt through the sand. The sediments in the fast flowing deep channel that meanders through the Front Lake are primarily coarser sands. Carbonate-rich shells are abundant in the sediments both from naturally occurring gastropods and bivalves, and also from commercially introduced oyster racks. There are abundant oyster racks throughout the shallow water areas of Merimbula Lake.

Samples were taken from different points within the Front Lake to gauge the influence of storm-water outlets, oyster farming and proximity to the township. In addition, beach sand samples were taken from the near-by "pristine" Pambula River for comparison with the Merimbula sands. The geochemistry of the sediment samples is outlined below (see also Table A.2 in Appendix 2).

Merimbula Lake – Top Lake

The Top Lake has a prograding bay head delta with angular coarse sands and gravels, representing deposition of the coarser grained terrigenous material coming down catchment. However this component is minor compared to the organic-rich silts and clays, including a mixture of smectite, chlorite, illite, and kaolinite which are found in the deeper basin of the Top Lake, trapped amongst mangrove roots and other aquatic vegetation, and in the tidal reaches of the input creeks. These muds grade into clayey/silty-sands due to mixing with beach sands in the delta connecting the Top Lake to the Front Lake. The organic inputs are from degrading terrestrial and marine-sourced plant and animal material and nutrients such as phosphorus and nitrogen from sewage and agricultural inputs.

An analysis of the sulfides in the sediments collected from the Top Lake showed a higher concentration of CRS (0.586 weight % sulfur) than the AVS (0.0386 weight % sulfur). The AVS is present as FeS or monosulfide black ooze (metastable intermediates, greigite, mackinawaite, etc) as well as hydrogen sulfide, but not pyrite. The CRS is Total Reduced Inorganic Sulfur (TRIS), which includes pyrite and the AVS (CRS = AVS + Pyrite sulfur).

The geochemistry of the sediment samples is outlined in Appendix 2 (Table A.3).

Merimbula Lake – Golf Lake

Golf Lake is a small and extremely shallow basin connected to the main Top Lake on its southern side. It receives direct runoff from an adjacent golf course, which is irrigated with treated sewage waste water. Golf Lake can also directly receive overspills from the

sewage treatment plant during peak seasons, when the treatment plant experiences overloading problems. There are several oyster leases also present in this section of the lake. The sediments are dominated by beach sands; however, a shallow depth and a large covering of sea grasses also ensure high sediment trapping efficiency. The geochemistry of the sediment samples is given in Appendix 2 (Table A.4).

Back Lagoon

Back Lagoon is a separate system located north of Merimbula Township. The sedimentary inputs are nearly identical to that of Merimbula Lake; however the freshwater flow into Back Lagoon is supplied by a different source to that of the main lake. Merimbula Creek drains a catchment to the north of Merimbula Township. The lower reaches of the creek and the lagoon are situated at the base of a steep hill upon which a housing estate has been developed over the past decade. The lagoon has a large quantity of grasses and reeds, and, in contrast to Merimbula Lake, is only open to the ocean approximately twice a year on average. Consequently, the sediment trapping efficiency is high and the flushing rate is low. This sedimentary component, although separate from Merimbula Lake, gives valuable information on the regional pollutant fluxes into the aquatic system. As it is not flushed daily by tides, mangroves do not grow along its shoreline, nor do aquaculture infrastructure associated with oyster leases exist in the Lagoon. This may have implications for anthropogenic changes to sediment geochemistry compared to Merimbula and Pambula Lakes. The geochemistry of the sediment samples is given in Appendix 2, Table A.5.

Pambula Lake

Pambula Lake, to the south of Merimbula, is regarded by the national estuarine classification system, OzCoasts, as a pristine system, and is therefore an ideal comparison to Merimbula Lake. The Pambula River drains into Pambula Lake through a large floodplain immediately to the south of Pambula Township. Coarse grained arkosic sands and gravels are very prominent along the lower course of this river where tidal water daily submerges the sands. These flats are the same as the bay head delta found where creeks drain into Merimbula Lake, but on a much larger scale. The samples obtained from Pambula ranged from clean beach sands on the ocean side, to organic-

rich muds in the central basin and arkosic gravels further upstream. The geochemistry of the sediment samples is outlined in Appendix 2, Table A.6).

4.3.2. Sediment mineralogy and textures

In terms of the estuary sediment textures, there is a contrast in sediment maturity between the well rounded beach sands and the angular sands and gravels discharging from the mouths of the various freshwater creeks and rivers that deliver new detrital material down catchment (Figures 4.2 – 4.3)

Figure 4.2: Well rounded quartz sand from Merimbula Beach. Minor fragments of carbonate are seen amongst the variably coloured and iron stained quartz grains.

Figure 4.3: Poorly sorted angular to subrounded quartz and pink feldspar grains deposited from Millingandi Creek where it flows into Merimbula Lake.

In contrast, sediment from the deeper lake bottom at Merimbula consists of a mixture of these sources, together with fragmented biogenic carbonate and other organic matter (Figures 4.4 – 4.5)

Figure 4.4: Sediment from Merimbula Top Lake (sampled from deeper water below tidal range). Note the well rounded quartz grains of variable colour, together with fragments of various bivalves and gastropod shells.

Figure 4.5: Merimbula Top Lake bottom sediment revealing broken echinoid pieces as well as foraminifera shells and some angular quartz grains.

The quartz present in the beach sands and flood delta sands is noteworthy in its colour variations, even within the one sample (Figure 4.6). The yellow colour imparted to sand grains is due to a variable thickness of iron hydroxide coatings. Many grains lack these iron coatings, and the proportions of coated to uncoated grains imparts an overall variation to the beach sand pigmentation.

These sands are monotonous in appearance and colour as a function of depth within the aerated beach itself. In contrast the same sands tidally flushed within the prograding flood delta of the estuary show an abrupt colour change from cream yellow to dark grey at depth, indicating the biogenic reduction of sea water sulfate to sulfide (Figures 4.7 and 4.8).

Figure 4.6: Merimbula flood delta sands, Merimbula Front Lake.

Figure 4.7: Merimbula flood delta sand. The exposed sand is yellow, typical of the beaches, whereas at only 10-20 cm depth it abruptly changes to grey due to the effects of sulfate-reducing bacteria in the substrate.

Figure 4.8: Merimbula flood delta sands (under reducing conditions), Merimbula Front Lake.

Where worm holes were intersected in the darker layer, a distinct reddish, oxidised tube was apparent against the grey sand, demonstrating that the burrows enabled oxygenated water to circulate at depth and reverse the reduction. The grey colour could be lightened in a matter of hours by exposing the dark sand to air, or in minutes by placing the reduced grey sand in a weak nitric acid solution. The sand immediately effervesced with the release of copious quantities of pungent hydrogen sulfide gas. The reacted sand revealed once again the presence of a range of coloured quartz grains, some with yellow iron oxide coating, and others without (Figure 4.9). This indicates that burial and sulfate reduction did not remove the pre-existing iron oxide films into solution. The oxidised-reduced boundary moves with tides, and it is not unusual in many of these estuaries to observe a thin film of whitish-grey bacteria forming a distinct band on quartz sands where deeper channels have exposed this layer.

Figure 4.9: Grey sand that was treated with weak nitric acid and reverted to yellow sand, preserving the variable intensities of the surface sand yellow iron coatings.

Besides the dominant quartz, there are a number of accessory minerals that control much of the trace element composition of these materials. There are a number of resistate minerals present, typical of beach sands worldwide, as well as some reflecting a local source geology. The phases found in these sediments (besides quartz, and organic matter and extremely fine grained sulfide) are listed below (Table 4.1). Most of the detrital minerals are found in all sediment types, while others are so rare as to be insignificant in terms of bulk mineralogical and chemical compositions (Tables 4.2 and 4.3). For example a single grain of chrome spinel has been found, indicating the presence of an ultramafic rock in the catchment.

	Pambula River beach sand	Merimbula beach sand	Merimbula Top Lake	Boggy Creek	Bald Hills Creek	Back Lagoon
Al-P	Y					
Amphibole	Y		Y (Hbld)			
Andalusite	Y					
Apatite			Y			
Biotite	Y		Y (weathered)	Y		Y
Carbonate		Y	Y	Y	Y	
Chlorite				Y		Y
Cr-Spinel						Y
Clay	Y		Y		Y	
Corundum	Y					
Epidote	Y	Y	Y	Y	Y	Y
Fe-Al-P			Y			
Feldspar (Alkali)				Y		
Feldspar (Plagioclase)					Y	Y
Pseudorutile	Y					
Garnet		Y				
Hematite						
Ilmenite		Y	Y		Y	
Goethite	Y	Y	Y	Y	Y	Y
Goethite-Rutile Intergrowth	Y		Y	Y	Y	
Magnetite						
Monazite						Y
Quartz	Y	Y	Y	Y		
Rutile	Y	Y	Y	Y		Y
Rutile/ Quartz Intergrowth	Y	Y		Y		Y
Titanite	Y		Y			
Tourmaline	Y	Y	Y			
Zircon	Y	Y	Y	Y	Y	
Na-Zr-S				Y ?		
Fe-Al-Si-Mg-S-P					Y	
S-P-Clay						Y

Table 4.1: Presence (Y) of grains identified by electron microprobe analysis of the various mineral separates from each sediment type. Most grains are single-phase; some are intergrowths or aggregates. Mineral separates were polished in epoxy blocks prior to analysis. Goethite refers to presence of Fe-oxides with low totals by EPMA, not necessarily only goethite.

	Locality	SiO_2	TiO_2	Al_2O_3	Cr_2O_3	Fe_2O_3	FeO	MnO	MgO	CaO	Na_2O	K_2O	P_2O_5	SO_3	ZrO_2
Al-Phosphate	**1**	1.42	0	24.76	0	0	0.4	0	0.27	0.56	0	0	25.05	1.27	0
Al-Phosphate	**1**	0	0	24.15	0	0	0	0	0	0.46	0	0	25.8	0.85	0
Iron Hydroxide with P	**2**	3.46	0	3.6	0	72.91	0	0.32	0.56	0.12	0.46	0	0.49	0.45	0
AlSi-P-S	**3**	51.75	0	46.27	0	0	0.53	0	0.28	0	0	0	0.26	0.44	0
Monazite	**3**	0.58	0	0	0	0	0	0	0	0.6	0	0	26.29	0	0
Intergrowth with quartz	**5**	28.01	2.93	15.35	0	0	4.43	0	1.02	0.39	0.2	2.45	0	0.87	0
Intergrowth with quartz	**5**	56.26	0.59	12.5	0	0	4.07	0	0.98	0.35	0.18	1.74	0	0.81	0
Needle-like	**5**	27.51	0.42	14.08	0	0	5.81	0	1.06	0.7	0.17	1.36	0.3	1.47	0
Zircon	**2**	31.3	0	0	0	0	0	0	0	0	0	0	0	0	68.7
K-feldspar	**2**	64.25	0	17.94	0	0	0	0	0	0	0.31	15.28	0	0	0
Albite	**5**	65.91	0	19.22	0	0	0.11	0	0	0.61	9.71	0.15	0	0	0
Tourmaline	**1**	35.57	0.27	34.22	0	0	9.21	0.22	3.59	0.18	1.49	0	0	0	0
Epidote	**3**	37.26	0	21.85	0	0	13.86	0.25	0.24	22.36	0	0	0	0	0
Titanite	**3**	29.99	37.81	1.68	0	0	1.43	0	0	27.46	0	0	0	0	0
Weathered biotite	**3**	47.39	1.99	25.01	0.22	0	4.45	0	2.62	0	0.13	9.37	0	0	0
Amphibole	**3**	49.93	0.6	6.03	0	0	12.1	0.3	16.04	11.2	0.59	0.12	0	0	0
Pseudorutile	**1**	0	64.26	0.43	0	31.55		1.88	0.25	0.1	0.22	0	0.19	0	0

Table 4.2: Representative electron microprobe analyses of accessory minerals. Electron microprobe analyses of minerals found with estuary sediments. Iron sulfide was too fine grained for this analytical method but is detected by XRD. 1.Pambula River beach; 2. Merimbula Beach/Flood Delta; 3. Merimbula Top Lake; 4. Bald Hills Creek; 5. Boggy Creek. Electron microprobe data is reported as FeO. This has been converted to ferric iron in some cases in this table.

	Locality	Oxygens pfu	Si	Ti	Al	Cr	Fe^{3+}	Fe^{2+}	Mn	Mg	Ca	Na	K	P	S	Zr	Cation Total
Al-Phosphate	**1**	5	0.07	0	1.41	0	0	0.02	0	0.02	0.03	0	0	1.02	0.05	0	2.61
Al-Phosphate	**1**	5	0	0	1.43	0	0	0	0	0	0.02	0	0	1.1	0.03	0	2.58
Iron Hydroxide with P	**2**	3	0.1	0	0.13	0	1.66	0	0.01	0.03	0	0.03	0	0.01	0.01	0	1.98
AlSi-P-S	**3**	2	0.55	0	0.58	0	0	0	0	0	0	0	0	0	0	0	1.15
Monazite	**3**	2	0.02	0	0	0	0	0	0	0	0.02	0	0	0.77	0	0	0.82
Intergrowth with quartz	**5**	2	0.58	0.05	0.37	0	0	0.08	0	0.03	0.01	0.01	0.06	0	0.01	0	1.2
Intergrowth with quartz	**5**	2	0.78	0.01	0.2	0	0	0.05	0	0.02	0.01	0	0.03	0	0.01	0	1.11
Needle-like	**5**	2	0.59	0.01	0.36	0	0	0.1	0	0.03	0.02	0.01	0.04	0.01	0.02	0	1.19
Zircon	**2**	4	0.97	0	0	0	0	0	0	0	0	0	0	0	0	1.03	2
K-feldspar	**2**	8	3.02	0	0.99	0	0	0	0	0	0	0.03	0.92	0	0	0	4.96
Albite	**5**	8	3	0	1.03	0	0	0	0	0	0.03	0.86	0.01	0	0	0	4.92
Tourmaline	**1**	31	7.51	0.04	8.51	0	0	1.63	0.04	1.13	0.04	0.61	0	0	0	0	19.5
Epidote	**3**	12	3	0	2.07	0	0	0.93	0.02	0.03	1.93	0	0	0	0	0	7.97
Titanite	**3**	5	1	0.95	0.07	0	0	0.04	0	0	0.98	0	0	0	0	0	3.03
Weathered biotite	**3**	22	6.68	0.21	4.16	0.02	0	0.52	0	0.55	0	0.04	1.69	0	0	0	13.87
Amphibole	**3**	23	7.25	0.07	1.03	0	0	1.47	0.04	3.47	1.74	0.17	0.02	0	0	0	15.26
Pseudorutile	**1**	9	0	3.21	0.03	0	1.58	0	0.11	0.02	0.01	0.03	0	0.01	0	0	4.99

Table 4.3: Representative electron microprobe analyses of accessory minerals. Electron microprobe analyses of minerals found with estuary sediments. Iron sulfide was too fine grained for this analytical method but is detected by XRD. 1.Pambula river beach; 2. Merimbula Beach/Flood Delta; 3. Merimbula Top Lake; 4. Bald Hills Creek; 5. Boggy Creek. Electron microprobe data is reported as FeO. This has been converted to ferric iron in some cases in this table.

In terms of heavy minerals, andalusite is probably of local catchment origin, sourced from contact aureoles as well as regional metamorphic rocks of the Lachlan Fold Belt. Andalusite is the hardest of the three Al_2SiO_5 polymorphs which explains its selective preservation as a detrital mineral. Tourmaline, ilmenite and feldspar would be derived from the Lachlan Fold Belt granites although some ilmenite and feldspar could also be sourced more locally from the basalts of the Devonian Rift system metabasalts (Figure 2.5). It is noteworthy that no magnetite (or titanomagnetite) has been found in any of these estuary sediments. Many granites of the Lachlan Fold Belt contain magnetite instead of ilmenite, but it is thoroughly weathered to the usual hydrated iron oxides within the catchment weathering profile. This is also consistent with the concentration of ilmenite in contrast to magnetite in heavy mineral placer deposits.

Subangular to angular epidote is present in all the sediment types and locations within the estuaries (Figure 4.10). It is sourced locally within the catchment from the greenschist facies epidote metabasalts within the Devonian Rift system volcanics.

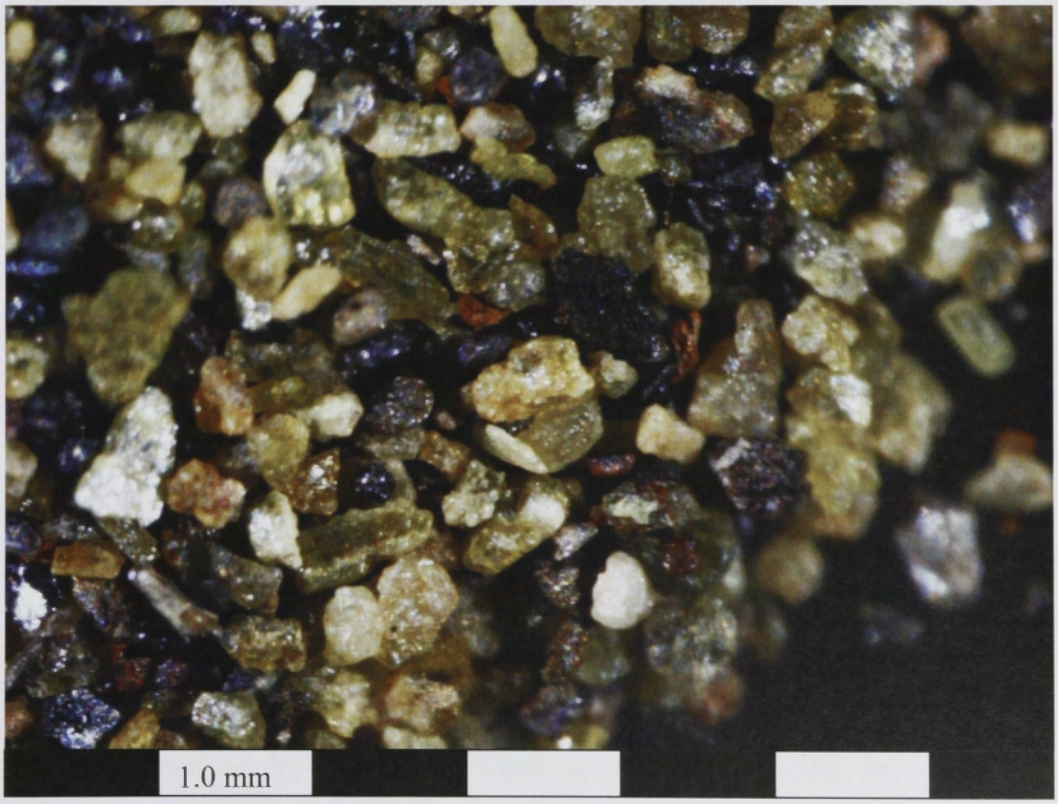

Figure 4.10: Angular green epidote together with black ilmenite

Also of local source are small lithic clasts of the Devonian Merimbula Group red bed mudstones (Figure 2.5). These are especially evident in the inlet creeks draining into Merimbula top lake (Figure 4.11).

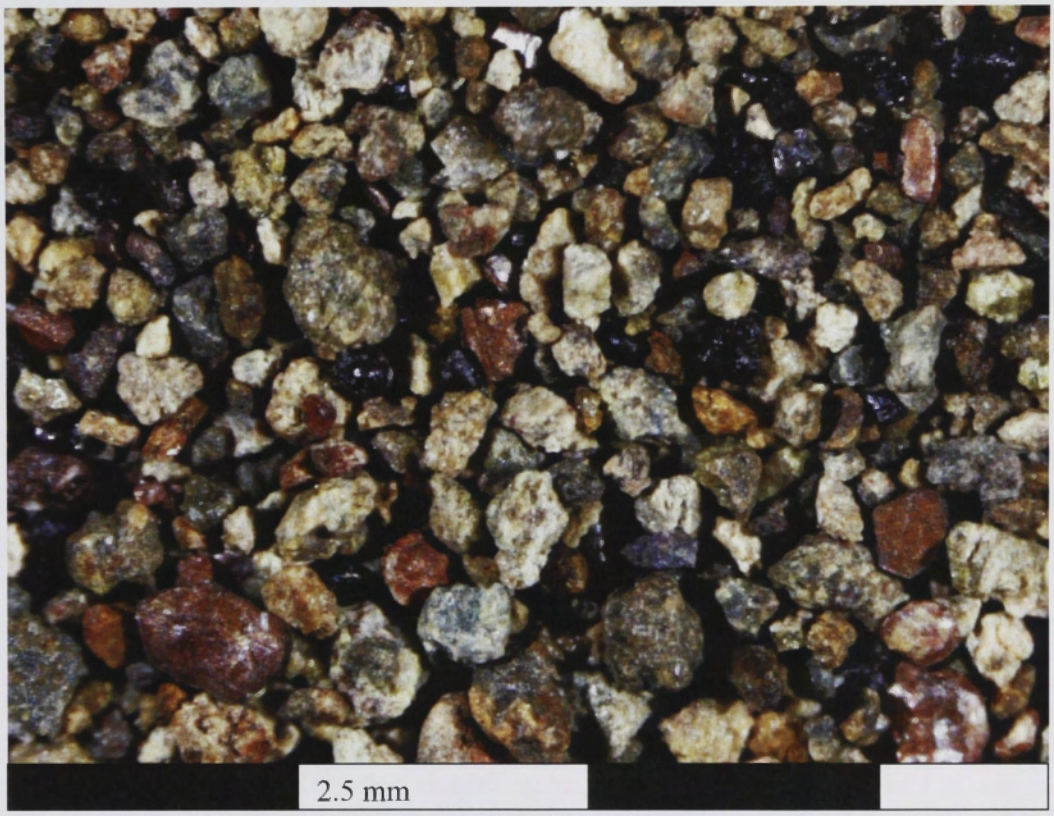

Figure 4.11: Millingandi Creek showing fine grained angular to rounded clasts of Devonian Merimbula Group red beds, together with rounded ilmenite, feldspar and quartz.

Zircon and quartz can be from a variety of sources, extending beyond the present catchment boundary. The incoming creeks contain detrital biotite which is highly weathered in terms of chemical composition where present within the lake proper. It is apparently absent from the beach sands and prograding flood delta. In some cases sulfur is detected in the analysis of the biotites, indicating reaction under reducing conditions to produce iron sulfide.

The rutile/anatase/leucoxene is of several origins. Individual rounded rutile grains of uniform appearance are most likely of detrital origin. Even though anatase is the most predominant TiO_2 phase produced by *in situ* catchment weathering and regolith

formation (Banfield *et al.*, 1993), post-depositional weathering within the estuary has altered some of the detrital ilmenite to secondary minerals such as limonite, pseudorutile and anatase intergrowths. There are round grains that consist of quartz-anatase intergrowths and also of limonite (*senso lato*)-anatase intergrowths together with pseudorutile. Pseudorutile is a common, hydrated intermediate in the alteration of ilmenite to rutile/anatase and is a common alteration product, for example in heavy mineral deposits of the Murray Basin (Grey *et al.*, 1999; Pownceby, 2010).

According to Grey and Reid (1975) pseudorutile is a distinct intermediate alteration product of ilmenite in which all the iron has been oxidized to the trivalent state and one-third of it has been leached out, to give the stoichiometry $Fe_2Ti_3O_9$ (Gupta *et al.*, 1991). Grey and Reid (1975) also note that pseudorutile stoichiometry corresponds to the maximum removal of iron from the ilmenite structure without concomitant removal of oxygen:

$$3Fe^{2+}TiO_3 + O_2 + 2H^+ \rightarrow Fe_2^{3+}Ti_3O_9 + Fe^{2+}{}_{(aq)} + H_2O$$

These authors state further removal of iron by leaching to eventually produce rutile must involve removal of oxygen, according to:

$$Fe_2^{3+}Ti_3O_9 \rightarrow 3TiO_2 + 2Fe^{3+} + 3O^{2\square}(Fe_2O_3)$$

The assumption is that Ti is perfectly immobile. The Ti:O ratio is 1:3 in both ilmenite and pseudorutile, but it must come down to 1:2 for rutile, so either Ti adds (which is unlikely) or O leaves.

In many cases it was impossible to get a pure rutile analysis, and leucoxene should perhaps be used to describe the inhomogeneous, cryptocrystalline, high TiO_2 products of ilmenite alteration following the nomenclature of Temple (1966) and Frost *et al.*, (1983) (Pownceby, 2010).

The presence of unaltered ilmenite together with the above pseudomorphs reflects the mixing of material sourced from different depositional environments, and subsequent sedimentation, in which fresh, unaltered detrital grains are continually brought into the estuary. In contrast, detrital magnetite is absent from these sediments, even though it is present in many granites from the catchment. This reflects the relative ease with which it is converted to secondary hydrated iron oxides during in situ weathering within the catchment.

There are also rounded grains that consist of intergrowths of quartz-anatase in the estuary sediments. These are interpreted here as post depositional pseudomorphs after detrital titanite within the estuary as they pseudomorph individual rounded detrital grains:

$$CaTiSiO_5 + 2H^+ = Ca^{2+} + TiO_2 + SiO_2 + H_2O$$

$$4FeTiO_3 + O_2 + 6H_2O = 4FeOOH + 4TiO_2 + 8H^+$$

(Fitzsimons, 2003).

Very rare apatite has been found in these estuary sediments. It is known to be susceptible to chemical breakdown during weathering of granite at source (Banfield, 1985). Electron microprobe data detected phosphorus as an authigenic/biogenic component adsorbed to the secondary iron hydroxides. Thus the secondary iron hydroxides and Fe-Al phases contain detectable phosphorus (Tables 4.1 – 4.2). It is well known that such phases act as local sinks for P precipitated out of solution.

4.3.3. Heavy mineral fraction

The mineralogy of a variety of coastal sediments in south-eastern Australia has been determined by XRD and electron microprobe analysis (quantitative and semiquantitative analysis). The accessory minerals present in sediments dominated by either quartz or clay were processed for heavy mineral separation at RSES by Mr Shane

Paxton. The heavy mineral fractions were initially separated on the basis of density in order to concentrate various accessory minerals and are labelled as follows in the tables of data:

2.96 H = Fraction of minerals that sank in a heavy liquid of Tetrabromoethane (TBE) with a density of 2.96 gm/cm^3.

2.96H 3.3L = Fraction of minerals that sank in a heavy liquid with a density of 2.96 gm/cm^3 but floated in the TBE liquid with a density of 3.3 gm/cm^3.

3.3H = Fraction of minerals that sank in a heavy liquid of Methylene Iodide (MI) with a density of 3.3 gm/cm^3.

Further separation of each density grouping of minerals was then based on magnetic separation, using a Chas W Cook Isodynamic separator, namely:

M1A = Fraction was magnetic at 1 amp setting
NM 1A= Fraction was non-magnetic at 1 amp setting

For example, the following labelling is explained:

2.96 H 3.3L NM1A = Non magnetic fraction of the minerals whose densities lie between 2.96 and 3.3 gm/cm3.

3.3H = Heavy minerals whose densities were greater than 3.3 gm/cm^3, but which were not further separated on the basis of magnetic properties.

Sands and the separated fractions were examined with a binocular microscope and digitally photographed, using a Nikon SMZ1500 (0.75 - 11.25 zoom and 10 × 20 eyepieces). Digital images were obtained with an attached Nikon Digital Sight DS-U1 and the software programACT-2U version 1.60.134.386.

Epoxy grain mounts of the various separates were then prepared as polished blocks in order to obtain quantitative and semiquantitative compositional data for the minerals. These mounts were examined in a JEOL 6400 scanning electron microscope, equipped with an Oxford Instruments light element dispersive spectrometer (EDS) detector and Link ISIS analytical software (Nguyen, 2007). Operating conditions for the energy-dispersive X-ray analyses (EDXA) were 15 kV accelerating voltage, 1 nA beam current, and a range of beam diameters (higher current, focused beam for garnet; lower current, beam defocused to 5 μm for micas and plagioclase). Natural mineral standards and the ZAF matrix correction routine were used (Whitney and Bozkurt, 2002). The following standards were used: sanidine for Si and K; albite for Na and Al; diopside for Ca, TiO_2 and pure Ti for Ti; Fe_2O_3 for Fe; Cr_2O_3 for Cr; MgO for Mg; pure Mn for Mn; pure apatite for P; zircon for Zr and Hf; calcite for Ca; and pyrite for S. All samples were polished with 1 μm diamond paste and carbon-coated to approximately 20 nm thickness. In addition to spot analyses, the SEM was used to construct X-ray maps for Fe, Mg, Ca, and either Al or Si by using a beam current of 100 nA, 50 ms dwell time, and 5–9 mm scanned area. These maps facilitated the identification of minerals in backscattered electron images, and the location of uncommon accessory minerals. SEM analyses and carbon coating were carried out at the Electron Microscopy Unit, RSBS, at the ANU.

The various estuary sediments contain the following groups of minerals -

- physically rounded to angular and abraded detrital minerals that have largely preserved their chemical compositions since being derived from their source.
- detrital iron- and iron-titanium oxides that have undergone weathering and hydrolysis
- those minerals that have either precipitated directly within the estuarine environment (e.g. carbonate, iron hydroxides) or have been modified post deposition in this environment.

A study of the processes and products of weathering within the catchment is beyond the scope of this thesis, but can be found in Hough (1983) for the Eden area and Banfield (1985) for further inland in the Lachlan Fold Belt granites. Hough (1983) studied the

weathering of a variety of igneous and sedimentary rock types in the Eden area. In the granites and rhyolites he found that the order of persistence of the dominant minerals was quartz > alkali feldspar >> plagioclase feldspar. Apatite was intermediate between the alkali feldspar and plagioclase feldspar, and zircon was more persistent than quartz. This is consistent with the rarity of detrital plagioclase compared to alkali feldspar in the Merimbula and Pambula estuaries. The clay mineral assemblages of the clay size fractions in the Eden area catchment are dominated by kaolinite, illite and dioctahedral vermiculite. Hough (1983) found the relative proportion is dependent on the degree of weathering of the regolith and its parent rock. With increasing weathering the tendency is to form kaolinite. The Ordovician and Silurian flysch sequences with the catchment are consistent with original detrital mineralogy consisting dominantly of illite and quartz (Wyborn and Chappell, 1983).

4.4. Depth profile variations

Six sediment cores were obtained from Merimbula Lake estuary; four from the Front Lake and two from the Top Lake (Figure 4.12). The sampling of sediments with increasing depth provided information on the change in concentration of elements with depth and with changing geochemical conditions. Obtaining data pertaining to both spatial and depth profiles allows a comprehensive analysis of the sedimentary composition of the estuary. The information obtained from the core samples also provided baseline data with respect to the concentrations of metals and other elements pre-settlement of the region. The baseline data from the cores could then be compared to the baseline data obtained from freshwater sediments from within the catchment.

The cores were sectioned into 1cm slices, then analysed. The slices which were selected for analysis were based upon obvious compositional changes, such as colour variation, additions of shelly or organic layers, and grain-size variations. Descriptions of the cores are given below.

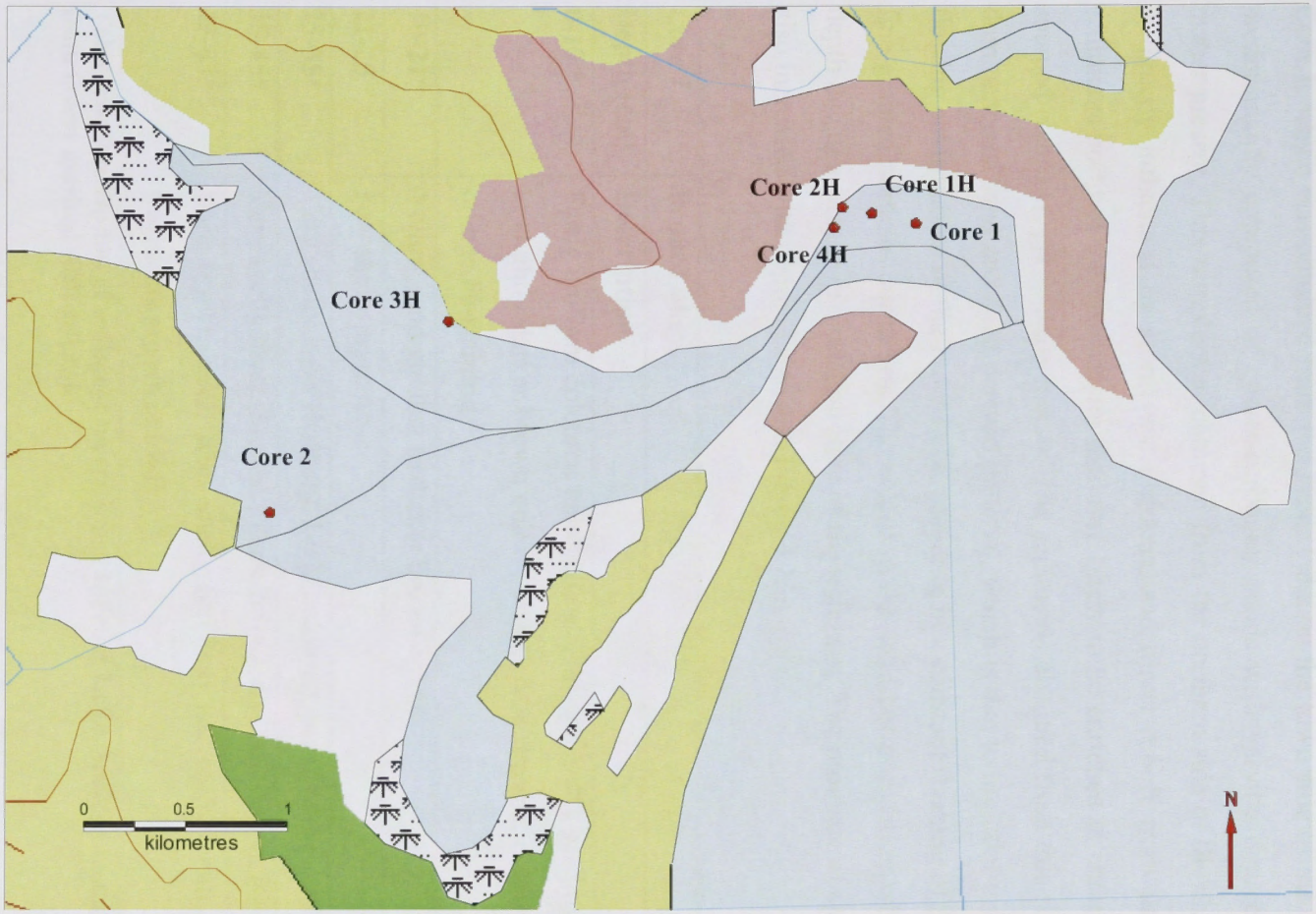

Figure 4.12: Location of cores in Merimbula Lake.

4.4.1. Depth profile variations - Core 1

Core 1, which was obtained from the Front Lake on the town side of the channel, was predominantly composed of quartz-carbonate sands with varying degrees of organic matter present. This sample was obtained from the northern side of the channel, which is directly influenced by storm water drains, and direct runoff from the town. The sediments north of the channel are therefore likely to be enriched in anthropogenically sourced elements, particularly metals. The sediments obtained from this core showed a dominance of sand and shell derived material, which is due to the tidal-influenced, fast flowing environment of the Front Lake, resulting in a constant flushing of the water and fine-grained particles out to sea. The colour of the sand became darker with increasing depth due to a change in oxidation state of the sediment. The presence of shelly material also increased with depth (Table 4.4; Figure 4.13).

Core 1	**Front Lake**
Depth (cm)	**Description**
0-10 *	Fairly uniform coloured pale yellow sand, gradually grading downwards to slightly darker brown colour. Worm tube present, coloured by bright orange Fe-staining
10-21*	Yellow sand grading to darker brown colour
21-25	Few shells present
25-35*	Very shelly layer (broken). Light coloured, pale yellow sand
35-45*	Very shelly layer (broken). Dark coloured yellow-brown sand
45-63*	Dark brown sand, with shells (broken) decreasing with depth. Shell fragments are white (old)

Table 4.4: Description of sediment layers, Core 1, Front Lake. Sediment samples analysed from layers marked with asterisk.

4.4.2. Depth profile variations - Core 2

Core 2 was obtained from the edge of Top Lake within an area of thick mangrove growth. These sediments are representative of an environment which undergoes less water movement and less flushing than the front lake; higher levels of organic matter;

and, higher concentrations of fine-grained sediments. The sediment core was predominantly composed of an organic rich muddy-sand on the surface, grading down to a dense, clay-rich sequence. Shell remnants were observed only in the top 40cm of the core (Table 4.5; Figure 4.13).

Core 2	**Top Lake**
Depth (cm)	**Description**
0-8*	Muddy/sandy layer with a large component of organic material
8-19	Sandy/gravelly layer
19-34	Large shells grading into finer broken shell layer. Dark brown muddy/sandy matrix
34-39	Muddy/sandy, very dark brown layer
39-50*	Clay layer, becoming lighter with depth (black-brown - yellow-brown)
50-68*	Clay layer with yellow, orange, red and grey mottles

Table 4.5: Description of sediment layers, Core 2, Top Lake. Sediment samples analysed from layers marked with asterisk.

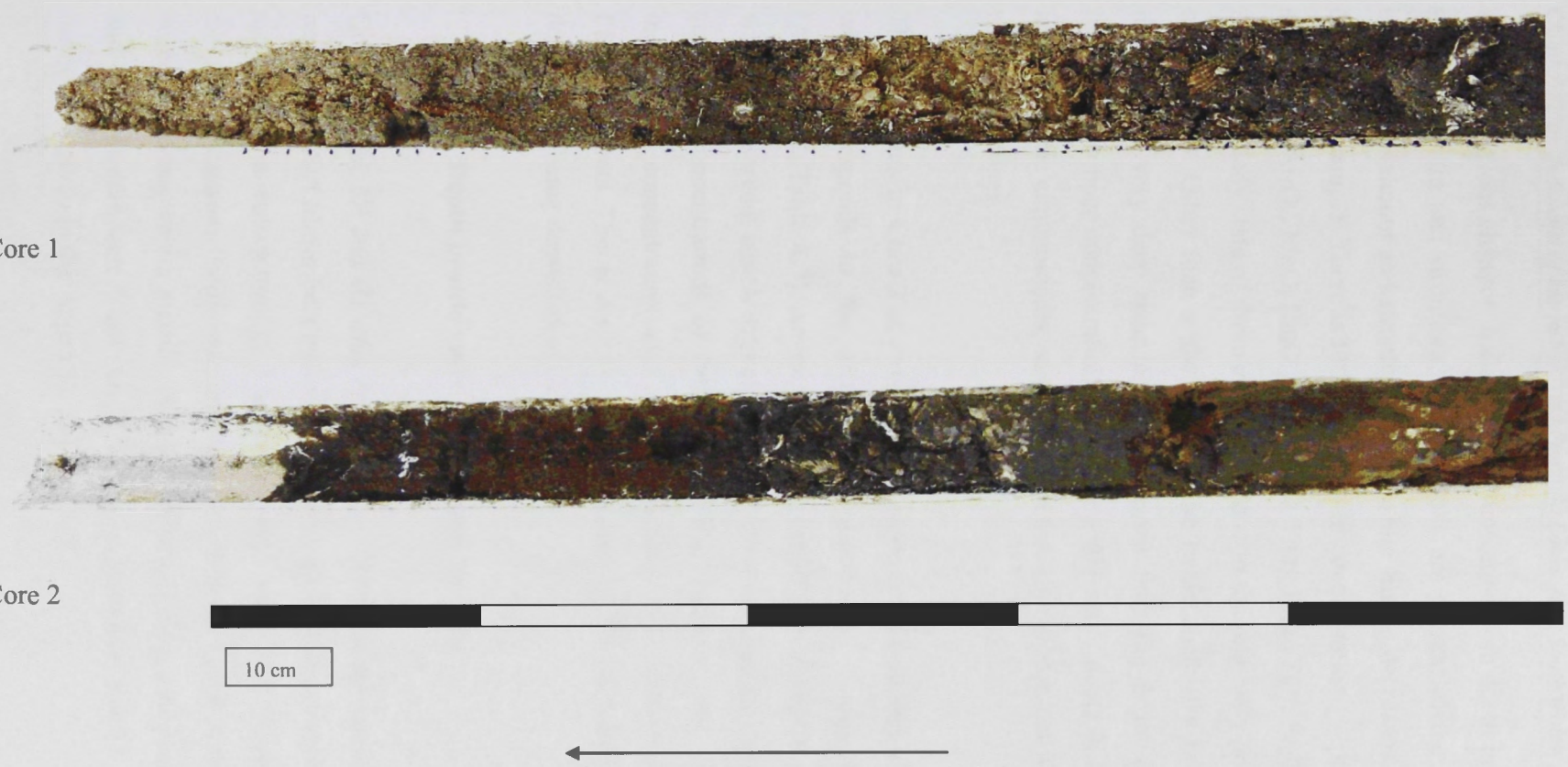

Figure 4.13: Images showing sediment layers present in Cores 1 and 2. The arrow points upwards, to the surface of the cores.

The most obvious changes in elemental composition with depth in the sediment involve silicon, calcium and strontium. Where shells are present in the sediment core, sharp increases of calcium and strontium occur, while silicon decreases as a result of dilution of the total sample. There is little variation in concentration (<1ppm) with depth in the sediment of Al_2O_3, MgO, MnO, Na_2O, K_2O, TiO_2, P_2O_5, SO_3, Fe_2O_3 (Appendix 2, Table A.7). The steady state of these elements is due to the relatively homogenous carbonate-quartz sands. Other than a shelly layer, the oxide chemistry is relatively consistent, indicating a very deep reducing zone (deeper than the depth of the core). A large increase in copper concentration within the sediment at depth is likely to be from past anthropogenic contaminants, such as the use of copper-rich antifouling paints used for boating purposes.

The sediments in Core 2 showed a slight increase of iron and aluminium with depth, which corresponds to the increasing concentration of clay minerals with depth (Appendix 2, Table A.7). An increase in concentrations of Cr, Cu, Ni and Zn with depth was also observed, which is likely to be directly related to the change in sediment-grain size. The concentrations of the REE behave conservatively with one another, and increased in concentration with depth. This behaviour is converse to that of the Front Lake sediments. This is due to an increased load of detrital heavy minerals transported down creek being deposited in the Top Lake.

4.4.3. Depth profile variations – Cores 1H – 4H

Cores 1H, 2H, 3H and 4H were collected from characteristic sites within the Front Lake and Top lake of Merimbula estuary. In general, all four cored sediment samples showed similarities in sedimentology and mineralogy, with little physical or mineralogical differences between them other than in isolated layers (Table 4.6; Figure 4.14). All the cored sediments were a mixture of reworked beach sand, terrestrial clay, organic matter and biogenic carbonate fragments (bivalve and gastropod shells). The geochemistry of the cores is given in the Appendix 2, Table A.8.

Core 1H	**Front Lake**
Depth (cm) from surface	**Description**
0-14	The upper section of the core consists of a strongly defined, moderately coarse sandy layer with broken bivalve shells.
14-36	Mottled organic/sandy layer. Higher concentration of organic matter, however the overall composition is still moderately coarse sand.
36-52	Whole shells, greater concentration of organic matter, with the presence of rootlets and decomposing organic matter. Dominant material moderately coarse sand.
52-75	With depth, the core becomes sandier, with less organic material.
Core 2H	**Front Lake**
0-13	Moderately coarse sandy layer.
13-20	Layer of whole bivalves.
20-34	Darker organic layer, with fine roots present.
34-39	Small gastropods, slightly finer material, lighter in colour.
39-75	Gradational mixture between moderately coarse sand material and organic material with reworked shelly fragments.
Core 3H	**Top Lake**
0-16	Clear coarse sandy layer on top 16cm.
16-75	Increasing organic matter with depth. Sediment grain size consistent. No shells present.
Core 4H	**Front Lake**
0-15	Pale moderately coarse sand
15-29	Increased concentration of organic material, fine broken shelly material.
29-46	Sand becoming darker with increased concentrations of organic matter, greater abundance of broken shells present, with some whole bivalve and gastropod shells also present.
46-56	Large pieces of decaying organic matter present, darker, finer sediment, no shells present.
56-75	Slightly sandier, paler colour suggests less organic material present, single shells with no reworking.

Table 4.6: Description of sediment layers, Cores 1H, 2H, 3H and 4H.

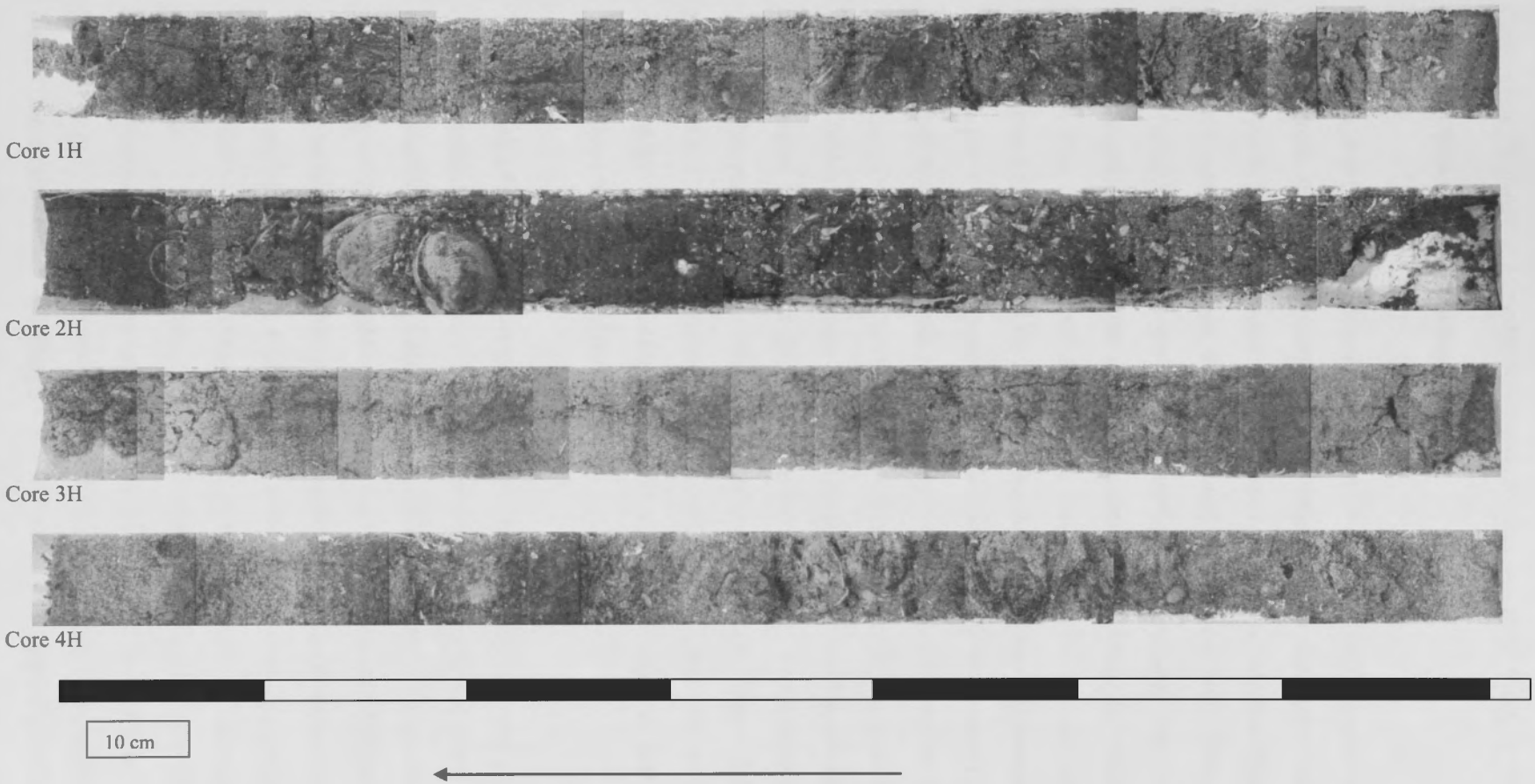

Figure 4.14: Images showing sediment layers present in Cores 1H, 2H, 3H, 4H. The arrow points upwards, to the surface of the cores.

4.5. Carbonate shell geochemistry

In order to determine the biogenic addition of elements to the sediments, the shells of eight different species of gastropods and bivalves from the Front Lake at Merimbula were analysed. These included bivalves (surf clam, *Dosinia caerulea*; Sydney Rock Oyster, *Saccostrea glomerata*; ark shell, *Anadara granosa*; pipi, *Plebidonax deltoides*; mussel, *Mytilus edulis*) and gastropods (families *Turrutellidae* and *Batillariidae*). The shells were collected from the surface sediment and from rocky outcrops. At time of collection, only the gastropod shells were alive. These were sectioned, embedded in resin, polished and analysed by LA-ICPMS. A 137-micron spot size and a scan rate of 25 micron per second were used to traverse across the growth zones of each shell. This data was averaged to get a bulk composition of each shell per traverse. Where more than one traverse of a shell was performed, the data is presented in separate tables. In the following tables and discussion, the trace element concentrations are given on a volotile free readjusted basis so that data can later be compared with sediment geochemistry, which is also presented on a volatile free total of 100 wt.%. Pure calcite has 56.03 wt. percent CaO, 43.97 wt. percent CO_2, readjusted to a CO_2 free 100 wt. % CaO value by multiplying by 1.785.This factor is applied to each trace element concentration below. Three bivalves were analysed by XRD.

The ark shell (*Anadara granosa)*, oyster (*Saccostrea glomerata)* and mussel (*Mytilus edulis*) consisted of aragonite, calcite and calcite-aragonite respectively. A list of the minerals associated with the Calcite Group and the Aragonite Group is listed below (Table 4.7). Overall these eight species had low concentrations of magnesium carbonates as expected for primary aragonite (Figure 4.15). The exception was the Sydney Rock Oyster (Figure 4.15) which contained 8879 ppm Mg. All other shells had less than 1200 ppm Mg. The trigonal calcite structure is able to incorporate more magnesium in its structure than the orthorhombic aragonite, therefore this difference was to be expected. The substitution of trace elements for the major cation Ca in carbonates is strongly influenced by the $CaCO_3$ polymorph. As noted by Viezer (1983, Fig. 1), the larger cell of the orthorhombic aragonite preferentially incorporates cations larger than Ca with an ionic radius larger than Ca (0.99A) such as Sr, Pb, Ba, U,

whereas the smaller rhombohedral cell of calcite favours incorporation of cations with a smaller ionic radii than calcium (eg. Mg, Fe, Zn, Cu, Cd).

Calcite Group (Trigonal)	**Aragonite Group (Orthorhombic)**
Calcite $CaCO_3$	Aragonite $CaCO_3$
Magnesite $MgCO_3$	Witherite $BaCO_3$
Siderite $FeCO_3$	Strontianite $SrCO_3$
Rhodochrosite $MnCO_3$	Cerussite $PbCO_3$
Sphaerocobaltite $CoCO_3$	
Smithsonite $ZnCO_3$	
Otavite $CdCO_3$	
Gaspeite (Ni, Mg, Fe)CO_3	

Table 4.7: Significant orthorhombic and trigonal calcium carbonate groups.

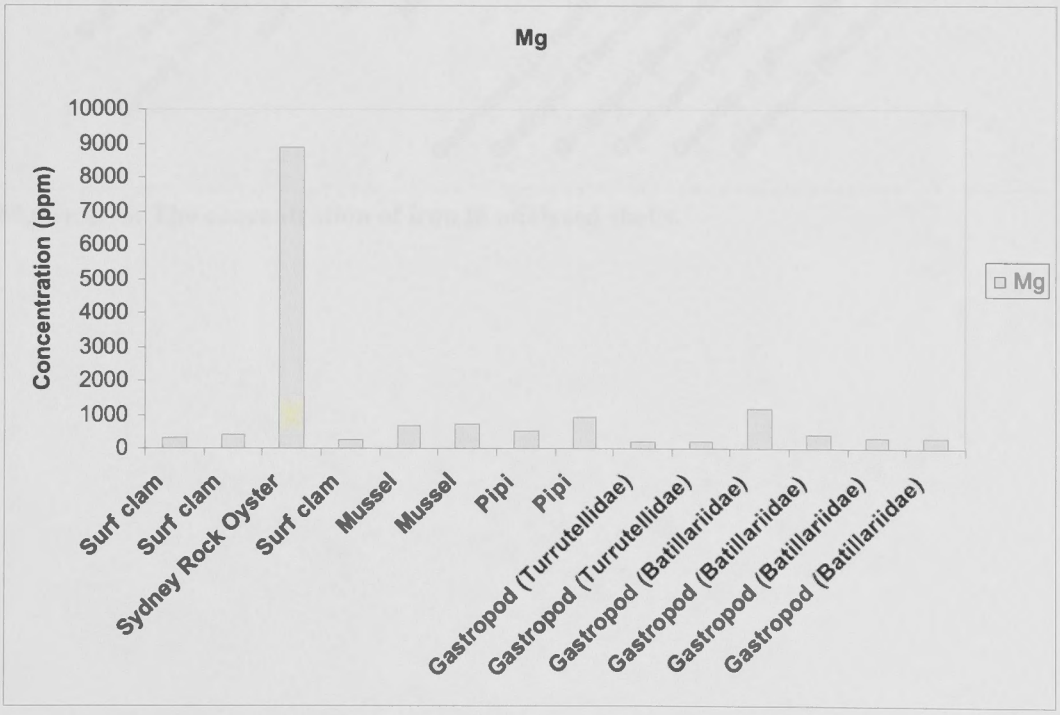

Figure 4.15: The concentration of magnesium in analysed shells (volatile-free basis).

Compared to magnesium, iron showed an order of magnitude lower concentration in these shells but largely followed magnesium. The oyster and gastropod (*Batillariidae)*

were notable in their higher concentrations compared to all other bivalves and gastropods (Figure 4.16). Manganese was also higher in the oyster and the gastropod (*Batillariidae)*, but overall iron and manganese were found at concentrations less than 50 and 2 ppm respectively, for the rest of the shells (Figure 4.17).

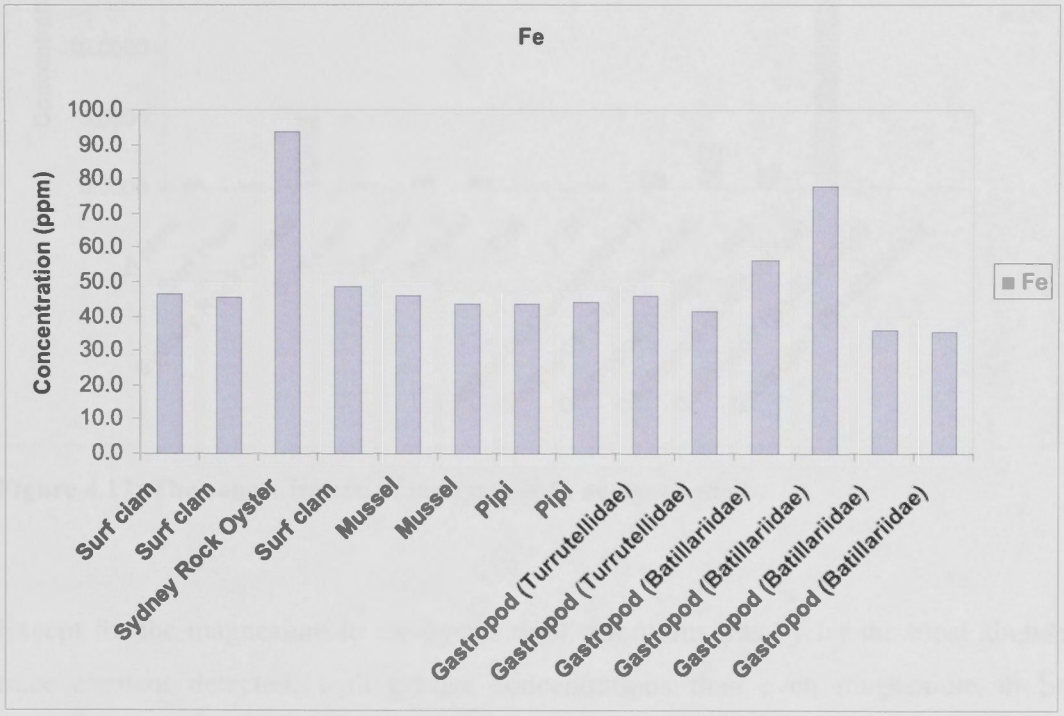

Figure 4.16: The concentration of iron in analysed shells.

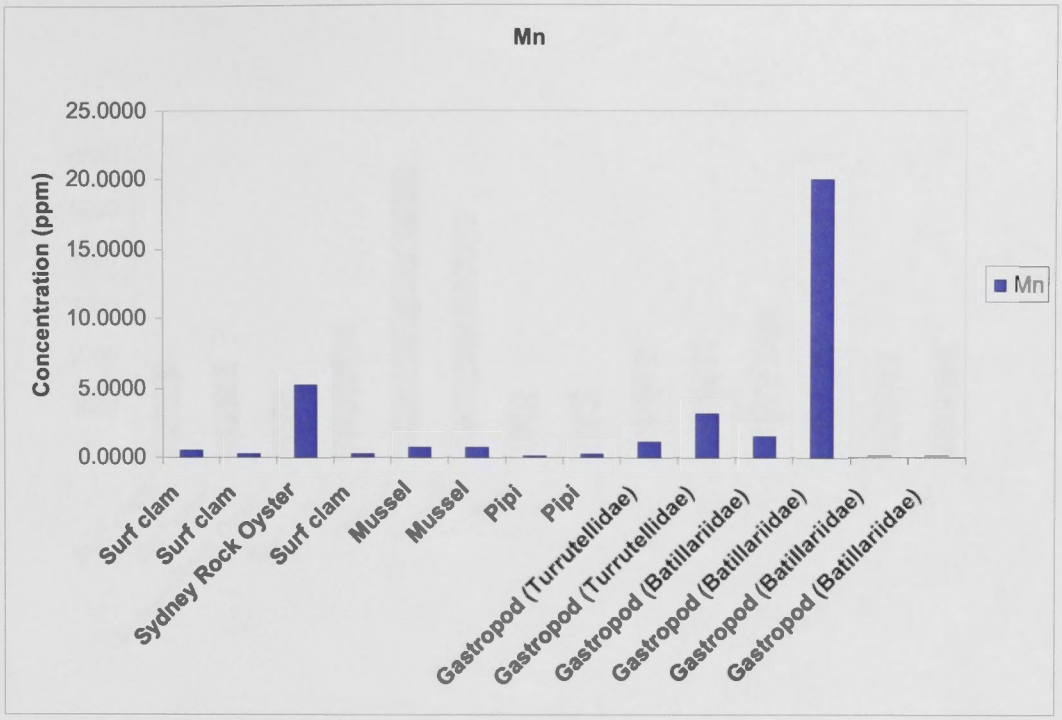

Figure 4.17: The concentration of manganese in analysed shells.

Except for the magnesium in the oyster shell, strontium was by far the most abundant trace element detected, with greater concentrations than even magnesium in both gastropods and bivalves (Figure 4.18). This was consistent with the crystal chemical substitutions in orthorhombic aragonite compared to trigonal calcite. An average of all gastropod data gave 2386 ppm strontium, whereas the bivalves (excluding the mussel) gave 1745 ppm strontium. The mussel is an exception, which averages strontium concentrations of 4843 and 5834 ppm over two separate laser scans. The mussel data was excluded from these averages as it was extremely limited in distribution and abundance within the studied estuaries. In contrast, the significant mussel aquaculture at Twofold Bay, Eden, would be expected to add significant biogenic accumulation of strontium in the underlying sediments.

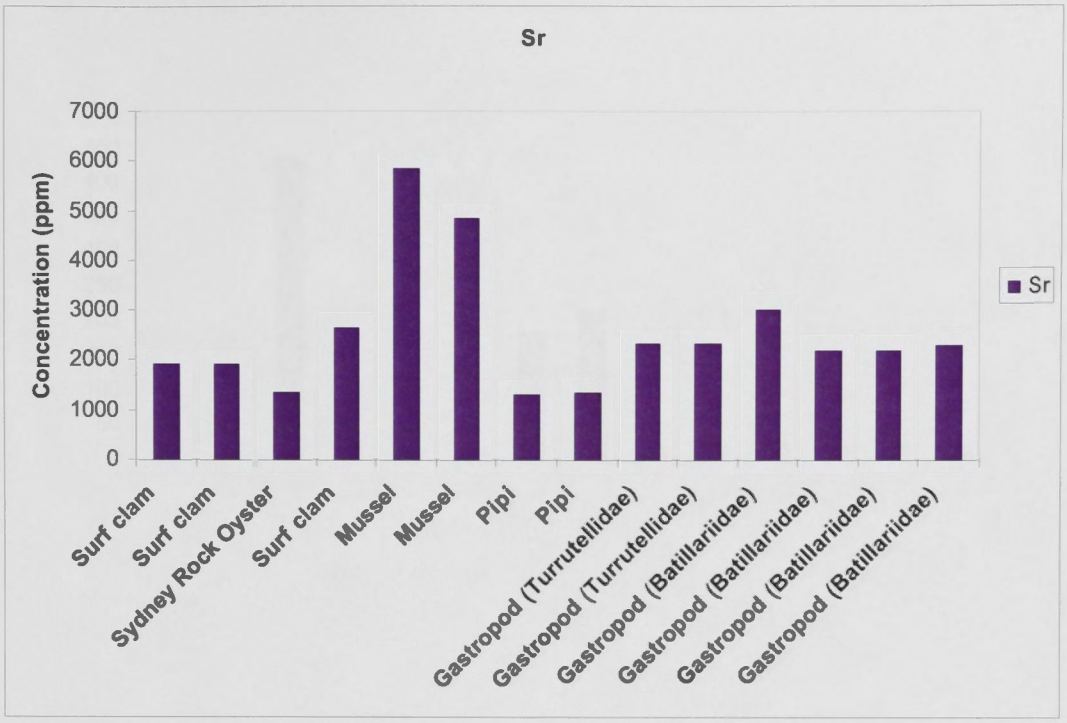

Figure 4.18: The concentration of strontium in analysed shells.

The phosphorus concentrations within the shells were generally less than 30 ppm, with several exceptions, most likely reflecting the presence of trapped organic matter (algae, chitin) within the growth layers of the shells (Figure 4.19). Even though not part of the aragonite/calcite structure, this data shows that shell contamination during growth will contribute elements such as phosphorus to the biogenic component of the accumulating sediments. For comparison, a soldier crab shell was also analysed from the Front Lake of Merimbula, which when readjusted to a volatile free basis, contained around 12 wt% MgO, approximately 2.5 wt% P_2O_5 and 8000 ppm Sr.

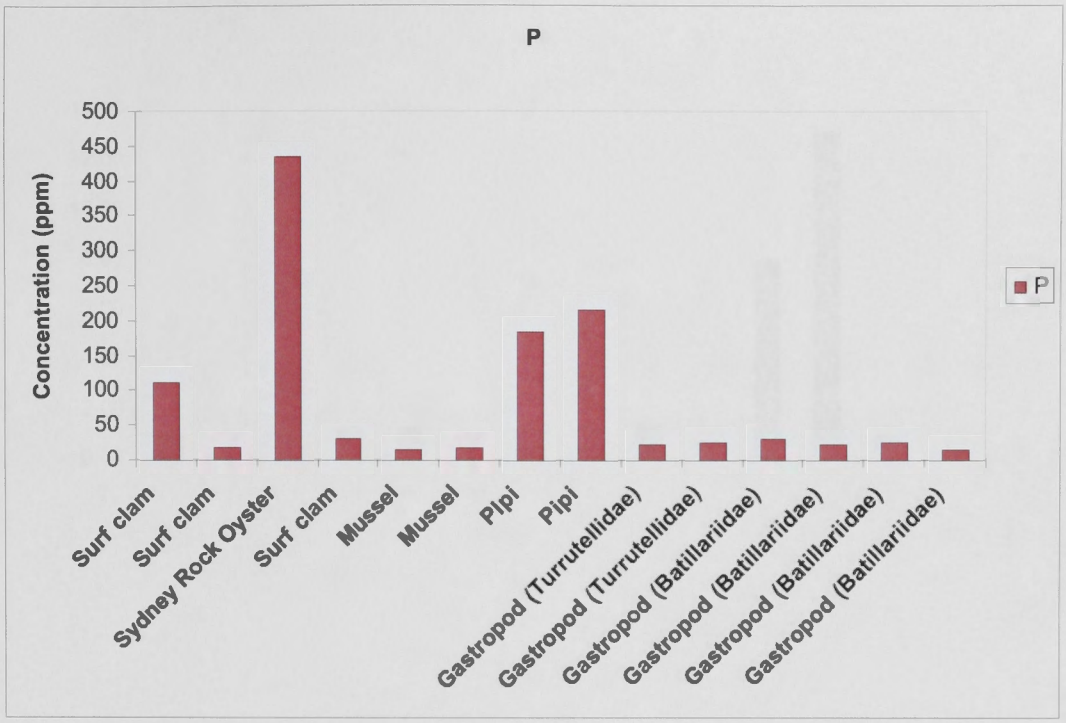

Figure 4.19: The concentration of phosphorus in analysed shells.

Lead and zinc are known to substitute readily into carbonate structures, especially the structure aragonite. Most of the analysed gastropod and bivalve species showed lead concentrations of less than 1 ppm, with some notable exceptions. The Sydney Rock oyster and the gastropod (*Batillariidae)* had lead concentrations of between 11-13 ppm (Figure 4.20).

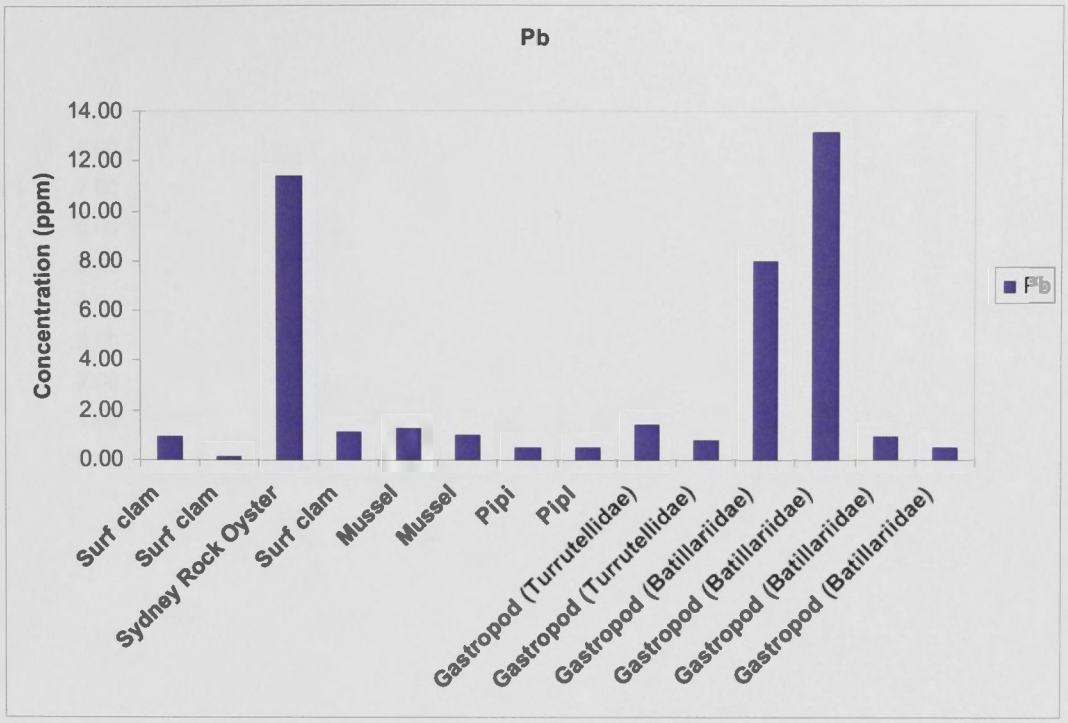

Figure 4.20: The concentration of lead in analysed shells.

In terms of potential contribution to sediment geochemistry, a concentration of 7 ppm lead in an oyster shell equates to 12.5 ppm lead on a volatile (CO_2 - free) readjusted total.

The oyster and the gastropod (*Batillariidae*) also had higher zinc concentrations than the other bivalves and gastropods, with the majority having less than 0.5 ppm zinc (Figure 4.21). The oyster and the gastropod (*Batillariidae*) contained 8.07 and 1.79 ppm of zinc respectively. Both lead and zinc are well known anthropogenic pollutants, and this data reflects such processes with the estuary.

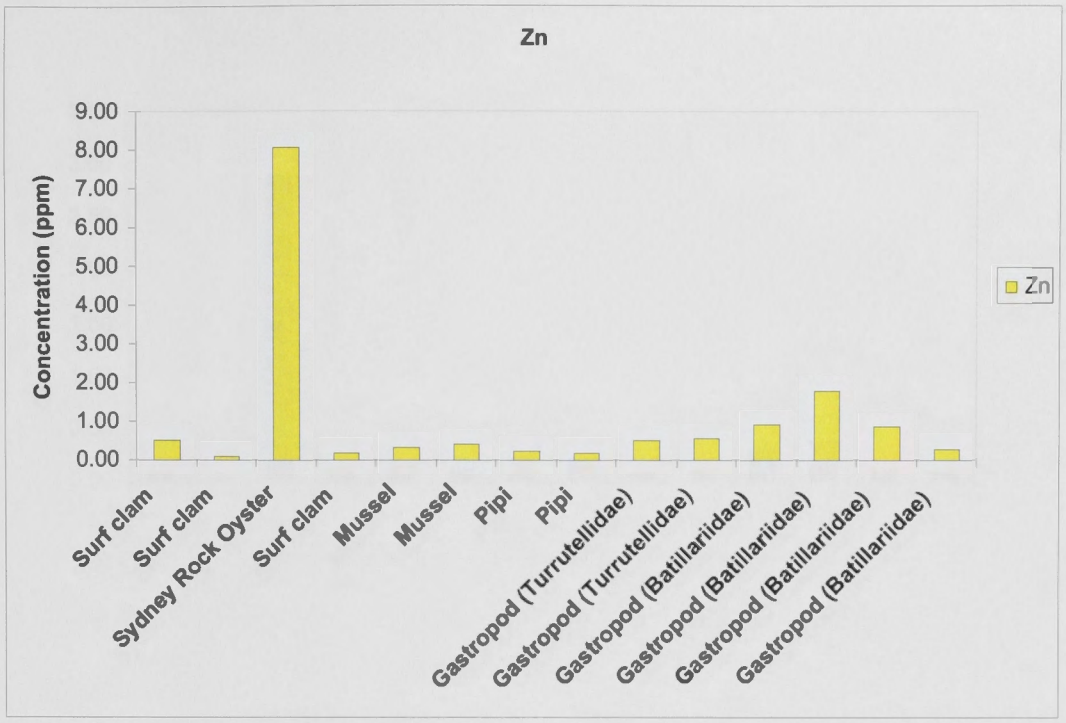

Figure 4.21: The concentration of zinc in analysed shells.

Copper also showed higher concentrations within the oyster and slightly so in the gastropod (*Batillariidae*) compared to the others (Figure 4.22). Most shells had less than 0.2 ppm copper whereas the oyster has 2.8 ppm. The gastropod (*Batillariidae*) had 0.31-0.39 ppm copper. Barium was higher in the oyster and mussel than any of the other analysed shells (Figure 4.23).

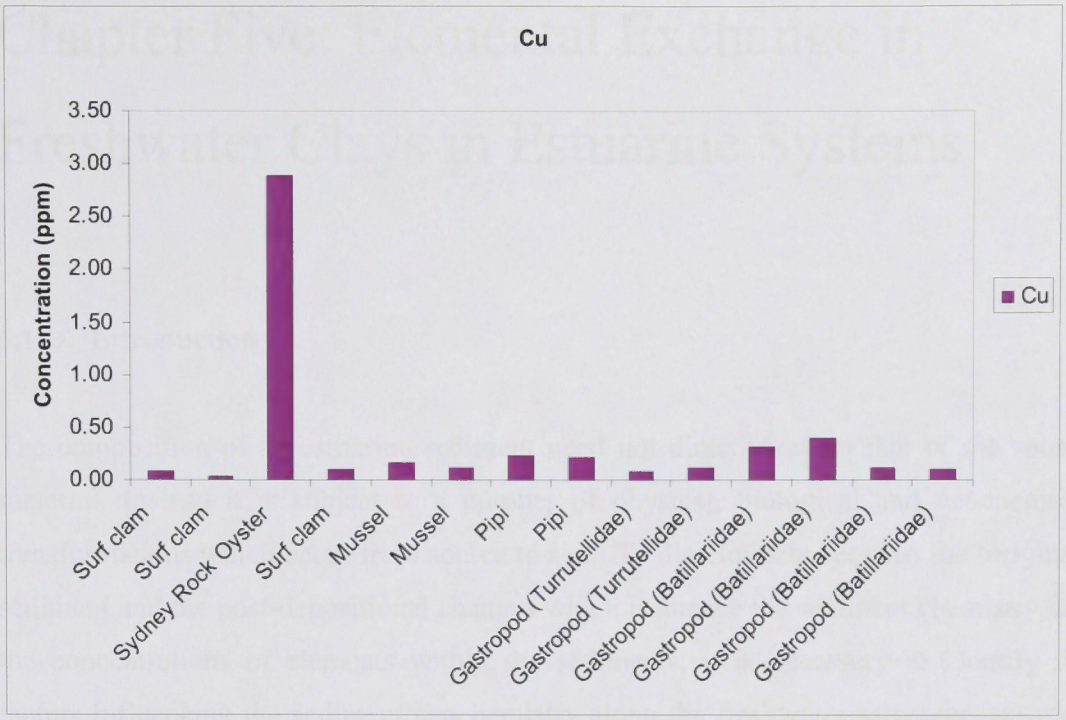

Figure 4.22: The concentration of copper in analysed shells.

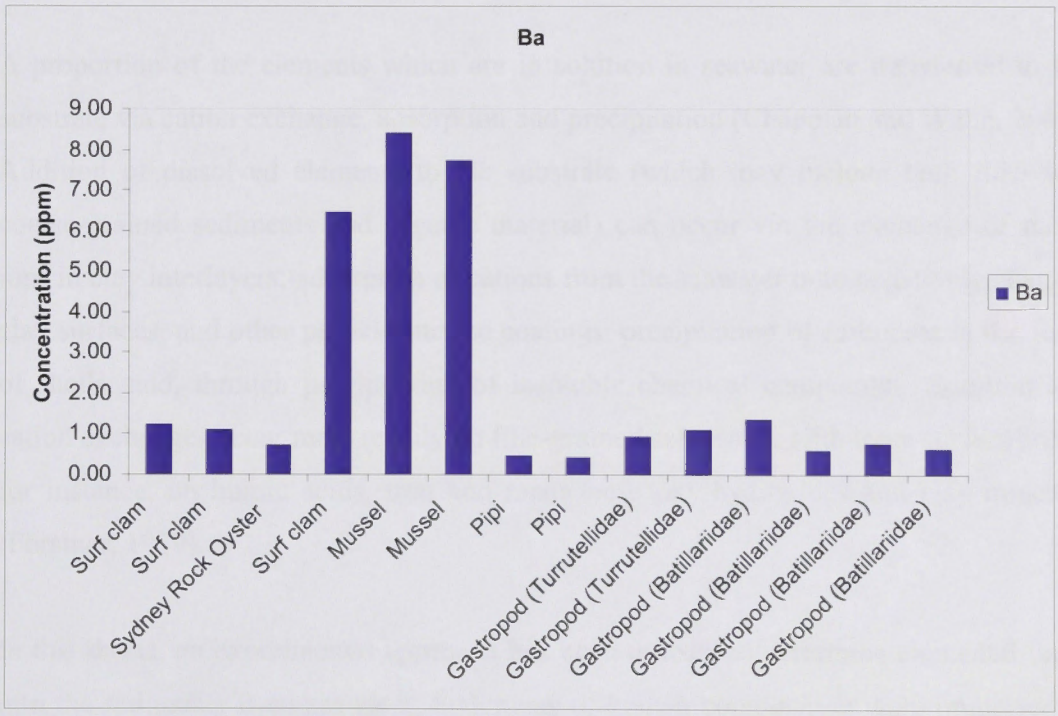

Figure 4.23: The concentration of barium in analysed shells.

Chapter Five: Elemental Exchange in Freshwater Clays in Estuarine Systems

5.1. Introduction

The composition of an estuarine sediment need not directly reflect that of the source material. Instead it is subject to a number of physical, biological and geochemical transformations which occur from source to sink. To discriminate between the 'original' sediment and the post-depositional changes which influence the sediment chemistry and the concentrations of elements within the sediments, it is necessary to identify the factors influencing the sediment geochemistry along the freshwater-saltwater pathway. The most obvious of these is the influence of seawater on freshwater sediments.

A proportion of the elements which are in solution in seawater are transferred to the substrate via cation exchange, adsorption and precipitation (Chapman and Wang, 2001). Addition of dissolved elements to the substrate (which may include both fine- and coarse-grained sediments and organic material) can occur via the exchange of metal ions in clay interlayers; adsorption of cations from the seawater onto negatively charged clay surfaces, and other particle surface coatings; precipitation of carbonate in the form of shells; and, through precipitation of insoluble chemical compounds. Sorption and cation exchanges occur most readily on fine-grained substances with large surface areas, for instance, on humic acids, iron and manganese oxy-hydroxides and clay minerals (Förstner, 1979).

In this thesis, an experimental approach has been utilised to determine elemental input into the sediments from seawater. Sediments of known composition were immersed in seawater so that the exchange from seawater to sediment could be identified and quantified. Five freshwater clays of known composition (kaolinite; chlorite and illite mixture; Ca-montmorillonite; goethite; illite; and halloysite) were suspended in PVC

pipes in the estuarine water column for a period of five months. These clays were selected to represent the range of geochemical changes occurring to different clay types in an estuarine environment. The aims for these experiments were to determine: (a) the *behaviour* of freshwater clays in the estuarine water column; (b) the *effect* of precipitated seawater contamination on the total geochemical concentration; and (c) the *changes* in elemental concentrations of the freshwater clays due to interaction with seawater. These sediments were suspended in the water column in order to exclude processes that occur in the *in situ* sediment column. This ensured that the effect of seawater on the sediment could be isolated, allowing discrimination of post-depositional inputs into the sediments prior to burial. These experiments were undertaken to test the hypothesis that the final concentration of a sample may reflect many post-depositional additions and subtractions to the original sediment. As dissolved and suspended metal inputs have a strong affinity for clay minerals in the estuarine environment, these experiments identify the effectiveness of different clay minerals in filtering out 'dissolved' pollutants from the water column, and examine the extent to which coastal lakes and estuaries create anomalies of particular elements within the environment, via the fine-grained sediment component.

5.2. Background

The fine-grained sediments which accumulate in estuaries are highly correlated with metals (Thorne and Nickless, 1981 *in* Moore *et al.*, 1989). All fine-grained materials with a large surface area are capable of accumulating (adsorbing) heavy metal cations at the solid-liquid interface as a result of intermolecular forces, with clays being able to do so within their crystalline structure (Förstner and Wittman, 1981). Solution pH also influences adsorption equilibria (Salomons, 1980; Millward and Moore, 1982; Tessier *et al.*, 1985). Fine-grained materials in the suspended sediment load of a fluvial system include clay minerals, iron oxyhydroxides and organic matter. These phases can undergo cation exchange whereby the surface of the particle will adsorb cations from solution and release equivalent amounts of other cations into solution. Cation exchange occurs based on the sorptive properties of negatively charged sites (SiOH, $AlOH_2$ and

AlOH groups in clay minerals; FeOH groups in iron hydroxides; and OH groups in organic substances) towards positively charged ions (Förstner and Wittman, 1981).

In order to balance the negative charges within the lattice, preferential adsorption of specific cations takes place, with release of equivalent charges associated with other cations (Förstner and Wittman, 1981). The degree to which cation exchange occurs is dependent on clay type, or the cation exchange capacity (CEC) of the clay (see Table 5.1).

Clay Minerals	**Na^+ (meq/100g)**	**Mg^{2+} (meq/100g)**	**Ca^{2+} (meq/100g)**	**K^+ (meq/100g)**	**Sum**
Montmorillonite	30.4	4.1	-33.58	1.88	69.96
Kaolinite	2	1	-1.2	0.35	4.55
Illite	7.8	3.88	-10.7	0.3	22.68
Mixed layer	21.38	5.2	-17.1	-0.2	43.88

Table 5.1: The cation exchange quantity of clay minerals in equilibrium with seawater (Sayles and Mangelsdorf, 1977). Note: positive value indicates that species is adsorbed, negative is released.

Cation exchange is the process by which a cation bound to the surface of a particle is replaced by a cation from solution. The CEC refers to the surface charge on a clay mineral which is a function of a net imbalance of charges originating from the silicate layers of the mineral (Guggenheim *et al.,* 2009). The capacity for exchange correlates with the size of the net negative charge on the 2:1 layer (Guggenheim *et al.,* 2009) and hence on the type of clay. The exchange capacity increases with decreasing grain size and the associated increase in the surface area/volume ratio (Vaithiyanathan *et al.*, 1992). Very fine grain size results in adsorption to negatively charged surfaces and cation exchange in the layers (for instance Ca^{2+} replaces Na^+ in montmorillonite). CEC increases markedly in the order: montmorillonite > halloysite > illite > chlorite > kaolinite. The preference of ion exchange follows the order: $Ba^{2+} > Pb^{2+} > Sr^{2+} > Ca^{2+} > Ni^{2+} > Cd^{2+} > Cu^{2+} > Co^{2+} > Zn^{2+} > Mg^{2+} > Ag^+ > Cs^+ > Rb^+ > K^+ > NH^{4+} > Na^+ > Li^+$ (Helfferich, 1962) or more simply, $Al^{3+} > Ca^{2+} > Mg^{2+} > K^+ = NH^{4+} > Na^+$ (Sparks, 2003). The exchange capacity of organic substances is particularly high, especially that of humic acids, so a low percentage of organic material can cause a

considerable increase in the exchange capacity of the total sediment (Förstner and Wittman, 1981).

In terms of the accumulation of anthropogenically derived pollutants (such as metals) into the sediments, it is the fine-grained component of the sediment which has the greatest capacity to be modified, and is therefore the most important in terms of monitoring anthropogenic change.

5.2.1. Clay structures

The crystal structures of clay minerals are based on composite layers built from components with tetrahedrally and octahedrally coordinated cations (Bennett *et al.*, 1991). Most occur as platy particles in fine-grained aggregates which, when mixed with water, yield materials with varying degrees of plasticity (Kearey, 1993). Chemically, all are hydrous silicates (principally of aluminium or magnesium). The clays can be divided into groups based upon their structures and chemistry. The four important layered clay mineral groups are kaolinites, illites, smectites and vermiculites. The various clay species are distinguished through either the substitution of cations, or through variations in the stacking sequence of the tetrahedral and octahedral cation sheets. The tetrahedral sheets consist of silicon (and sometimes aluminium) cations, with oxygen atoms that surround each cation at the corners of a tetrahedron. The individual tetrahedra are each connected to three adjacent tetrahedra by sharing the basal corner oxygens to form a hexagonal mesh-like structure (Figure 5.1).

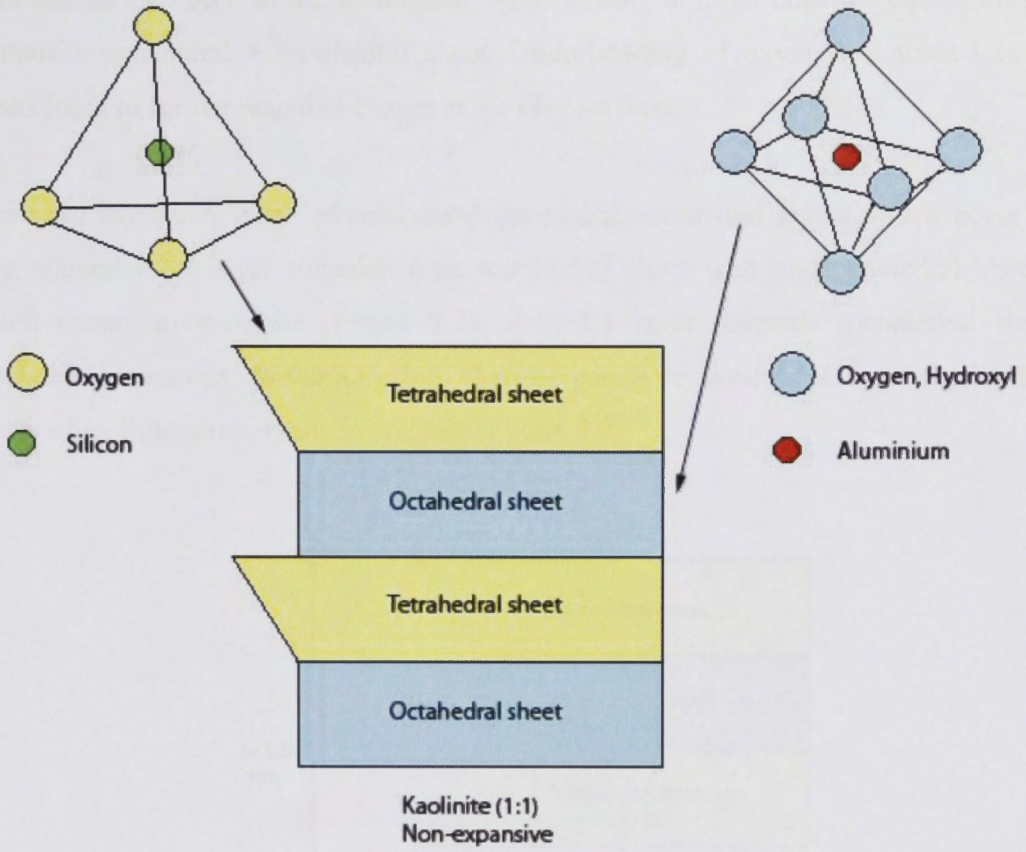

Figure 5.1: Schematic representation of the tetrahedral and octahedral sheets within a 1:1 kaolinite structure.

Octahedral sheets comprise medium-sized cations such as aluminium (effective ionic radius 58.3 pm: Shannon, 1969; Shannon and Prewitt, 1970; Shannon and Prewitt, 1976), at the centre of each individual octahedron, with oxygens at each of the six corners. The individual octahedra are linked laterally to neighbouring octahedra and also to at least one tetrahedral sheet through sharing of oxygens. The plane of joining tetrahedral and octahedral sheets also includes shared oxygens, as well as unshared hydroxyls. These OH^- groups are located at the centre of each hexagon at the same level as the apical oxygens.

Octahedral sheets are similar in structure to gibbsite, $Al(OH)_3 = Al_2(OH)_6$, in the case of dioctahedral clays or to brucite, $Mg(OH)_2 = Mg_3(OH)_6$ in the case of trioctahedral species. Al^{3+} may be replaced by divalent cations such as Mg^{2+} or Fe^{2+} in the octahedral

layer and Si^{4+} by Al^{3+} in the tetrahedral layer, leading to a net negative charge on the composite octahedral + tetrahedral sheet. Underbonding of oxygens at the edges of sheets leads to further negative charge at the clay surface.

There are two main types of compound octahedral-tetrahedral layers which occur in clay minerals: 1:1 layer minerals (one tetrahedral sheet with one octahedral sheet), which occurs in kaolinite (Figure 5.1); and, 2:1 layer minerals (octahedral sheet sandwiched between two tetrahedral sheets), which is typical of montmorillonite, vermiculite, illite, primary mica, and talc (Figure 5.2).

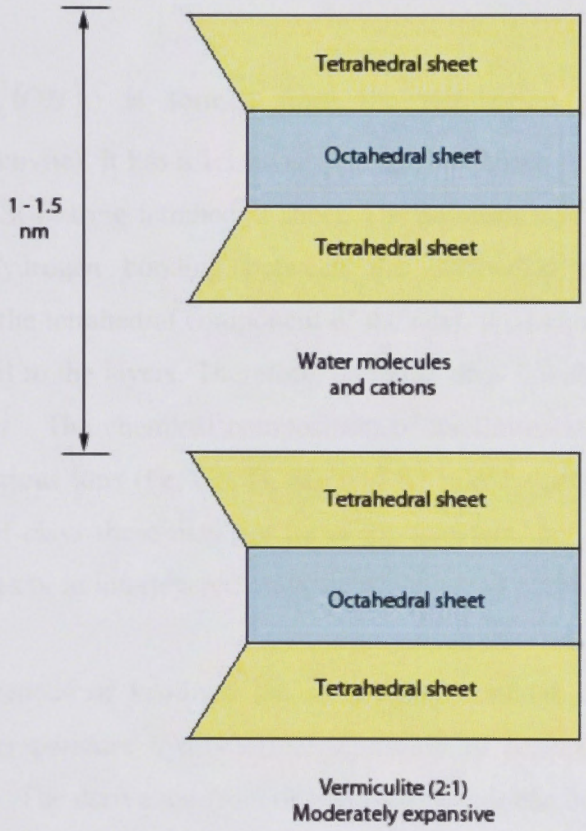

Figure 5.2: Schematic representation of the tetrahedral and octahedral sheets within a 2:1 vermiculite structure.

These layers are separated by an interlayer space. If the layers are electrostatically neutral, the interlayers will be devoid of additional cations and anions. However, most clays have an excess of layer negative charge, which requires neutralization by loosely

bound interlayer cations such as Ca^{2+}, Mg^{2+}, Na^{+}, K^{+} and H^{+}. The bonding energy is generally in the order Ca > Mg > K > H > Na, although in certain clay minerals (e.g. kaolinite), the bonding energy is Mg > Ca (Carroll and Starkey, 1958; Sparks, 2003). The cations with the higher bonding energy preferentially occupy the exchange sites in the interlayers and on the mineral surfaces, and displace more weakly bound cations, all else being equal. Thus, the replacing power of Na^{+} ions in seawater is reduced by the presence of Ca^{2+} and Mg^{2+} ions that have higher bonding energy (Carroll and Starkey, 1958), as calcium and magnesium out-compete sodium for the same site.

The individual clays may be identified by a number of properties, as follows:

Kaolinite

Kaolinite ($Al_4Si_4O_{10}(OH)_8$) is formed from the weathering of aluminosilicates (plagioclase and muscovite). It has a 1:1 layer structure, with one Al-bearing octahedral sheet bonded to one Si-bearing tetrahedral sheet. The adjacent layers are held together firmly by strong hydrogen bonding between the octahedral component of one compound layer and the tetrahedral component of the next, producing a structure which cannot expand normal to the layers. Therefore, kaolinite does not shrink or swell when in contact with water. The chemical composition of kaolinite shows little variation. Small amounts of various ions (Fe, Cr, Ti, Mg and K) may be present, but due to the fine-grained nature of clays these may not be in the structure, but occur as impurities such as Fe or Ti oxides or in interlayered mica, or adsorbed on particle surfaces.

The principle occurrences of kaolinite are as primary residual deposits formed by weathering or low-temperature hydrothermal alteration of feldspars, muscovite and other Al-rich silicates. The derivation from orthoclase feldspar can be expressed as:

$$4KAlSi_3O_8 + 4H^+ + 2H_2O \rightarrow 4K^+ + Al_4Si_4O_{10}(OH)_8 + 8SiO_2$$

During weathering, the silica and K^{+} are leached away. If potassium is not completely lost, then illite rather than kaolinite is likely to form (Deer *et al.*, 1992).

Halloysite

Halloysite ($Al_4[Si_4O_{10}](OH)_8$) is a hydrated member of the kaolinite group, and hence is found in nature as a precursor to kaolinite formation. It has a 1:1 layer structure, with a single layer of water molecules in each interlayer space. The presence of interlayer water increases the layer spacing (d_{001}) from the characteristic 7.2 Å of kaolinite to approximately 10 Å in halloysite. Dehydration occurs readily, causing the collapse of the structure to a form which is similar to kaolinite (dehydrated halloysite has $d_{001} \sim 7$ Å). The halloysite sheets are characteristically rolled into a tubular form.

Montmorillonite

Montmorillonite (typical formula, $(({}^1/_2 Ca, Na)_{0.7}(Al_{3.3}Mg_{0.7})[Si_8O_{20}](OH)_4 \times nH_2O)$ (Deer *et al.*, 1992) is a major member of the class of smectites, which are characterised by a small crystal size. It is formed from the alteration of potassic feldspars and diagenesis of muscovite. Montmorillonite has a 2:1 layer structure, with one Al-dioctahedral sheet sandwiched between two Si-tetrahedral sheets. There is no direct bonding between layers, and furthermore the layers have a slight negative charge as a result of minor substitution of $(Mg, Fe)^{2+}$ for octahedral Al^{3+}. Typically one sixth of the Al-ions are replaced by Mg in the octahedral layer. The charge imbalance is satisfied by exchangeable interlayer cations such as Ca^{2+} or Na^{+}. Water molecules are also attracted to the interlayer space. Insertion of these interlayer species cause expansion of the lattice structure, so montmorillonite is classified as a swelling and shrinking clay.

Illite

Illite (typical formula $K_{1.5\square 1.0}Al_4(Al_{1.5\square 1.0}Si_{6.5\square 7.0}O_{20})(OH)_4$) (Deer *et al.*, 1992) has a 2:1 layer structure and is formed from the weathering or hydrothermal alteration of muscovite-phengite. Illite may also form through the authigenic alteration of K-feldspar or the recrystallisation of smectites in marine sediments. Illite is a hydrated clay, but is incapable of expanding and contracting due to the potassium ions maintaining the interlayer spacing.

Vermiculite

Vermiculite ($(Mg,Ca)_{0.6\square 0.9}(Mg,Fe^{3+},Al)_6[(Si,Al)_8O_{20}](OH)_4 \times nH_2O$) (Deer *et al.*, 1992) has a trioctahedral 2:1 layer structure. Vermiculite is essentially a hydrated mica in which interlayer potassium is replaced by $[(Mg,Ca)(H_2O)_6]^{2+}$ complexes.

Chlorite

Chlorite ($(Mg^{2+},Al^{3+},Fe^{2+},Fe^{3+})_6[(Si.Al)_4O_{10}](OH)_8$) is closely related to the mica minerals. The chlorite minerals have a mica type 2:1 layer intercalated with an additional brucite-like sheet. Chlorites are formed by the hydrothermal alteration of mafic minerals in tuffs, andesites and sediments, as well as crystallising as primary phases in low-grade metamorphic rocks.

Oxides

The oxides $Fe^{3+}O(OH)$ (polymorphs goethite and lepidocrocite) and Fe_2O_3 (hematite), $5Fe_2O_3.9H_2O$ (ferrihydrite) and $Al(OH)_3$ (gibbsite) are very stable, and amorphous phases, which occur in association with clay minerals. Aluminium in soils is usually in the form of a hydroxide, and iron in the form of an oxyhydroxide. Both aluminium and iron oxyhydroxides occur as clay-sized crystals with structures based on hexagonal and cubic close-packed oxygen anion frameworks, and also, in the case of aluminium hydroxide, within interlayers of vermiculites and smectites. Oxides can develop positive surface charge at low pH, thus becoming capable of adsorbing anions (phosphate and sulfate).

Goethite commonly substitutes minor Al, Mn and Ni for Fe. It also has a very high surface area and a high sorptive capacity for cations, including Cu, Pb and Zn, and anions, especially phosphate (Eggleton, 2001).

5.3. Study site

The site for the *in situ* clay pipe experiments was selected on the basis of being a locality where the experiments would be undisturbed; where the pipes would undergo

semi-diurnal tidal flushing; distance from highly populated land use; and, proximity to a nearby freshwater creek containing sediments of a high sulfur content (Figure 5.3). These factors were considered to be essential in discriminating the potential transformations occurring to the freshwater sediment geochemistry with respect to sulfur concentrations, which were elevated in sediments associated with inflow points around the lake. The clay pipes were therefore placed in the south-western corner of the Top Lake in Merimbula, near Bald Hills Creek (Figure 5.3).

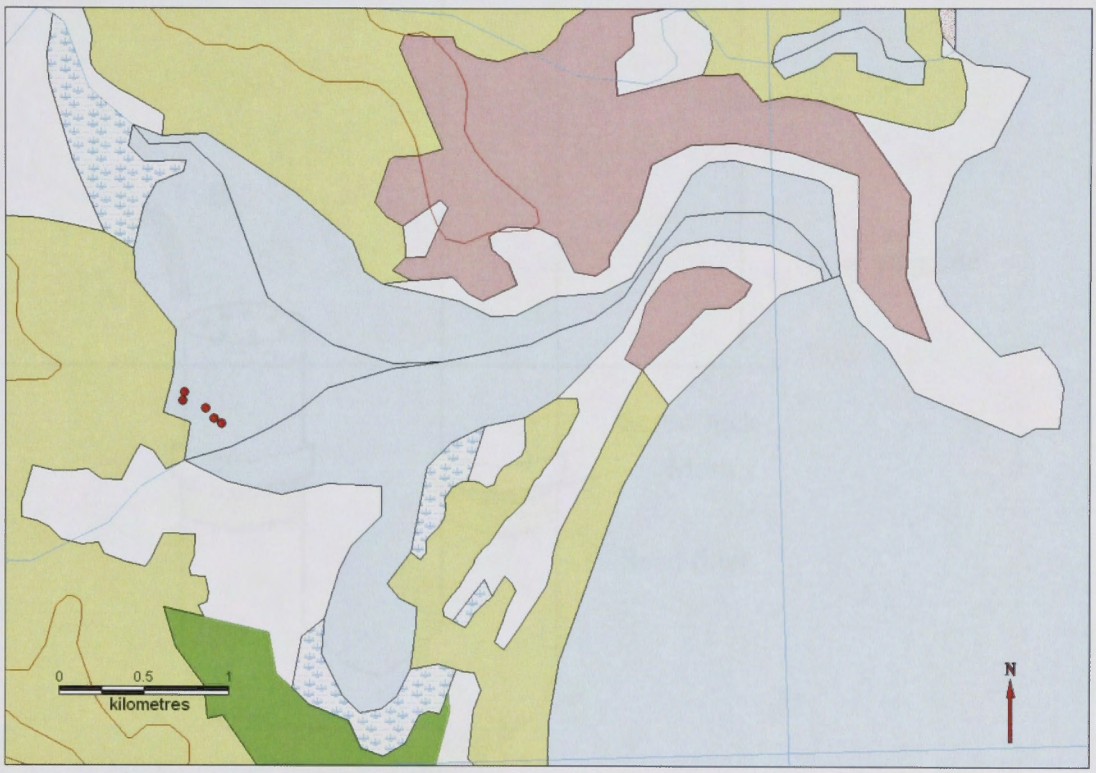

Figure 5.3: Location of *in situ* clay pipe experiments in Merimbula Lake (red dots).

5.4. Methodology

5.4.1. Field methods

In situ experiments were initially conducted using well characterised freshwater clays of known elemental compositions. The clays were placed in PVC pipes within the estuary in order to establish the additions and subtractions of metals in the estuarine environment. With each tide cycle, seawater alternately flowed from pipe opening A to

B as the tide ebbed, and then from pipe opening B to A as the tide rose. This enabled four cycles of flushing approximately every day (Figure 5.4).

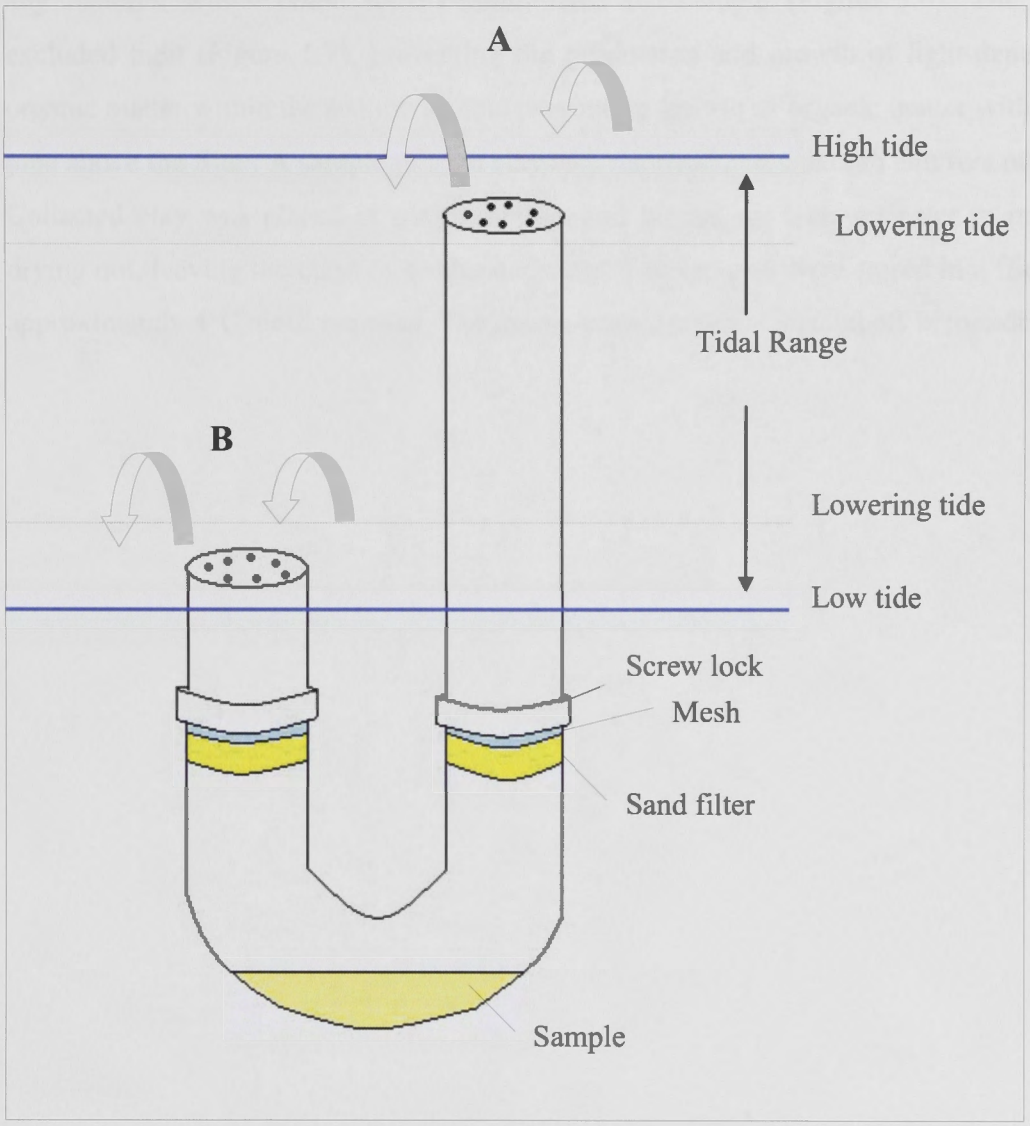

Figure 5.4: Pipes were positioned so that water would be expelled from the pipe during high and low tide.

Clay samples included: (a) a kaolinite, chlorite and illite mixture; (b) Ca-montmorillonite from Texas; (c) crushed goethite; (d) Muloorina illite; (e) Halloysite, NZCC Matauri Bay. All were samples obtained from Professor Tony Eggleton, (RSES, ANU). The pipes were attached onto oyster poles within the water column, at a depth that would allow for tidal flushing through the pipe twice daily (Figure 5.5).

Approximately 10g of each clay were placed within the "U" section of a pipe, which was then sealed with a 200μm microfibre material filter, and capped with a sand filter. This would prevent the loss of the clay sample to the water column, or the addition of any material which could have contaminated the sample (Figure 5.6). The pipes excluded light (Figure 5.7), preventing the production and growth of light-dependent organic matter within the sediments, and preventing growth of organic matter within the pipe above the filter. A sample of each clay was removed at one month and five months. Collected clay was placed in plastic bottles and topped up with seawater to prevent drying out, leaving the clays in a saturated state. The samples were stored in a fridge at approximately 4°C, until required. The excess seawater was decanted off before drying.

Figure 5.5: PVC pipe clay experiments in the estuary (above), and retrieved (below).

Figure 5.6: Sand filter over meshing in PVC pipe, trapping fine grained material in the seawater.

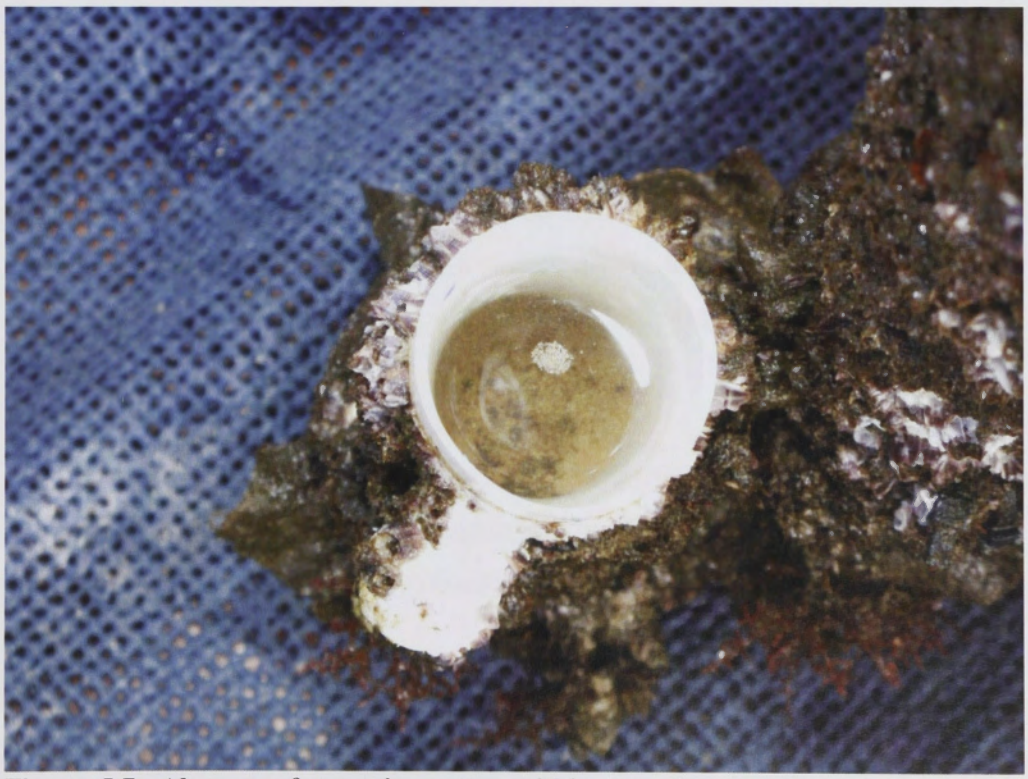

Figure 5.7: Absence of organic matter within the pipe, as opposed to abundance of barnacles on outside of pipe.

5.4.2. Analytical methods

A total of 18 samples were crushed and milled to obtain the whole rock and trace element compositions. Previous studies on sediments saturated with seawater have either involved methodologies where sediment samples have been rinsed with deionised water with consequent errors (Sayles and Mangelsdorf, 1977), or have been experiments conducted within the laboratory (Russell, 1970; Mathew *et al.*, 1997; Charlet and Tournassat, 2005).

In this study, the experiments were conducted *in situ*, saturating the sediment samples with a frequent flushing of seawater. This ensured that natural processes (flooding and rain pulses, evaporation, tidal flushing) were taken into account. The excess seawater was decanted, and the wet clay samples were placed on a watch glass and oven-dried overnight at 40°C. The dried sediments were crushed in a mortar and pestle, and then passed through a 500μm sieve. An aliquot of 2g was milled in a micronising mill with ethanol for 10 minutes, and then oven-dried overnight at 40°C.

Whole-rock major elements were analysed using a PW2400 wavelength-dispersive X-ray fluorescence (XRF) spectrometer, and whole-rock and individual mineral trace elements were analysed by laser ablation inductively-coupled plasma mass spectrometry (LA-ICP-MS) by the methods outlined by Spandler *et al.*, 2003 and Gingele *et al.*, 2007. Major elements Na, Mg, Al, Si, P, S, K, Ca, Ti, Mn, Fe, F and Cl were determined by XRF with a Phillips (now PANalytical) PW2400 wavelength-dispersive X-ray fluorescence spectrometer.

For detailed descriptions of analytical methods see Section 4.2.2. For selected samples, a second aliquot of 2g was hand crushed in a mortar and pestle, then packed into glass slides for quantification of phase mineralogy, including clay type, by X-Ray Diffraction (XRD).

5.5. Results

Samples were collected wet and stored in contact with the seawater. Samples were not rinsed so as to prevent loss of artefacts associated with ion exchange (Sayles and Mangelsdorf, 1977).

The analyses of the clay and goethite samples in Table 5.2 show the major, minor and trace elements for the original composition of the samples, and the compositions after one month and five months immersed in seawater. There were only limited variations in concentrations of the elements. Of the major and minor elements, decreases in concentrations were observed for CaO, and increases in concentrations were observed for Na_2O and SO_3. The changes in concentrations of the major and minor elements can be attributed to cation exchange and adsorption from the seawater. Of the trace elements, increases in concentration were observed in Cr, Ni, Cu, Zn, As, Mo and Pb. The increases in these trace elements, particularly copper, cannot be attributed to interaction with seawater alone, given their very low seawater abundances (Table 5.3, below). Such large elevations in concentration must therefore be due to anthropogenic additions to the seawater.

The XRD data showed only minor changes to the mineralogical composition of the clays over time (Table 5.2). However changes over time in the mineral peaks observed in the XRD scans showed chemical change to some of these minerals as a result of cation exchange (Appendix 3). The addition of salt to all samples was due to the evaporation of seawater following the sampling of the wet samples. Observed increases in Na_2O correlate with increases of halite in the samples. Authigenic changes were also observed, with the Ca-montmorillonite gaining small amounts of gypsum, as a precipitate from the seawater, and the illite sample showing the appearance of some kaolinite after five months as a result of the weathering of the micas in the sample.

Sample number	Clay type	Origin	Original freshwater sample	Freshwater sample after 5 months in estuarine water column
1	Kaolinite + Illite	Unknown	Kaolinite > Illite > Smectite	Kaolinite > Illite > Halite
2	Ca-montmorillonite	Standard clay sample, STx-1: Manning Formation, Jackson Group (Eocene), Texas, USA	Montmorillonite > Quartz > Opal	Montmorillonite > Halite > Gypsum > Quartz
3	Goethite	Crushed goethite rock sample, from RSES, ANU. Original source unknown.	Goethite	Goethite
4	Illite	Muloorina, South Australia	Illite > Halite > Quartz	Illite > Halite > Quartz > Kaolinite
5	Halloysite	Matauri Bay New Zealand China Clay	Halloysite > Kaolinite > Quartz > Montmorillonite	Halloysite > Kaolinite > Quartz > Halite

Table 5.2: Phase makeup of results of clay and goethite sample as determined by XRD before and after immersion in seawater.

5.6. Discussion

Merimbula Lake is a pristine estuarine system, especially with respect to the water quality which is strictly monitored due to the restrictions enforced by the local oyster farming industry. In studying the chemistry of the estuarine sediments to determine which constituents are naturally derived and which are anthropogenic, it is important to discriminate what is added to the sediments after deposition. The first step is to identify and quantify the geochemical changes occurring in freshwater sediments purely as a result of the addition of seawater. This was undertaken with the *in situ* clay pipe experiments.

5.6.1. Post-collection precipitated seawater contamination

Fine-grained clay minerals can absorb ions internally within the crystal structure, bind them to the surface by reversible adsorption, and temporarily bind large amounts of water (Schulz and Zabel, 2006). In addition, as it is almost impossible to avoid some contamination from seawater when analysing sediments which have been immersed in

seawater and then dried for analysis, salts from the seawater may precipitate within the sample, forming an additional component of the sediment. It is therefore imperative to determine the extent to which the compositions of these clays are modified by the salts which crystallise during the drying out process of the sediments within the laboratory. In order to account for these precipitates, the concentration of seawater present in each collected sample before drying must be estimated. This was done using the concentration of Cl^- present in the dried sediment. As chlorine is present in high concentration in seawater (19400 ppm at 3.5% salinity, Table 5.3), and only in trace amounts in terrestrial samples (120-553 ppm for freshwater clay samples 1, 2, 3 and 5, Tables 5.4 - 5.8), effectively all the chlorine present in the samples was from the addition of seawater. The exception was the illite sample (sample number 4), which was deposited in a lacustrine environment during the Oligocene (Muloorina, South Australia) (Norrish and Pickering, 1983) (Table 5.7), and hence started out with a significant salt content.

.

Detailed composition of seawater at 3.5% salinity				
Element	**ppm**		**Element**	**ppm**
Hydrogen H	110,000		Yttrium Y	0.000013
Oxygen O	883,000		Zirconium Zr	0.000026
Sodium Na	10,800		Niobium Nb	0.000015
Chlorine Cl	19,400		Molybdenum Mo	0.01
Magnesium Mg	1,290		Ruthenium Ru	0.0000007
Sulfur S	904		Silver Ag	0.00028
Potassium K	392		Cadmium Cd	0.00011
Calcium Ca	411		Tin Sn	0.00081
Bromine Br	67.3		Antimony Sb	0.00033
Helium He	0.0000072		Iodine I	0.064
Lithium Li	0.17		Xenon Xe	0.000047
Beryllium Be	0.0000006		Cesium Cs	0.0003
Boron B	4.45		Barium Ba	0.021
Carbon C	28		Lanthanum La	0.0000029
Nitrogen ion	15.5		Cerium Ce	0.0000012
Fluorine F	13		Praesodymium Pr	0.00000064
Neon Ne	0.00012		Neodymium Nd	0.0000028
Aluminium Al	0.001		Samarium Sm	0.00000045
Silicon Si	2.9		Europium Eu	0.0000013
Phosphorus P	0.088		Gadolinium Gd	0.0000007
Argon Ar	0.45		Terbium Tb	0.00000014
Scandium Sc	<0.000004		Dysprosium Dy	0.00000091
Titanium Ti	0.001		Holmium Ho	0.00000022
Vanadium V	0.0019		Erbium Er	0.00000087
Chromium Cr	0.0002		Thulium Tm	0.00000017
Manganese Mn	0.0004		Ytterbium Yb	0.00000082
Iron Fe	0.0034		Lutetium Lu	0.00000015
Cobalt Co	0.00039		Hafnium Hf	<0.000008
Nickel Ni	0.0066		Tantalum Ta	<0.0000025
Copper Cu	0.0009		Tungsten W	<0.000001
Zinc Zn	0.005		Rhenium Re	0.0000084
Gallium Ga	0.00003		Gold Au	0.000011
Germanium Ge	0.00006		Mercury Hg	0.00015
Arsenic As	0.0026		Lead Pb	0.00003
Selenium Se	0.0009		Bismuth Bi	0.00002
Krypton Kr	0.00021		Thorium Th	0.0000004
Rubidium Rb	0.12		Uranium U	0.0033
Strontium Sr	8.1			

Table 5.3: Detailed composition of seawater at 3.5% salinity (Turekian, 1976).

In order to account for seawater contamination, the cations and anions in seawater need to be reconstituted as salts to establish the total percentage sea salt content of the salt-contaminated sediment, and the cations converted to oxides to compare directly with the geochemical data.

The sea salt correction was applied as follows. The ratio of Cl content in the analysed sample to Cl in sea water gave the proportion of sea water that had contaminated any analysis. The weight percentage of salt in the contaminated sediment was estimated as:

$$wt\%\ (\text{salt}) = wt\%(\text{Cl}_{initial}) \times wt\%(\text{total salt}_{seawater})/wt\%(\text{Cl}_{\text{seawater}})$$

The ratio $\text{wt\%}(\text{Cl}_{initial})/\text{wt\%}(\text{Cl}_{\text{seawater}})$, multiplied by a particular element concentration in seawater, was then subtracted from the raw analytical data to get the pre-contamination concentration, using the following equation, applied for each element, *X*:

$$\textit{Corrected concentration in clay} = wt\%X_{initial} - \left[\frac{wt\%Cl_{initial}}{wt\%Cl_{seawater}} \times wt\%X_{seawater}\right]$$

These concentrations were then rescaled to compensate for the fact that some of the initial weight was due to sea salt rather than uncontaminated sediment:

$$\textit{Rescaled concentration} = \textit{corrected concentration} \times 100\% / (100\% - wt\%(\text{salt}))$$

This provided the effective concentration of the elements after the removal of the contributions from seawater, which was applied to all elements analysed in each of the five clay samples (Appendix 2, Table A.9). The results of these calculations are given in Tables 5.4 – 5.8. The data in these tables is arranged in groups corresponding to the original analysis of the freshwater sample, the sample after one month and the five months in the estuary. In each case, the difference between the sample and the sample with the sea salt removed provides the change in concentration of each element due to the presence of precipitated sea salt. The elements which showed the greatest addition as a result of seawater precipitation were those that were most abundant in seawater: chlorine, sodium, magnesium, sulfur, calcium, potassium and strontium. Other elements

showed no change due to seawater precipitation as they are of such low concentrations in seawater (see Table 5.3).

Clay 1: Kaol + Chl +Ill							
	CaO (wt%)	**MgO (wt%)**	**Na_2O (wt%)**	**K_2O (wt%)**	**SO_3 (wt%)**	**Cl (wt%)**	**Sr (ppm)**
Freshwater Clay	0.343	0.266	0.094	0.320	0.000	0.014	25.340
Freshwater Clay (sea salt removed)	0.343	0.264	0.084	0.319	0.000	0.000	25.288
Aliquot of element which is attributable to the sea salt content	0.000	0.002	0.011	0.000	0.000	0.014	0.051
1 month	0.114	0.462	1.045	0.389	0.088	0.829	29.951
1 month (sea salt removed)	0.090	0.371	0.422	0.368	0.000	0.000	26.915
Aliquot of element which is attributable to the sea salt content	0.025	0.091	0.622	0.020	0.088	0.829	3.036
5 months	0.191	0.708	2.781	0.390	0.428	2.714	37.401
5 months (sea salt removed)	0.111	0.408	0.745	0.324	0.112	0.000	27.468
Aliquot of element which is attributable to the sea salt content	0.081	0.299	2.037	0.066	0.316	2.714	9.933

Table 5.4: Concentration of elements attributable to the influence of sea salt precipitation in kaolinite, chlorite and illite sample. Zero values are below detection limit, where not the result of subtraction.

Clay 2: Ca-Montmorillonite							
	CaO (wt%)	**MgO (wt%)**	**Na_2O (wt%)**	**K_2O (wt%)**	**SO_3 (wt%)**	**Cl (wt%)**	**Sr (ppm)**
Freshwater Clay	1.777	3.659	0.392	0.096	0.000	0.036	90.522
Freshwater Clay (sea salt removed)	1.776	3.655	0.365	0.095	0.000	0.000	90.396
Aliquot of element which is attributable to the sea salt content	0.001	0.004	0.027	0.001	0.000	0.036	0.126
1 month	0.683	3.978	5.911	0.403	0.786	5.527	58.570
1 month (sea salt removed)	0.519	3.368	1.764	0.268	0.142	0.000	38.343
Aliquot of element which is attributable to the sea salt content	0.164	0.609	4.147	0.135	0.644	5.527	20.227
5 months	0.367	4.047	4.972	0.397	0.501	3.971	40.806
5 months (sea salt removed)	0.249	3.609	1.992	0.300	0.039	0.000	26.145
Aliquot of element which is attributable to the sea salt content	0.118	0.438	2.980	0.097	0.463	3.971	14.661

Table 5.5: Concentration of elements attributable to the influence of sea salt precipitation in Ca-montmorillonite sample. Zero values are below detection limit, where not the result of subtraction.

Clay 3: Goethite							
	CaO (wt%)	MgO (wt%)	Na_2O (wt%)	K_2O (wt%)	SO_3 (wt%)	Cl (wt%)	Sr (ppm)
Freshwater Clay	0.040	0.173	0.125	0.023	0.000	0.036	4.713
Freshwater Clay (sea salt removed)	0.039	0.169	0.098	0.022	0.000	0.000	4.580
Aliquot of element which is attributable to the sea salt content	0.001	0.004	0.027	0.001	0.000	0.036	0.132
1 month	0.062	0.231	0.312	0.032	0.028	0.273	7.504
1 month (sea salt removed)	0.054	0.201	0.108	0.026	0.000	0.000	6.498
Aliquot of element which is attributable to the sea salt content	0.008	0.030	0.204	0.007	0.028	0.273	1.006
5 months	0.094	0.317	0.891	0.046	0.147	0.813	11.494
5 months (sea salt removed)	0.070	0.227	0.281	0.026	0.053	0.000	8.475
Aliquot of element which is attributable to the sea salt content	0.024	0.090	0.610	0.020	0.095	0.813	3.019

Table 5.6: Concentration of elements attributable to the influence of sea salt precipitation in goethite sample. Zero values are below detection limit, where not the result of subtraction.

Clay 4: Illite							
	CaO (wt%)	MgO (wt%)	Na_2O (wt%)	K_2O (wt%)	SO_3 (wt%)	Cl (wt%)	Sr (ppm)
Freshwater Clay	1.578	3.937	4.066	5.940	0.479	3.482	54.952
Freshwater Clay (sea salt removed)	1.475	3.553	1.453	5.855	0.073	0.000	41.349
Aliquot of element which is attributable to the sea salt content	0.103	0.384	2.613	0.085	0.406	3.482	13.603
1 month	1.611	4.268	0.526	6.572	0.049	0.352	42.661
1 month (sea salt removed)	1.601	4.229	0.262	6.563	0.008	0.000	41.307
Aliquot of element which is attributable to the sea salt content	0.010	0.039	0.264	0.009	0.041	0.352	1.354
5 months	1.353	3.973	1.442	6.155	0.162	1.281	39.836
5 months (sea salt removed)	1.315	3.832	0.480	6.124	0.012	0.000	34.853
Aliquot of element which is attributable to the sea salt content	0.038	0.141	0.962	0.031	0.149	1.281	4.983

Table 5.7: Concentration of elements attributable to the influence of sea salt precipitation in illite sample. Zero values are below detection limit, where not the result of subtraction.

Clay 5: Halloysite							
	CaO (wt%)	**MgO (wt%)**	**Na_2O (wt%)**	**K_2O (wt%)**	**SO_3 (wt%)**	**Cl (wt%)**	**Sr (ppm)**
Freshwater Clay	0.015	0.000	0.104	0.022	0.006	0.068	0.229
Freshwater Clay (sea salt removed)	0.013	0.000	0.052	0.021	0.000	0.000	0.000
Aliquot of element which is attributable to the sea salt content	0.002	0.000	0.051	0.002	0.006	0.068	0.229
1 month	0.107	0.167	1.416	0.104	0.216	1.592	8.296
1 month (sea salt removed)	0.059	0.000	0.222	0.066	0.030	0.000	2.557
Aliquot of element which is attributable to the sea salt content	0.047	0.167	1.194	0.039	0.185	1.592	5.739
5 months	0.302	0.270	2.125	0.186	0.379	2.016	20.984
5 months (sea salt removed)	0.242	0.048	0.611	0.136	0.144	0.000	13.647
Aliquot of element which is attributable to the sea salt content	0.060	0.222	1.513	0.049	0.235	2.016	7.336

Table 5.8: Concentration of elements attributable to the influence of sea salt precipitation in halloysite sample. Zero values are below detection limit, where not the result of subtraction.

The original freshwater samples 1, 2, 3 and 5 had only small amounts of chlorine present. Accordingly, when the equation to determine the sea salt contributions of each element was applied, only negligible changes were seen. However, the original illite sample (number 4) showed relatively enriched concentrations of calcium, magnesium, sodium, potassium, sulfur, chlorine and strontium, due to the sample being formed in an inland, high-salinity lacustrine environment. Over the five-month period, the concentrations of precipitated salts in the illite showed an initial decrease followed by an increase from the original sample. This is most likely due to dissolution of the original high salt content during initial contact with the seawater at the commencement of the *in situ* experiment, followed by acquisition of new salt.

The correction to analyses for salt content is in general small, but it is necessary since the concentrations change significantly for elements that are abundant in seawater relative to freshwater sediments, such as Na and Sr.

5.6.2. *In situ* clay pipe experiments

The changes which occur to freshwater clays as they interact with the marine environment can have major effects on concentrations of elements within the clays. The extent of change depends on a number of variables including: bonding energies of the major cations Ca^{2+}, Mg^{2+}, K^{+} and Na^{+} ions; the cations originally in the exchangeable sites in/on the clay minerals; the variation in charge of the exchange positions; the ionic activity of the seawater; and the buffer mechanism of the seawater in terms of pH (Carroll and Starkey, 1958; Keller, 1963). This study focuses on the effect seawater has on the concentration of selected elements in a freshwater clay sediment, independent of the chemistry occurring at the seafloor sediment surface or with burial.

The reactions of clay minerals in seawater occur rapidly, with changes occurring within ten days of immersion in the seawater (Mackenzie and Garrels, 1965), as a result of ion exchange reactions between seawater and river-derived suspended matter rapidly reaching equilibrium in the ocean (Sayles and Mangelsdorf, 1977). During the five months that the clay samples were suspended in the estuarine water column, analysis detected minor changes to the overall chemical composition of the clays (Appendix 2, Table A.9). These changes were in general compatible with the comparison of freshwater particulates and marine sediments by Martin and Whitfield (1983), showing increases in concentration of sodium, strontium, sulfur and some other cations that are more abundant in seawater than in freshwater (Table 5.9). However, the changes in concentration of elements in the *in* situ experiments also showed dependence on the clay type. In order to determine post-depositional additions and transformations in the clays, this study plots variation of a range of elements against the immobile component Al_2O_3 to determine the relative additions and transformations occurring within the sediments. Aluminium has been shown to be a conservative element, with its concentration remaining stable in the estuarine environment (Kemp, 1976; Kemp and Thomas, 1976; Wasserman, 2001).

	Rivers		Ocean	
Element	**Dissolved (ppb)**	**Particulate (ppm)**	**Water (ppb)**	**Deep sea clays (ppm)**
As	0.3	0.07	0.04	0.1
Al	50	94000	0.5	95000
As	1.7	5	1.5	13
Au	0.002	0.05	0.004	0.003
B	18	70	4440	220
Ba	60	600	20	1500
Br	30	5	67000	100
Ca	13300	21500	412000	10000
Cd	0.02	1	0.01	0.23
Ce	0.08	95	0.001	100
Co	0.2	20	0.05	55
Cr	1	100	0.3	100
Cs	0.035	6	0.4	5
Cu	1.5	100	0.1	200
Er	0.004	3	0.0008	2.7
Eu	0.001	1.5	0.0001	1.5
Fe	40	48000	2	60000
Ga	0.09	25	0.03	20
Gd	0.008	5	0.0007	7.8
Hf	0.01	6	0.007	4.5
Ho	0.001	1	0.0002	1
K	1500	20000	380000	28000
La	0.05	45	0.003	45
Li	12	25	180	45
Lu	0.001	0.5	0.0002	0.5
Mg	3100	11800	$1.29x10^6$	18000
Mn	8.2	1050	0.2	6000
Mo	0.5	3	10	8

Table 5.9: The concentrations of dissolved and particulate elements in river water, and concentrations of elements in water and deep sea clays in the ocean (Martin and Whitfield, 1983).

	Rivers		Ocean	
Element	**Dissolved (ppb)**	**Particulate (ppm)**	**Water (ppb)**	**Deep sea clays (ppm)**
Na	5300	7100	$1.077x10^7$	20000
Nd	0.04	35	0.003	40
Ni	0.5	90	0.2	200
P	115	1150	60	1400
Pb	0.1	100	0.003	200
Pr	0.007	8	0.0006	9
Rb	1.5	100	120	110
Sb	1	2.5	0.24	0.8
Sc	0.004	18	0.0006	20
Si	5000	285000	2000	283000
Sm	0.008	7	0.0005	7
Sr	60	150	8000	250
Ta	<0.002	1.25	0.002	1.0
Tb	0.001	1.0	0.0001	1.0
Th	0.1	14	0.01	10
Ti	10	5600	1	5700
Tm	0.001	0.4	0.0002	0.4
U	0.24	3	3.2	2.0
V	1	170	2.5	150
Y	-	30	0.0013	32
Yb	0.004	3.5	0.0008	3
Zn	30	250	0.1	120

Table 5.9 (continued): The concentrations of dissolved and particulate elements in river water, and concentrations of elements in water and deep sea clays in the ocean (Martin and Whitfield, 1983).

By using a range of different clays, it was possible to account for the variations in concentrations of elements according to the different clay chemistry, mineralogy and structure. A large number of elements showed minimal changes over the five-month period. However, the elements which did show change gave insight into the evolving geochemistry of the clays as influenced by oxygenated seawater only. Plotting Al_2O_3 against Na_2O in the clays shows two clear groups of samples (not including the Fe-oxide): those which are high aluminium (the 1:1 dioctahedral clays, kaolinite and halloysite) and those which are low aluminium (the 2:1 clays, illite and smectite) (Figure 5.8). Whereas the aluminium concentrations remain relatively unchanged as expected, the sodium concentrations show an increase over time in all the clay samples except the illite. This is also to be expected, since sodium has a high concentration in seawater, is adsorbed readily to the surface of negatively charged clay particles, and also substitutes for Ca^{2+}, Mg^{2+}, Al^{3+} and K^+. The Ca-montmorillonite shows the largest

increase in sodium, reflecting a combination of both surface adsorption and also cation exchange, replacing the calcium.

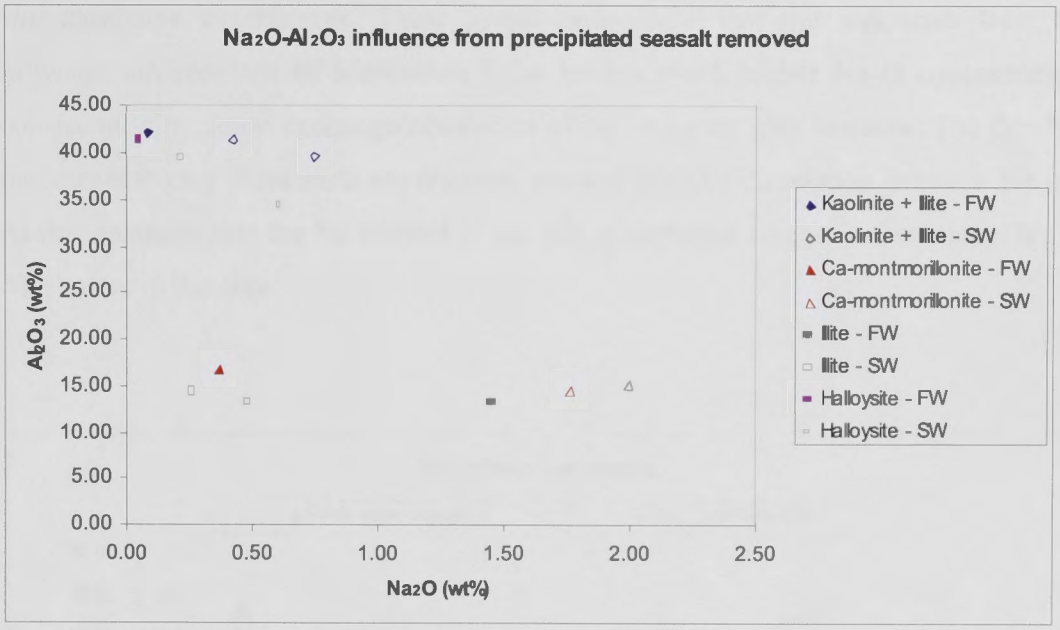

Figure 5.8: Change in sodium concentration in clay samples over a five month period. The values are plotted with the influence of precipitated sea salt removed, and readjusted to 100%. Freshwater samples, FW, (filled symbols) are indicative of the original sample. Saltwater samples, SW, (empty symbol) represent the sample after a five month period in this and subsequent figures.

The illite sample shows evidence of its original hypersaline lake source, through an initial decrease in concentration of sodium from the original sample, to those samples taken after one month and five months. The halloysite sample (Figure 5.8) shows a slight decrease in aluminium and a slight increase in sodium over time. The slight decrease in aluminium is likely due to exchange processes occurring between the halloysite sample and the seawater, whereby exchangeable Al is replaced by Ca^{2+}, Mg^{2+}, K^{+} or Na^{+} (Hendershot *et al.*, 1996; Mkadam *et al.*, 2006). The slight increase of sodium in the halloysite sample may be due to adsorption and/or exchange.

The trends observed in the clay pipe experiments can also be observed in nature. A comparison of the freshwater and saltwater samples collected *in situ* from Merimbula Lake estuary and catchment show a linear correlation between the Na_2O concentrations relative to Al_2O_3 (Figure 5.9), particularly with respect to the saltwater sediments. The freshwater sediments sourced from the creeks and dams in the catchment show low

Na_2O, with no strong correlation between Al_2O_3 and Na_2O, because sodium and aluminium are largely decoupled during the weathering cycle as Na^+ goes into solution. The increase in sodium relative to aluminium is consistent with the trends seen in the *in situ* clay pipe experiments. These graphs also show that the sediments from the saltwater environment of Merimbula Lake have a much higher Na_2O concentration, consistent with cation exchange/adsorption of Na^+ onto the clay surfaces. The fact that the seawater clay incubation experiments show a positive correlation between Na and Al demonstrates that the Na content is not due to saltwater contamination alone, but to Na content in the clay.

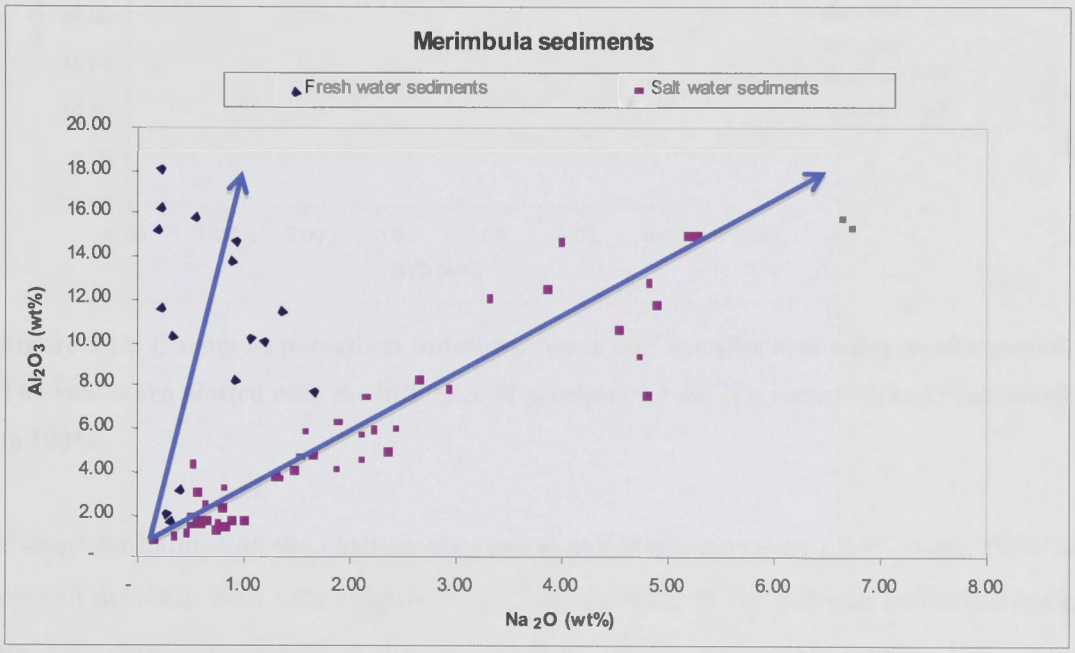

Figure 5.9: A comparison of the freshwater and saltwater samples collected *in situ* from Merimbula Lake estuary, and freshwater inputs from within the catchment.

In contrast to the behaviour of Na_2O, K_2O shows no change in the clay pipe experiments, for the kaolinite and halloysite sample (Figure 5.10). These 1:1 clay minerals have a low cation exchange capacity, and are therefore unable to adsorb potassium ions within the interlayer spacings. In contrast, the 2:1 layer group, which includes the Ca-montmorillonite and illite sample, shows slight increases in K_2O with time. The structure of montmorillonite and illite are similar, with the interlayer spacings being occupied by K^+ ions (Bergaya *et al.*, 2006). The increase of potassium in these

samples is due to adsorption from the seawater (Weaver, 1967). In part this increase in potassium may correspond accordingly with an inferred reduction of particle size and the related increase of surface area (Vaithiyanathan *et al.*, 1992) of the Ca-montmorillonite and illite, compared to the kaolinite and halloysite samples.

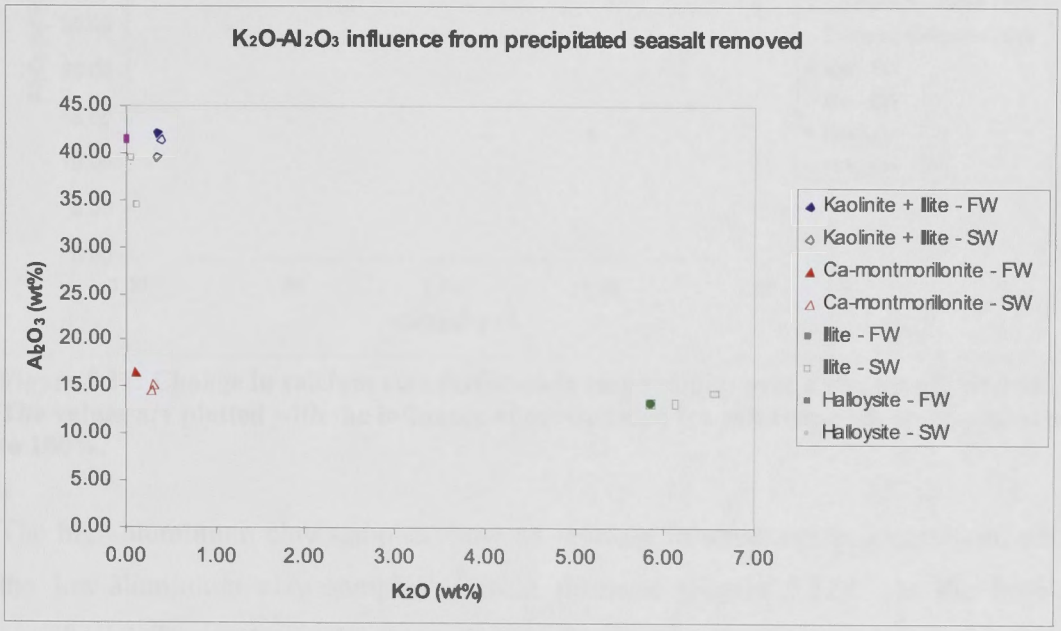

Figure 5.10: Change in potassium concentration in clay samples over a five month period. The values are plotted with the influence of precipitated sea salt removed, and readjusted to 100%.

Except for halloysite, the calcium concentrations in the clay pipe experiments show an overall decrease with time (Figure 5.11). The decrease in the calcium concentration in the clay pipe experiments is due to cation exchange, with exchangeable Ca^{2+} being replaced primarily by Na^{+}, and also Mg^{2+} and K^{+} from the seawater (Sayles and Mangelsdorf, 1977, 1979). The halloysite shows an increase in calcium, due to halloysite having a stronger bonding energy for Ca^{2+} than Mg^{2+} in seawater (Carrol and Starkey, 1958).

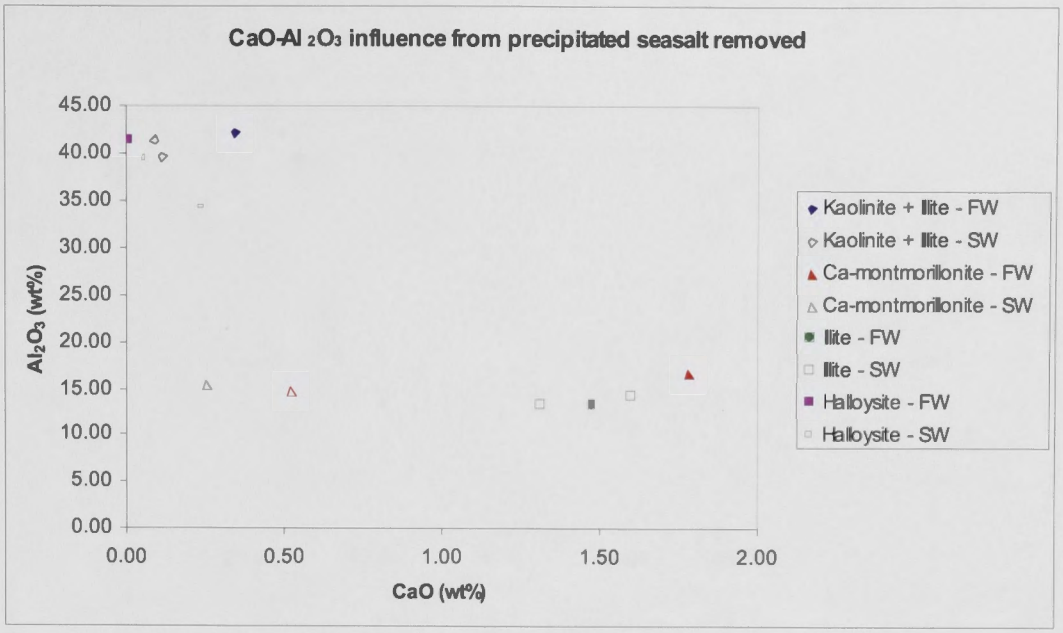

Figure 5.11: Change in calcium concentration in clay samples over a five month period. The values are plotted with the influence of precipitated sea salt removed, and readjusted to 100%.

The high-aluminium clay samples show an increase in strontium concentration, while the low-aluminium clay samples show a decrease (Figure 5.12). In the high-Al samples, Sr^{2+} may be both adsorbed onto the surface particles and undergo cation exchange in the lattice of the mineral, whereas in the low-Al samples the decrease in the strontium concentration is due to cation exchange, with Sr^{2+} being replaced by Na^{+}, Mg^{2+} and K^{+} from the seawater. Since strontium is similar in charge and bonding energy to calcium, it would be expected to decrease with calcium. Sr will substitute for Ca in minerals including plagioclase feldspar, apatite, sulfides (gypsum and anhydrite), and carbonates (dolomite, calcite and aragonite) (Capo *et al.*, 1998).

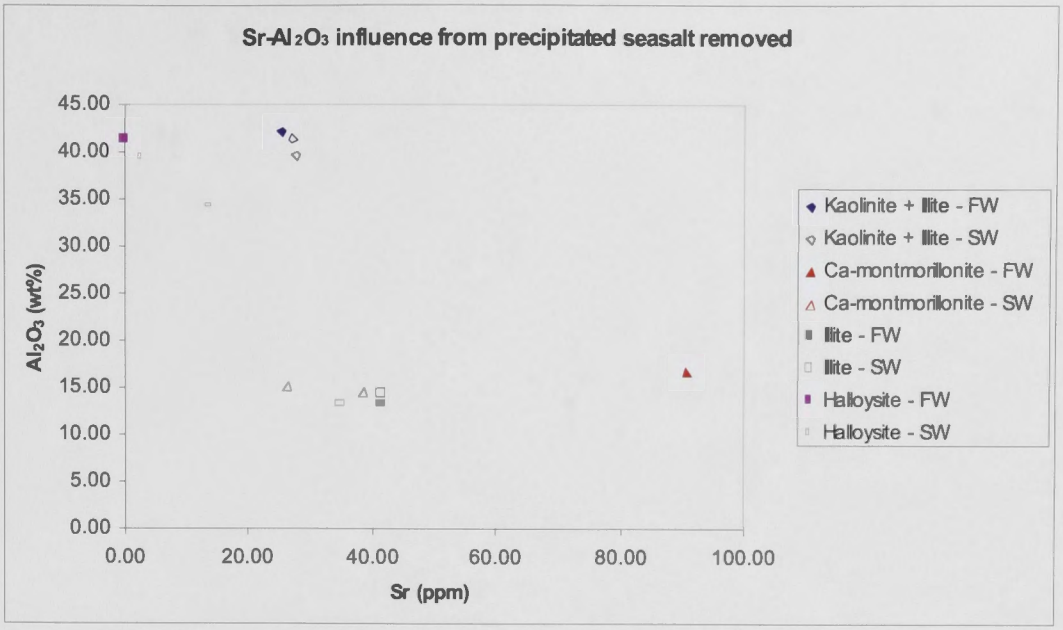

Figure 5.12: Change in strontium concentration in clay samples over a five month period. The values are plotted with the influence of precipitated sea salt removed, and readjusted to 100%.

Even though Mg^{2+} ions from seawater should move into the exchange positions in minerals in preference to Ca^{2+} and Na^{+} ions according to Carroll and Starkey (1958), Carter and Wilde (1972) and Sparks (2003), the magnesium in the clay pipe experiments shows very little change over time (Figure 5.13). Plotting magnesium against aluminium in the natural sediment samples from the estuary shows strong correlations in both the freshwater samples and the saltwater samples. This suggests that magnesium is mainly present in the structural layers of the clay component of the sediments. The magnesium concentration in the clay pipe experiments shows only a slight increase due to substitution within the clays.

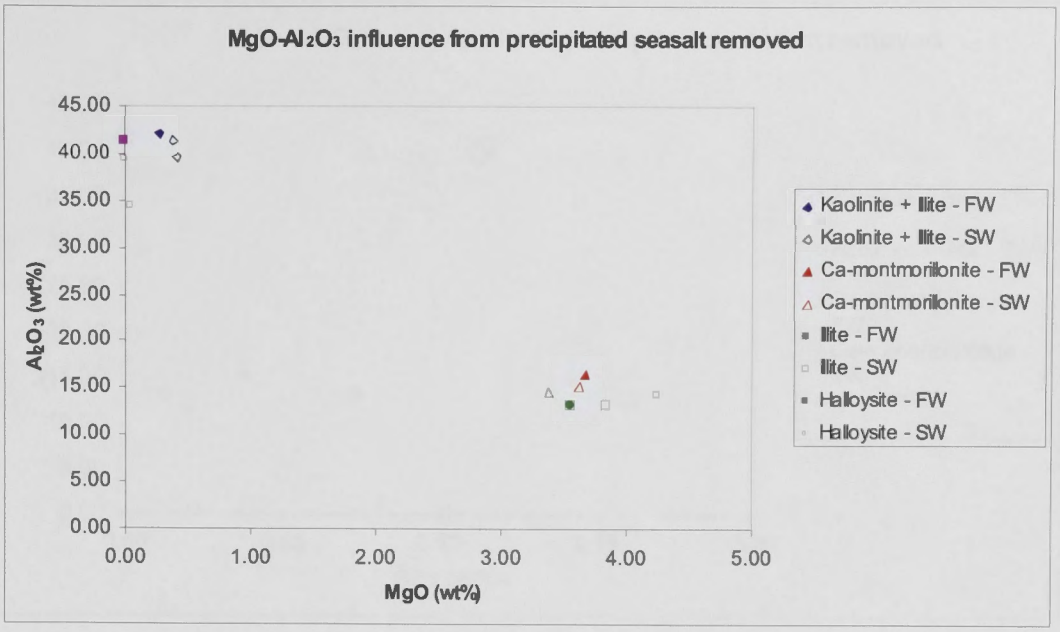

Figure 5.13: Change in magnesium concentration in clay samples over a five month period. The values are plotted with the influence of precipitated sea salt removed, and readjusted to 100%.

In the suspended clay pipes, none of the clay samples showed a significant change in iron content over time. The total concentration of iron in seawater is 0.0034 ppm, although in coastal waters the total amount of iron decreases rapidly with distance from the shore (Sugimura *et al.*, 1978), therefore iron content in the estuary may be higher. The ability of seawater to introduce iron into the clays is minimal, and iron that is already present in clays or oxyhydroxides would not be expected to be very mobile. In this study it is apparent that the influence of iron dissolved in seawater on the clays is minimal (Appendix 2, Table A.9).

Sulfur concentrations showed an increase in all clay types over the five month period (Figure 5.14). This sulfur is added from the aerated tidal ocean water (604 ppm) as sulfate (SO_4^{2-}), and is not sulfide formed by sulfate-reducing bacteria, as would occur in the sediment column of an estuary.

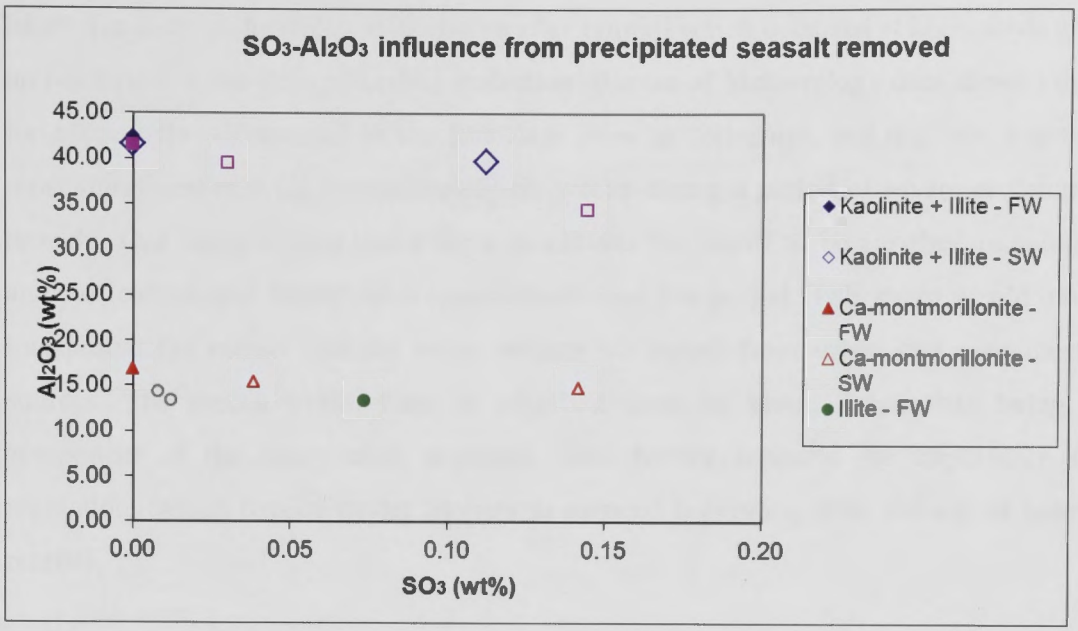

Figure 5.14: Change in sulfur concentration in clay samples over a five month period. The values are plotted with the influence of precipitated sea salt removed, and readjusted to 100%.

Bearing in mind that these clay pipe experiments were designed specifically to look at the influence of the seawater column upon sediments entering an estuary, some remarkable changes were observed in the trace element concentrations. These have nothing to do with subsurface authigenic/biogenic processes that are discussed in the next chapter, but only with the processes occurring specifically in the water column. Unusually large increases in copper and zinc occurred in the clay pipe experiments, particularly in the Ca-montmorillonite sample (Figure 5.15 and Figure 5.16). Elements such as Cu, Zn and Pb are of low concentration in seawater, or in the weathered rocks from the catchment, so large increases in concentrations in the clay pipe experiments over time are therefore likely to be indicative of anthropogenic additions to the seawater. Merimbula Lake is nominally a relatively pristine estuary system with little anthropogenic input of metals, especially in respect to the water quality which is strictly maintained due to the local importance of the oyster farming industry. Hence, high concentrations of potentially toxic elements were not expected. The analyses show a one-off peak in copper and zinc concentrations in the Ca-montmorillonite sample after one month, which then returned to previously low levels after five months (Appendix 2, Table A.9). This suggests equilibration with an ephemeral source of high Cu. It is most

likely due to an anthropogenic discharge after rainfall which occurred at Merimbula and up catchment in the days preceding collection. Bureau of Meteorology data showed that for Merimbula ~20mm fell in the four days prior to collection, and that this was the most significant rain for approximately six weeks during a period of severe prolonged drought. One could expect under those conditions for runoff to be enriched in solutes and particulates that would have accumulated over that period. This event would have transported the metals into the water column via runoff from urban and agricultural sources. The metals would then be adsorbed onto the clays, rather than being a component of the precipitated seawater. This further supports the importance of regulations which require oyster farmers to suspend harvesting after periods of heavy rainfall.

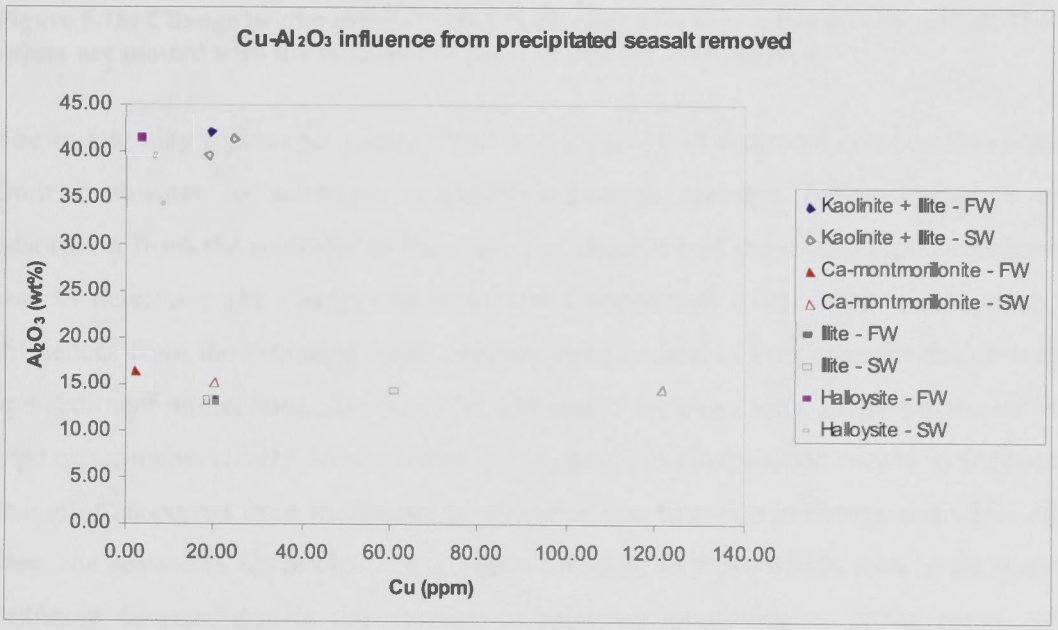

Figure 5.15: Change in copper concentration in clay samples over a five month period. The values are plotted with the influence of precipitated sea salt removed.

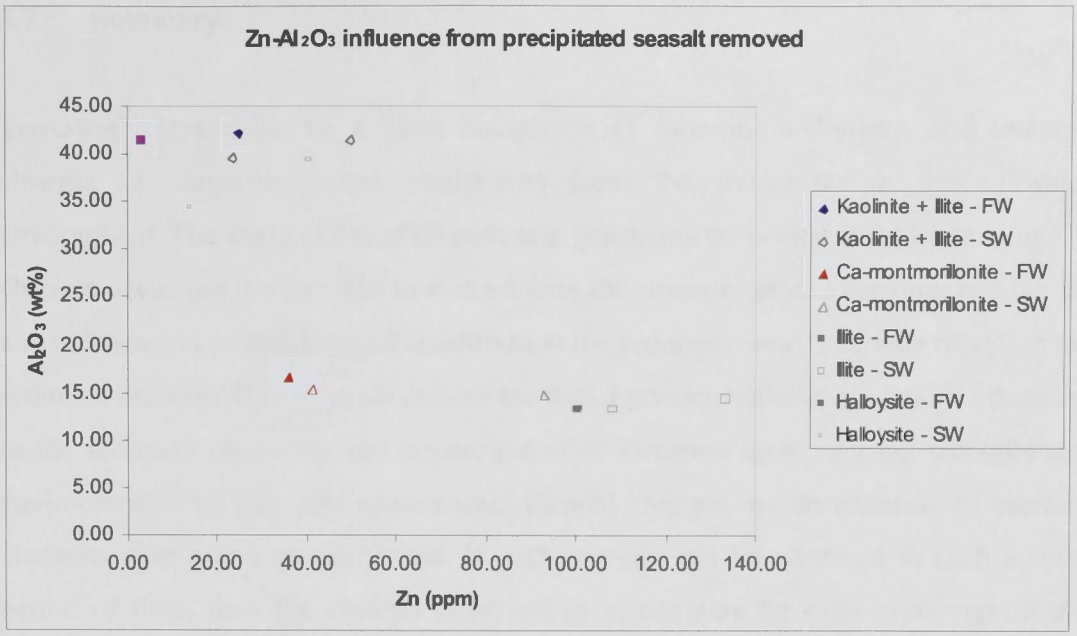

Figure 5.16: Change in zinc concentration in clay samples over a five month period. The values are plotted with the influence of precipitated sea salt removed.

The *in situ* clay pipe experiments show that a change in sediment composition occurs from freshwater to saltwater, whereby sediments undergo cation exchange and adsorption from the seawater to the clay. The objective of these clay pipe experiments was to determine the changes in elemental composition of the clays in response to influences from the estuarine water column, independent of later changes due to burial and sediment interactions. Although the changes in the clays were small, the *in situ* clay pipe experiments clearly demonstrated that a change in composition occurs in sediments that are transported from freshwater to saltwater, due to cation exchange and adsorption from the seawater. These changes are quite different to those trends seen in the natural sediment column, due to the absence of reducing environments in the pipes. This highlights the importance of the geochemistry of the environment on the potential uptake of elements by the sediments, which will be dependent on whether the sediments are *in situ* in the sediment column, or are in the water column.

5.7. Summary

Terrestrial clays make up a large component of estuarine sediments, and undergo changes in chemistry when transported from the freshwater to the saltwater environment. The study of estuarine sediment geochemistry is vital in understanding the changes occurring to clays due to contact with the seawater prior to settling and burial, and independent of geochemical conditions at the sediment-water interface or within the sediment column. This research defines the initial pre-depositional alterations occurring to the sediment chemistry and concentration of elements upon entering the saltwater environment. The clay pipe experiments showed changes in concentration of selected elements over a five month period. If such changes can be observed in such a short period of time, then the changes observed in nature may be even more significant. Variation of chemistry with time may also reflect climatic and anthropogenic factors. It is simple to observe changes in composition when the starting material is of a known composition. However, it is more of a challenge with natural sediment samples, which contain a range of species in varying proportions, mixed together from a variety of sources.

As the composition of seawater exerts a strong influence on the composition of the sediments in an estuary, this study shows that caution must be excercised in relating sediment geochemistry from estuaries to a geochemical signature that relates directly to the terrestrial source material. This study is pinpointing the geochemical changes occurring in the estuarine environment which may influence the total overall composition of the sediments. This is a valuable technique as it takes into account the original source material as well as additions and transformations of elements as a result of post-depositional geochemical alterations and processes.

Chapter Six: Geochemistry of Estuarine Sediments - Natural and Anthropogenic Factors

6.1. Introduction

Sediments which are classified as being polluted are generally assumed to have a concentration of a particular substance or element that is above baseline concentrations or standard sediment quality guidelines (Albanese *et al.*, 2007). In a fluvial system, pollutants such as metals, organic and inorganic chemicals and nutrients are added to the sediments via a range of mechanisms including runoff, leaching, and dumping. These inputs, which may be from anthropogenic and sometimes naturally anomalous sources, are added to the original transported weathering product post-deposition. We are therefore presented with a before and after contamination scenario. In a heavily polluted environment, where point sources of pollutants are obvious, pollutant loadings may be compared to baseline data to identify the enrichment factor within the sediment. In systems where the pollutant levels are only small, it can be more difficult to discriminate what is associated with the original weathering product, and what is added post-deposition.

In the last chapter the effects of cation exchange and adsorption on clays immersed in seawater were examined. These effects were especially evident for the elements Na, K, Ca and Mg. The terrestrial sediments which have been deposited in the estuary have also undergone similar changes in geochemistry; however, as the estuarine sediments represent a mix of terrigenous and marine components, there is no 'original' sediment sample with which to make comparisons. To make observations regarding the post-depositional transformations and additions affecting the sediments we therefore need to compare the estuarine sediment samples to a baseline composition, which represents a mixture of clays and sands. Using a conservative element that remains unchanged

between the freshwater and marine environment further establishes a baseline in the data, which can be compared with other elements that may be modified by deposition in the marine environment.

This chapter presents the results of a field and geochemical study of the physical and chemical modifications which occur in sediments when they are transported from a freshwater to marine environment. Some of these modifications can be shown to occur naturally, whereas others are identified as being specifically due to anthropogenic influences. By linking regolith geoscience with coastal aquatic geochemistry, it is possible to identify the role that transported regolith plays in the concentration of potentially toxic elements in the depositional environment of an estuary. A close examination of the changing geochemistry of the sediments may also assist in understanding how urban centres impact on the transformations and accumulations of particular elements which lead to environmental problems.

6.2. Influences on the sediment geochemistry of Australian estuaries

As estuaries are important areas of urban and recreational growth and development, the impact of urbanisation on estuarine sediment geochemistry is significant, resulting in an increased pollutant load to both the water and the sediments. In many populated regions around the world, estuarine sediments are highly contaminated due to riverine transport of suspended sediments and their associated contaminants, derived from upstream industrialized or agricultural regions. In south-eastern Australia, where populations are spread out and industry along river systems is minimal, the estuaries are relatively pristine. For this reason, Australian estuaries provide the perfect setting to demonstrate, through sediment geochemistry, that upper catchment compositions do not necessarily reflect the final composition: there are post-depositional additions and transformations (authigenic, biogenic, anthropogenic, and terrigenous) and geochemical processes that alter the original sediment.

Many northern-hemisphere river catchments have long histories of concentrated settlement, industry and mining along vast river systems (Nelson *et al.*, 1993, Walther *et*

al., 2003). As a result, heavy metal pollution is added to terrigenous sediments during transport along these rivers, and heavy metals are already immobilised by their associations with fine particulate clay, organic material and oxide coatings. This process of heavy metal fixation to clays, organic matter and secondary oxides results in a positive correlation between heavy metal concentration and the proportion of sediment which falls in the finest size fractions. Thus upon final deposition within river beds, estuaries or out to sea, the heavy metal pollution is principally pre-depositional, and could have occurred hundreds or thousands of kilometres upstream from the final deposition site.

In contrast, small east Australian catchments such as Merimbula differ from typical northern-hemisphere catchments in that they lack upstream industry and population centres. In addition, a low flow rate, entrance and depositional morphologies and environments mean that sediments are essentially trapped within lake systems. The largest population centre in the catchment for Merimbula is the township of Merimbula itself, which is located adjacent to the estuary. Close to the township, any heavy metal pollution will be seen clearly to be a post-depositional feature, associated with the coarser-grained sediments of the Front Lake rather than finer-grained sediments of the Top Lake. This data therefore highlights some distinctive features of the Australian landscape.

Due to the fact that estuarine systems represent a sedimentary sink of marine and terrestrial components, as populations increase in coastal areas, so do the anthropogenic impacts on the estuarine systems (Prasad and Ramanathan, 2008). As drought conditions worsen and populations rise, the heavy metal inputs, and their fixation and immobilisation by additional nutrient loads entering the sediment may cause increased accumulation. Changing geochemical conditions within the sediment, such as redox boundaries, may increase the potential for remobilization of elements into the water column, and therefore increase bioavailability of potentially toxic elements. An understanding of the geochemistry of the original sediments and how they are transformed from freshwater into a marine setting is therefore vital in determining the contrasting geochemistry of anthropogenically added metals.

6.3. Geochemistry of sediments

The sediment types identified in Merimbula and Pambula Lakes include a mixture of mature beach sands; organic rich silt/clays, which dominate the Top Lake and creeks; minor, poorly sorted terrigenous sand/gravels of arkosic composition; and organic-free clay/silt sampled from the freshwater creeks and rivers upstream of the estuary. The sediments as a whole can be defined as a binary mixture of two components – (a) the terrestrial clay and detrital gravel component transported seaward from the local catchment sources, and (b) the mature, quartz-dominated beach sands. The mature beach sands dominate the seaward side of the estuary and form a prograding delta into the estuary, manifesting at sea level as a tide-dominated flat. Coming from the landward side is a clay-dominated terrigenous component that is principally transported into the estuary during high rainfall events in the upland catchment. These muds are concentrated in the deeper water below tide-dominated sections, but also intermix with the above mentioned beach sands. A third, though minor, component is a coarser-grained, gravelly arkosic sand, which is deposited within deltas at the small creek mouths. A simple physical-chemical mixing of these components would theoretically produce simple linear correlations between their components. However, the aims of this research are to determine and to show:

1. What geochemical and compositional changes occur in sediments upon transfer from the freshwater to the saltwater environment;
2. Whether there are geochemical differences, both in terms of overall composition and variability in chemical conditions within different areas of the estuary (either due to natural processes or pollutants); and
3. The degree to which the final composition of a sediment can reflect the original source material.

In order to do this, bulk rock geochemistry data has been used to examine the behaviour of authigenic, biogenic and potentially anthropogenically derived metal additions with respect to conservative elements (the rare earth elements, REE) in a range of sediments sourced from a single estuary.

The relationships between the REE and other metals, in most cases, follow two distinct trends: (a) a mixing line between the sedimentary end members (based on mineralogical composition); and (b) a trend which deviates from the sediment end member mixing line. These trends distinguish between original material and the material added to the sediment post-deposition. Discrimination of these two major groups within the sediments not only allows enrichment factors to be determined. It also shows that elements which have been added after deposition are not only associated with what is geochemically stable, but that increases in concentration in proximity to urban development are evident. This is important as it shows certain elements existing in two separate phases: what is original and what is added.

6.3.1. The use of conservative elements to define sediment mixing end-members

In order to recognise the addition of certain elements to the sediment post-deposition, the chemistry of the original sediment must be known. The rare earth elements lanthanum and cerium were selected as potential monitors of original sediment compositions and mixing within the estuary, due to their likely conservative mixing behaviour from the freshwater to the marine environment. In other words, they were expected to show no change in fractionation as a result of sediment-water interactions. Lanthanum was plotted against cerium for samples which were representative of the sediment end-members present in the estuary (beach sands and fine-grained freshwater clays) as shown in Figure 6.1. The two sediments lay on a single mixing line between the beach sand (with only a small concentration of REE) and the terrigenous clay (with high concentrations of REE).

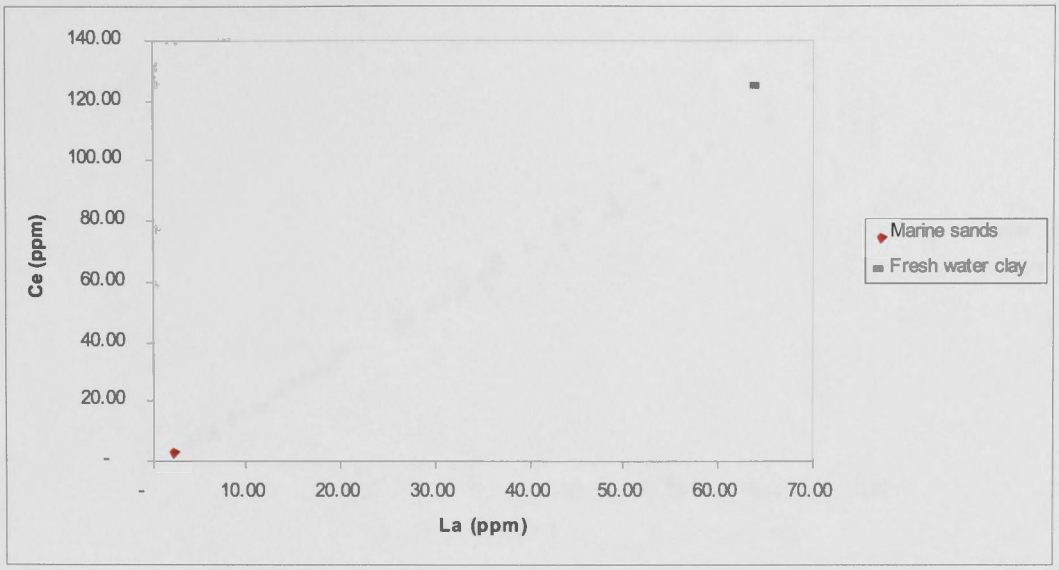

Figure 6.1: Relationship between Ce and La for the sedimentary end members: marine sands and freshwater clays.

All the available sediment samples from Merimbula Lake, Pambula Lake, Back Lagoon and from freshwater environments are mixtures of the same sediment types, so mixed sediment analyses from Merimbula Lake will plot between these two end-members (Figure 6.2). Freshwater and marine sediments all lay along a well-defined straight line trend ($R^2 = 0.9964$), demonstrating that seawater interaction does not perturb the Ce/La ratio, and hence that both elements behave conservatively. Locations of sediments are also distinguished in Figure 6.2, which shows no offsets or deviations away from the linear trend for any geographic location.

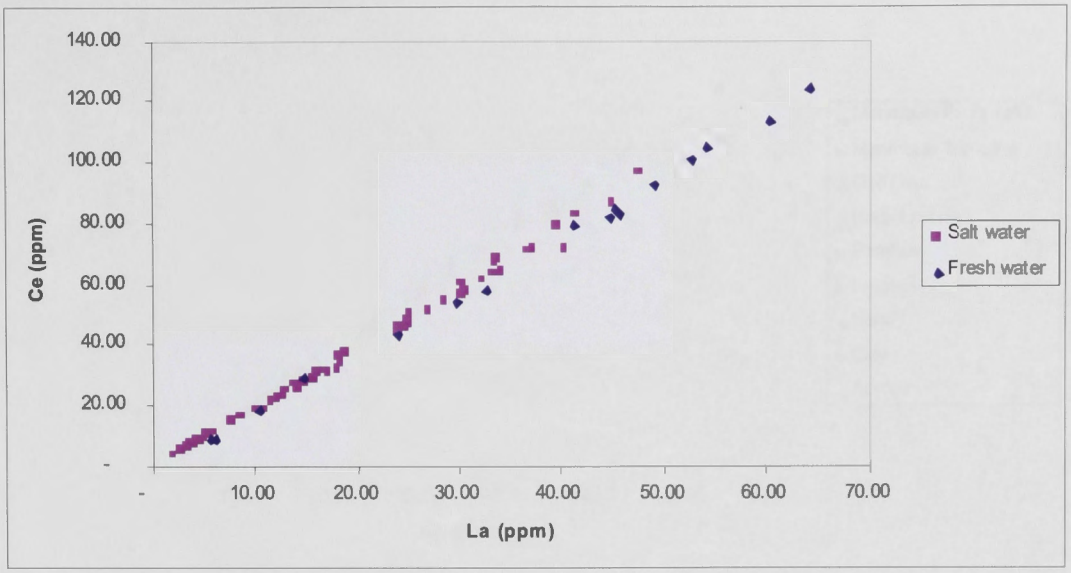

Figure 6.2: Mixing relationship between Ce-La in estuarine and freshwater sediments.

This data trend is thus consistent with the REE content of the sediments being unaffected by post-depositional, authigenic, biogenic and anthropogenic processes. Discriminating the source regions of the data collected illustrates that, independent of the variables in geochemistry with respect to the location from which the sample was collected, the REE ratio remains constantly linear ($R^2 = 0.9964$) (Figure 6.3). The REE remain unchanged as they change from freshwater to marine environments, with the freshwater REE samples following an identical pattern to the saltwater REE samples, thus showing the importance of the use of REE as conservative elements within this model. Similar constancy of ratios was also observed for the other REE.

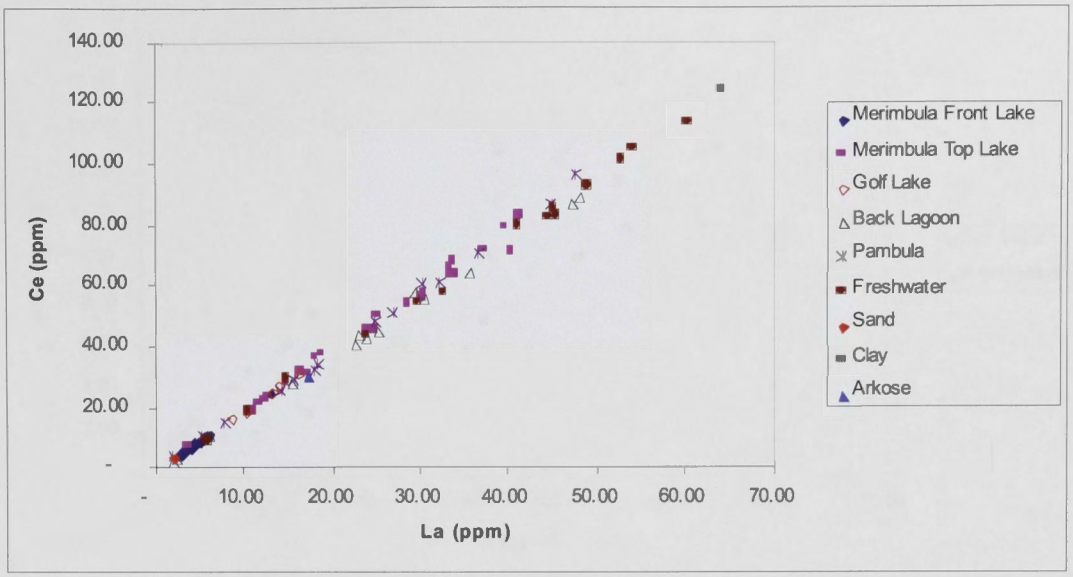

Figure 6.3: Mixing relationship between Ce-La in estuarine and freshwater sediments, by geographic location.

It is important to be able to recognise that the distributions of the REE in the system are in fact showing conservative behaviour. For comparison to the REE, aluminium is often used as a conservative tracer element (Weisberg *et al.*, 2000). In this system, although the behaviour of Al_2O_3 shows a positive correlation with lanthanum, there is a greater scatter in Al_2O_3 for a given La-content (Figure 6.4). The concentrations of aluminium do not correlate exactly with lanthanum, which could be a result of aluminium being partitioned through flocculation into colloidal and organically complexed forms (Xu *et al.*, 2002). This highlights the reliability of using the REE as the conservative elements for the model.

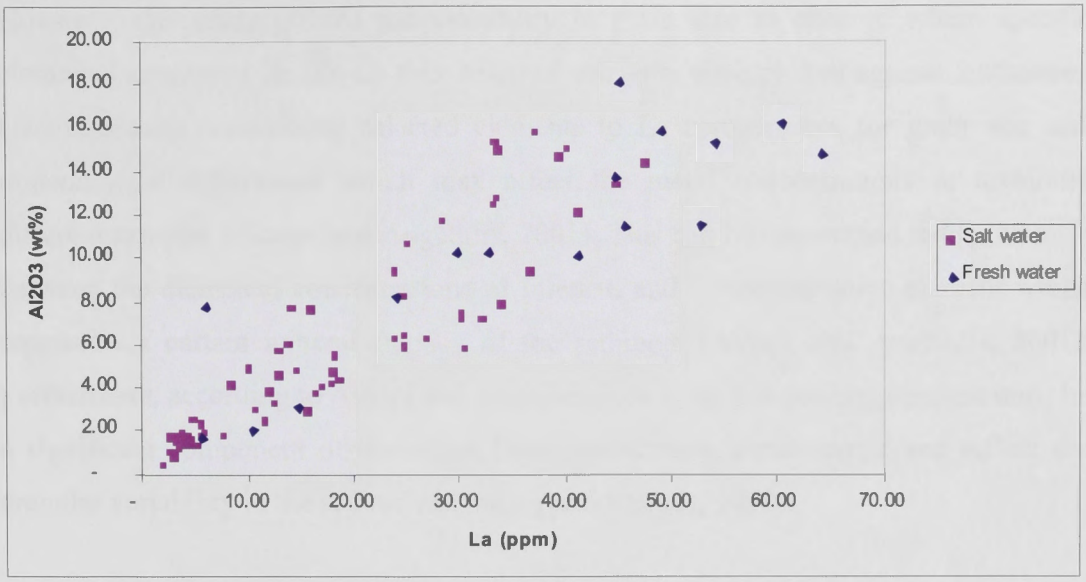

Figure 6.4: Mixing relationship between Al_2O_3-La in estuarine and freshwater sediments.

6.3.2. Normalisation of the geochemical data

Many elements, particularly metals, have higher concentrations in the finer grained sediments, which may be influenced by natural and anthropogenic sources. Since the different mineralogy of different particle size fractions may bias elemental concentrations within a sediment, normalisation techniques are generally used in order to correct for the influence of grain size on the concentration of elements in sediments (Loring, 1991; Loring and Rantala, 1992; Aloupi and Angelidis, 2001). Although there is no agreement on the exact methodology to be used for normalisation, there are two broad categories that are agreed upon: granulometric and geochemical (Daskalakis and O'Connor, 1995; Liaghati *et al.*, 2003). Granulometric techniques rely on normalisation against total weight percent fines (< 62.5 μm) or the total clay size particles within the sediments (< 4 μm) present in the sediment (Loring, 1991). Alternatively, geochemical methods of normalisation determine associations between concentrations of metals in the sediments with certain reference elements (Liaghati *et al.*, 2003). Commonly used reference elements include aluminium (Bruland *et al.*, 1974; Bertine and Goldberg, 1977; Sharman *et al.*, 1984; Windom *et al.*, 1989; Carral *et al.*, 1995; Daskalakis and O'Connor, 1995; Balls *et al.*, 1997; Trimble and Hoenstine, 1997), iron (Blomqvist *et al.*, 1992; Herut *et al.*, 1993; Tam and Yao, 1998; Fang and Hong, 1999), organic carbon (Daskalakis and O'Connor, 1995) and lithium (Loring, 1990, 1991).

However, this study utilises the variability in grain size to observe where specific elemental anomalies lie. To do this, selected elements were plotted against lanthanum. Geochemically normalising selected elements to La compensates for grain size and mineralogical differences which may affect the metal concentrations in texturally different samples (Aloupi and Angelidis, 2001). This can be determined using the ratio between the elemental concentrations of interest, and the conservative element which represents a certain mineral fraction of the sediment (Aloupi and Angelidis, 2001). Furthermore, according to Aloupi and Angelidis, 2001, the normalising element must be a significant component of the major fine-grained trace metal carrier and reflect the granular variability in the sediments (Loring and Rantala, 1992).

In order to provide further evidence for the conservative behaviour of the REE, the data from the sediments in the estuary were compared to that of the Post Archean Average Shale (PAAS) composition of Taylor and McLennan (1985). Normalising to chondrite shows the characteristic REE pattern of the average shale (Figure 6.5).

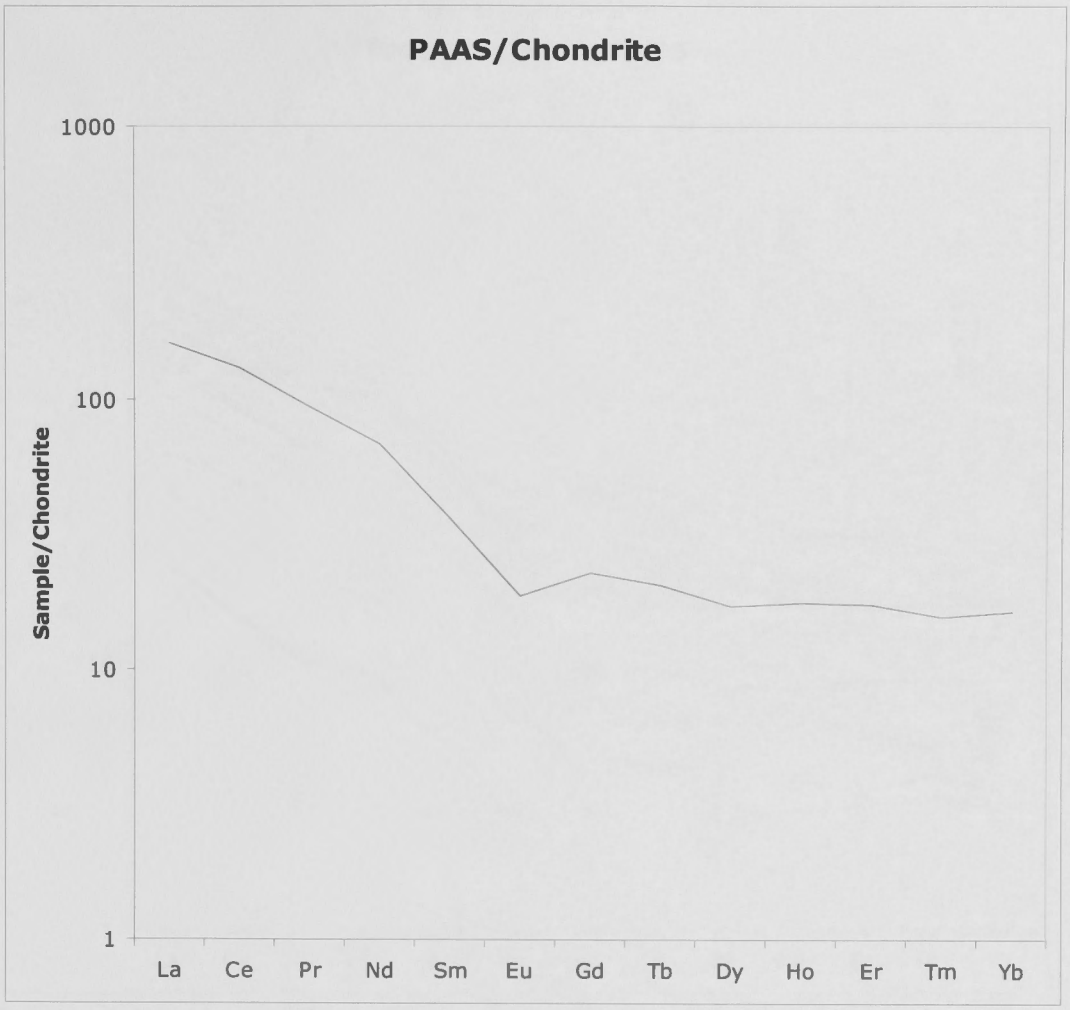

Figure 6.5: The Post Archean Average Shale REE normalised to chondrite abundances (Taylor and McLennan, 1985).

The steep LREE pattern, decreasing Eu anomaly and flat HREE pattern is typical of the upper crust. The REE for freshwater samples for this study are shown in Figure 6.6 for comparison. The most clay-rich samples show a normalised pattern that is remarkably similar to that of the PAAS. Note that the more quartz-rich samples have retained the same overall pattern, but with diminished overall concentration of the REE. This is consistent with the REE dominantly being found in the finer sediment fraction, with REE-poor quartz acting only as a diluent.

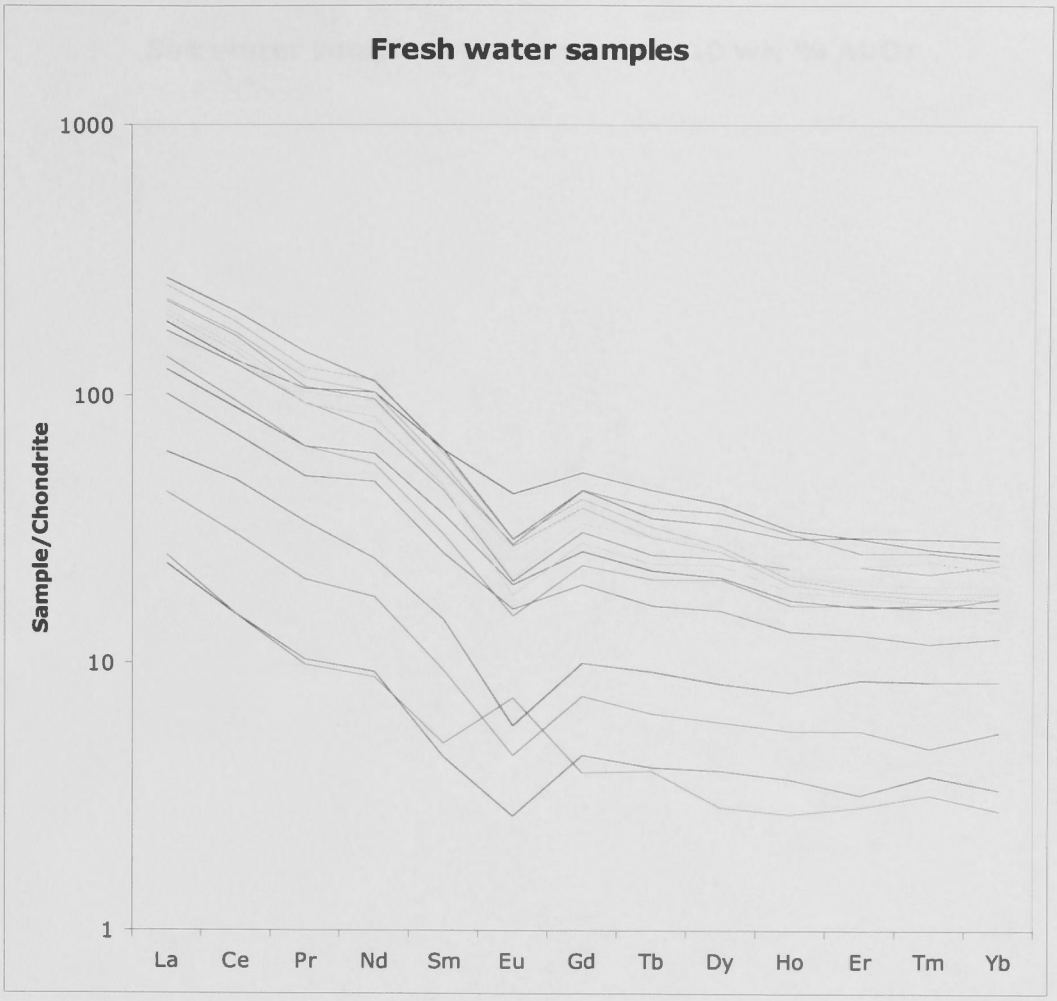

Figure 6.6: Freshwater REE sediment samples normalised to chondrite abundance.

Identical REE patterns were found in both the saltwater and freshwater sediment samples. This shows that the behaviour of the REE remains unchanged even as the geochemistry of the environment undergoes variability. In the saltwater sediment samples which contained more than 10% weight percent Al_2O_3, the pattern of the REE did indeed remain unchanged from the freshwater environment, and showed a narrower vertical spread due to the consistently high clay content (Figure 6.7).

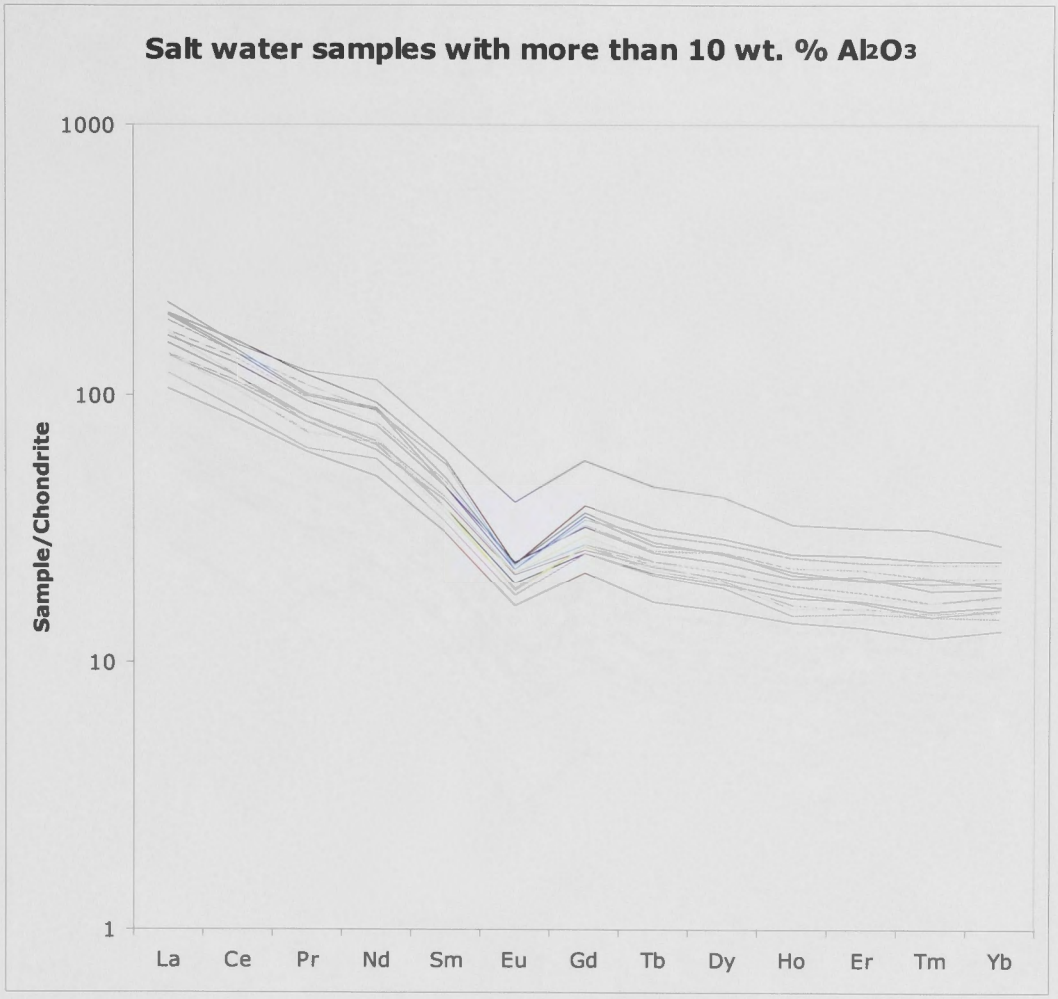

Figure 6.7: Saltwater REE sediment samples with more than 10 wt% Al_2O_3 normalised to chondrite abundance.

The saltwater sediments with 4-10 weight percent Al_2O_3 showed similar patterns of behaviour, but with a wider range of lower normalised abundances due to the larger proportion of REE-poor minerals (Figure 6.8).

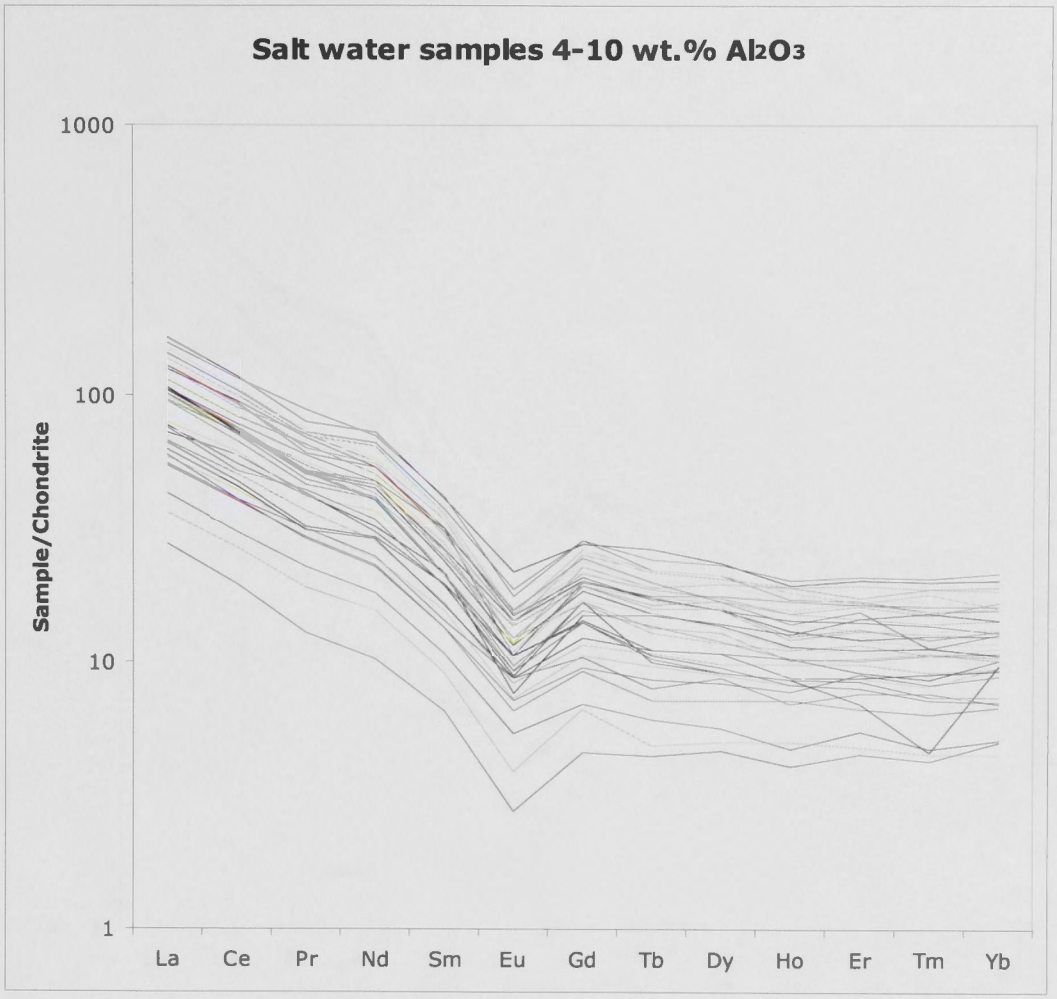

Figure 6.8: Saltwater REE sediment samples with 4 - 10 wt% Al_2O_3 normalised to chondrite abundance.

The behaviour of REE with less than 2% weight percent Al_2O_3 also showed similarities with the patterns observed previously, however there is a more erratic scatter of the data. This is a consequence of heavy minerals being incorporated into the analysis (Figure 6.9).

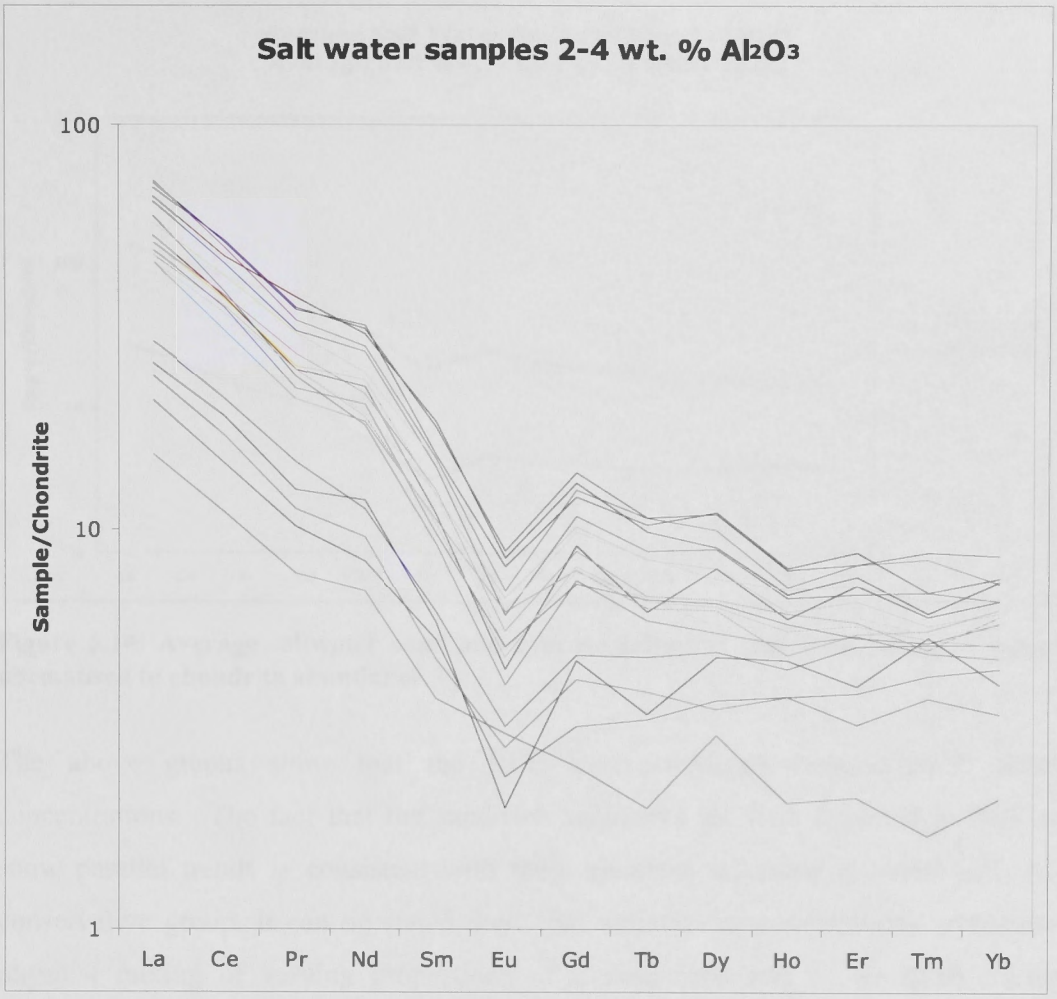

Figure 6.9: Saltwater REE sediment samples with 2 - 4 wt% Al_2O_3 normalised to chondrite abundance.

The averaged plots for saltwater sand and clay sediments, differentiated by SiO_2 content, were identical apart from vertical displacement, again showing that REE are truly conservative, and that quartz functions as an inert diluent (Figure 6.10).

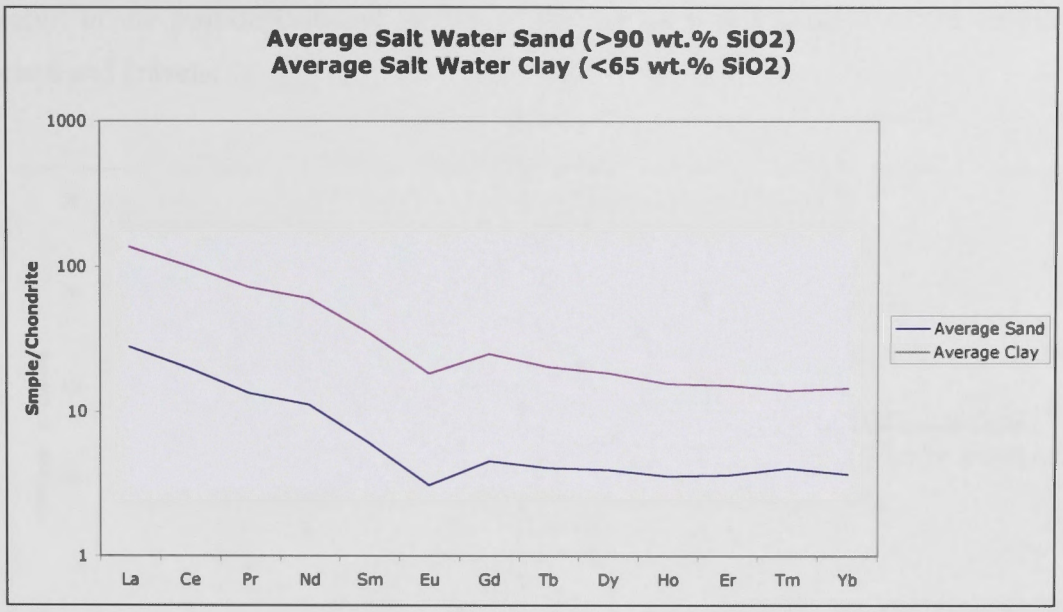

Figure 6.10: Average saltwater sand and average saltwater clay REE sediment samples normalised to chondrite abundance.

The above graphs show that the REE have preserved their original, detrital concentrations. The fact that the sand-rich sediments are both depleted in REE and show parallel trends is consistent with these elements behaving geochemically as a conservative group. It can be stated then, that variation in compositions represents a physical mixing of varying proportions of a sand-sized and a clay-sized fraction. Subsequent modifications to this mixing occur once the sediments have been deposited in the estuary.

6.3.3. Authigenic additions and transformations to the sediment geochemistry

Based on the conservative nature of the REE and the correspondence between the freshwater and estuarine REE sediment geochemistry, both the conservative and non-conservative behaviour of elements of interest, such as the metals, can be assessed. If all the elements behaved conservatively, then a plot of all data points will indicate a strong positive correlation (Figure 6.11). In this instance, the ratio between La and element *x*, will be the same for freshwater and saltwater sediments. The overall decrease in the concentration range of La for the saltwater sediments compared to the freshwater is a

result of the post-depositional mixing of the marine beach sands with the terrestrial clays and gravels.

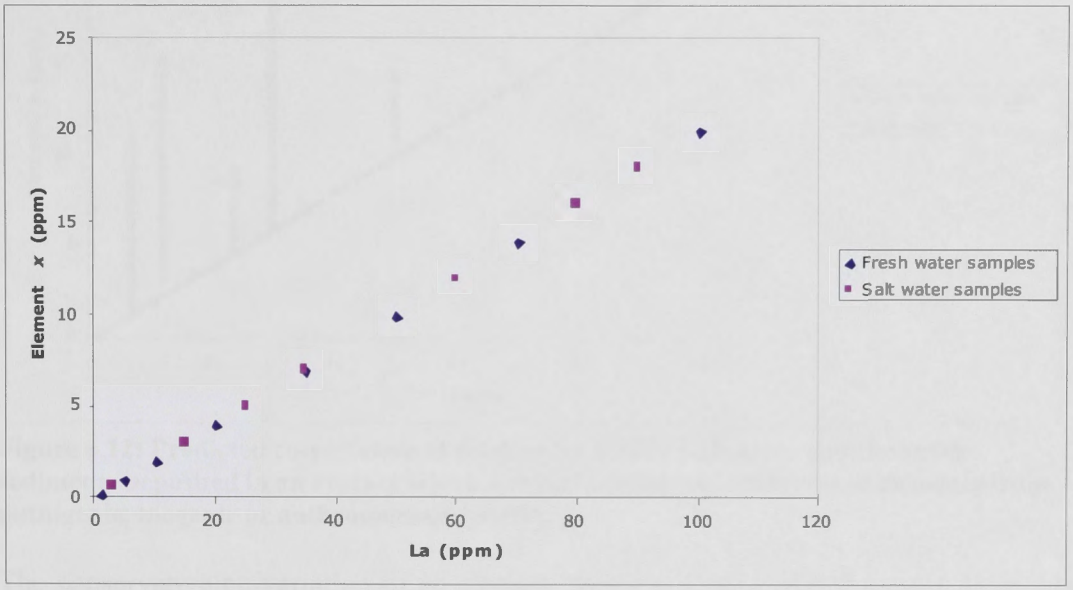

Figure 6.11: Predicted co-variation of freshwater source sediments and the same sediments deposited in an estuary when elements other than REE also behave conservatively. Based on an arbitrary set of data in which freshwater clay is mixed with quartz sands in estuary to lower overall concentrations of elements in clay, but not the element-La ratio

A sediment which has had subsequent additions of elements of authigenic, biogenic or anthropogenic origins can therefore be predicted to show an increase in the element in question, without changing the La concentration. Thus in a suite of estuarine sediment analyses, post-depositional addition of an element to some of the sediment samples will result in a greater scatter in estuary data compared to the freshwater data for a given La concentration (Figure 6.12). Superimposed upon a baseline trend with strong co-variation, the element which has been added post-deposition will show a significant scatter in the estuarine data population.

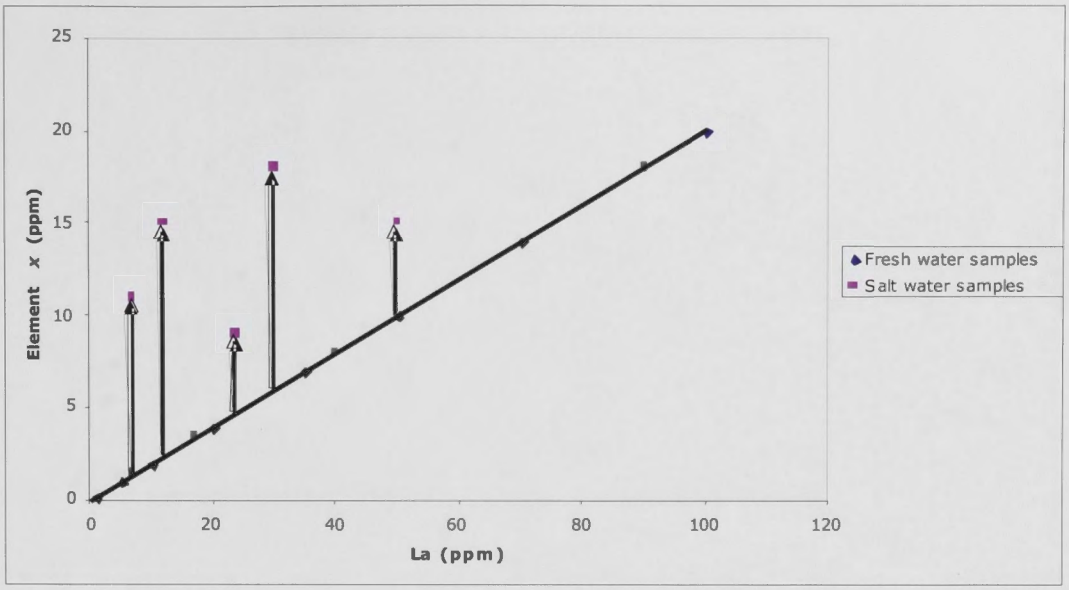

Figure 6.12: Predicted co-variation of freshwater source sediments and the same sediments deposited in an estuary which has had subsequent additions of elements from authigenic, biogenic or anthropogenic sources.

The conservative co-variation of an element with La illustrated in Figure 6.11 is now indicated by the straight line. Based on each sediment sample having a conservative La content, any post depositional addition of an element will cause that sediment to change as indicated by individual sample trends shown by arrows. Those estuarine sediments that are, for whatever reason, unaffected by an addition of element *x*, will share the common conservative baseline La-element *x* trend, but element *x* will show a scatter to higher values.

The saltwater sediments which have not had post depositional addition of element *x* still define a conservative La-element *x* baseline trend. However the overall scatter of data for element *x* is much greater in the saltwater samples due to addition of element *x* to some of the estuary samples. Furthermore, even though the maximum concentration of that element is no different between the freshwater and saltwater samples, this alone does not justify the assumption that "no significant heavy metal pollution" may have occurred in this estuary. Thus in Figure 6.13, the sample with a concentration of 20 ppm La has had a five fold increase in the concentration of element *x*.

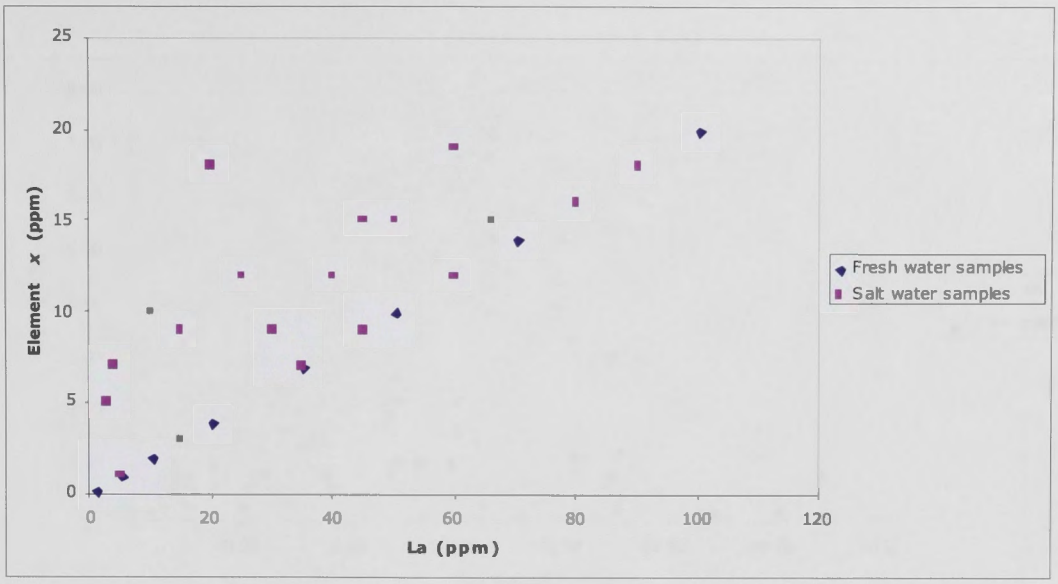

Figure 6.13: The saltwater sediments which have not had post depositional addition of element *x* still define a conservative La-element *x* baseline trend.

Using the conservative behaviour of the REE as a reference, elements which have been either added or removed from the sediments post-deposition in the estuary may therefore be distinguished. For instance, elements which are abundant in the seawater, such as sodium (10,800 ppm), will clearly be added to sediments post-deposition in the estuarine environment, and plotting Na_2O against La shows two distinct trends. The freshwater samples show a low Na_2O concentration trend, while the sediment samples obtained from the saltwater environment show a scatter of data marked by higher concentrations of Na_2O for a given concentration of La than the freshwater samples (Figure 6.14a). To ensure these trends are independent of the error incurred by the presence of various quantities of precipitated seawater within the samples post-collection, the amount of precipitated seawater within these samples was calculated (Appendix 2, Table A.10). With the salt precipitates removed, the plot of Na_2O against La shows a decreased concentration of Na_2O within the sediment, the trends between the freshwater and saltwater sediment samples are, however, still distinct (Figure 6.14b). The two trend lines differentiate between the freshwater and saltwater sediment samples because the sodium originates from different sources: seawater on the one hand and mature terrigenous weathering products on the other.

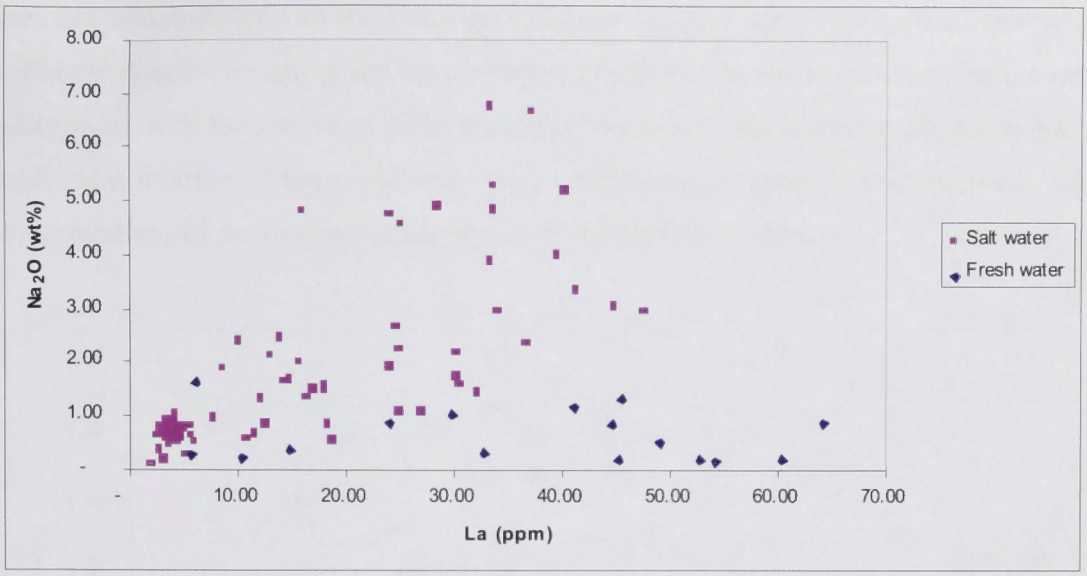

Figure 6.14a: Mixing relationship between Na_2O-La in estuarine and freshwater sediments.

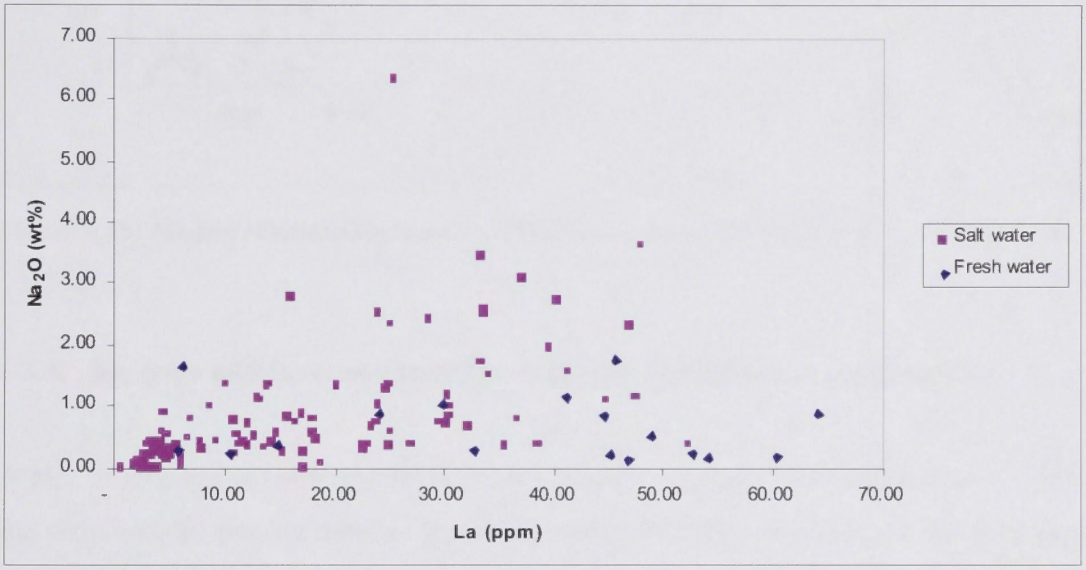

Figure 6.14b: Mixing relationship between Na_2O-La in estuarine and freshwater sediments, with contamination by dried seawater removed.

Magnesium shows a similar difference between the estuarine and freshwater sediments. As magnesium is present in high concentrations in the seawater and in low concentrations in the terrestrial freshwater sediment load, plotting MgO against La again shows two separate trends: the magnesium which is sourced from the freshwater component, and the magnesium which is sourced from the seawater (Figure 6.15).

Similar to Na_2O concentrations in the estuarine sediment samples, MgO also shows elevated concentrations in the estuarine sediment samples compared to the freshwater sediment samples for any given concentration of La. This is due to cation exchange and adsorption, with the source of these additions being from the seawater. As the estuary contains a mixture of terrestrial and marine sediments, an overlap exists between the concentrations of the freshwater and the saltwater sediment samples.

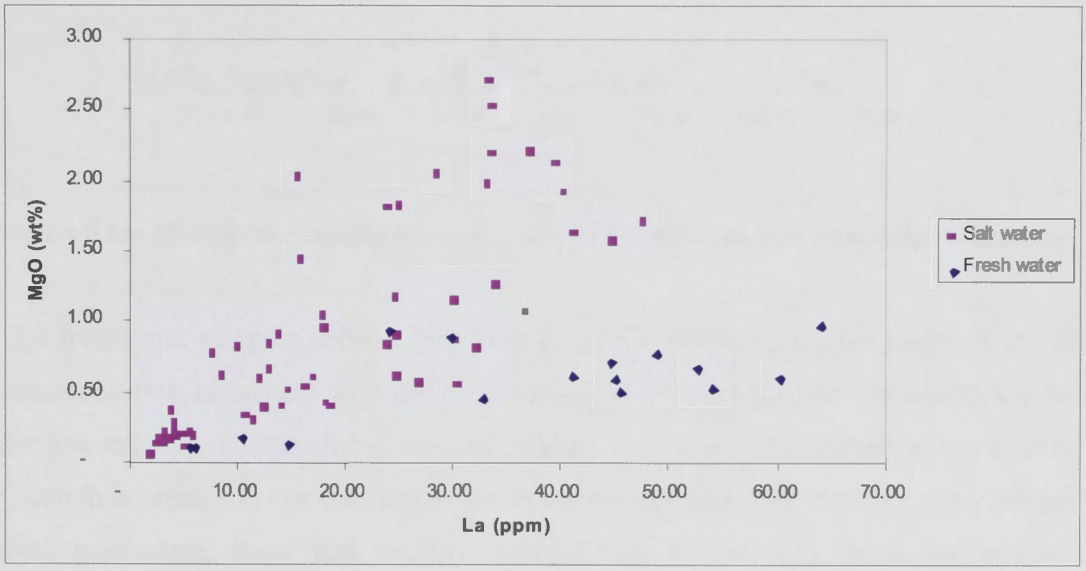

Figure 6.15: Mixing relationship between MgO-La in estuarine and freshwater sediments.

6.3.4. Biogenic additions and transformations to the sediment geochemistry

A plot of calcium against lanthanum shows that the calcium variation does not follow the simple linear mixing trend of the conservative REE (Figure 6.16), or the divergent trends shown by elements such as Na and Mg that are abundant in both mature sediments and seawater. This is almost entirely due to the fact that the majority of the calcium present in the sediments in the estuary is of a non-terrigenous origin, but is instead a post-depositional biogenic addition, sourced from the large concentration of gastropod and bivalve carbonate shells within the marine environment. The source of this $CaCO_3$ is the seawater, and thus bears no relationship to the lanthanum concentration that is of terrigenous, detrital origin.

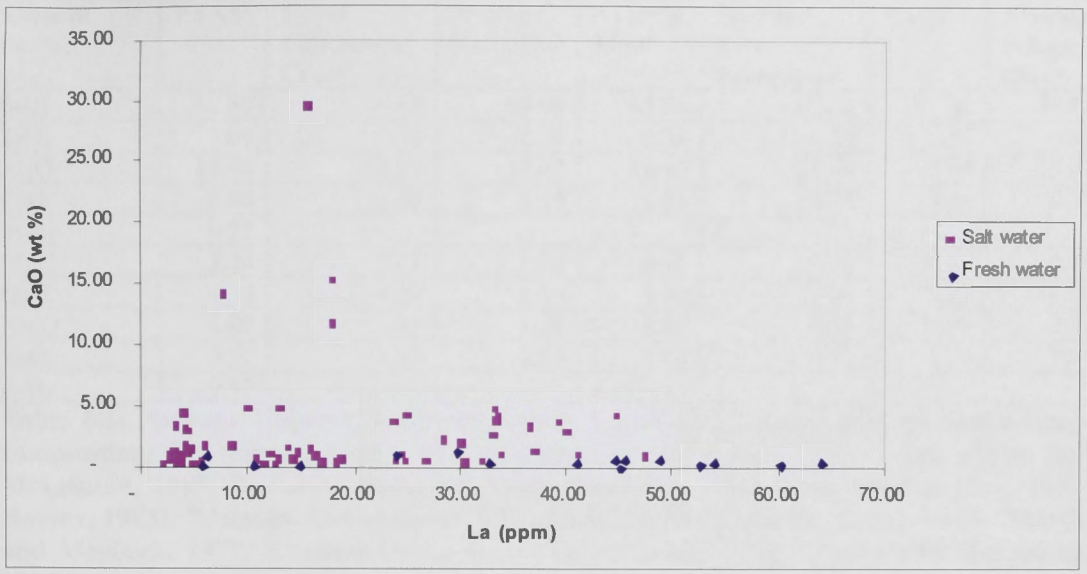

Figure 6.16: Mixing relationship between CaO-La in estuarine and freshwater sediments.

The freshwater samples show a very low Ca content over the entire range of the La concentrations, consistent with the Ca being taken into solution during weathering and the low-calcium, chemically weathered product then being transported to the estuary. Calcium is present in low concentrations in the average sediment, average mud, average river particulate, loess and average pelagic clay (Table 6.1). In a south-eastern Australian setting, the two mature weathering products which form the sedimentary end-members in Merimbula Lake are also low in calcium: quartz-dominated beach sand has 1.14%, while the average clay has 0.36%.

The estuary samples show a variable but overall increase in Ca content, which does not correlate with La content, due to the addition of biogenic carbonate. In a few cases, the samples are so rich in carbonate due to gastropod and mollusc shells, that up to 30 wt% CaO is present.

Element (wt%)	PAAS[a]	Upper Continental Crust[b]	Average Sediment[c]	Average Mud[d]	Average River Particulate[e]	Loess[f]	Average Pelagic Clay[g]
SiO_2	62.80	66.69	64.96	64.74	62.58	77.30	54.13
TiO_2	1.00	0.38	0.56	0.75	0.70	0.51	0.58
Al_2O_3	18.90	15.19	13.42	19.46	17.76	13.04	15.87
FeO	6.50	4.50	5.15	6.56	6.18	3.09	8.36
MnO	0.11	-	-	-	-	-	-
MgO	2.20	2.21	3.07	2.32	1.99	1.13	3.48
CaO	1.30	4.20	8.95	1.30	3.08	1.11	1.30
Na_2O	1.20	3.89	1.68	1.20	0.96	1.89	5.39
K_2O	3.70	3.37	2.83	3.85	2.41	2.29	3.01
P_2O_5	0.16	-	-	-	-	-	-

Table 6.1: Average Upper Continental Crust, PAAS and various average sedimentary compositions (McLennan, 1995). [a]From Taylor and McLennan, 1985; [b]From Taylor and McLennan, 1985; [c]Estimate based on geochemical data from many sources (Pye, 1987; Romov, 1983); [d]Volatile- and carbonate-free basis (Taylor and McLennan, 1985); [e]Martin and Meybeck, 1977; [f]Carbonate-free basis, Taylor *et al.*, 1983; [g]Taylor and McLennan, 1985.

Element (ppm)	PAAS[a]	Upper Continental Crust[b]	Average Sediment[c]	Average Mud[d]	Average River Particulate[e]	Loess[f]	Average Pelagic Clay[g]
Li	-	20	21	30	25	30	57
Be	-	3	2.2	3	-	2	2.6
B	100	15	75	100	70	-	230
P	-	700	665	700	1150	-	1500
Sc	16	11	14	16	18	8	19
V	150	60	110	140	170	73	120
Cr	110	35	74	100	100	44	90
Mn	-	600	680	850	1050	560	670
Co	23	10	16	20	20	11	74
Ni	55	20	40	60	90	20	230
Cu	50	25	40	50	100	18	250
Zn	85	71	65	85	350	60	200
Ga	20	17	16	20	25	14	20
Ge	-	1.6	1.5	2	-	-	2
Rb	160	112	110	160	100	85	110
Sr	200	350	385	200	150	192	18
Y	-	22	21	27	28	25	40
Zr	210	190	210	210	-	375	150
Nb	19	25	17	19	-	20	14
Mo	1.0	1.5	-	1.0	3	-	27
Cd (ppb)	-	98	-	-	1000	-	300
Sn	4.0	5.5	5	6	-	5	3.0
Cs	15	3.7	4.5	6	6	4	6
Ba	650	550	480	650	600	625	2300
La	38	30	28.3	38.2	46	35.4	42
Ce	80	64	58.9	79.6	88	78.6	80
Pr	8.9	7.1	6.52	8.83	9.0	8.46	10
Nd	32	26	24.9	33.9	33	33.9	41
Sm	5.6	4.5	4.23	5.55	7.0	6.38	8.0
Eu	1.1	0.88	0.86	1.08	1.5	1.18	1.8
Gd	4.7	3.8	3.61	4.66	5.4	4.61	8.3
Tb	0.77	0.64	0.60	0.774	0.89	0.81	1.3
Dy	4.4	3.5	3.61	4.68	5.4	4.82	7.4
Ho	1.0	0.80	0.76	0.991	1.1	1.01	1.5
Er	2.9	2.3	2.19	2.85	3.1	2.85	4.1
Tm	0.40	0.33	0.31	0.405	0.44	0.40	0.57
Yb	2.8	2.2	2.14	2.82	3.2	2.71	3.8
Lu	0.43	0.32	0.33	0.433	0.52	0.42	0.55
Hf	5.0	5.8	5.5	5.0	6	11.4	4.1
Ta	-	2.2	1.5	2	1.25	-	1
W	-	2.0	2.1	2.7	-	1.6	1
Pb	20	20	17	20	150	13	30
Bi	-	127	-	250	-	-	550
Th	14.6	10.7	10.4	14.6	14	11.3	13.4
U	3.1	2.8	2.3	3.1	3	2.5	2.6

Table 6.1 (continued): Average Upper Continental Crust, PAAS and various average sedimentary compositions (McLennan, 1995). [a]From Taylor and McLennan, 1985; [b]From Taylor and McLennan, 1985; [c]Estimate based on geochemical data from many sources (Pye, 1987; Romov, 1983); [d]Volatile- and carbonate-free basis (Taylor and McLennan, 1985); [e]Martin and Meybeck, 1977; [f]Carbonate-free basis, Taylor *et al.*, 1983; [g]Taylor and McLennan, 1985.

The relationship between calcium and strontium concentrations in the sediment provides further evidence for the addition of these elements to the sediment after deposition in the estuary. Referring back to Table 6.1 (Taylor and McLennan, 1985), the concentrations of CaO are only 1.3 – 3.1 wt% in river particulates, mud and pelagic sediments. The freshwater sediment of the current study similarly have < 1.4wt% CaO (Figure 6.17). In the terrigenous sediments from Taylor and McLennan (1985), detrital plagioclase feldspar is the principal source of calcium in greywackes, while in more mature marine sediments (either clay or beach sands), little calcium remains. In this study, the estuarine environment of the study area means higher concentrations of calcium present in the sediment are sourced from seawater derived calcium (for instance shellfish, algae, invertebrates, phytoplankton and zooplankton).

Strontium typically substitutes for calcium in a range of minerals, such as plagioclase feldspar. Immature sediments will therefore show a correlation between detrital Ca and Sr from unweathered feldspar (Figure 6.17).

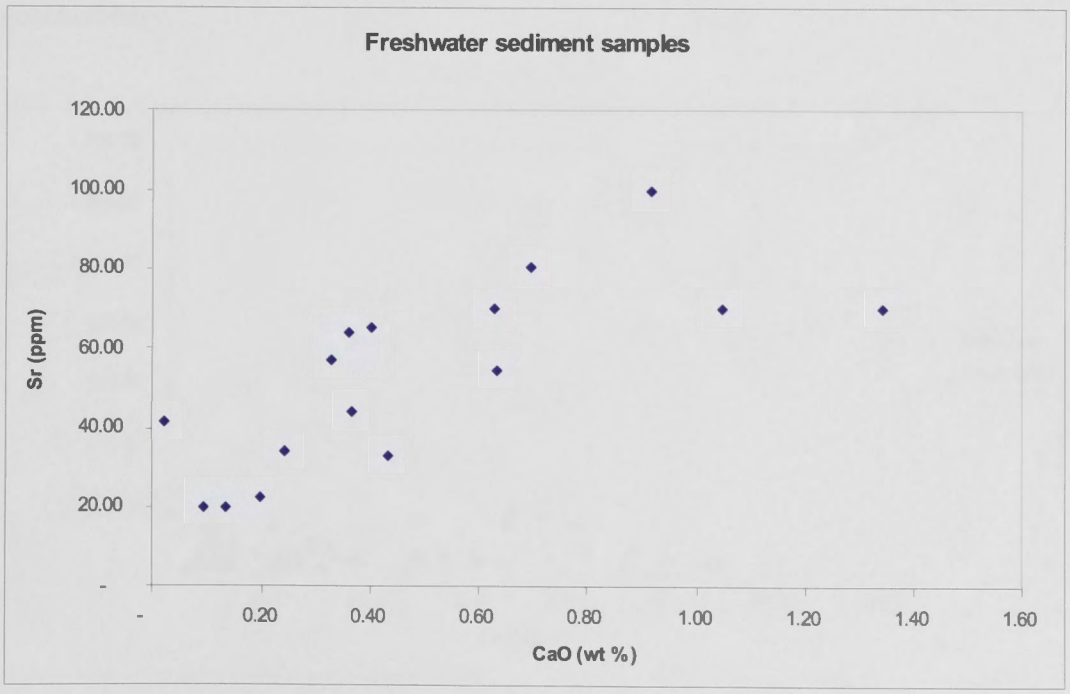

Figure 6.17: Mixing relationship between Sr-CaO in freshwater sediments.

The prolonged weathering that is characteristic of the Australian regolith explains the great maturity of the sediments transported to Merimbula estuary, and hence their depletion in terrigenous CaO.

When Sr is plotted against La for all sediments, some estuarine samples show much higher Sr than the freshwater samples of Figure 6.14, but no linear trend is observed. Instead, a pattern is seen very similar to that for Ca against La (Figure 6.18). This implies that there remains a strong correlation between Sr and Ca, and that both have a source that is independent of the La-bearing clay.

When calcium and strontium are plotted against each other for all sediments (Figure 6.19), they do indeed show a strong positive correlation. It is also evident that the input from the seawater is much higher than that from terrigenous sources. It was hypothesised that significant amounts of both calcium and strontium were added to the saltwater sediments from the seawater and/or bivalve and gastropod shells, which were sufficient in some samples to constitute a large component of the overall sediment geochemistry.

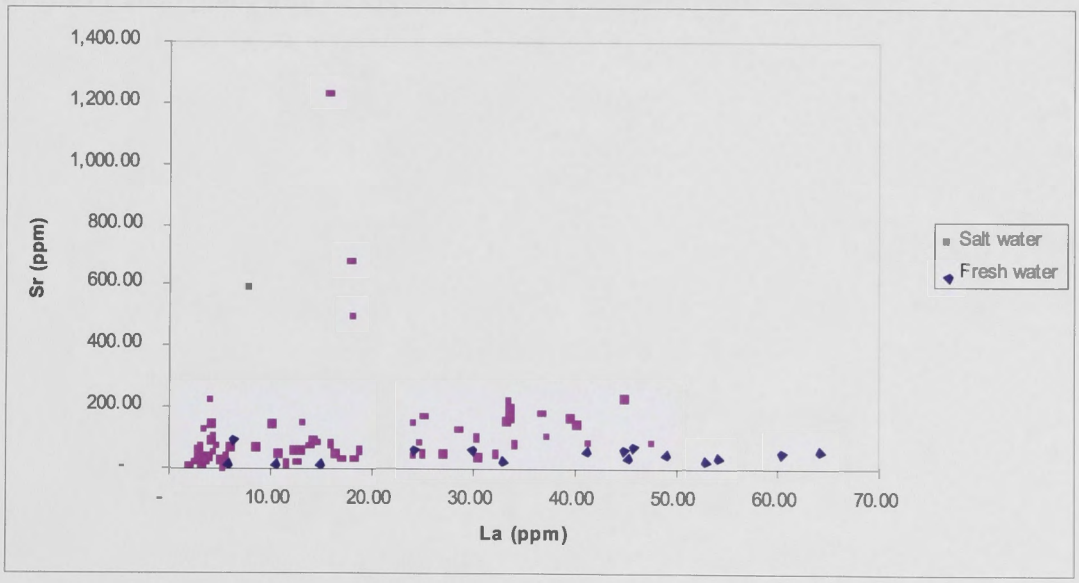

Figure 6.18: Mixing relationship between Sr-La in estuarine and freshwater sediments.

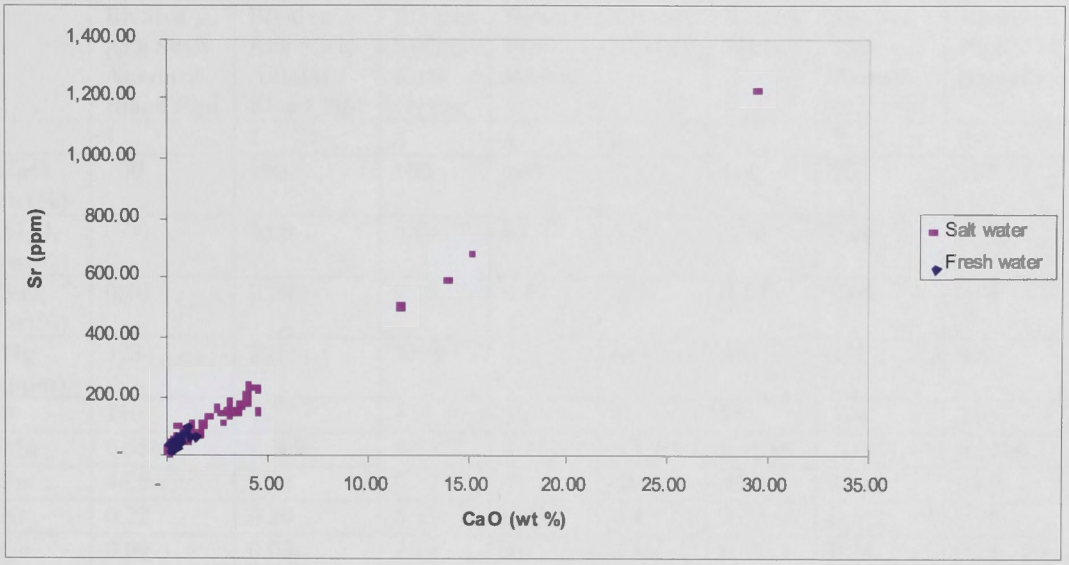

Figure 6.19: Mixing relationship between Sr-CaO in estuarine and freshwater sediments.

In addition to the sediments, different species of local gastropod and bivalve shells were also analysed. In order to compare this data directly with the sediments which are presented on a volatile-free basis with total readjusted to 100% , the shell data also needs to be readjusted to a volatile (CO_2)-free basis. Sr concentrations showed a range of 1309 - 5833 ppm, with an average of 2533 ppm, as seen in Table 6.2.

	Bivalve Ark Shell Anadara Blood Pipi	Bivalve Ark Shell Anadara Blood Pipi	Bivalve Sydney Rock Oyster	Bivalve Pipi Ribbed	Bivalve Mussel	Bivalve Mussel	Bivalve Pipi Smooth	Bivalve Pipi Smooth
	1	2	3	4	5	6	7	8
CaO (wt%)	100	100	100	100	100	100	100	100
Al_2O_3 (wt%)	0.00	0.00	0.03	0.00	0.00	0.00	0.00	0.00
SiO_2 (wt%)	0.10	0.08	0.15	0.07	0.09	0.10	0.08	0.08
Mg (ppm)	323	391	8879	233	643	693	492	903
P	110	17	434	30	16	18	184	214
Mn	0.5589	0.3096	5.2077	0.2224	0.7595	0.7858	0.1841	0.3120
Fe	46.5	45.5	93.2	48.4	46.1	43.6	43.4	43.9
Ni	0.22	0.20	0.32	0.21	0.19	0.19	0.20	0.22
Cu	0.09	0.03	2.88	0.11	0.16	0.12	0.24	0.21
Zn	0.49	0.08	8.07	0.17	0.33	0.40	0.21	0.18
Rb	0.02	0.01	0.18	0.02	0.01	0.01	0.01	0.01
Sr	1917	1895	1349	2662	5834	4843	1309	1343
Cd	0.00	0.00	0.02	0.00	0.03	0.02	0.00	0.00
Cs	0.00	0.00	0.00	0.00	0.00	0.00	0.00	0.00
Ba	1.25	1.10	0.72	6.44	8.41	7.74	0.48	0.44
La	0.04	0.04	0.85	0.02	0.14	0.09	0.01	0.01
Ce	0.04	0.03	1.51	0.01	0.13	0.10	0.02	0.01
Pr	0.00	0.00	0.18	0.00	0.01	0.01	0.00	0.00
Nd	0.02	0.02	0.69	0.01	0.06	0.02	0.00	0.01
Sm	0.01	0.00	0.12	0.00	0.01	0.00	0.00	0.00
Eu	0.00	0.00	0.02	0.00	0.00	0.00	0.00	0.00
Gd	0.01	0.00	0.18	0.00	0.00	0.01	0.01	0.01
Tb	0.00	0.00	0.01	0.00	0.00	0.00	0.00	0.00
Dy	0.00	0.01	0.02	0.00	0.01	0.01	0.00	0.00
Ho	0.00	0.00	0.00	0.00	0.00	0.00	0.00	0.00
Er	0.00	0.00	0.01	0.00	0.00	0.01	0.00	0.00
Tm	0.00	0.00	0.00	0.00	0.00	0.00	0.00	0.00
Yb	0.00	0.00	0.00	0.00	0.00	0.01	0.00	0.01
Lu	0.00	0.00	0.00	0.00	0.00	0.00	0.00	0.00
Pb	0.90	0.12	11.41	1.14	1.25	1.02	0.50	0.52
Th	0.00	0.00	0.01	0.00	0.00	0.00	0.00	0.00
U	0.26	0.01	0.01	0.14	0.00	0.00	0.00	0.00

Table 6.2: LA-ICPMS data for the concentrations of major elements (wt % oxide) and other elements (ppm) in selected bivalves, readjusted to 100% on a volatile-free basis. Values of 0.00 are representative of samples below detection limit.

	Gastropod Turritella	Gastropod Turritella	Gastropod Top Shell Snail	Gastropod Top Shell Snail	Gastropod Snail	Gastropod Snail
	9	**10**	**11**	**12**	**13**	**14**
CaO	100	100	100	100	100	100
Al_2O_3	0.00	0.00	0.00	0.00	0.00	0.00
SiO_2	0.07	0.08	0.08	0.07	0.08	0.09
Mg (ppm)	228	217	1164	417	309	314
P	23	24	31	23	24	16
Mn	1.1197	3.1194	1.5155	20.0212	0.1342	0.1104
Fe	45.8	41.6	56.1	77.8	35.8	35.4
Ni	0.17	0.21	0.21	0.23	0.20	0.15
Cu	0.08	0.11	0.31	0.39	0.12	0.11
Zn	0.50	0.53	0.92	1.79	0.88	0.29
Rb	0.03	0.02	0.06	0.04	0.03	0.04
Sr	2323	2325	2995	2180	2199	2297
Cd	0.00	0.00	0.00	0.00	0.00	0.00
Cs	0.00	0.00	0.00	0.00	0.00	0.00
Ba	0.92	1.12	1.35	0.60	0.74	0.63
La	0.07	0.04	0.07	0.18	0.05	0.05
Ce	0.10	0.04	0.09	0.20	0.04	0.05
Pr	0.01	0.00	0.01	0.02	0.01	0.01
Nd	0.05	0.02	0.04	0.10	0.01	0.02
Sm	0.00	0.00	0.00	0.02	0.01	0.01
Eu	0.00	0.00	0.00	0.00	0.00	0.00
Gd	0.01	0.00	0.01	0.02	0.00	0.02
Tb	0.00	0.00	0.00	0.00	0.00	0.00
Dy	0.01	0.00	0.00	0.02	0.00	0.01
Ho	0.00	0.00	0.00	0.00	0.00	0.00
Er	0.00	0.00	0.01	0.00	0.00	0.00
Tm	0.00	0.00	0.00	0.00	0.00	0.00
Yb	0.00	0.00	0.00	0.00	0.00	0.00
Lu	0.00	0.00	0.00	0.00	0.00	0.00
Pb	1.42	0.77	7.98	13.18	0.92	0.49
Th	0.00	0.00	0.01	0.02	0.00	0.00
U	0.08	0.05	0.00	0.02	0.05	0.03

Table 6.2 (continued): LA-ICPMS data for the concentrations of major elements (wt % oxide) and other elements (ppm) in selected bivalves, readjusted to 100% on a volatile-free basis. Values of 0.00 are representative of samples below detection limit.

A comparison of the saltwater sediment data and the analysed shell data is given in Figure 6.20. A linear regression of all CaO-Sr estuary sediment data gives an excellent correlation (Sr ppm = 39.16*CaO + 21.9; R^2 = 0.95). Extrapolation of this trend predicts a Sr concentration of 3938 ppm corresponding to 100wt% CaO, in the centre of the range of Sr measured for the shells. Thus, it is clear that biogenic addition of carbonate primarily controls CaO and Sr additions to these estuary sediments.

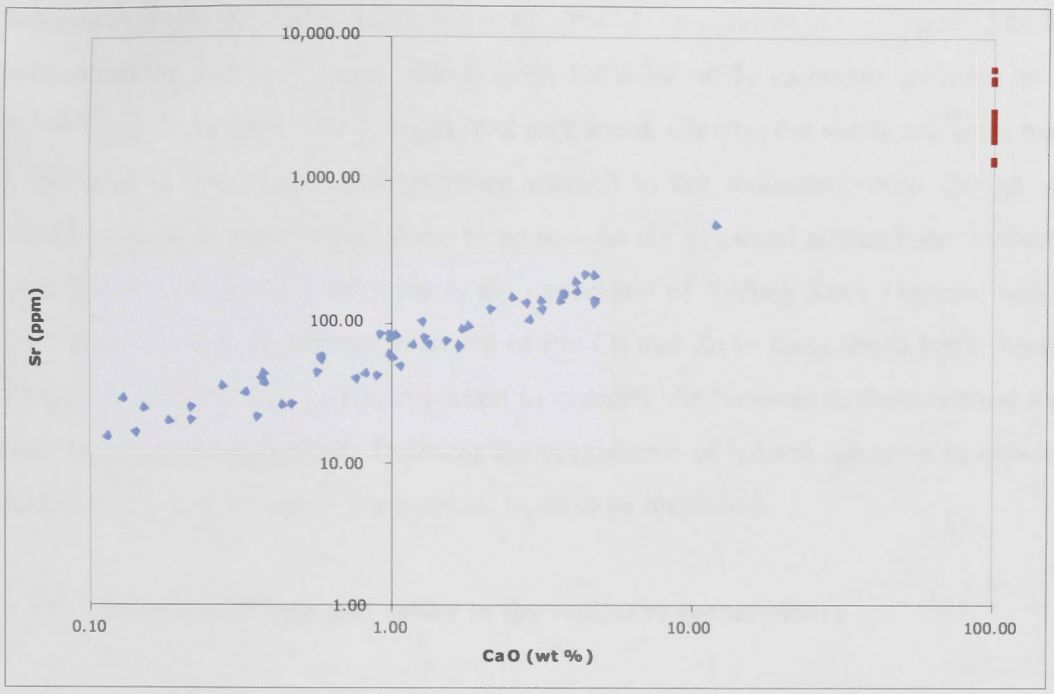

Figure 6.20: Relationship between Sr-CaO in saltwater sediments (blue) and shells (red).

On a volatile-free basis, the maximum CaO content of the analysed sediments in Merimbula Lake is 11.71 wt.% CaO, which is equivalent to a maximum of 20.9 wt.% biogenic carbonate addition. This is exceptional because most sediments are estimated to have had < 5 wt. % biogenic carbonate addition. However, since the Sr content of the freshwater sediments is so low, this represents a very significant Sr addition to the estuary sediments (more than doubling the Sr content in most cases).

The shells therefore explain the CaO and Sr contents of these sediments, above and beyond the small detrital component. However, it is also important to establish the contribution of the biogenic carbonate shell addition on other trace elements in the saltwater sediments compared to the freshwater material. Apart from the oyster, the shells are low in analysed trace elements other than Sr. On average there is only about 5 % addition of carbonate to the sediments, therefore very few of the trace elements present in the sediments are significantly sourced from biogenic carbonate. For example, in the shell analyses, lead is present in most samples at a concentration of less than 1 ppm (volatile-free basis), but several analyses show 8, 11 and 13 ppm lead respectively. This very significant amount is most likely due to point source pollution,

incorporated into the carbonate structure as a $PbCO_3$ component in the oysters. The lead concentrations average 3 ppm, which even for a 10 wt % carbonate addition to the sediment, only equates to a 0.3 ppm lead increment. Clearly, the shells are not a major contributor of lead (and other pollutant metals) to the sediments, even though they provide excellent monitors of these elements. As the principal aquaculture product in Merimbula and Pambula estuaries is the cultivation of Sydney Rock Oysters, and the shell data indicates significant presence of Pb, Cu and Zn in these shells (refer back to Figures 4.20, 4.21, 4.22), it is important to quantify the biogenic carbonate shell input into the estuarine sediments. Defining the coexistence of natural elements in estuarine sediments allows for a post-depositional input to be identified.

6.3.5. Additions of iron and sulfur to the sediment geochemistry

Iron and sulfur provide another example of post-depositional authigenic additions and transformations to the geochemistry of the sediment that may be detected by plotting against conservative elements. In an estuarine environment, these elements undergo additional modification by post-depositional processes, and can be added to the sediments from the seawater as insoluble iron sulfide under reducing conditions. A plot of SO_3 against La showed no correlation between the freshwater and saltwater sediments (Figure 6.21).

Sulfates from the seawater are adsorbed onto the fine-grained sediments, which, if then deposited in reducing environments, are transformed into insoluble sulfides, such as pyrite, in the sediments. In the organic- and clay-rich sediments, this process is catalysed by microbes, so the sulfur is of biogenic origin. It is extremely unlikely that sulfur is transported as sulfide into the lake, based upon the low sulfur concentrations being sourced from up-catchment (below XRF detection limit). Hence, the sulfur is added to the sediments entirely post-deposition from the seawater as a sulfate, which explains the lack of correlation between SO_3 and La, and between the freshwater and saltwater sample data.

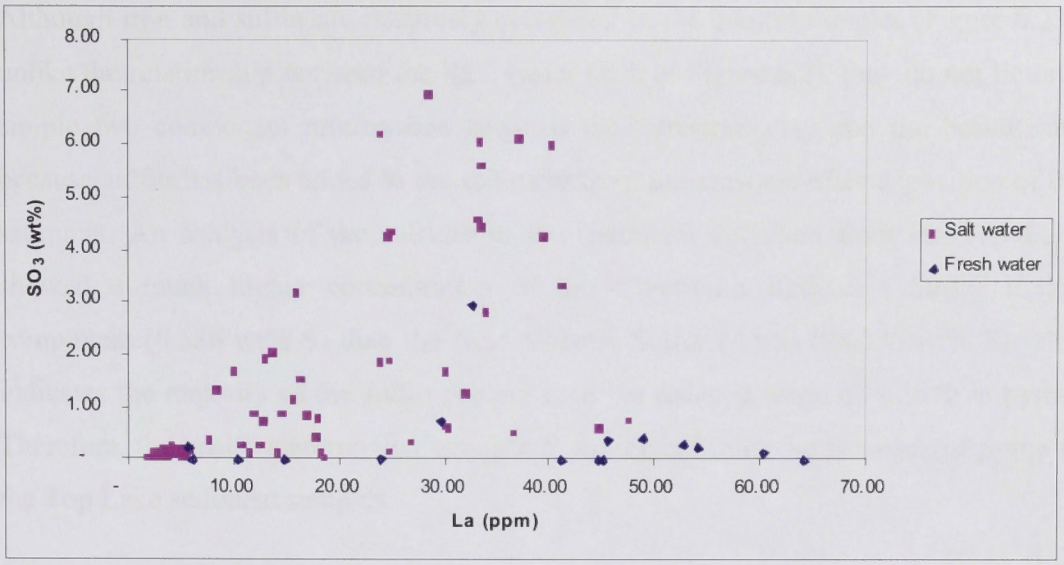

Figure 6.21: Mixing relationship between SO_3-La in estuarine and freshwater sediments.

In contrast, a comparison of iron with the conservative REE shows similar trends in both the freshwater and the saltwater sediment samples. As iron is present in very low concentrations in seawater, and local geology includes iron-rich bedrock, the iron in the samples from Merimbula is an original component of the terrestrial sediment, present before deposition in the estuarine environment (Figure 6.22).

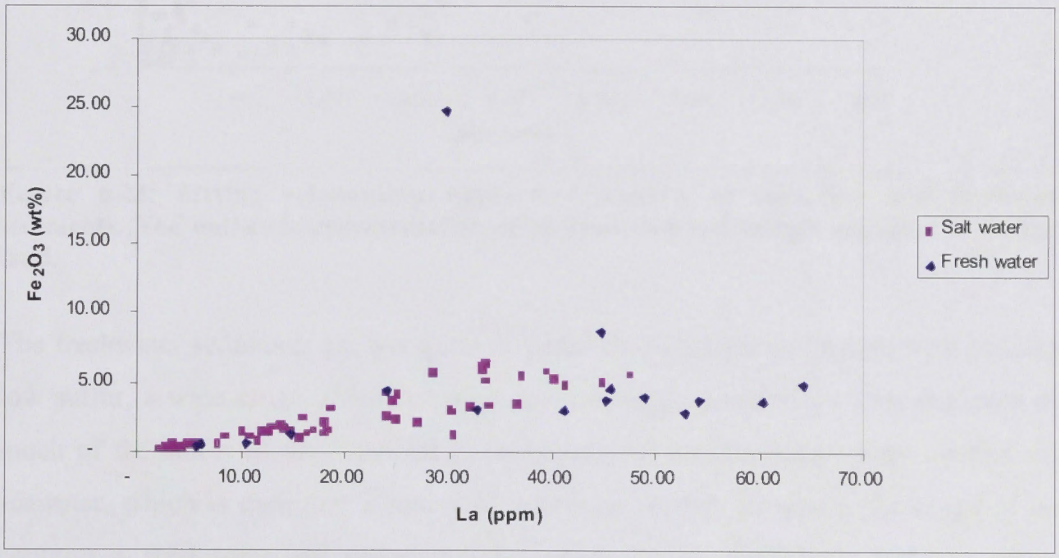

Figure 6.22: Mixing relationship between Fe_2O_3-La in estuarine and freshwater sediments. The outlier is representative of an iron-rich soil sample obtained from farm land.

Although iron and sulfur are positively correlated in the marine samples (Figure 6.23), unlike the relationship between the REE (refer back to Figure 6.2), they do not lie on a simple two component mixing line between the terrestrial clay and the beach sand because sulfur has been added to the sediment from the seawater after deposition of the sediment. An analysis of the sulfides in the sediments collected from the Top Lake showed a much higher concentration of the Chromium Reducible Sulfur (CRS) component (0.586 wt% S) than the Acid Volatile Sulfur (AVS) (0.0386 wt% S). This indicates the majority of the sulfur present is in the reduced form, as sulfide in pyrite. Therefore, the positive correlation between S and Fe indicates the presence of pyrite in the Top Lake sediment samples.

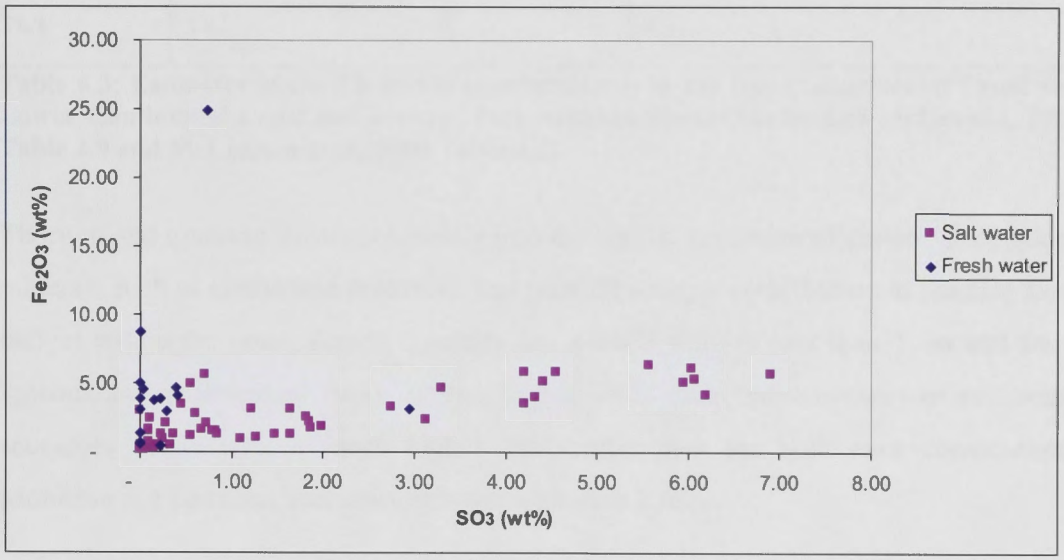

Figure 6.23: Mixing relationship between Fe_2O_3-SO_3 in estuarine and freshwater sediments. The outlier is representative of an iron-rich soil sample obtained from farm land.

The freshwater sediments show a quite different SO_3-Fe_2O_3 relationship, with generally low sulfur, a wide range of iron content, and no strong correlation. This indicates that much of the sulfur of the estuarine sediments is not present before they interact with seawater, which is therefore a source of additional sulfur. However, the range of iron contents in freshwater and estuarine sediments is similar, suggesting that it is sourced from terrigenous sediment.

6.3.6. Terrestrial additions and transformations to the sediment geochemistry

The use of multi-element comparisons in determining the original source of a material may also be observed in the relationship between thorium and uranium. These are highly incompatible, radioactive elements which are concentrated in the Earth's crust, where infracrustal differentiation further concentrates them in the upper crust relative to the lower-crust (Table 6.3).

	Upper Crust	Lower Crust	Post Archean Average Shale
Th (ppm)	10.7	2	14.6
U (ppm)	2.8	0.53	3.1
Th/U	3.82	3.77	4.7

Table 6.3: Estimates of the Th and U concentrations in the Upper continental Crust and Lower Continental Crust and average Post Archean Shale (Taylor and McLennan, 1985 Table 2.9 and McLennan *et al.*, 2006 Table 4.2).

Thorium and uranium substitute readily into the crystal structures of common accessory minerals such as zircon and monazite, and provide a major contribution to the heat flow budget within the crust. Zircon typically has a Th/U ratio of less than 1, so that most igneous and sedimentary rocks, with a higher Th/U ratio, must contain an additional accessory phase with a much higher Th/U ratio than the bulk rock composition. Monazite is a common accessory mineral with such a ratio.

The freshwater sediments from Merimbula-Pambula show a positive correlation between La and Th, consistent with the concentration of Th in the finer-grained sediments. Furthermore there is no significant difference in La-Th behaviour between freshwater and the saltwater samples from these estuaries (Figure 6.24).

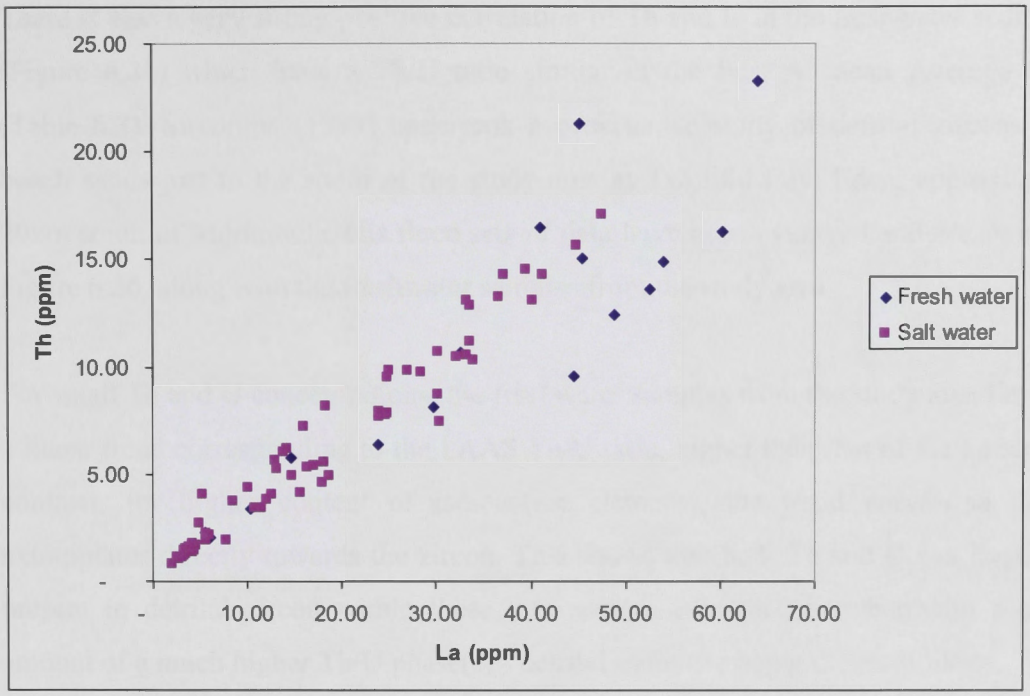

Figure 6.24: A plot of the La and Th concentrations in the freshwater and saltwater sediments.

Th and Zr also show a strong correlation, as would be expected since Th^{4+} readily substitutes for Zr^{4+} in zircon (Figure 6.25).

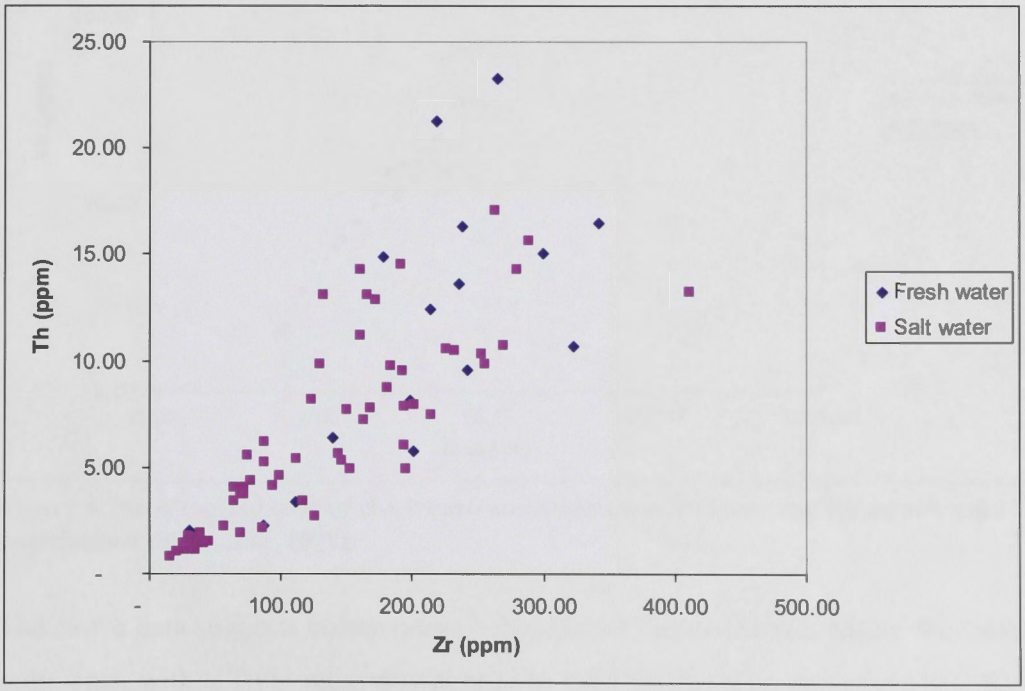

Figure 6.25: A plot of the Th and Zr concentrations in the freshwater and saltwater sediments.

There is also a very strong positive correlation of Th and U in the freshwater sediments (Figure 6.26) which have a Th/U ratio similar to the Post Achaean Average Shale (Table 6.3). Sircombe (1999) undertook a provenance study of detrital zircons from beach sands just to the south of the study area at Twofold Bay, Eden, approximately 20km south of Merimbula. His three sets of data have been averaged and are shown in Figure 6.26, along with the freshwater samples from the study area.

For small Th and U concentrations, the freshwater samples from the study area lie along a linear trend corresponding to the PAAS Th/U ratio, higher than that of the zircons. In contrast, for higher content of radioactive elements, the trend curves so that it extrapolates directly towards the zircon. This shows that both Th and U can largely be present in detrital zircon within these transported sediments, together with a minor amount of a much higher Th/U phase(s) - detrital monazite being the most likely.

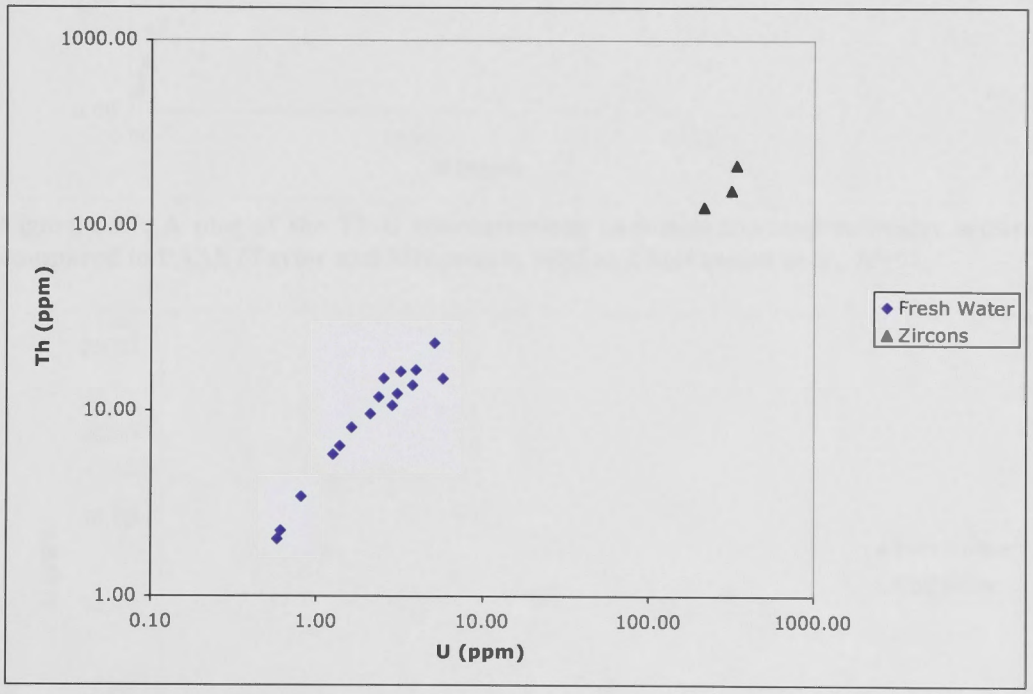

Figure 6.26: A log-log plot of the freshwater sediments and average for beach sand zircon populations (Sircombe, 1999).

The above data suggests conservative behaviour of these elements within the freshwater sediments, with a Th/U ratio very similar to the Post Archean Average Shale (PAAS). However, the estuary samples are enriched in U compared to the freshwater samples

and PAAS average shale (Figure 6.27). Note that the lower limit of U for these saltwater samples, over the entire La range, matches the freshwater baseline trend extremely well. However, at any given La concentration, saltwater samples range to higher uranium contents (Figure 6.28).

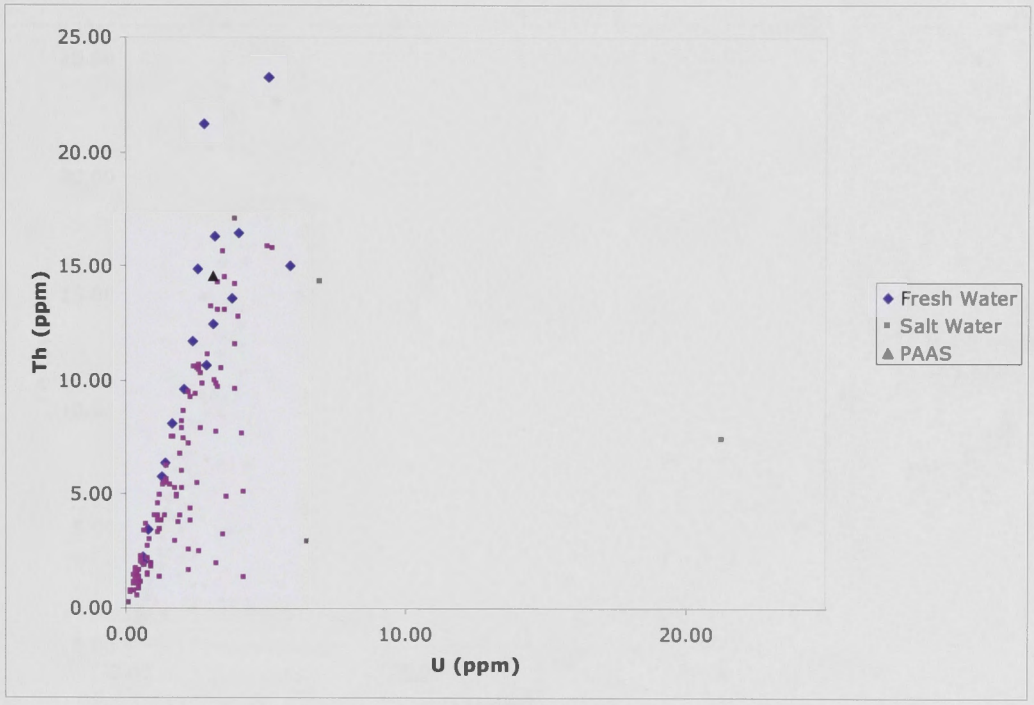

Figure 6.27: A plot of the Th-U concentrations in freshwater and saltwater sediments, compared to PAAS (Taylor and McLennan, 1985 and McLennan *et al.*, 2006).

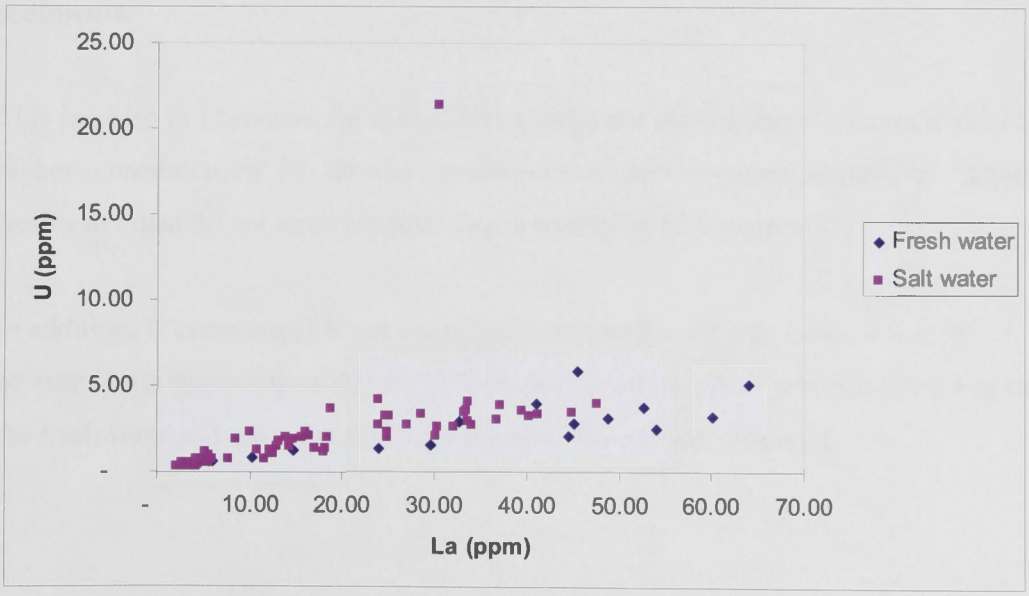

Figure 6.28: A plot of the uranium concentration in freshwater and saltwater sediments as a function of the conservative element La.

This difference is even more pronounced in the Th-U plot (Figure 6.29), since U extends to much higher concentrations in the saltwater samples for any given Th content. Again, the spread of data shows a sharp boundary on the low-U side, where baseline values are defined by freshwater samples and some of the saltwater samples.

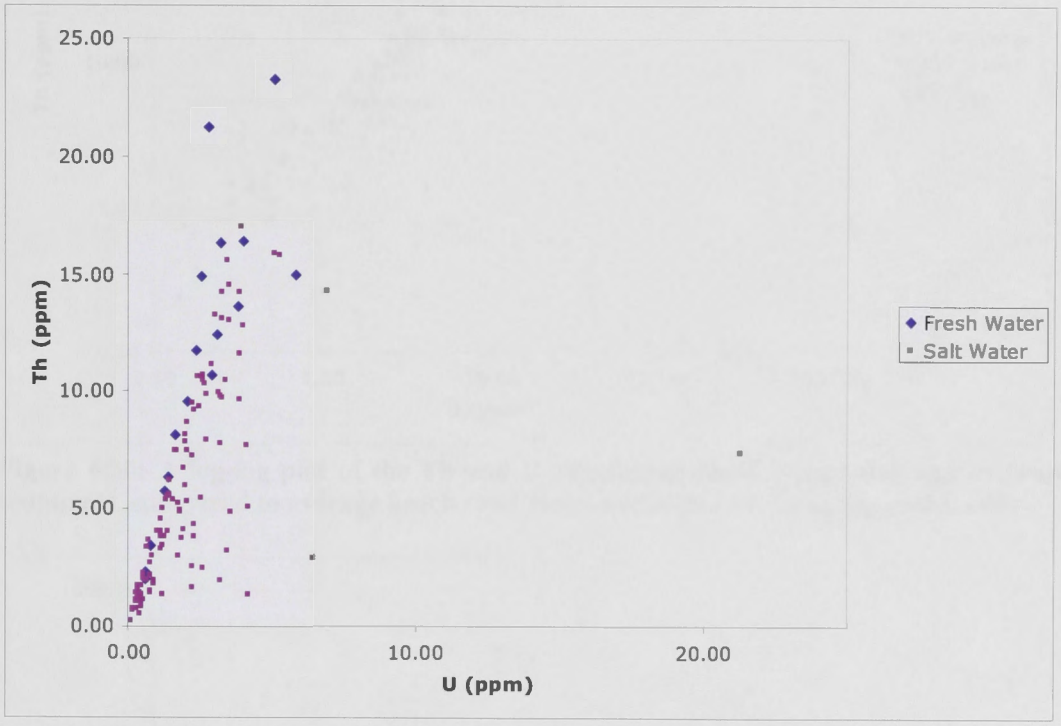

Figure 6.29: A plot of the Th-U concentrations in freshwater and saltwater sediments.

This increase in U content for the saltwater sediment array cannot be explained by local higher concentration of detrital zircon, since the saltwater departures from the freshwater data do not trend towards zircon control of U (Figure 6.30).

In addition, U enrichment is not restricted to one sediment type (clay, sand, etc). A plot of sands with greater than 90 wt. % SiO_2 shows an excellent correspondence between the freshwater and saltwater sands for many of the samples (Figure 6.31).

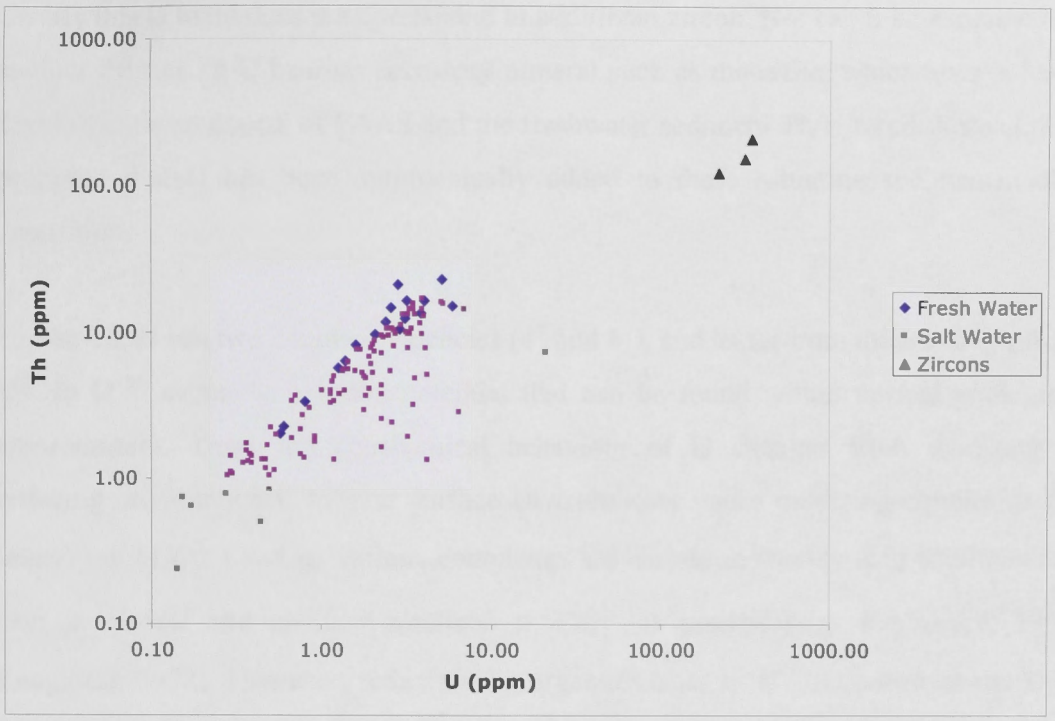

Figure 6.30: A log-log plot of the Th and U concentrations in freshwater and saltwater sediments, compared to average beach sand zircons (zircon data from Sircombe, 1999).

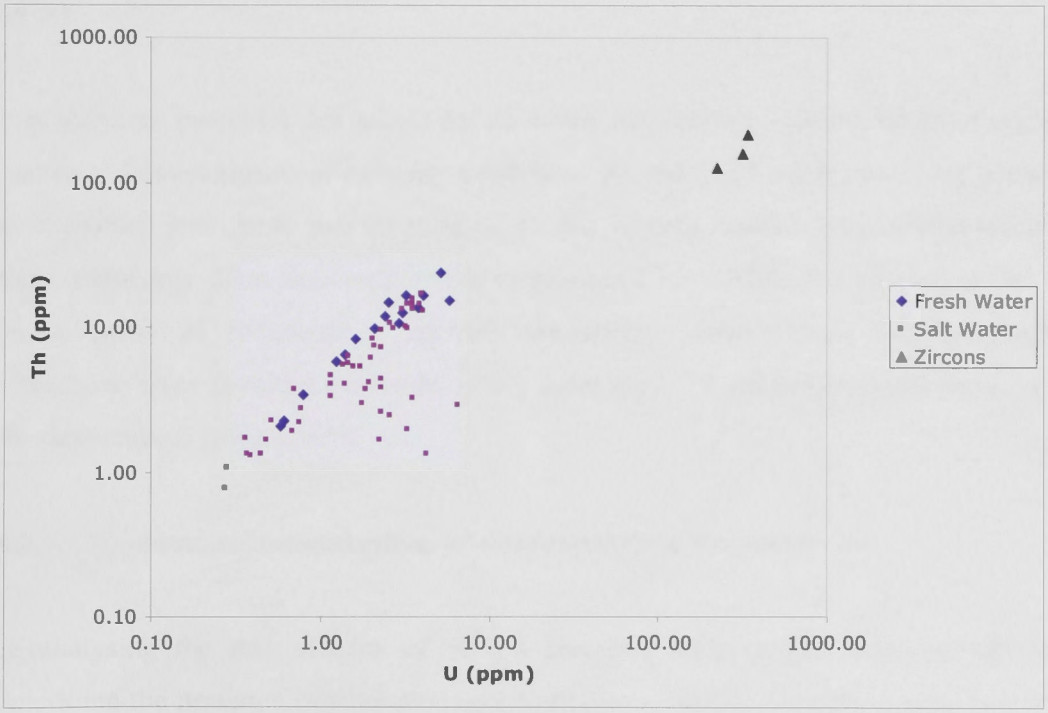

Figure 6.31: A log-log plot of the Th and U concentrations in freshwater and saltwater sands with greater than 90 wt. % SiO_2, compared to average beach sand zircons (zircon data from Sircombe, 1999).

Clearly this U trend does not correspond to additional zircon. Nor can it be explained by another detrital Th-U bearing accessory mineral such as monazite, which always has a Th/U ratio far in excess of PAAS and the freshwater sediment Th/U trend. Instead, it is proposed that U has been authigenically added to these estuarine sediments, after deposition.

Unlike Th, U has two common valencies (4^+ and 6^+), and as for iron, the transition from U^{4+} to U^{6+} occurs at a redox potential that can be found within normal geological environments. Thus, the geochemical behaviour of U changes from oxidising to reducing environments. In near surface environments under oxidizing conditions the uranyl ion (UO_2^{2+}) and its various complexes are mobile in weakly acid solutions and also in neutral and alkaline solutions if $CO_3^{2\square}$ is present (e.g. Krauskopf, 1967; Langmuir, 1978). However, reduction by organic matter to U^{4+} immobilises the U as highly insoluble uraninite (UO_2). The solubility of uranium in water is greatly reduced under anoxic conditions where uraninite and U^{4+} complexes are important (Langmuir, 1978).

It is therefore proposed that within the estuarine environment, accumulation of organic matter and development of reducing conditions, promoted by sulfate reducing bacteria, also enables authigenic precipitation of U that slightly modifies the composition of these sediments. This has considerable implications for studies that attempt to use the geochemistry of sediments to identify the specific source rocks for fine-grained sediments, since uranium cannot be safely assumed to be immobile or conservative in the depositional environment.

6.3.7. Anomalous concentrations of elements within the sediments

In analysing the relationships of certain elements with one another, we can also determine the presence of anomalous concentrations, and whether these concentrations are sourced from natural or anthropogenic sources. This is particularly important in terms of determining whether elements, which are present at low concentrations, pose future risks to the health of the estuary.

The Australian and New Zealand Sediment Quality Guidelines for Estuaries (ANZECC/ARMCANZ, 2000) give the concentrations at which a particular metal is deemed to pose toxic risks to living organisms in the sedimentary environment. These concentrations may be sourced from both natural and anthropogenic origins. The lower sediment quality guideline, or the 'trigger value', represents the concentration above which further ecosystem-specific investigation is recommended. The upper sediment quality guideline is a concentration corresponding to sediments which are highly contaminated and are likely to have a biological impact.

The data presented for Merimbula Lake shows that the highest value for a particular metal does not necessarily mean it is anomalous, above sediment quality guidelines, or above background readings which are interpreted from freshwater sediment samples (Table 6.4). The baseline data presented here is characterised by the fine-grained terrestrial weathered sediment component being transported and deposited within the estuary from up-catchment. This sample, a fine-grained clay collected from Boggy Creek (MC 030506-1a), represents the terrestrial sedimentary end-member. In many samples, the freshwater baseline sample concentration exceeds the lower range in Merimbula Lake. This is due to the mixing between the fine-terrestrial clays, and the coarser marine sands causing dilution of total concentrations. In this case, it is the concentrations which exceed the baseline data which are representative of post-depositional inputs.

Contaminant	Freshwater concentrations (baseline)	Merimbula Range	ISQG-Low (Trigger value)	ISQG-High
METALS (ppm)				
Antimony	1.14	0.1 – 5.3	2	25
Cadmium	0.04	0.0 – 2.5	1.5	10
Chromium	68.04	13.0 – 146	80	370
Copper	65.59	3.0 – 250	65	270
Lead	19.64	2.0 – 28.5	50	220
Nickel	14.96	5.2 – 79.0	21	52
Silver	0.48	0.1 – 2.8	1	3.7
Zinc	46.65	2.0 – 133	200	410
METALLOIDS (ppm)				
Arsenic	5.04	1.0 – 22.2	20	70

Table 6.4: Merimbula and freshwater data for selected elements, compared with recommended sediment quality guidelines (ANZECC/ARMCANZ, 2000).

The data shows that the concentrations of the metals in Merimbula Lake (with the exception of Ni) are always below the upper sediment quality guideline, with most metals being less than, or close to, the lower trigger value. However, significant enrichment of some elements in some samples compared to baseline data is evident, which warrants further investigation.

It should be noted that concentrations elevated above the regional mean do not necessarily imply the existence of local anomalies, since the local background will vary depending on the nature of the sediment. The methodology outlined in this research can nevertheless identify such anomalies, including local accumulation of anthropogenic additions in the sediment. Consequently, potential future environmental risks become evident, even when the anomalies are below baseline trigger values and would not otherwise be considered significant. Furthermore, the identity and location of the anomalous element and its behaviour relative to conservative species allows natural and anthropogenic contaminants to be distinguished.

In terms of biological risks, the trigger value for Pb (50 ppm) and the ISQG-High Value for Pb (220 ppm) (Table 6.4) are not supported by appropriate data for discussing the likelihood of biological affects. In any sediment analysis, some of the Pb is held in the crystal structure of detrital minerals (e.g. alkali feldspar, zircon), therefore ingestion and excretion by animals will have little or no effect on biota. It is therefore necessary to determine the proportion of Pb in a sediment, which is adsorbed to clays and iron hydroxides, that can be biologically taken up by plants and animals. For example, the clay-rich, fine-grained sediment with 30 ppm Pb may in fact have little impact on biota due to the concentration of Pb being locked within the crystal lattices, and therefore unavailable for biological uptake. In contrast, another sediment with only 20 ppm Pb, may have much of this as highly bioavailable Pb. Ingestion of large amounts of this sediment is consequently just as adverse as a small amount of the ISQG high trigger value sediment with high anthropogenic Pb contamination. Indeed it is misleading to think of a whole rock analysis with a trigger value. It is the biologically available contaminant that is critical, not the total concentration. Thus a bottom feeding fish ingesting sediment with a small amount of biologically reactive Pb, will take up, over a

long period of time, just as much Pb toxin from a contaminated sediment with a total Pb concentration well below ANZECC guidelines, as a "one-off" ingestion of a high concentration sample.

In order to determine whether an element has been added or removed from the estuarine sediment, it is necessary to compare the concentration of the elements in the estuary to baseline data. Elements in Merimbula Lake were normalized to lanthanum in the freshwater sediment sample (Figure 6.32). This allowed elements with anomalous concentrations relative to the freshwater data to be identified, defining the latter as an effective baseline. Elevation of elements above the baseline (1.00, or 100% of the total concentration of the baseline sample) therefore indicates post-depositional additions to the estuarine sediments. Elements which showed concentrations > 1.00 above baseline, included Sr and the metals Ni, Cu, Zn, Mo, Ag, Cd, Sn and Pb. These were considered to be significantly elevated in concentration with respect to the freshwater samples.

Compared to the chondrite normalising diagrams (Figures 6.5-6.10), in which the pattern of the REE did not change from clay to sand, but simply showed a decrease in concentration of REE with increasing quartz content of the sediments, normalising other elements to a baseline clay shows significantly different behaviour. For instance, normalising metals to the baseline shows anomalies which are independent of the clay-quartz component.

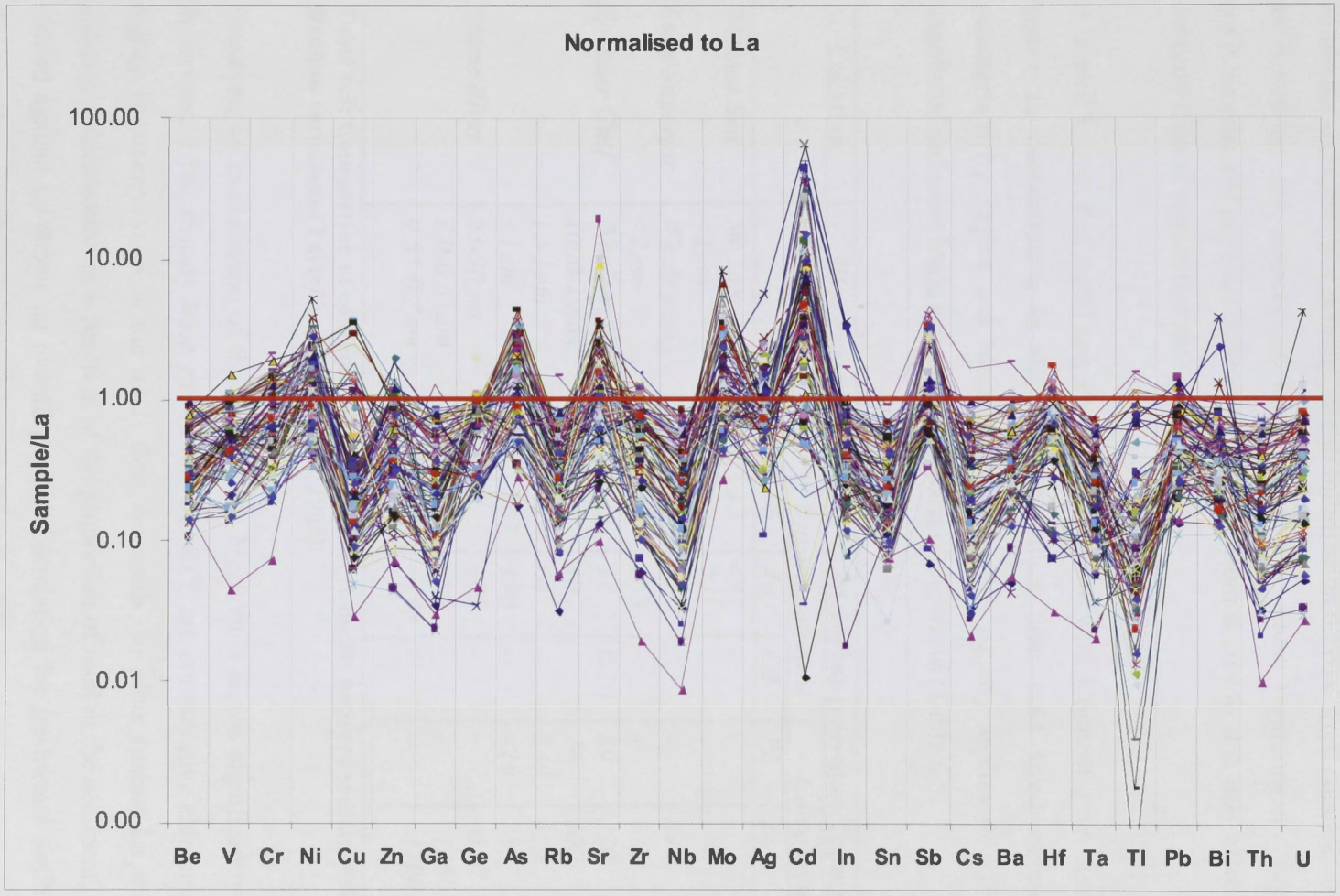

Figure 6.32: Metal concentrations in sediments from Merimbula Lake, normalized to lanthanum in freshwater baseline sample.

However, it is not enough to simply note the fact that certain elements are enriched within the sediment. Nor is there enough information derived from concentrations alone to determine the sources of these anomalies, since variations in geochemical environments and physical controls which exist from source to sink may affect the final concentration of elements within a sediment.

It is well known that metal concentrations correlate with sediment grain size, and are higher in concentration in the clay-rich rather than sand sized sediments. As summarized by Taylor and McLennan (1985), this equally applies to polluted and unpolluted sediment loads across various parts of the world (Table 6.5).

Location	Size Fraction	Metal concentration (ppm)					
		Uncontaminated			*Contaminated*		
		Pb	*Zn*	*Cd*	*Pb*	*Zn*	*Cd*
Barents Sea	*50-2μm*	***17***	*49*	-	-	-	-
	<2μm	***53***	*245*	-	-	-	-
Lake Superior	*Whole sample*	-	*91*	-	-	*64*	-
	<2μm	-	*166*	-	-	*530*	-
Spencer Gulf	*Whole sample*	***9.5***	*14*	*0.10*	***89***	*230*	*2.7*
	1000-10μm	***7.5***	*10*	-	***70***	*200*	*2.3*
	10-1μm	***41***	*64*	-	***340***	*620*	*9.4*
	<1μm	***107***	*190*	-	***410***	*780*	*8.0*
Rhine River	*63-20μm*	-	*~65*	-	-	*~350*	-
	2.0-0.63μm	-	*~90*	-	-	*~1260*	-
	0.63-0.2μm	-	*~170*	-	-	*~1700*	-

Table 6.5: Comparison of concentrations of various elements between sediment size fraction variations (Taylor and McLennan, 1985).

However, an examination of the Pb data for Merimbula shows significantly different behaviour. It has already been shown that the REE are conservative elements that are higher in concentration in the muds than the sands, so plots against La should also indicate concentration as a function of the proportion of mud in the sediment. Pb, when plotted against La shows an overall positive correlation for freshwater sediments, but does not do so for the saltwater sediments (Figure 6.33).

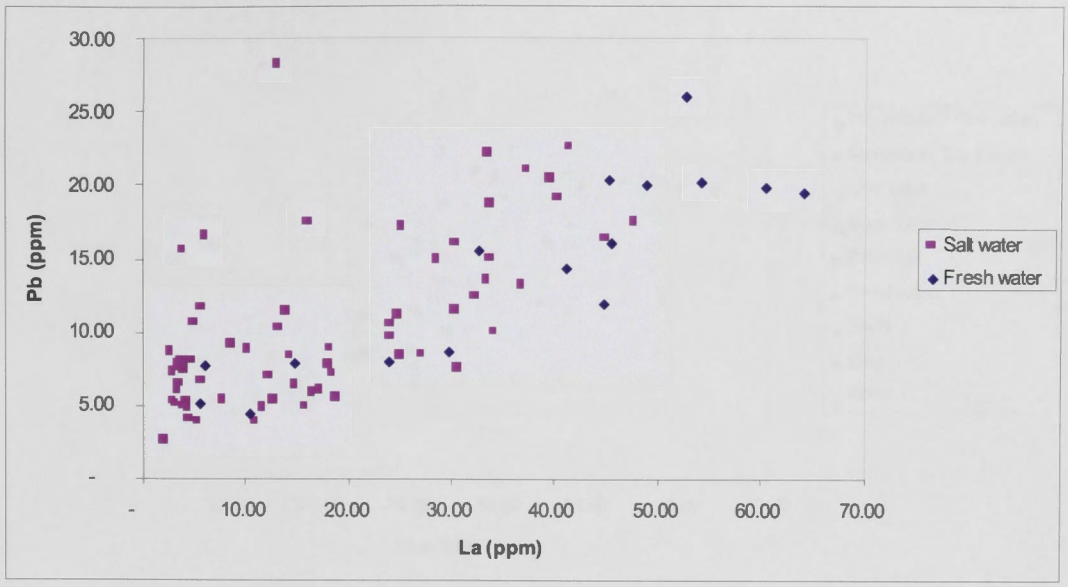

Figure 6.33: Relationship between Pb-La in estuarine and freshwater sediments.

The freshwater trend can be explained as domination by a terrigenous sourced variation. However, for the low-La saltwater samples, there is a range of observed Pb concentrations that cannot be explained by terrigenous mixing processes, and are presumably post-depositional additions.

The La-Pb data can be discriminated further by geographical location, and individual localities do in general show overall positive correlations between La and Pb, as expected from the decrease in grain size and subsequent increase in sediment surface area (Figure 6.34). However, the sediments in the Front Lake of Merimbula show a range of Pb concentrations to very high values, irrespective of changing grain size. This trend suggests that Pb is being added to the sediment after deposition. As the Front Lake of Merimbula is in close proximity to the township, it can be deduced that elevated Pb in the sediments correlates to anthropogenic contributions. These can be compared with the natural baseline delineated by the freshwater samples, which is not constant but increases systematically with La content.

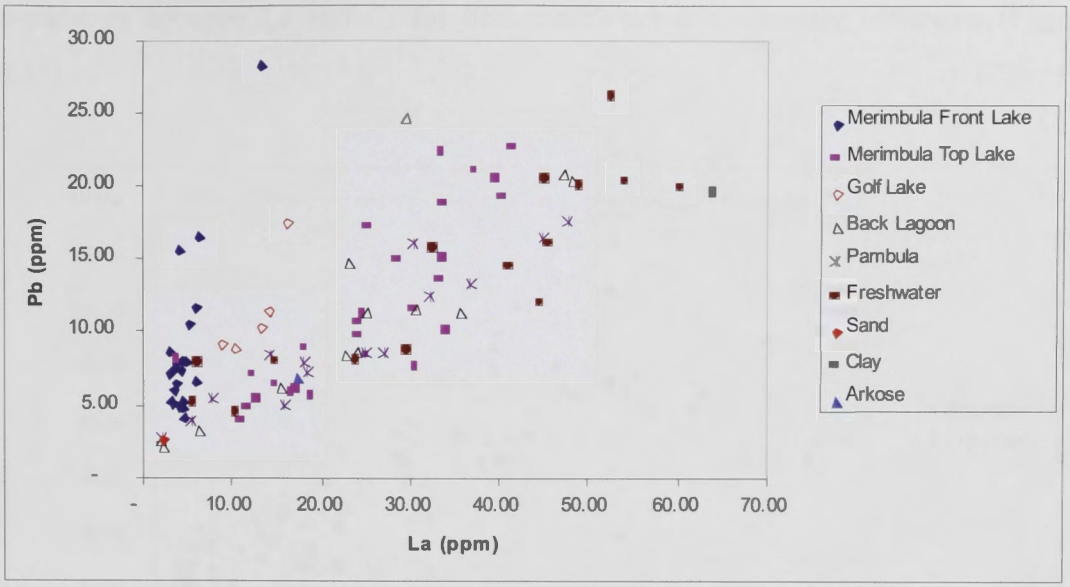

Figure 6.34: Mixing relationship between Pb-La in estuarine and freshwater sediments, by geographic location.

It is interesting to observe that when compared to the most La-rich freshwater clay sample, the sediments of the estuary do not appear to be particularly enriched in terms of absolute Pb concentration (Figure 6.34). The difference is only apparent when comparing sediments of similar La content. The Front Lake sediment samples, which have been deduced to show anthropogenic contamination, are mostly below baseline concentrations, as a result of the quartz in the sands diluting the elements that are concentrated in clay, such as Pb. Therefore, definition of an absolute concentration as a baseline would not detect the enrichment in the estuary. Absolute concentrations of elements do not always provide enough information to deduce whether the element is of original or post-depositional origin. Where sediment types vary between locations, as is the case in Merimbula Lake, anomalies do not necessarily reflect the highest absolute concentrations in the region, but instead must be identified relative to a baseline concentration which varies depending on the nature of the local sediment. This may be especially the case for regions with relatively weak signals. Consideration of inter-elemental trends, rather than individual concentrations, is vital for this to be achieved.

The distributions of other metals such as Cr, Ni, Cu, Zn, As, Cd, and Sn can be analysed in a similar way. The relationship between lanthanum and chromium shows a positive

correlation between La and Cr for both freshwater and seawater sediments (Figure 6.35).

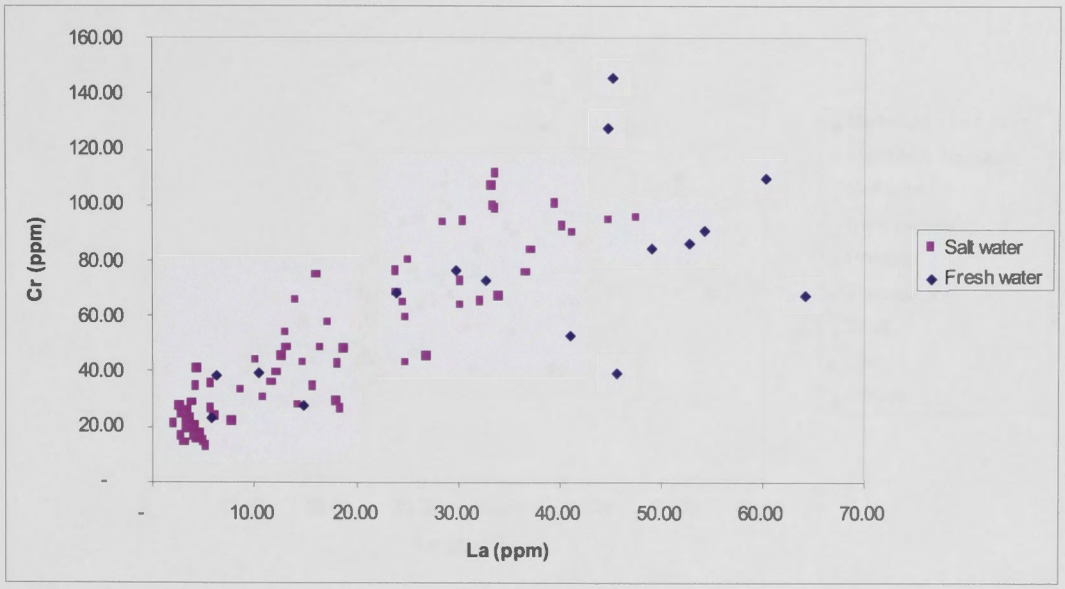

Figure 6.35: Relationship between Cr-La in estuarine and freshwater sediments.

Looking at the data in more detail to observe the distribution of chromium concentration with respect to geographic location, all samples appear to be enriched relative to the freshwater baseline samples. However, the Front Lake sediments show a very different trend to the sediments of the Top Lake (Figure 6.36). Although higher absolute concentrations of Cr are correlated with the finer-grained sediments of the Top Lake, the cluster of sediments in the Front Lake, which is known to have experienced anthropogenic inputs of Pb, also shows post-depositional input of Cr. Tin also shows similar behaviour (Figure 6.37).

Compared to the freshwater samples at Merimbula, the Front Lake sands are enriched in Sn. In contrast, at Pambula, it is the more clay-rich samples that are enriched in Sn. The major source of the Sn is most likely from anti-fouling paint, which is applied to the outer, underwater surfaces of boats and ships in order to inhibit the growth of barnacles and other marine organisms. Anti-fouling paints commonly consist of copper and tributyl tin, which may enter the water column and sediments due to leaching, flaking, or through maintenance of the vessel. In Merimbula, boats are moored in the sandy

Front Lake, whereas in Pambula Lake, there is a ship maintenance yard on the southern shoreline.

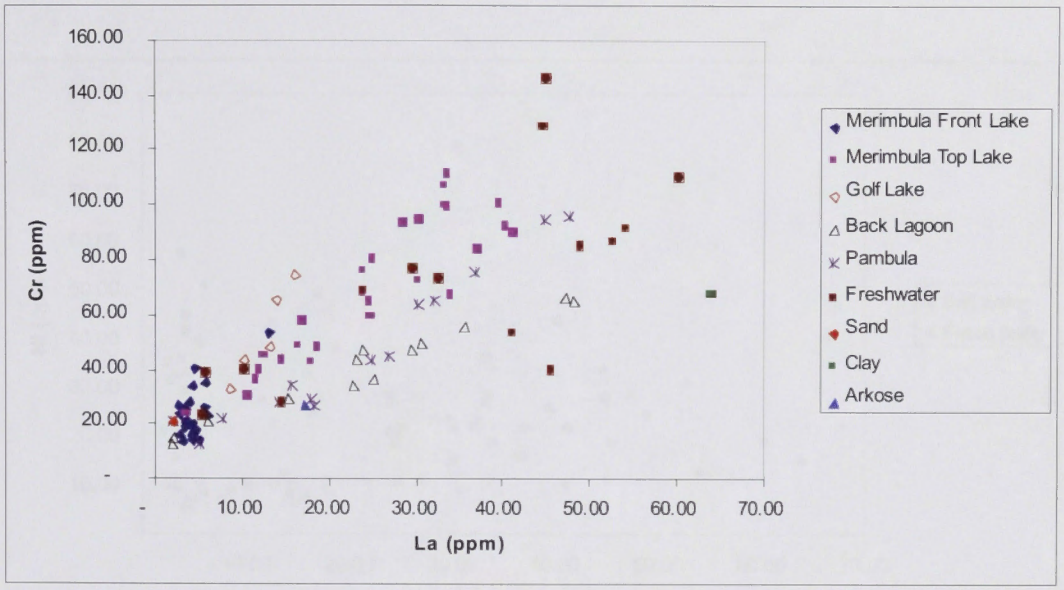

Figure 6.36: Mixing relationship between Cr-La in estuarine and freshwater sediments, by geographic location.

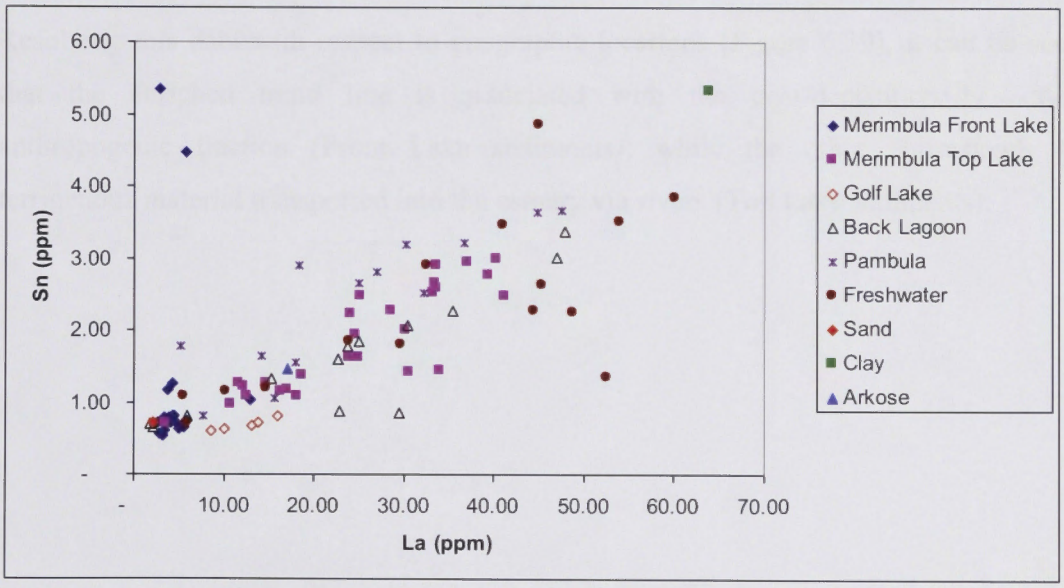

Figure 6.37: Mixing relationship between Sn-La in estuarine and freshwater sediments, by geographic location.

The relationship between nickel and lanthanum shows two trend lines in the data for saltwater samples, one following the freshwater baseline, while the other again shows substantial enrichment above the baseline (Figure 6.38).

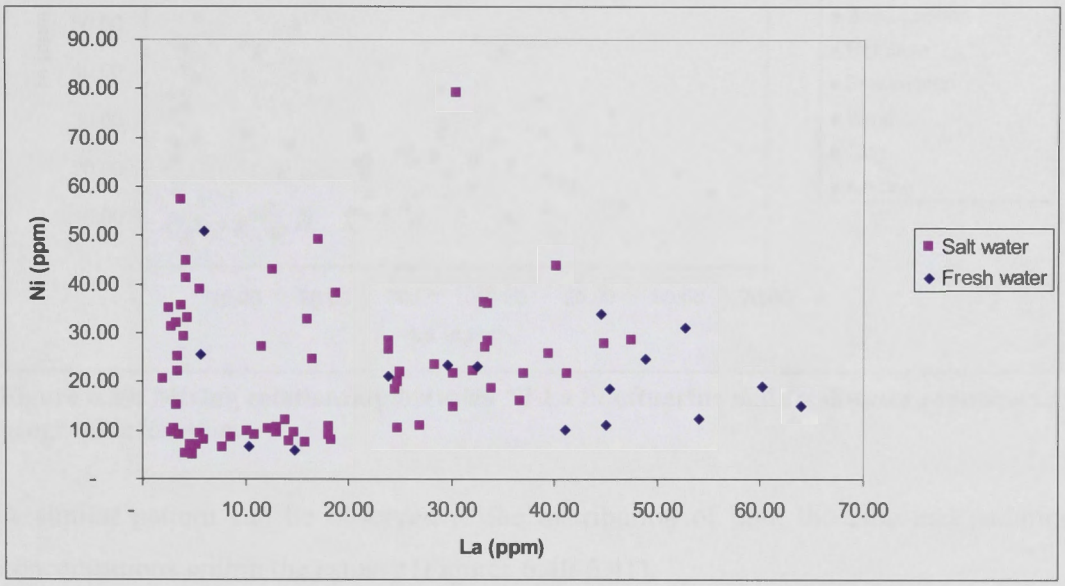

Figure 6.38: Relationship between Ni-La in estuarine and freshwater sediments.

Resolving this data with respect to geographic locations (Figure 6.39), it can be seen that the enriched trend line is associated with the post-depositionally added anthropogenic fraction (Front Lake sediments), while the other corresponds to terrigenous material transported into the estuary via rivers (Top Lake sediments).

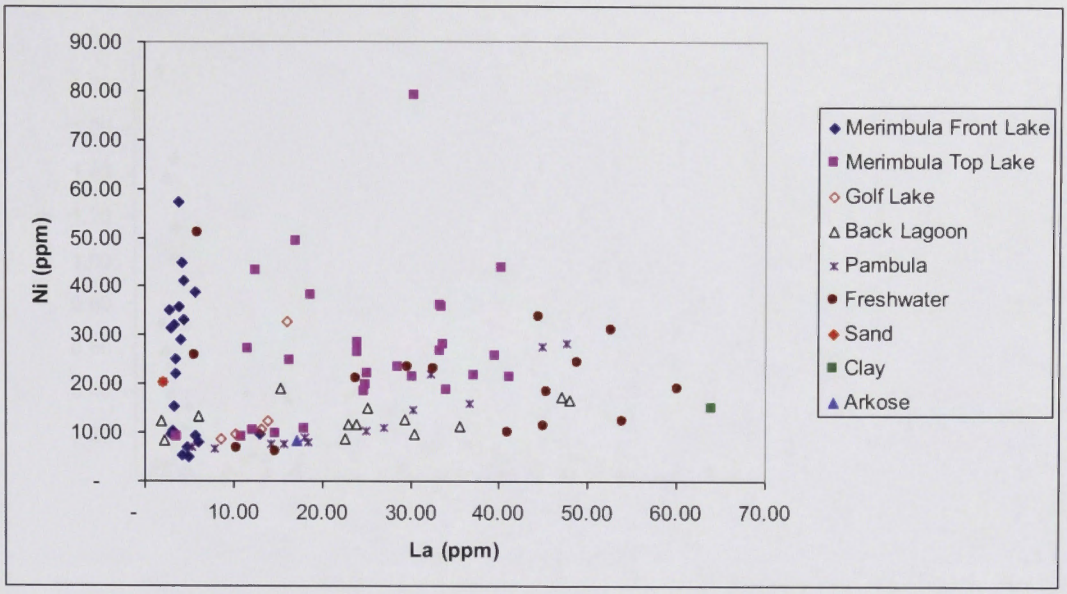

Figure 6.39: Mixing relationship between Ni-La in estuarine and freshwater sediments, by geographic location.

A similar pattern can be observed in the distribution of both the zinc and cadmium concentrations within the estuary (Figures 6.40-6.41).

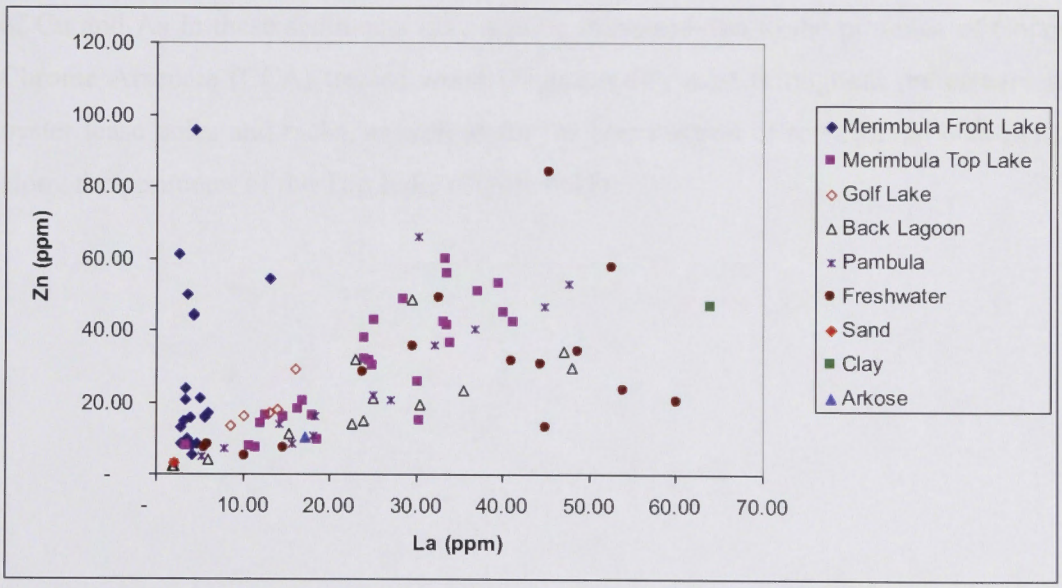

Figure 6.40: Mixing relationship between Zn-La in estuarine and freshwater sediments, by geographic location.

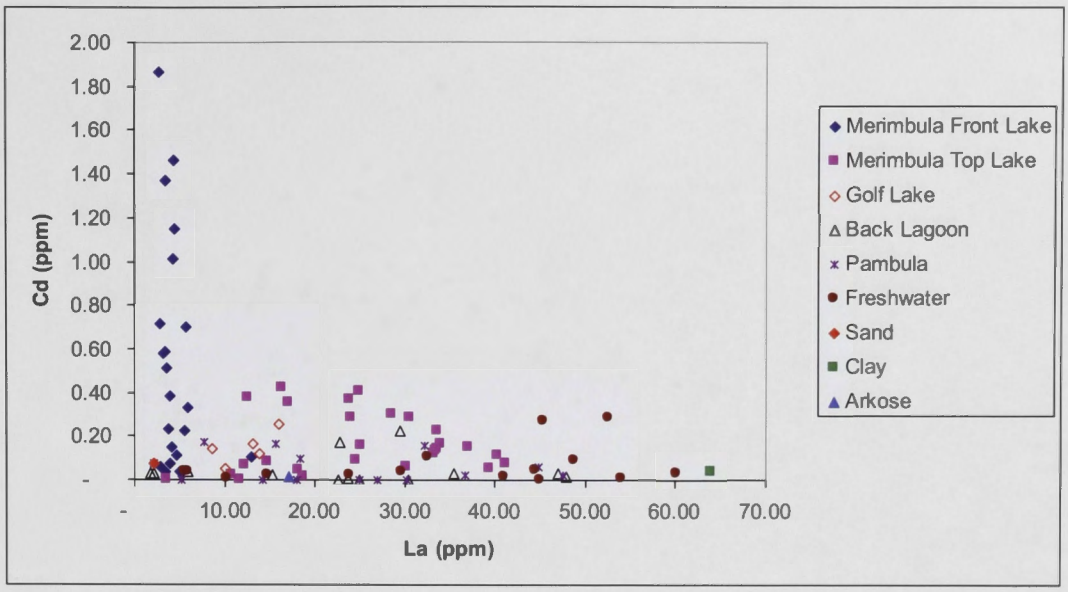

Figure 6.41: Mixing relationship between Cd-La in estuarine and freshwater sediments, by geographic location.

The distribution of arsenic and copper concentrations in the system shows a greater spread of the data, particularly in the Top Lake sediments, where these elements may be strongly adsorbed onto finer-grained sediments (Figure 6.42 – 6.43). The concentrations of Cu and As in these sediments may also be increased due to the presence of Copper Chrome Arsenate (CCA) treated wood (Figure 6.44), used throughout the estuary for oyster lease poles and racks, as well as for the construction of recreational boardwalks along the perimeter of the Top Lake (Figure 6.45).

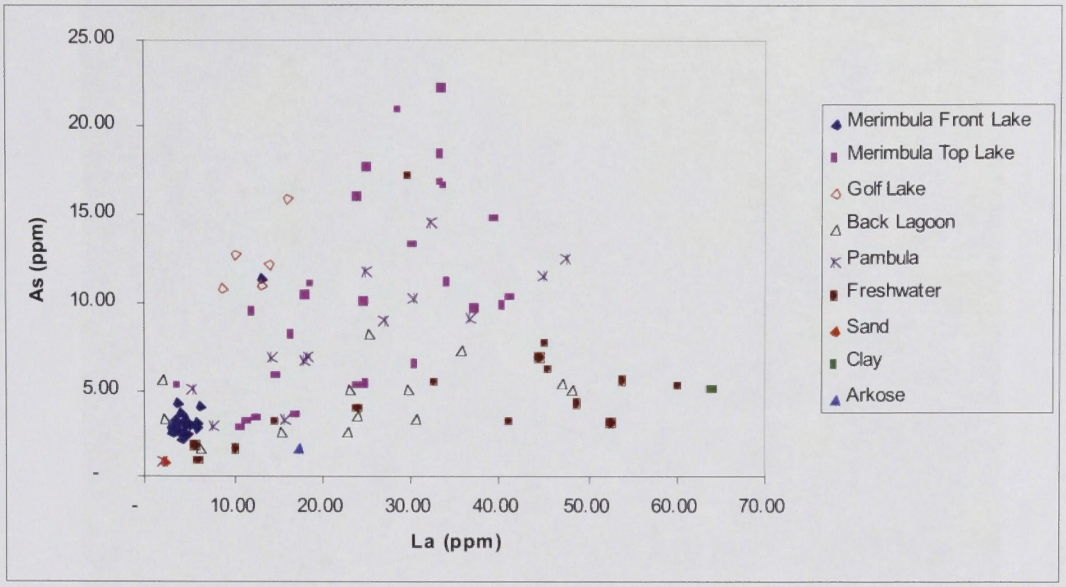

Figure 6.42: Mixing relationship between As-La in estuarine and freshwater sediments, by geographic location.

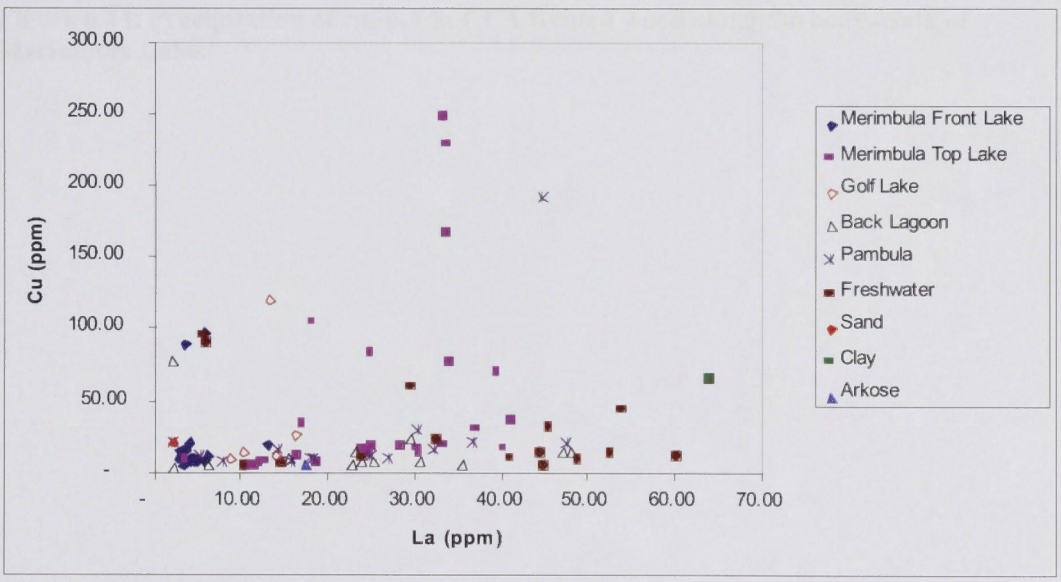

Figure 6.43: Mixing relationship between Cu-La in estuarine and freshwater sediments, by geographic location.

Figure 6.44: Precipitation of copper in CCA treated wood along the boardwalk of Merimbula Lake.

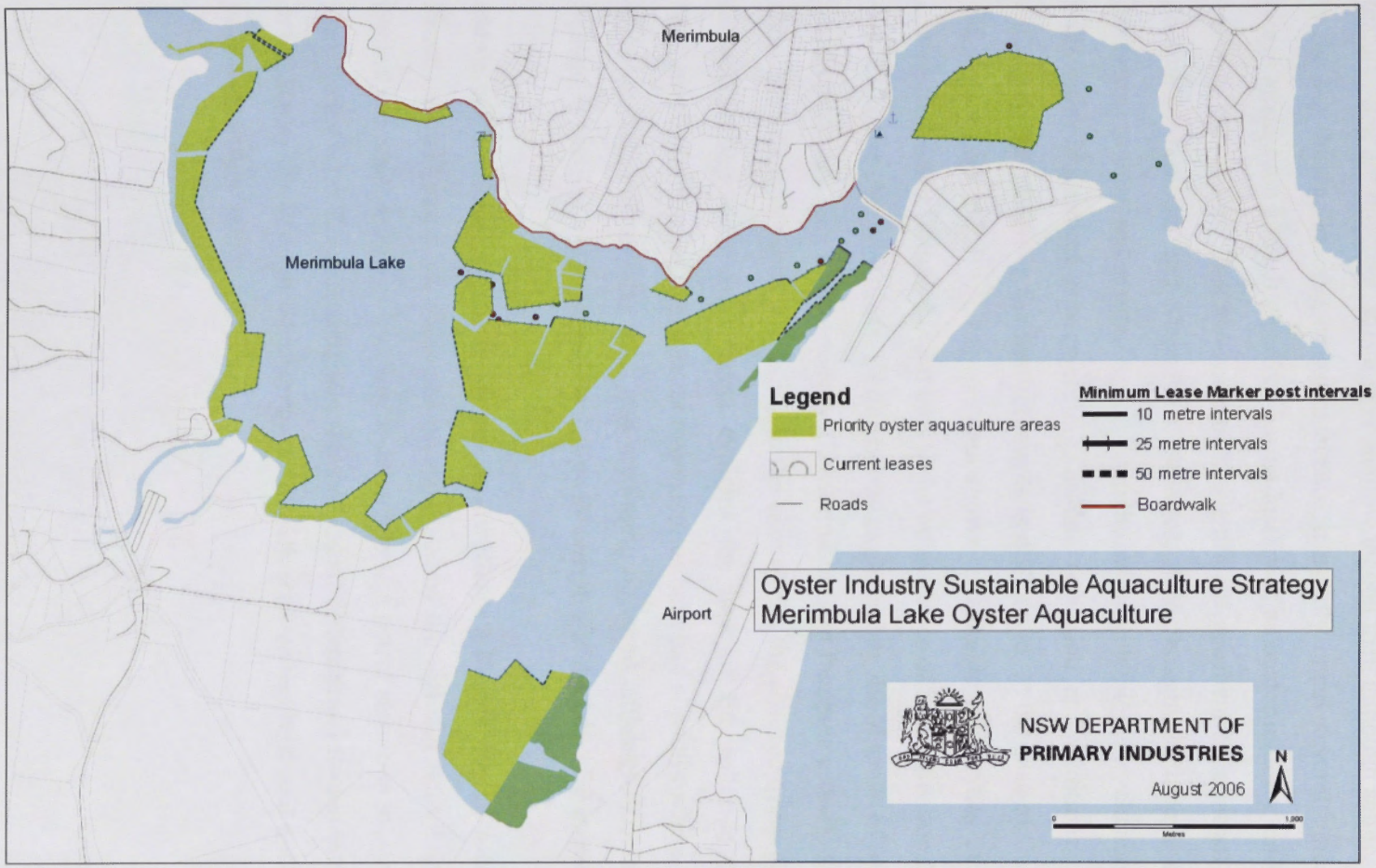

Figure 6.45: Map of oyster leases (green) and boardwalk (red line) at Merimbula Lake. A large quantity of the wooden oyster lease poles and the boardwalk have been treated with CCA.

Back Lagoon has the lowest concentration of any metal for a given La-content for all the estuarine sediment samples, and it matches the freshwater sample most closely. In contrast to Merimbula and Pambula estuaries, Back Lagoon has a number of physical features that are different. It is a very shallow lagoon that, although saline, is only open to the sea during flooding or storm events. It usually opens several times a year and closes again soon after. It therefore has no history of an oyster industry, and there are no boats in the lagoon. This has resulted in significant geochemical contrast to the wave dominated Pambula and Merimbula estuaries, even though all three share the same catchment source sediments. Apart from the authigenic/biogenic changes associated with redox dependent processes (e.g. sulfate reduction and addition), the style of anthropogenic additions to these sediments is distinctive. In the case of Cu, Cr, Ni, Zn, Cd, As and Sn, the Back Lagoon data shows remarkable similarities to the baseline source freshwater sediments, and thus show no evidence of contamination (Figures 6.35 – 6.42). In the case of Cu, As, Cr this can be explained by the absence of oyster farming and treated logs, as it is the site-specific Merimbula and Pambula estuary sediments that show the effects of these pollutants. In the case of Sn, the absence of Sn-based paint as an anti-fouling agent from boats explains the lack of Sn pollution compared to Merimbula and Pambula. The latter two estuaries both had slipways where maintenance of boats including sanding back and repainting occurred, although this has now been banned in Merimbula. A commercial slipway operates in the lake of Pambula estuary.

However, the Back Lagoon shows just as significant a Pb addition as does Merimbula Front Lake (Figure 6.34). This can be explained by the fact that Back Lagoon extends behind the main streets of Merimbula town where a petrol station is located on the hill slope to the lake. This demonstrates that individual differences between estuaries can be predicted on the basis of whether they are tidal, with aquaculture and boating, or non-tidal and shallow water.

6.4. Conclusions

In order to provide evidence for, and explanation of, the movements and concentrations of particular elements in estuarine sediments, a number of sampling methodologies and experiments was undertaken. The primary dataset consisted of bulk geochemical analyses from a collection of sediment samples. Many elements are concentrated in the fine-grained clay components of the terrigenous freshwater sediments, and some of these in turn are susceptible to removals or additions from seawater or other influences, while others, the "conservative" elements, are not. Variation in the non conservative elements due to such interactions may be disguised by dilution of the clay with a coarser-grained sand fraction. A methodology was developed whereby highly conservative elements (the REE) were identified. The ratios of concentrations of these elements show a constant pattern which remains unchanged irrespective of dilution of the clay by sand, or perturbations from other inputs. The absolute concentrations of one such element plotted against another show linear mixing trends between sand-rich and clay-rich end-member sediment types. Plotting other elements against a conservative species allowed anomalous concentrations to be identified. Once an understanding of the post-depositional elemental concentrations and relationships were determined, a second look at the bulk geochemistry allowed new patterns in multi-elemental relationships to be observed. Other inter-element plots also show distinct trend lines which are indicative of the origins of the elements in the sediments. For example, linear relationships exist between elements such as Ca and Sr which have crystallised together in detrital minerals such as feldspar, or have been post-depositionally introduced from seawater or as a biogenic shell component. Correlation between Fe and S demonstrates their occurrence in post-depositional pyrite. Conversely, Th and U correlate when present in detrital heavy minerals, but deviation away from the trend in seawater-influenced sediments demonstrates post-depositional addition of U. This methodology and approach to interpreting elemental relationships is particularly useful in defining anthropogenic contributions from, primarily, the estuarine water column. For example, the small Pb contribution from freshwater clays, which correlates with La content, can be distinguished from anthropogenic additions which do not.

It can be concluded that the elemental chemistry of the estuarine sediment is not simply a product of original source material, but also shows a number of post-depositional additions, transformations and significant post-depositional geochemical changes. In many cases, it is possible to identify these perturbations, the process responsible, and the source. Use of a baseline determined by local concentration of a conservative element also allows quite subtle anomalies to be identified and localised.

The compositions of the Front Lake sediments show anthropogenic anomalies that correlate with the presence of Merimbula Township nearby. The sediments have metal concentrations above a defined baseline compared with any other location in Merimbula Lake, even when the absolute concentrations are not higher. This is primarily due to runoff from the township directly into the Lake, including a large number of storm water outlets which run directly from the township into the Front Lake, as well as high boat traffic, large oyster leases, and recreational usage.

This research has significant implications for the oyster farming industry in terms of how to define a pristine environment. Regions which are utilised for aquaculture have strict sediment and water quality guidelines in place. In most cases, these environments are relatively pristine and are monitored carefully. Sediment Quality Guidelines provide trigger values, with lower and upper limits. In Merimbula and Pambula, in almost all samples collected, values were well within the safe range. However, through analysis of inter-element relationships, it becomes obvious that the highest concentration of an element does not necessarily mean it is anomalous, or has the greatest enrichment above an appropriately chosen baseline. Anomalies can nevertheless be identified that are above such a baseline, but below absolute concentration limits. At what concentration then, is an element defined as being of concern?

Elements that show concentrations deviating significantly from baseline levels should be observed over time to determine accumulated concentrations to support planning for future risks arising from acid sulfate soil formation, dredging and changes in sea level, temperature and nutrient levels, which may remobilise accumulated and concentrated elements from the sediment column.

Although this study is mainly concerned with identification of post-depositional inputs into estuarine sediments, it also has implications for other areas of Earth Science and industry. In mineral exploration, it is common practice to gather a large amount of elemental concentration data from surface material and contour this data spatially, in order to identify a potential exploration target underlying the highest concentration in cover. However, this study shows that a uniform zero or regional mean concentration is not necessarily an effective choice as a baseline for identification of geochemical anomalies. If the nature of the host material varies from locality to locality, then the baseline concentrations must be adjusted to reflect that variation. Absolute maxima in concentration need not necessarily identify locations with the greatest addition, while significant anomalies above a low local baseline may not show up as high absolute concentrations.

Chapter Seven: Using Isotopes to Verify Anthropogenic Inputs into Estuarine Sediments

7.1. Introduction

Isotopes are important tools for identification of the sources of particular elements in the environment. Strontium isotopes analyses were undertaken on a number of sediment samples obtained from Merimbula Lake, Pambula Lake and up catchment in order to define the proportion of strontium sourced from the terrestrial weathering products, and the proportion added from marine biogenic sources. Similarly, lead isotope analyses were undertaken on the same sediment dataset in order to identify what proportion of lead in the sediments is from anthropogenic sources, and what proportion is from naturally occurring sources. The results of these analyses were then compared with the distributions of strontium and lead, relative to a baseline defined by the conservative REE, as described in the previous chapter. Combining these two types of data further strengthens the ability to discriminate and quantify fluxes of trace elements from different sources.

7.2. Strontium Isotopes

Strontium has four stable, naturally occurring isotopes: ^{84}Sr, ^{86}Sr, ^{87}Sr and ^{88}Sr. ^{87}Sr is a radiogenic isotope, generated by emission of a negative beta particle from ^{87}Rb (Veizer, 1989). The decay constant for Rb^{87} is 1.42×10^{-11} yr^{-1} (Steiger and Jäger, 1977); hence its half life is 48.6 Gyr. On geological timescales, the total inventory of isotopes ^{84}Sr, ^{86}Sr and ^{88}Sr remain constant, in contrast to ^{87}Sr, and their mutual abundance ratios do not vary (Veizer, 1989). Strontium isotopic composition is not fractionated by processes such as phase separation, chemical speciation, evaporation or biological assimilation (Smith, *et al.*, 2009).

The strontium isotopic composition of terrestrial inputs from rivers depends upon the lithology of the catchment. The $^{87}Sr/^{86}Sr$ ratio can be used as a tracer to determine if a source rock was a mantle-derived magma or was a result of more extensive processing in the crust. For mantle-derived rocks, the isotopic ratio ranges from $^{87}Sr/^{86}Sr \approx 0.699 - 0.706$; and, for crustal involvement, $^{87}Sr/^{86}Sr \approx 0.705\text{-}0.735$. The average $^{87}Sr/^{86}Sr$ ratio for global runoff from major river systems is 0.7119 (Palmer and Edmond, 1989).

Strontium is present in the oceans at a concentration of approximately 8.1 ppm at 3.5% salinity and has a long residence time ($2\text{-}5 \times 10^6$ yr) compared to the relatively short mixing time of water in the oceans ($\sim 10^3$ yr) (Xu and Marcantonio, 2007). As a result, the strontium in the world's oceans is isotopically homogenous ($^{87}Sr/^{86}Sr = 0.70906$, Faure, 1986), and biogenic and authigenic precipitates everywhere in the ocean incorporate strontium of the same isotopic signature (Xu and Marcantonio, 2007). However, changes in the strontium isotopic signature in the oceans have occurred over geological time, which relate to changes in contributions from hydrothermal inputs at ocean ridges versus those from weathering of rocks on the continents. Isotopic ratios of sources range from $^{87}Sr/^{86}Sr = 0.704$ for young volcanic rocks to 0.708 in marine carbonates and 0.720 for older continental crust (Faure, 1986; Palmer and Edmond, 1989; Xu and Marcantonio, 2007). Rain has a similar strontium isotopic composition to seawater (Åberg *et al.*, 1989; Bain and Bacon, 1994).

The $^{87}Sr/^{86}Sr$ ratio in sediments can be used to identify the source of sediments in estuarine systems (Faure, 1986; Douglas *et al.*, 1995; Rachold *et al.*, 1997; Négrel *et al.*, 2000; Singh and France-Lanord, 2002; Douglas *et al.*, 2003; Bayless *et al.*, 2004; Smith *et al.*, 2009). In the mixing environment of an estuary, the strontium isotopic signature of the sediments reflects contributions derived from the ocean water (precipitated carbonates, silicates, oxides and sulfides) and terrestrial weathering products (Faure, 1986). In contrast, the authigenic and biogenic component will reflect a $^{87}Sr/^{86}Sr$ ratio of the water body from which it was derived (Négrel *et al.*, 2000; Smith *et al.*, 2009), while the sediments deposited from the terrestrial environment will have a $^{87}Sr/^{86}Sr$ ratio which represents an average composition of the weathered, eroded and transported material (Smith *et al.*, 2009). As the sediment component includes strontium from

multiple sources, with each source having distinct and uniform isotopic compositions, it is possible to determine which proportion of strontium in the sediment is derived from each of the sources (Bain and Bacon, 1994).

7.3. Lead isotopes

Concentrations of lead and lead isotope ratios can be used to identify contamination in the environment (Munksgaard and Parry, 1998). Mining practices, emissions by industrial sources and the burning of fossil fuels have all introduced various forms of lead into the environment (Saint-Laurent *et al.*, 2010). Although the atmospheric lead source constitutes a major flux to the environment, the inputs from fluvial transport are also extremely important.

Lead isotopes can be used to distinguish between anthropogenic and natural sources (Kehoe, 1965; Erel *et al.*, 1997; Wilson *et al.*, 2006; Saint-Laurent, 2010). Lead consists of four stable isotopes: ^{204}Pb; ^{206}Pb; ^{207}Pb; and ^{208}Pb. Three of these, ^{206}Pb, ^{207}Pb, and ^{208}Pb, are radiogenic end products, derived from ^{238}U, ^{235}U, and ^{208}Th respectively. These isotopes have increased in abundance as a result of the decay rate of their parent isotopes since the formation of the Earth (Munksgaard and Parry, 1998). The signatures of these isotopes vary with respect to geological sources, and the isotopic composition of lead ores is usually different to that of bedrock (Brown, 1962; Faure, 1986; Renberg *et al.*, 2002). This differentiation between the two sources makes it possible to use lead isotope compositions to determine the presence of anthropogenic (mined) lead in the environment (Renberg *et al.*, 2002).

Lead exists as a pollutant in an Australian setting primarily from the past use of leaded petrol (gasoline), which was dispersed throughout the environment due to its high concentration in the atmosphere. The isotopic signature of lead used in Australian petrol is unique, due to the dominant use of lead from the early Proterozoic Pb-Zn ore deposits in Broken Hill, N.S.W., and Mt Isa, Qld (Gulson *et al.*, 2006). These deposits were formed at 1700 Ma and have a distinct signature of the $^{206}Pb/\ ^{204}Pb$ ratio of 16.0 (± 0.02%) for Broken Hill, and 16.1 (± 0.02%) for Mt Isa (Gulson *et al.*, 2006). This

contrasts with the signature found in younger (400 Ma) Pb-Zn deposits from Australia and other parts of the world which have a $^{206}Pb/^{204}Pb$ ratio of 18.1 (Gulson, 1996). In contrast, lead derived from other sources, such as paint and batteries may have different isotopic values, based upon their origin. For instance, batteries which are often made from scrap lead, and therefore derived from mixed sources may have a range of $^{206}Pb/^{204}Pb$ values. Townsend and Snape (2008) reported discarded batteries as having $^{206}Pb/^{204}Pb$ values ranging from 15.97 – 17.87. Similarly, leaded paint produced using Australian lead will have isotopic values of Broken Hill and Mt Isa, whereas if derived from different sources, may exhibit $^{206}Pb/^{204}Pb$ values similar to another major source, for instance, Idaho USA (16.90) (Townsend and Snape, 2008). Lead isotopes therefore provide a valuable method for tracing anthropogenically-derived heavy metal pollution in the environment (Kober *et al.*, 1999).

Lead is adsorbed to clays and FeOOH, and thus is potentially mobile in the sedimentary environment, although it may become immobilised due to decreasing pH or high levels of organic material (de Matos *et al.*, 2001; Backstrom *et al.*, 2006; Saint-Laurent *et al.*, 2010). Lead is also readily bioaccumulated. However, its isotopic composition is not significantly affected by physical or chemical processes (Bollhoffer and Rosman, 2001).

This study uses lead isotopes to distinguish between natural and anthropogenic lead in the estuarine environment of Merimbula and Pambula. The results are incorporated into the REE-adapted baseline methodology in Chapter 6 to provide further information regarding the sources of anthropogenic lead and other metals, as well as biogenic, authigenic and terrestrial post-depositional additions to the estuarine sediment.

7.4. Analytical methods

Sr and Pb isotopic data was obtained using Inductively Coupled Plasma Mass Spectrometry (ICP-MS) at the Australian Institute of Nuclear Science and Engineering (AINSE) within the Australian Nuclear Science and Technology Organisation (ANSTO) facility and from RSES, ANU. An initial set of approximately 50 samples were analysed for lead isotopes at ANSTO in the AINSE facility by ICP-MS. Due to

large analytical errors, these results could not be used. A subset of 10 samples were subsequently analysed for lead and strontium isotopes at RSES, ANU. Ten sediment samples, one USGS standard (MAG-1) and one procedural blank were analysed by MC-ICPMS (NEPTUNE), along with SRM 987 Sr and SRM 981 Pb solution standards.

Sample aliquots containing ~ 1 μg Pb and a few μg Sr, but comprising less than 100 mg total sample were digested in HF/HNO_3 on a hotplate in Teflon "bombs". A second aliquot of HF/HNO_3 was then added and the bombs were assembled in stainless steel jackets, transferred to an oven at ~ 190°C and heated at least overnight. After cooling, the bomb contents were evaporated on a hotplate until dry. 6M HNO_3 was then added and evaporated, followed by dissolution in 2M HNO_3 ready for ion exchange column separation. Six of the samples required further treatment with HCl and HNO_3 to derive accurate solutions in 2M HNO_3. All the samples were centrifuged before introduction to the columns, and a few samples left significant undissolved fluoride residues.

All samples were loaded on pre-prepared 0.15 mL Sr spectrometer ion exchange columns. The major elements and most trace elements were eluted prior to collecting the Sr fraction and then the Pb fraction.

7.4.1. Strontium

The first round of dilutions gave variable yields that did not correlate with the presence of undissolved residues. Hence, several samples were measured twice at different dilutions. Washout or instrument blanks were measured before each sample and comprised <0.1% of the sample signal for most isotopes and were ignored in data reduction. A procedural blank also had < 0.1% of the sample signal for most isotopes for most of the samples (when calculated at the same dilution as sample solutions) and it too was ignored. Krypton interference (from the Ar gas) on ^{84}Sr and ^{86}Sr was subtracted as an instrumental blank. The ion exchange chemistry did not completely eliminate Rb from some samples, so the ^{87}Rb correction on ^{87}Sr was significant in those cases. Instrumental mass bias was corrected utilising $^{86}Sr/^{88}Sr$ (based on an assumed $^{86}Sr/^{88}Sr$ value of 0.1194).

7.4.2. Lead

In contrast to Sr, the Pb yields were consistent and predictable, so that only one round of dilutions was necessary. Thallium (SRM 997) was added to each sample solution to allow correction for mass bias utilising $^{205}Tl/^{203}Tl$. Washout or instrumental blanks and the procedural blank were <0.1% for most isotopes, and were ignored in the data reduction, just as for the Sr analyses. Mercury interference on ^{204}Pb varied from ~0.05% - ~0.4% and was subtracted by monitoring ^{202}Hg.

7.5. Results and Discussion

7.5.1. Strontium

A total of 10 sediment and rock samples were analysed for strontium isotopes (Table 7.1). This table gives results for freshwater clays and gravels, the local Devonian red beds as well as estuarine muds and sands. The strontium results, together with isotopic values obtained from McCulloch and Woodhead (1993) from the Bega Batholith, Berridale Batholith and selected Ordovician sediments are shown in Table 7.2, a $^{87}Sr/^{86}Sr$- total Sr diagram (Figure 7.1) and a $^{87}Sr/^{86}Sr$-$^{85}Rb/^{86}Sr$ diagram (Figure 7.2).

The Merimbula Group sample, which is a representative rock sample from the Late Devonian red bed mudstone which outcrops significantly in this catchment, shows a high $^{87}Sr/^{86}Sr$ signature of 0.78841. The average modern seawater has an $^{87}Sr/^{86}Sr$ value of 0.70918 (Hodell *et al.*, 1989), and modern shells in sediments should reflect this seawater value. All samples analysed for strontium isotopes plot between these two end-members. The freshwater clay sample (MC 030506-1a) has a relatively high $^{87}Sr/^{86}Sr$ value of 0.74034, which reflects its terrestrial source. With the addition of marine biogenic components to the sediments in the estuary, the $^{87}Sr/^{86}Sr$ is lowered, becoming closer to that of seawater. Variability in the total strontium concentration is due to the mixing between the mature weathering products, and biogenically derived marine strontium, as solid solution in the bivalves and gastropods. As the estuarine sediments are a combination of terrestrial and authigenic components, the $^{87}Sr/^{86}Sr$ value will

reflect the mixing of these components. The Bega River gravels (111107-14), are representative of the coarse material transported from the catchment and deposited in a freshwater environment, has a $^{87}Sr/^{86}Sr$ ratio of 0.72019, which is similar to the estuarine sediments, implying that terrestrial input into the estuary cannot always be unambiguously distinguished by its high $^{87}Sr/^{86}Sr$. This is further emphasised by the similar $^{87}Sr/^{86}Sr$ data from local Ordovician sediments (McCulloch and Woodhead 1993) (Table 7.1, Figure 7.1). However, if Sr and Rb data are considered together, terrigenous and marine origins can still be distinguished.

Sample number	Location	$^{87}Sr/^{86}Sr$	$^{84}Sr/^{86}Sr$	$^{85}Rb/^{86}Sr$	Sr (ppm)
MC 030506-1a	Freshwater clay (Boggy Creek)	0.74034 ± 0.00001	0.05652 ± 0.00000	0.00743 ± 0.00002	63.93
MLI 080307-04	Soils from banks of Millingandi Creek	0.71710 ± 0.00002	0.05650 ± 0.00000	0.00946 ± 0.00002	70.22
111107-14	Gravels (Bega River)	0.72019 ± 0.00003	0.05651 ± 0.00001	0.03352 ± 0.00004	99.93
Merimbula Group	Devonian red beds	0.78841 ± 0.00004	0.05660 ± 0.00000	0.10612 ± 0.00007	41.92
BST. A1	Merimbula Front Lake sands	0.71910 ± 0.00002	0.05648 ± 0.00000	0.00774 ± 0.00002	58.73
ML 130406-05 (18)	Merimbula Top Lake delta	0.71458 ± 0.00004	0.05646 ± 0.00002	0.02790 ± 0.00007	219.20
C2-0	Merimbula Top Lake - Core 2, surface	0.71253 ± 0.00003	0.05646 ± 0.00000	0.00605 ± 0.00005	99.10
C2-68	Merimbula Top Lake - Core 2, 68cm depth	0.71871 ± 0.00002	0.05654 ± 0.00000	0.01624 ± 0.00002	67.50
GL 161006-03	Golf Lake sands	0.71754 ± 0.00002	0.05649 ± 0.00000	0.00326 ± 0.00002	75.53
PR 120406-01	Pambula River sands	0.71706 ± 0.00002	0.05647 ± 0.00000	0.00484 ± 0.00004	8.71
Average modern seawater (Hodell *et al.*, 1989)		0.70918			8.10
Global average runoff (Palmer and Edmond, 1989)		0.7119			

Table 7.1: Isotope results for $^{87}Sr/^{86}Sr$, $^{84}Sr/^{86}Sr$, $^{85}Rb/^{86}Sr$ and Sr (ppm) for Merimbula and Pambula estuaries; freshwater clays, gravel and Devonian basement; average seawater; global average runoff (Palmer and Edmond, 1989); and samples from Bega Batholith and Berridale Batholith and Ordovician sediments (McCulloch and Woodhead, 1993).

Sample number	Location	$^{87}Sr/^{86}Sr$
Bega Batholith (McCulloch and Woodhead, 1993)	Moruya	0.70408
	Cobargo	0.70466
	Kameruka	0.70560
	Candelo	0.70566
	Bemboka	0.70897
	Glenbog	0.70869
	Tonghi	0.70869
Berridale Batholith (McCulloch and Woodhead, 1993)	Merumbago	0.71082
	Delegate	0.70682
	Jindabyne	0.70769
	Cootralantra	0.71206
Ordovician sediments (whole rock) (McCulloch and Woodhead, 1993)		0.71993

Table 7.2: Isotope data for $^{87}Sr/^{86}Sr$ for samples from Bega Batholith and Berridale Batholith and Ordovician sediments (McCulloch and Woodhead, 1993).

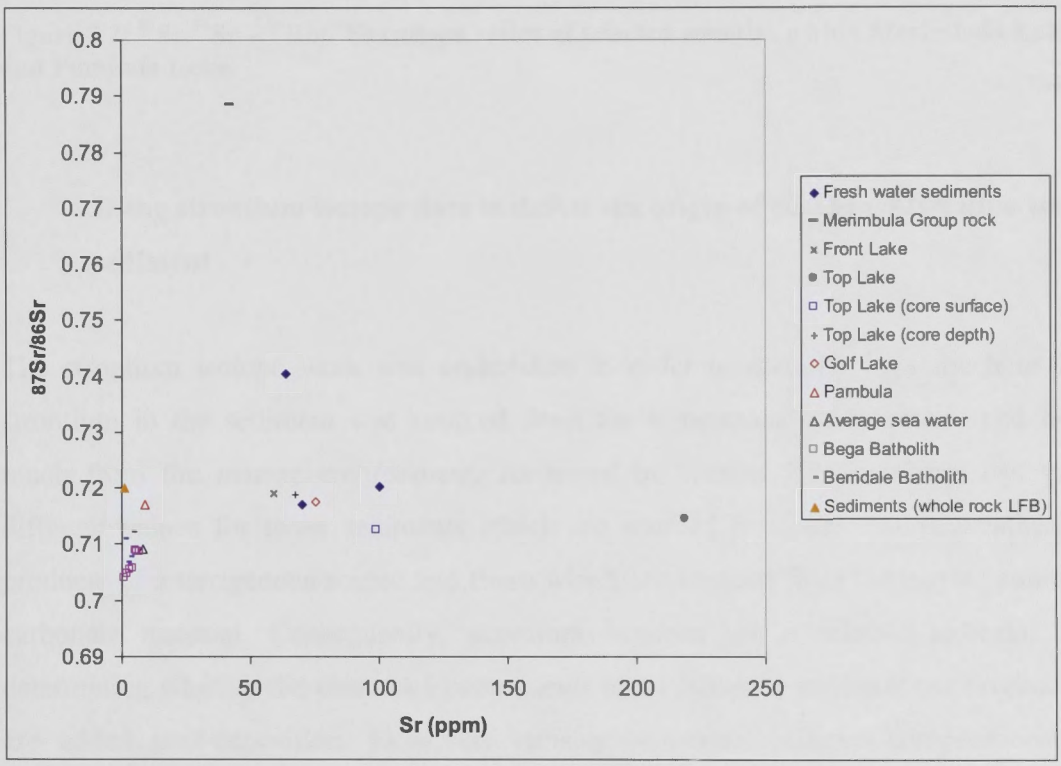

Figure 7.1: $^{87}Sr/^{86}Sr$ – total Sr isotope ratios of selected samples from Merimbula Lake and Pambula Lake, with the inclusion of $^{87}Sr/^{86}Sr$ signatures from Bega Batholith, Berridale Batholith and Ordovician sediments (McCulloch and Woodhead 1993).

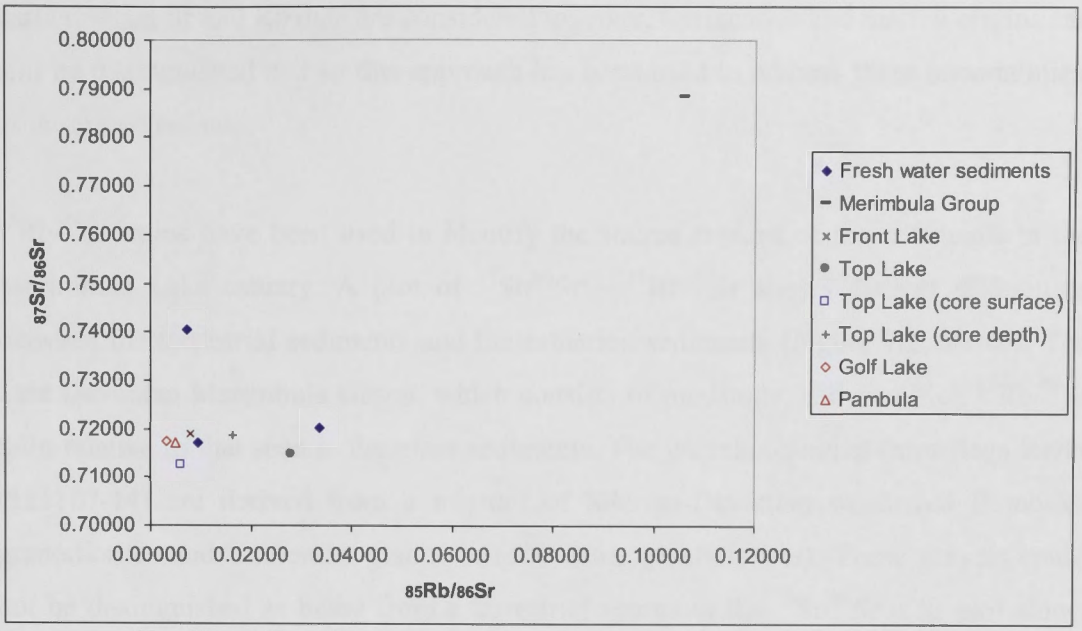

Figure 7.2: $^{87}Sr/^{86}Sr$ – $^{85}Rb/^{86}Sr$ isotope ratios of selected samples within Merimbula Lake and Pambula Lake.

Using strontium isotope data to define the origin of components within the sediment

The strontium isotope work was undertaken in order to quantify how much of the strontium in the sediment was sourced from the terrigenous environment, and how much from the marine environment. As noted in Section 7.2, strontium has very different values for those sediments which are sourced from the mature weathering products of a terrigenous source and those which are sourced from the marine sourced carbonate material. Consequently, strontium isotopes are a reliable indicator for determining whether the elemental components of an estuarine sediment are original or are added post-deposition. However, utilising strontium isotopic compositions to distinguish between marine and land sourced sediments may encounter uncertainties, due to ongoing estuarine geochemical and biogeochemical processes that affect those samples obtained from estuaries. The formation of Fe-Mn oxyhydroxide and organic matter coatings, and exchangeable carbonates on the surfaces of the sediment particles, may have altered surface particle interactions, causing Sr to be incorporated from the seawater, with concomitant reduction of the $^{87}Sr/^{86}Sr$ ratio (Smith *et al.*, 2009). As noted

earlier, when Sr and Rb data are considered together, terrigenous and marine origins can still be distinguished and so this approach has been used to address these uncertainties, as described below.

$^{85}Rb/^{86}Sr$ ratios have been used to identify the source regions of the sediments in the Merimbula Lake estuary. A plot of $^{87}Sr/^{86}Sr$ – $^{85}Rb/^{86}Sr$ shows distinct differences between the terrestrial sediments and the estuarine sediments (Figure 7.2, above). The Late Devonian Merimbula Group, which consists of mudstone, shows a high $^{85}Rb/^{86}Sr$ ratio relative to that seen in the other sediments. The gravels obtained from Bega River (111107-14) are derived from a mixture of Silurian-Devonian weathered Bemboka granodiorites and Kameruka granodiorites (biotite granodiorites). These gravels could not be distinguished as being from a terrestrial source in the $^{87}Sr/^{86}Sr$ – Sr plot alone. However, the higher $^{85}Rb/^{86}Sr$ value relative to the marine sediment samples confirms a terrestrial origin.

The sample obtained from the Top Lake basin of Merimbula Lake estuary, ML 130406-05 (18), shows a value between the gravels and the marine beach sands, consistent with the composition being a mixture between the two sources. A lower $^{85}Rb/^{86}Sr$ ratio in the clay sample is indicative of a different source material to the Bega River gravels and the Merimbula Group red beds. The lower $^{85}Rb/^{86}Sr$ ratio in the freshwater clays reflects the source material from which the creek drains, the Late Devonian Boyd Volcanic Complex. The transported clays represent a mixture of acid volcanics, basalts and quartz porphyries, and hence show a lower radiogenic signal.

The similarity between the clays and the marine end-member in terms of the $^{85}Rb/^{86}Sr$ value ensures that all the samples obtained from the estuary plot in Figure 7.2 as a tight cluster. This also shows that the clays from the input creeks reflect the greatest terrigenous source to the estuarine sediments.

7.5.2. Lead

A total of 10 sediment and rock samples were analysed for lead isotopes (Table 7.3). This table gives results for freshwater clays and gravels, the local Devonian red beds,

estuarine muds and sands and reference material from Broken Hill (Chiaradia *et al.*, 1997). The McCulloch and Woodhead (1993) data are for K-feldspars from the Bega Batholith, Berridale Batholith and whole-rock Ordovician sediments from the Lachlan Fold Belt (whole rock LFB), and are given in Table 7.4.

In addition to discriminating parent source materials, lead isotope studies can also be effective in differentiating natural from anthropogenic sources of lead (Bindler *et al.*, 2001). Lead concentrations in lake and estuarine sediments can be derived from a range of natural and anthropogenic sources derived from surrounding drainage systems transporting the weathered products of catchment soils, bedrock and mineral matter from the catchment (Renberg *et al.,* 2002) and anthropogenic contaminants.

Selected sediment samples from Merimbula and Pambula were analysed for lead isotopes and plotted on the $^{207}Pb/^{204}Pb$-$^{206}Pb/^{204}Pb$ graph (Figure 7.3), together with isotopic data derived from McCulloch and Woodhead (1993. Figure 7.3 also includes data for the Proterozoic lead from Broken Hill (Chiaradia *et al.,* 1997. The Broken Hill lead may be taken to represent the end member composition of any suspected anthropogenic input into the sediment, such as from the synthetic tetraethyl lead formerly added to petrol.

	Location	$^{206}Pb/^{204}Pb$	$^{207}Pb/^{204}Pb$	$^{208}Pb/^{204}Pb$	$^{207}Pb/^{206}Pb$	$^{208}Pb/^{206}Pb$	Pb (ppm)
MC 030506-1a	Freshwater clay (Boggy Creek)	19.1354 ± 0.0008	15.6801 ± 0.0008	39.2804 ± 0.0019	0.8194 ± 0.0000	2.0528 ± 0.0000	19.64
MLI 080307-04	Soils (Millingandi Creek)	18.9474 ± 0.0008	15.6716 ± 0.0008	39.1593 ± 0.0019	0.8271 ± 0.0000	2.0667 ± 0.0000	8.84
111107-14	Gravels (Bega River)	18.4595 ± 0.0008	15.6421 ± 0.0008	38.5250 ± 0.0018	0.8474 ± 0.0000	2.0870 ± 0.0000	7.84
Merimbula Group	Devonian red beds	19.0220 ± 0.0007	15.6791 ± 0.0008	39.2713 ± 0.0018	0.8243 ± 0.0000	2.0645 ± 0.0000	20.49
BST. A1	Merimbula Front Lake sands	17.4208 ± 0.0010	15.5376 ± 0.0010	37.2316 ± 0.0024	0.8919 ± 0.0000	2.1372 ± 0.0000	28.25
ML 130406-05 (18)	Merimbula Top Lake delta	18.1065 ± 0.0007	15.5965 ± 0.0007	38.1303 ± 0.0017	0.8614 ± 0.0000	2.1059 ± 0.0000	22.30
C2-0	Merimbula Top Lake - Core 2, surface	17.7169 ± 0.0008	15.5679 ± 0.0009	37.6992 ± 0.0022	0.8787 ± 0.0000	2.1279 ± 0.0000	12.30
C2-68	Merimbula Top Lake - Core 2, 68cm depth	18.9743 ± 0.0010	15.6724 ± 0.0010	39.2377 ± 0.0024	0.8260 ± 0.0000	2.0679 ± 0.0001	14.14
GL 161006-03	Golf Lake sands	18.4237± 0.0008	15.6278 ± 0.0008	38.4260 ± 0.0021	0.8483 ± 0.0000	2.0857 ± 0.0001	11.47
PR 120406-01	Pambula River sands	19.0994 ± 0.0010	15.7203 ± 0.0010	39.2100 ± 0.0025	0.8231 ± 0.0000	2.0530 ± 0.0001	2.68
Broken Hill (Chiaradia *et al.*, 1997)		16.003			0.9617	2.2283	

Table 7.3: Isotope results for ^{204}Pb, ^{206}Pb, ^{207}Pb and ^{208}Pb from Merimbula and Pambula estuaries and the catchment and Broken Hill (Chiaradia *et al.*, 1997).

	Location	$^{206}Pb/^{204}Pb$	$^{207}Pb/^{204}Pb$	$^{208}Pb/^{204}Pb$
Bega Batholith	Moruya	18.170	15.581	38.042
	Cobargo	18.179	15.599	38.132
	Kameruka	18.154	15.619	38.179
	Candelo	18.185	15.620	38.197
	Bemboka	18.160	15.630	38.207
	Glenbog	18.149	15.629	38.203
	Tonghi	18.142	15.622	38.182
Berridale Batholith	Merumbago	18.134	15.643	38.248
	Delegate	18.153	15.621	38.163
	Jindabyne	18.226	15.633	38.253
	Cootralantra	18.107	15.641	38.229
Sediments (whole rock LFB)		20.720	15.812	41.454

Table 7.4: Pb isotopic composition of K-feldspar from Bega Batholith, Berridale Batholith and whole rock sediments from the LFB (from McCulloch and Woodhead, 1993).

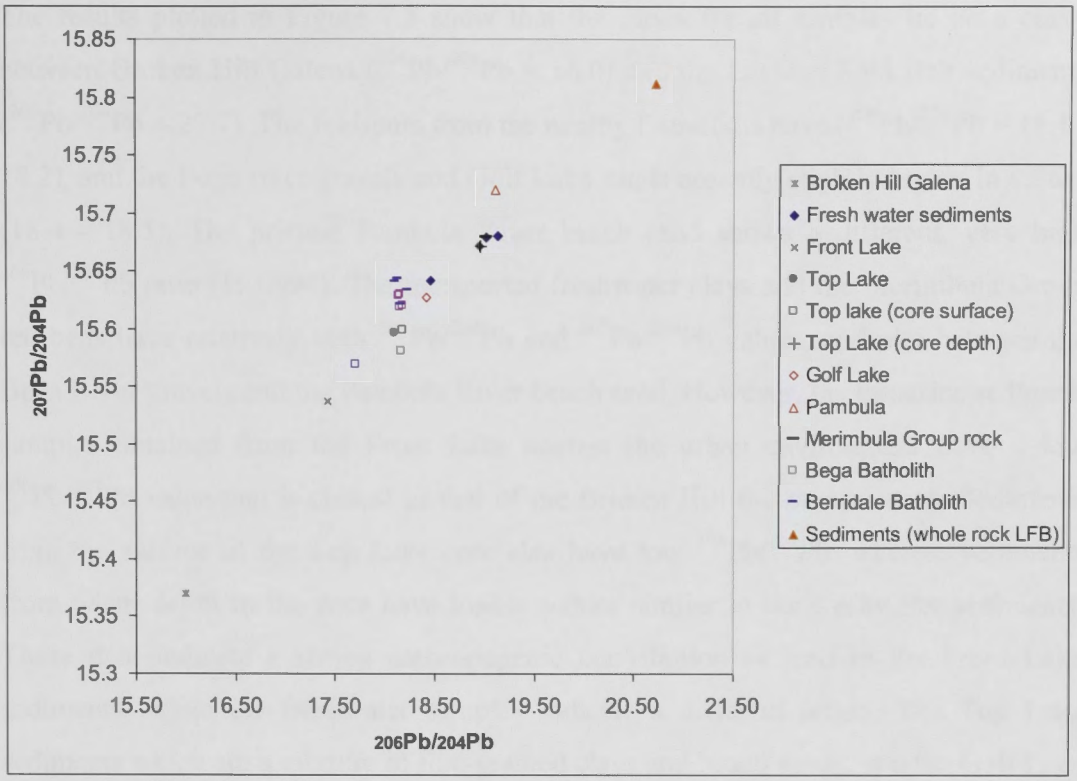

Figure 7.3: $^{207}Pb/^{204}Pb$-$^{206}Pb/^{204}Pb$ isotope ratios of samples within Merimbula Lake and Pambula Lake, compared to Broken Hill galena (Chiaradia *et al.*, 1997) and Bega Batholith, Berridale Batholith and Ordovician sediments (McCulloch and Woodhead 1993).

Using lead isotope data to define the origin of components within the sediment

Lead isotope analysis was undertaken specifically to determine how much of the lead in the sediment was derived from anthropogenic sources. The focus of this study was to determine the source of a range of elements by analysing the relationships between the element of interest and a conservative element. Therefore, an investigation of lead isotopes was a vital step in further elaborating on the deductions of Chapter 6, where the correlation between Pb and La in the estuaries and catchment shows the data to follow two distinct types of behaviour. While some of the data follows the mixing line between the two sedimentary end-members, a large number of samples show comparative enrichment above the base line, which is a result of post-depositional addition in the estuary (refer to Figure 6.34).

The results plotted in Figure 7.3 show that the ratios for all samples lie on a curve between Broken Hill Galena ($^{206}Pb/^{204}Pb$ = 16.0) and the Lachlan Fold Belt sediments ($^{206}Pb/^{204}Pb$ = 20.7). The feldspars from the nearby Batholiths have ($^{206}Pb/^{204}Pb$ = 18.1 - 18.2), and the Bega river gravels and Golf Lake sands are only slightly higher in values (18.4 - 18.5). The pristine Pambula River beach sand shows a different, very high $^{206}Pb/^{204}Pb$ ratio (19.0994). The transported freshwater clays and the Merimbula Group red beds have relatively high $^{206}Pb/^{204}Pb$ and $^{207}Pb/^{204}Pb$ values, and plot between the Bega River gravels and the Pambula River beach sand. However, the estuarine sediment samples obtained from the Front Lake nearest the urban environment have a low $^{206}Pb/^{204}Pb$ value that is closest to that of the Broken Hill ore composition. Sediments from the surface of the Top Lake core also have low $^{206}Pb/^{204}Pb$, whereas sediments from 68cm depth in the core have higher values similar to the freshwater sediments. These data indicate a strong anthropogenic contribution of lead to the Front Lake sediments, while the freshwater samples indicate a different origin. The Top Lake sediments which are a mixture of fine-grained clays and beach sands, and the Golf Lake sediment samples, which receive runoff from treated sewage, represent a mixing of the natural and anthropogenic signals. The spread of data therefore indicates a distinction between what is a natural lead signal, and what is an anthropogenic lead signal in the Merimbula Lake sediments.

To put the Merimbula and Pambula data in a broader context, $^{207}Pb/^{206}Pb$-$^{208}Pb/^{206}Pb$ ratios from this study were compared with data from Broken Hill, and data also given by Chiaradia *et al.*, (1997) for Mt Isa (lead, silver, copper and zinc), leaded petrol, Cobar (copper, lead, zinc and silver mine in northern N.S.W.), Captains Flat (previously mined for gold, silver, lead, zinc, copper and iron), Port Kembla (heavily industrialized seaport, steelworks, copper smelter, and coal terminal in N.S.W.), Lake Illawarra (in the vicinity of Port Kembla), and Woodlawn (zinc, lead and copper sulfide deposit in southern N.S.W.) (Table 7.5, Figure 7.4).

Sample	$^{206}Pb/^{204}Pb$	$^{208}Pb/^{206}Pb$	$^{207}Pb/^{206}Pb$
Australian ore deposits			
Broken Hill	16.003	2.2283	0.9617
Captains Flat	18.065	2.1122	0.8643
Cobar	18.105	2.1078	0.8631
Mt Isa	16.112	2.2224	0.9586
Woodlawn	18.087	2.1087	0.8633
Other potential lead sources			
Gasoline	16.403	2.2015	0.9432
Air	16.588	2.1886	0.9335
Sediments			
Lake Illawarra; sediment sample	18.772	2.0667	0.8326
Mullet Creek; sediment sample	17.215	2.1492	0.9007
Lake Illawarra; sediment sample	17.684	2.1264	0.8798
Lake Illawarra; sediment sample	17.579	2.1275	0.8833
Port Kembla Inner Harbour; sediment sample	18.286	2.0571	0.8544

Table 7.5: $^{206}Pb/^{204}Pb$, $^{208}Pb/^{206}Pb$ and $^{207}Pb/^{206}Pb$ values for Australian ore deposits, gasoline, air and sediments obtained from polluted estuarine environments on the south eastern coast of Australia (from Chiaradia *et al.*, 1997)

Pambula River sand and the freshwater sediments show extremely low ratios on this plot (young radiogenic lead), whereas the data from Broken Hill, Mount Isa, gasoline and air lie at the other extreme. Woodlawn, Cobar and Captain's Flat mine sites in younger host rocks that are expected to have a very high absolute content of lead, are at intermediate ratios. One Lake Illawarra sediment sample is higher than these, strongly suggesting anthropogenic contamination with 'old' lead from lead ore. The Merimbula Front Lake and Top Lake core surface samples of this study are similarly high in $^{207}Pb/^{206}Pb$ and $^{208}Pb/^{206}Pb$ ratios, implying that the same applies at these localities.This is in strong contrast to the majority of sediment samples of this study, which show ratios lower than Cobar, Captain's Flat and Woodlawn, while the sediments from Top Lake are similar to those mine sites. The isotopic values from the Front Lake and the Top Lake core surface are uniquely high. It should be noted that the Front Lake of Merimbula is surrounded by the township, with high levels of runoff and stormwater drainage discharging directly into the Lake, whereas Pambula Lake is bordered by national parks. Thus, Front Lake has sources of anthropogenic contamination that lower-ratio sites such as Pambula do not. This data therefore shows that the lead concentrations in the sediments of the Front Lake of Merimbula are of anthropogenic origin, while the sands obtained from Pambula River, and the freshwater sediments have little anthropogenic influence.

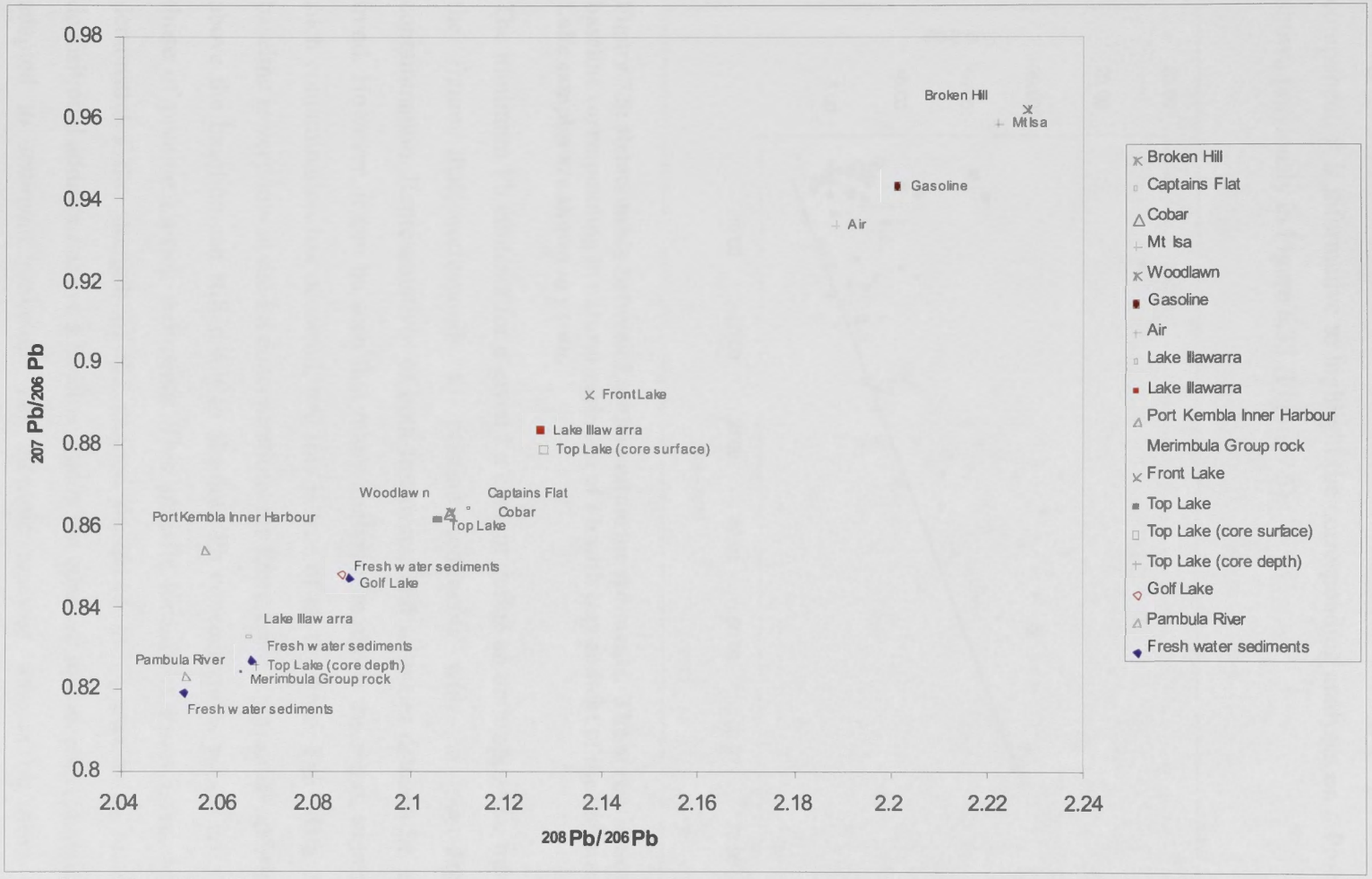

Figure 7.4: $^{207}Pb/^{206}Pb$-$^{208}Pb/^{206}Pb$ with location of sampling sites, Broken Hill Galena and other locations for comparison (from Chiaradia *et al.*, 1997).

Having identified the lead of the Front Lake sediments as having a high anthropogenic component, it is informative to highlight the corresponding analyses on a Pb-La plot as shown previously in Figure 6.33 (Figure 7.5).

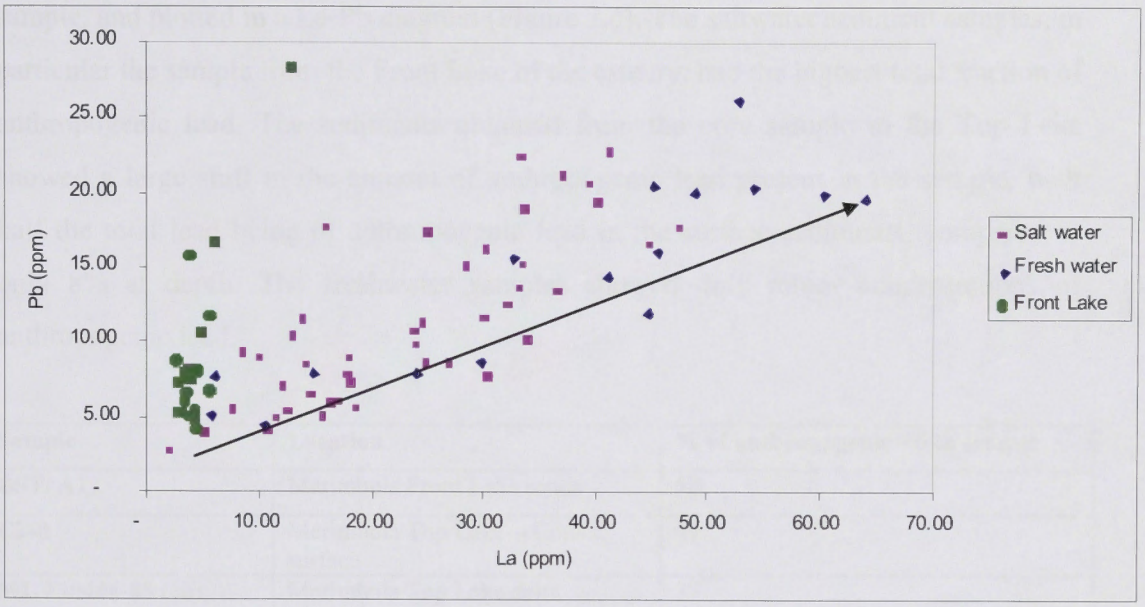

Figure 7.5: Relationship between La-Pb in estuarine sediments. The arrow indicates a baseline corresponding to natural variation of Pb with clay content of the sediment. Front Lake samples are shown in green.

The minimum Pb contents for a given La content define an anthropogenic trend line in the figure that corresponds to pristine sediments with no post-depositional contamination. Representatives of both freshwater and saltwater datasets lie along this trend. However, it can be seen that many analyses lie above the trend, indicating that such contamination has occurred, and this is true of all the Front Lake data. Since the baseline is very low at the La concentrations for Front Lake, substantial additions of Pb above the baseline can still result in absolute Pb concentrations which are similar to those of pristine La-rich sediments. This specific locality at Front Lake, Merimbula demonstrates the strength of the method described in Chapter 6 to identify post depositional additions above a baseline that is not constant in concentration but which is adapted to sediment make-up. The isotopic analysis follows on from this and demonstrates that the added Pb can be identified as anthropogenic, which correlates with the proximity of Merimbula Township.

Based upon these isotope data, the amount of lead in each sample which could be attributed to an anthropogenic source (defined by the leaded petrol value) was determined using simple fractions. The percentage of anthropogenic lead in each sample is given in Table 7.6. The anthropogenic fraction of lead was removed from the total sample, and plotted in a La-Pb diagram (Figure 7.6). The saltwater sediment samples, in particular the sample from the Front Lake of the estuary, had the highest total fraction of anthropogenic lead. The sediments obtained from the core sample in the Top Lake showed a large shift in the amount of anthropogenic lead present in the sample, with half the total lead being of anthropogenic lead in the surface sediments, compared to only 8% at depth. The freshwater samples showed only minor concentrations of anthropogenic lead.

Sample	Location	% of anthropogenic Pb in sample
BST. A1	Merimbula Front Lake sands	58
C2-0	Merimbula Top Lake - Core 2, surface	49
ML 130406-05 (18)	Merimbula Top Lake delta	35
111107-14	Gravels (Bega River)	23
GL 161006-03	Golf Lake sands	23
MLI 080307-04	Soils (Millingandi Creek)	8
C2-68	Merimbula Top Lake - Core 2, 68cm depth	8
Merimbula Group	Devonian red beds	6
PR 120406-01	Pambula River sands	1
MC 030506-1a	Freshwater clay (Boggy Creek)	0

Table 7.6: Percentage of anthropogenic lead fraction in each sample. This is calculated by the formula for a sample (totalPb-baseline Pb at a particular La value) divided by total Pb content of the sample.

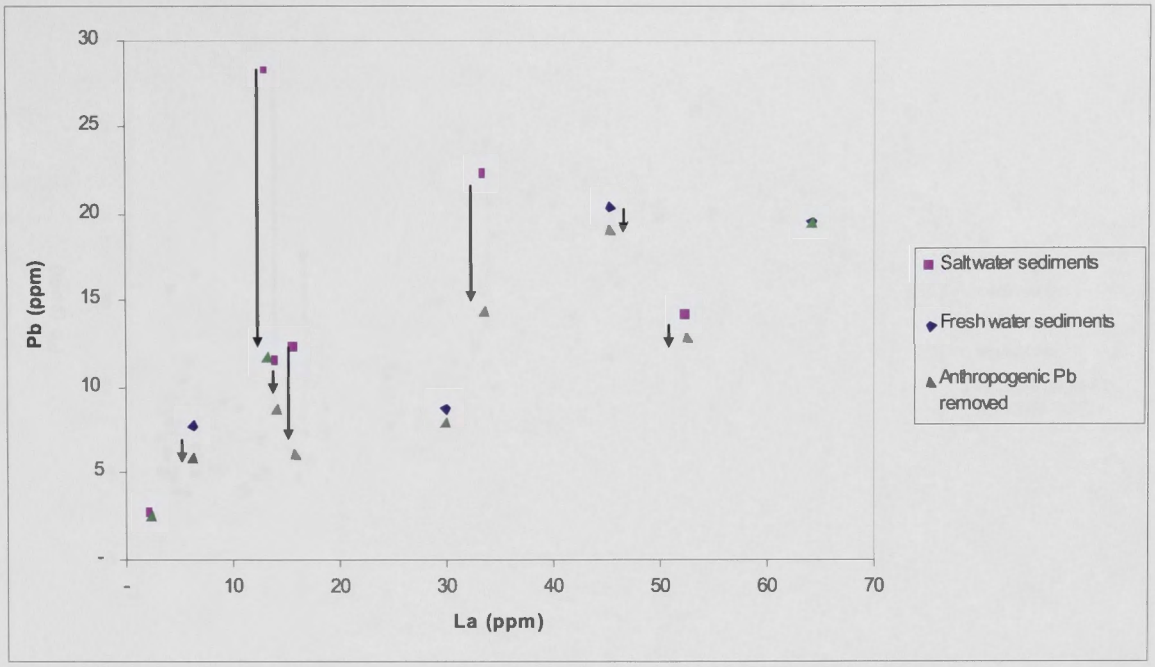

Figure 7.6: The anthropogenic fraction of lead removed from the total sample, and plotted on a La-Pb diagram.

Plotting the data with the anthropogenic fraction of lead removed (green triangles) against all saltwater and freshwater sediment samples, showed a shift towards the baseline data (Figure 7.7). This not only futher substantiates the accuracy of using the baseline data for comparison, but it provides futher evidence for the concentration of anthropogenically derived material being in the estuarine component of the dataset, with the highest concentrations being in the Front Lake of the estuary.

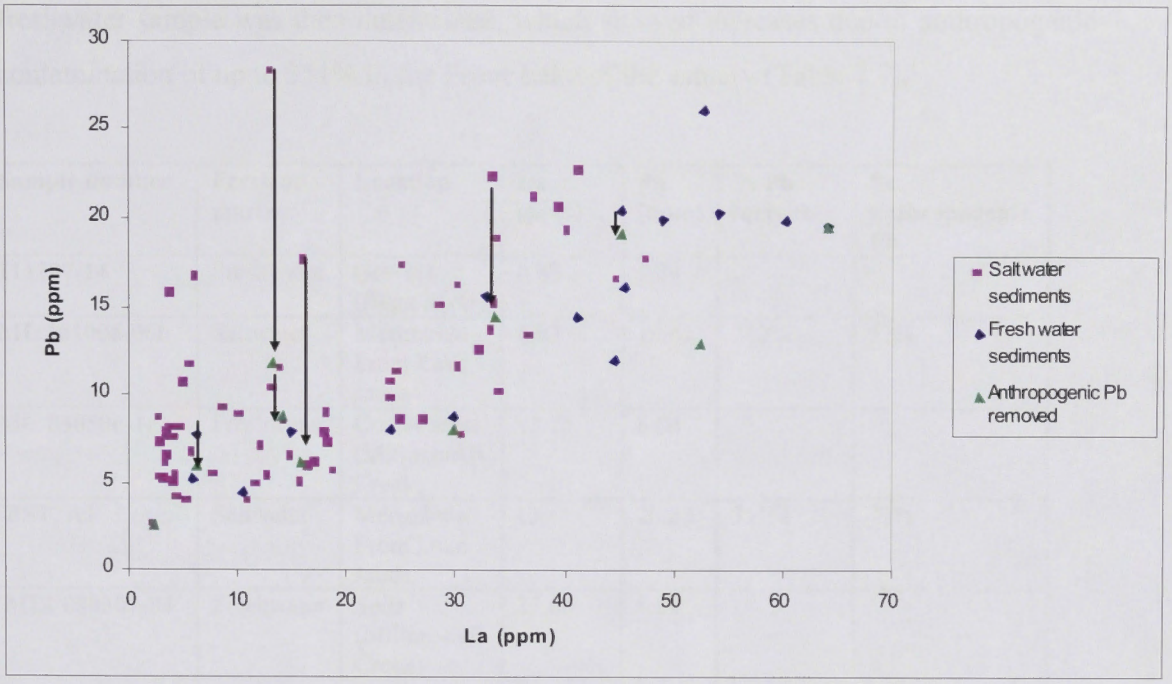

Figure 7.7: La-Pb plot of the data with the anthropogenic fraction of lead removed (green triangles) against all saltwater and freshwater sediment samples.

The previous estimates of the amount of anthropogenic Pb added were based on the Pb-isotopic composition of sediment. An independent estimate can also be made through comparison of the amount of Pb individual samples lying above the La-Pb baseline trend, at a given La concentration. As can be seen from Figure 7.7 for each La value, the saltwater samples have Pb concentrations that are similar to freshwater samples ranging up to much higher values. Table 7.7 lists freshwater sediment samples and saltwater sediments samples at the same La concentration, and reports the maximum Pb values for a given La. This shows that between 36% and 72% of the entire Pb is added to these sediments – a result similar to the Pb-isotope calculation.

The fraction of anthropogenic lead in the sediment samples can also be used to define the enrichment of lead above baseline levels. Four freshwater sediment samples with a range of La concentrations were compared with saltwater sediment samples that have high Pb concentrations, but similar La. Through a comparison of this data, the percentage of anthropogenic Pb in each sample was determined, which ranged from 36% - 72%. The percentage increase of this concentration compared to the baseline

freshwater sample was then determined, which showed increases due to anthropogenic contamination of up to 351% in the Front Lake of the estuary (Table 7.7).

Sample number	Fresh or marine	Location	La (ppm)	Pb (ppm)	% Pb increase	% anthropogenic Pb
111107-14	Freshwater	Gravels (Bega River)	6.02	7.84		
ML 181006-06b	Saltwater	Merimbula Front Lake sands	6.02	16.61	212%	53%
MC 030506-1c	Freshwater	Coarse sand (Millingandi Creek)	14.86	8.04		
BST. A1	Saltwater	Merimbula Front Lake sands	13	28.25	351%	72%
MLI 080307-04	Freshwater	Soils (Millingandi Creek)	29.66	8.84		
BL 181006-01	Saltwater	Back Lagoon sands	29.43	24.71	280%	64%
MC 030506-1b	Freshwater	Fine clays (Millingandi Creek)	41.01	14.52		
ML 130406-07 (20)	Saltwater	Merimbula Top Lake clays	41.26	22.67	156%	36%

Table 7.7: Freshwater samples and saltwater samples at the same La concentration, and the % increase of lead above baseline levels, and the fraction which is of anthropogenic origin.

The Top Lake of Merimbula also had a significant fraction of anthropogenic lead present in the sediments, and an enrichment above baseline concentrations of 156% (Tables 7.6 - 7.7). Although the Top Lake is not in as close proximity to urban development as the Front Lake, the dominantly fine-grained sediments, lower flushing times and deeper water conditions in the Top Lake are likely to accumulate contaminants which are input via runoff, freshwater creeks and tidal movement from the Front Lake. The accumulated anthropogenic fraction of lead in the Top Lake sediments therefore indicate temporal trends in response to development in the Front Lake.

Defining the proportion of anthropogenic lead in the sediments, together with the geographical location of this anthropogenic lead enrichment gives insight into the movement of pollutants in the estuarine environment. By then comparing this data to

freshwater baseline values, the impact of urbanization and associated anthropogenic fluxes may be identified and quantified accurately.

7.6. Conclusions

Lead and strontium isotope analyses have been used to distinguish the sources of these elements in the Merimbula and Pambula Lake sediments. Strontium isotopes distinguish different source rock contributions and marine biogenic contributions from calcium carbonate shells. Lead isotopes show the distinctive contribution of anthropogenic products such as petrol additives in Australia, due to the Proterozoic age of the giant ore body at Broken Hill. These results are consistent with the methodology of the previous chapter, whereby plotting the variation of an element of interest such as Pb against a conservative species can locate anomalous behaviour even where they are not obvious from single-element concentration data alone.

Chapter Eight: Conclusions

The conclusions of this thesis can be condensed into a number of major points:

1) Transported regolith undergoes significant post-depositional geochemical changes that do not necessarily reflect the original source composition, specifically due to additions, subtractions and transformations occurring from the freshwater to marine environment.

2) Using the conservative rare earth element lanthanum, which remains unchanged in concentration for a particular sediment type between the freshwater and marine environment, allows a baseline trend in the data to be established. Other elements, which have been modified by deposition in the marine environment, can be compared against this baseline trend. This enables detailed evaluation of authigenic, biogenic and anthropogenic geochemical modifications within the south coast estuaries.

3) Binary mixing relationships have been established for a wide range of estuarine sediment compositions, based upon the sedimentary end members, which include the catchment source rocks and the mature beach sands. Post depositional modifications to this binary baseline data are demonstrated by variation between the three water bodies in this study. The tide dominated estuaries of Merimbula and Pambula as well as the Back Lagoon (an ICOLL), share the same authigenic and biogenic modifications to the sediment chemistry. However, in contrast to Merimbula and Pambula Lakes, Back Lagoon lacks many of the anthropogenic modifications which are evident in the tide dominated estuaries due to the absence of an aquaculture industry, boats and associated infrastructure.

4) Based on the baseline binary mixing relationships and examination of the elemental concentrations of various elements against the conservative REE lanthanum, a number of important observations were made. In particular, compared to the overall range in concentration of a specific element for this baseline binary mixture, pollution may not be evident if examined data are only compared to a threshold value as defined by sediment quality guidelines, or to a local maximum background value. It has been demonstrated that the greatest modifications to elemental additions need not exceed the uppermost value of a baseline data set. For example, no estuarine sediment has a Pb concentration in excess of the most Pb-rich (clay-rich) terrigenous transported freshwater material. Yet estuarine sediments that are a mixture of sand and clay can have more than double their baseline Pb contents due to pollution.

5) Lead and strontium isotope analyses may be used to differentiate between natural and anthropogenic, and terrestrial and marine sources, respectively, of specific elements into the estuarine system.

6) This work has also identified significant authigenic accumulation of reduced uranium within the reduced sediments. The extent to which this U is biologically available once exposed to subaerial weathering and re-oxidation is an unknown question.

This work forms the basis for predicting future environmental risks, caused by the accumulation and concentration of anthropogenically and naturally derived elements within the estuarine sediments. By determining which elements are being concentrated in the estuarine sediments we are able to provide insights into the current state of the estuary, with important consequences for future monitoring of the health of the estuary as populations and associated pressures increase. Although this study is mainly concerned with identification of post-depositional inputs into estuarine sediments, it also has implications for other areas of Earth Science and industry. In mineral exploration, it is common practice to gather a large amount of elemental concentration data from surface material and contour this data spatially, in order to identify a potential

exploration target underlying the highest concentration in cover. However, this study shows that a uniform zero or regional mean concentration is not necessarily an effective choice as a baseline for identification of geochemical anomalies. If the nature of the host material varies from locality to locality, then the baseline concentrations must be adjusted to reflect that variation. Absolute maxima in concentration need not necessarily identify locations with the greatest addition, while significant anomalies above a low local baseline may not show up as high absolute concentrations.

This research also has implications for the oyster farming industry regarding the definition of a pristine environment. In Merimbula and Pambula, in almost all samples collected, values were well below the trigger value of the Sediment Quality Guidelines. However, through analysis of inter-element relationships, it becomes clear that the highest concentration of an element within a population of data points does not necessarily mean that it is anomalous, or has the greatest enrichment above a natural baseline. Furthermore, anomalies can be identified that are above such a baseline, but below the maximum measured concentration limits.

The question has been posed in this thesis: at what concentration then, is an element defined as being of concern? The methodology developed here identifies those elements accumulating in the estuarine sediments which are of post-depositional origin, when at very low concentrations. A comparison of this data then identifies whether these elements are anomalous. Elements that show concentrations deviating significantly from baseline levels should be observed over time to determine accumulated concentrations. This can then be used to plan against future risks arising from, for example: acid sulfate soils; dredging; and, changes in variables including, but not limited to, sea level, water temperature and nutrient levels. Such processes may remobilise accumulated and concentrated elements from the sediment column.

The development of a methodology which can be used as a tool to define the sources of elements associated with estuarine sediments has a number of important implications. It not only has the potential to provide a cost-effective method of identifying post-depositional additions to a sediment, and clearly shows that estuarine sediments are not

simply a transported form of their catchment counterpart. This methodology clearly demonstrates that a final sediment composition does not necessarily reflect its original source material, but may have certain components added and removed before it is finally deposited. In addition, this methodology identifies elements which are present in very low concentrations but are linked to an anthropogenic source. Using such an approach, elements which are significant, in terms of what will contribute to pollution in the future, can be identified long before it is perceived as being a problem. This is important for monitoring pollutants in coastal systems which are increasingly dynamic regions of pressure and change.

References

Åberg, G., Jacks, G. and Hamilton, P.J. (1989). Weathering rates and 87Sr/86Sr ratios: an isotopic approach. *Journal of Hydrology*, **109**: 65–78.

Abrahim, G. M. S., Parker, R. J. and Nichol, S. L. (2007). Distribution and assessment of sediment toxicity in Tamaki Estuary, Auckland, New Zealand. *Environmental Geology*, **52** (7): 1315-1323.

Acevedo-Figueroa, D., Jimenez, B.D. & Rodrguez-Sierra, C.J. (2006). Trace metals in sediments of two estuarine lagoons from Puerto Rico. *Environmental Pollution*, **141** (2): 336-342.

Albanese, S., De Vivo, B. and Cicchella, D. (2007). Geochemical background and baseline values of toxic elements in stream sediments of Campania region (Italy). *Journal of Geochemical Exploration,*
93 (1): 21-34.

Algeo, T.J. and Maynard, J.B. (2004). Trace-element behavior and redox facies in core shales of Upper Pennsylvanian Kansas-type cyclothems. *Chemical Geology,* **206**: 289–318.

Aloupi, M. and Angelidis, M.O. (2001). Geochemistry of natural and anthropogenic metals in the coastal sediments of the island of Lesvos, Aegean Sea. *Environmental Pollution,* **113**: 211–219.

Andrews, J.E., Brimblecombe, P., Jickells, T.D., Liss, P.S. and Reid, B.J. (2004). An Introduction to Environmental Chemistry. 2nd Edition. Blackwell Publishing, 296 pp.

Åström, M. (1998). Partitioning of transition trace metals in oxidized and reduced zones of sulphide-bearing fine-grained sediments, *Applied Geochemistry,* **13** (5): 607–617.

Australian and New Zealand Environment and Conservation Council, and Agriculture and Resource Management Council of Australia and New Zealand (ANZECC/ARMCANZ) (2000).

National Water Management Strategy. Paper No. 4. Australian and New Zealand Guidelines for Fresh and Marine Water Quality. Volume 1. The Guidelines. Environment Australia, Department of Environment and Heritage, Canberra.

Australian Bureau of Statistics (ABS) (1996). Census of Population and Housing, cat. No. 2035.0, Canberra.

Australian Bureau of Statistics (ABS) (2006). Census data, Commonwealth of Australia. http://www.abs.gov.au Accessed 20/06/2008.

Australian Bureau of Statistics (ABS), 2008. Australian population distribution - June 2006, 1301.0 - Year Book Australia, 2008. Australian Demographic Statistics. http://www.abs.gov.au/ausstats/abs@.nsf/bb8db737e2af84b8ca2571780015701e/5A717784C2562A99CA2573D20010FF17?opendocument

Australian National Resources Atlas (ANRA), (2007). Coasts - Understanding Processes – Australia. 2000-2002 National Land and Water Resources Audit theme assessments. http://www.anra.gov.au/topics/coasts/processes/index.html

Australian National Resources Atlas (ANRA) (2002). Australian Catchment, River and Estuary Assessment 2002. http://www.anra.gov.au/topics/coasts/pubs/estuary_assessment/est_introduction.html

Bäckström, M., Bohlin, H., Karlsson, S. and Holm, N. G. (2006). Element (Ag, Cd, Cu, Pb, Sb, Tl and Zn), element ratio and lead isotope profiles in a sediment affected by a mining operation episode during the late 19th century. *Water, Air, and Soil Pollution*, **177** (1–4): 285–311.

Badri, M.A. and Aston, S.R. (1985). Heavy metal occurrence and geochemical fractionation: The relationships of catchment soils to associated estuarine sediments. *Environmental Pollution Series B, Chemical and Physical.* **10** (1): 61-75.

Baeyens, W., Elskens, M., Gillain, G. and Goeyens, L. (1998). Biogeochemical behaviour of Cd, Cu, Pb and Zn in the Scheldt estuary during the period 1981–1983. *Hydrobiologia,* **366:** 15-44.

Bain, D.C. and Bacon, J.R. (1994). Strontium isotopes as indicators of mineral weathering in catchments. *Catena*, **22**: 201-214.

Balls P.W., Hull S., Miller B.S., Pirie J.M., Proctor W. (1997). Trace metal in Scottish estuarine and coastal sediments. *Marine Pollution Bulletin*. **34**: 42 – 50.

Banfield, J.F. (1985). The mineralogy and chemistry of granite weathering. PhD thesis, The Australian National University.

Banfield, J.F., Bischoff, B.L. and Anderson, M.A. (1993) TiO2 accessory minerals: coarsening, and transformation kinetics in pure and doped synthetic nanocrystalline materials. *Chemical Geology*, **110**: 211-231.

Bayless, E.R., Bullen, T.D., Fitzpatrick, J.A., 2004. Use of 87Sr/86Sr and δ11B to identify slag affected sediment in southern Lake Michigan. *Environmental Science and Technology* **38:** 1330–1337.

Bega Valley Shire Council (BVSC) (2001). Estuary Program, 2001. Bega, NSW. http://www.begavalley.nsw.gov.au/Environment/estuaries/estuaries.htm Accessed 20/03/2006.

Bega Valley Shire Council (BVSC) (2008). Merimbula District Structure Report, July, 2008. Bega, NSW. 54 pp.

Bell F.C., and Edwards, A.R. (1980). An environmental inventory of estuaries and coastal lagoons in New South Wales. Total Environment Centre, Sydney, 187 pp.

Bennett, R.H., Bryant, W.R. and Hulbert, M.H. (Editors) (1991). Microstructure of Fine-Grained Sediments: From Mud to Shale. Frontiers in Sediment Geology. Springer-Verlag, New York. 589 pp.

Bergaya, F., Theng, B.K.G. and Lagaly, G. (2006). Handbook of clay science. 1st Edition, Elsevier, Amsterdam, Boston, London. 1224 pp.

Berner, R.A. (1969). Migration of iron and sulfur within anaerobic sediments during early diagenesis. *American Journal of Science*, **267**(1): 19-42.

Berner, R.A. (1981). A new geochemical classification of sedimentary environments. *Journal of Sedimentary Research*, **51**(2): 359-365.

Bertine, K.K., Goldberg, E.D. (1977). History of heavy metal pollution in southern California coastal zone - reprise. *Environmental Science and Technology,* **11**: 297-299.

Bierwirth, P.N. and Brodie, R.S. (2005). Identifying acid sulfate soil hotspots from airborne gamma-radiometric data and GIS analysis. Bureau of Rural Sciences, Australian Government, Commonwealth of Australia.

Bindler, R., Renberg, I., Anderson, N.J., Appleby, P.G., Emteryd, O. and Boyle, J. (2001). Pb isotope ratios of lake sediments in West Greenland: inferences on pollution sources. *Atmospheric Environment*, **35**: 4675–4685.

Blomqvist, S., Larsson, U. and Borg, H. (1992). Heavy metal decrease in the sediments of a Baltic bay following tertiary sewage treatment. *Marine Pollution Bulletin,* **24**: 258-266.

Boening, D.W. (1999). An Evaluation of Bivalves as Biomonitors of Heavy Metals Pollution in Marine Waters. *Environmental Monitoring and Assessment,* **55** (3): 459-470.

Bollhöfer, A. and Rosman, K. J. R. (2001). Isotopic source signatures for atmospheric lead: the Northern Hemisphere. *Geochimica et Cosmochimica Acta*, **65** (11): 1727–1740.

Borrego, J., López-González, N. and Carro, B. (2004). Geochemical signature as paleoenvironmental markers in Holocene sediments of the Tinto river estuary (southwestern Spain). *Estuarine, Coastal and Shelf Science,* **61**: 631–641.

Boyd, R., Dalrymple, R., and Zaitlin, B. A., (1992) Classification of clastic coastal depositional environments. *Sedimentary Geology,* **80**: 139-150.

Brooke, B. (2003). The role of sedimentological information in estuary management. Proceedings of Coast to Coast 2002 - "Source to Sea" Conference, Tweed Heads, pp. 31-34.

Brown, J.A.H. and Millner, F.C. (1989). Aspects of meteorology and hydrology of the Australian Alps, *in* Good, R. (Editor). The Scientific Significance of the Australian Alps. *Fenner Conference of the Environment, 1st, The Australian Alps National parks Liason Committee, Proceedings:* 297-329.

Browne W. R. (1947). A short history of the Tasman Geosyncline of eastern Australia. *Science Progress*, **140**: 623–637.

Bruland, K.W., Bertine, K., Koide, M., Goldberg, E.D. (1974). History of metal pollution in Southern California Coastal zone. *Environmental Science and Technology*, **8**: 425-432.

Burton, J.D. and Liss, P.S. (Editors) (1976). Estuarine Chemistry. Academic Press. New York, London, San Francisco. Chapter 1, Basic Properties and processes in estuarine chemistry. Pp. 229.

Butcher, S.S., Charlson, R.J., Orians, G.H. and Wolfe, G.V. (eds) (1992). Global biogeochemical cycles Academic Press, London. 379 pp.

Calvert, S.E. and Pedersen, T.F. (1993). Geochemistry of Recent oxic and anoxic marine sediments: implications for the geological record, *Marine Geology,* **113:** 67–88.

Capo, R.C., Stewart, B.W. and Chadwick, O.A. (1998). Strontium isotopes as tracers of ecosystem processes; theory and methods. *Geoderma,* **82**: 197-225.

Carman C.M. Ip, Xiang-Dong Li, Gan Zhang, Onyx W.H. Wai & Yok-Sheung Li (2007). Trace metal distribution in sediments of the Pearl River Estuary and the surrounding coastal area, South China. *Environmental Pollution,* **147**: 311-323.

Carral, E., Villares, R., Puente, X., Carballeira, A., (1995). Influence of watershed lithology on heavy metal levels in estuarine sediments and organisms in Galicia (north-west Spain). *Marine Pollution Bulletin,* **30**: 604-608.

Carroll, D. and Starkey, H.C. (1958). Effect of Sea-Water on Clay Minerals. *Clays and Clay Minerals,* **7**: 80-101.

Carter, R.C. and Wilde, P. (1972). Cation exchange capacity of suspended material form coastal sea water off central California. *Marine Geology*, **13**: 107-122.

Censi, P., Spoto, S. E., Saiano, F., Sprovieri, M., Mazzola, S., Nardone, G., Di Geronimo, S. I., Punturo, R., Ottonello, D. (2006). Heavy metals in coastal water systems. A case study from the north-western Gulf of Thailand. *Chemosphere*, **64**: 1167–1176.

Cha, H., Choi, M.S., Lee, C and Shin, D. (2007). Geochemistry of surface sediments in the southwestern East/Japan Sea. *Journal of Asian Earth Sciences*, **29** (5-6): 685-697.

Chapman, P. M. and Wang, F. (2001), Assessing sediment contamination in estuaries. *Environmental Toxicology and Chemistry*, **20**: 3–22.

Charlet, L. and Tournassat, C. (2005). Fe(II)–Na(I)–Ca(II) Cation Exchange on Montmorillonite in Chloride Medium: Evidence for Preferential Clay Adsorption of Chloride – Metal Ion Pairs in Seawater. *Aquatic Geochemistry*, **11**: 115–137.

Chau, K.W. (2006). Persistent organic pollution characterization of sediments in Pearl River estuary. *Chemosphere*, **64**: 1545–1549.

Chester, R. (1990). Marine Geochemistry. xviii + 698pp. Unwin Hyman: London, Boston, Sydney, Wellington.

Chester, R. (2003). Marine Geochemistry. Second Edition. 520 pp. Blackwell Science: Malden, Oxford, Melbourne, Berlin.

Chiaradia, M., Chenhall, B.E., Depers, A.M., Gulson, B.L. and Jones, B.G. (1997). Identification of historical lead sources in roof dusts and recent lake sediments from an industrialised area: indications from lead isotope. *The Science of the Total Environment,* **205:** 107-128.

Cho, Y.G., Lee, C.B. and Choi, M.S. (1999). Geochemistry of surface sediments off the southern and western coasts of Korea. *Marine Geology*, **159**: 111–129.

Collins, W.J., Beams, S.D., White, A.J.R. and Chappell, B.W. (1982). Nature and origin of A-type granites with particular reference to southeastern Australia. *Contributions to Mineralogy and Petrology,* **80**: 189-200.

Coney P. J., Edwards A., Hine R., Morrison F. and Windrim D. (1990). The regional tectonics of the Tasman Orogenic system, eastern Australia. *Journal of Structural Geology*, **12**: 519–543.

Cortesao, C. and Vale, C. (1995) Metals in sediments of the Sado estuary, Portugal. *Marine Pollution Bulletin*, **30:** 34–37.

Cox, M. E. and Preda, M. (2005). Trace metal distribution within marine and estuarine sediments of western Moreton Bay, Queensland, Australia: relation to land use and setting. *Geographical Research*, **43**: 173–193.

Crecelius, E.A., Trefry, J.H., Steinhauer, M.S. and Boehm, P.D. (1991). Trace metals in sediments from the inner continental shelf of the western Beaufort Sea. *Environmental Geology*, **18** (1): 71-79.

Crook, K.A.W. (1980). Fore-arc evolution in the Tasman Geosyncline: the origin of southeastern Australian continental crust. *Journal of the Geological Society of Australia*, **27**: 215-232.

Dalrymple, R.W. and Choi, K. (2007). Morphologic and facies trends through the fluvial–marine transition in tide-dominated depositional systems: A schematic framework for environmental and sequence-stratigraphic interpretation. *Earth-Science Reviews*, **81**: 135–174.

Daskalakis, K.D. and O'Connor, T.P. (1995). Normalization and elemental sediment contamination in the coastal United States. *Environmental Science and Technology,* **29** (2):470–477.

Davranche, M., Bollinger, J.-C. and Bril, H. (2003). Effect of reductive conditions on metal mobility from wasteland solids: an example from the Montagne-du-Nord site (France). *Applied Geochemistry*, **18**: 383–394.

Deer, W.A., Howie, R.A. and Zussman, J. (1992). An Introduction to the Rock-Forming Minerals. Second Edition. New York: Wiley. 696 pp.

de Matos, A. T., Fontes, M. P. F., da Costa, L. M. and Martinez, M. A. (2001). Mobility of heavy metals as related to soil chemical and mineralogical characteristics of Brazilian soils. *Environmental Pollution*, **111** (3): 429–435.

Department of Natural Resources, DNR, (2008). Estuaries in NSW, Major issues for NSW estuaries, http://www.dnr.nsw.gov.au/estuaries/issues.shtml accessed 10/12/2008

Department of Natural Resources (DNR) (2009). Estuaries in NSW: Pambula Lake. http://www.dnr.nsw.gov.au/estuaries/inventory/pambula.shtml Accessed 7/6/2009.

Department of Primary Industries (DPI) (2008). Regional Geology of NSW - Craton and Orogens
http://www.dpi.nsw.gov.au/minerals/geological/overview/regional#Lachlan Accessed 22/10/2009.

de Villiers, S. and Nelson, B.K. (1997) from Low-temperature hydrothermal flux controls on seawater chemistry: evidence from non-conservative behaviour of "conservative" elements. *Science*, **285**: 721-723.

Department of Land and Water Council (DLWC) (2004). Merimbula Lake. http://www.naturalresources.nsw.gov.au/estuaries/inventory/merimbula.shtml Accessed 03/09/2004.

Douglas, G., Ford, P., Palmer, M., Noble, R., and Packett, R. (2005). Identification of sediment sources in the Fitzroy River Basin and Estuary, Queensland, Australia Nutrient and carbon cycling in subtropical estuaries Fitzroy - FH1 . in: Noble, Bell, R., Tilden, A., and Fitzroy J Fitzroy in Focus: Coastal science for the Fitzroy region, CRC for Coastal Zone Estuary and Waterway Management: 18-19 and p 67-72.

Douglas, G.B., Gray, C.M., Hart, B.T. and Beckett, R. (1995). A strontium isotopic investigation of the origin of suspended particulate matter (SPM) in the Murray-Darling River system, Australia. *Geochimica et Cosmochimica Acta*, **59**: 3799–3815.

Douglas, G. B., Ford, P. W., Palmer, M., Noble, R. M. and Packett, R. (2006). Fitzroy River, Queensland, Australia. II. Identification of Sources of Estuary Bottom Sediments. *Environmental Chemistry,* **3**: 377–385.

Douglas, G., Palmer, M. and Caitcheon, G. (2003). The provenance of sediments in Moreton Bay, Australia: a synthesis of major, trace element and Sr–Nd–Pb isotopic geochemistry, modeling, and landscape analysis. *Hydrobiologia*, **494**: 145–152.

Douglas, I. (1985). Urban sedimentology. *Progress in Physical Geography*, 255–280.

Duinker, J.C., Hillebrand, M. T. J., Nolting, R. F. and Wellershaus, S. (1985). The river EMS: processes affecting the behaviour of metals and organochlorines during estuarine mixing. *Netherlands Journal of Sea Research*, **19** (1): 19-29.

Du Laing, G. Rinklebe, J. Vandecasteele, B. Meers, E. and Tack, F.M.G. (2009). Trace metal behaviour in estuarine and riverine floodplain soils and sediments: a review. *Science of the Total Environment*, **407**: 3972–3985.

Eggins, S.M. (2003) Laser ablation ICP-MS analysis of geological materials as lithium borate glasses. *Geostandards Newsletter: The Journal of Geostandards and Geoanalysis*, **27**: 147-162.

Eggleton, R.A. (Editor) (2001). The Regolith Glossary: surficial geology, soils and landscapes. Cooperative Research Centre for Landscape Evolution and Mineral Exploration (CRCLEME).

Elder, J.F. (1988). Metal Biogeochemistry in Surface-Water Systems - A Review of Principles and Concepts. *U.S. Geological Survey Circular*, 1013.

Erel, Y., Veron, A. and Halicz, L. (1997). Tracing the transport of anthropogenic lead in the atmosphere and in soils using isotopic ratios. *Geochimica et Cosmochimica Acta*, **61** (21): 4495–4505.

Erskine, W.D. and Warner, R.F. (1988). Geomorphic effects of alternating drought and flood dominated regimes on NSW coastal rivers. *In* Warner, R.F. (ed), (1988). Fluvial Geomorphology of Australia. Academic Press.

Fan, D. J., Neuser, R. D., Sun, X. G., Yang, Z. S., Guo, Z. G. and Zhai, S. K. (2008). Authigenic iron oxide formation in the estuarine mixing zone of the Yangtze River. *Geo-Marine Letters*, **28** (1): 7-14.

Fang, T, and Hong, E. (1999). Mechanisms influencing the spatial distribution of trace metals in surficial sediments off the Southwestern Taiwan. *Marine Pollution Bulletin,* **38** (11): 1026–1037.

Faure, G. (1986). Principles of Isotope Geology. 2nd edition. Wiley. New York, 589 pp.

Ferland, M.A., Roy, P.S. and Murray-Wallace, C.V. (1995). Glacial lowstand deposits on the outer continental shelf of southeastern Australia. *Quaternary Research*, **44**: 294–299.

Fergusson C. L. and Fanning C. M. (2002). Late Ordovician stratigraphy, zircon provenance and tectonics, Lachlan Fold Belt, south-eastern Australia. *Australian Journal of Earth Sciences*, **49**: 423–436.

Fergusson, C.L., Cas, R.A.F., Collins, W.J., Craig, G.Y., Crook, K.A.W., Powell, C.McA., Scott, P.A. and Young, G.C. (1979). The Late Devonian Boyd Volcanic Complex, Eden. N.S.W: a reinterpretation. *Geological Society of Australia, Journal,* **26**: 87-105.

Förstner, U. (1979). Sources and sediment associations of heavy metals in polluted coastal regions. *Physics and Chemistry of The Earth*, **11**: 849-866.

Förstner, U. and Wittmann, G. T. W. (1979). Metal Pollution in the Aquatic Environment. Springer, Berlin, 486 pp.

Förstner, U. and Wittman, G.T.W. (1981). Metal Pollution in the Aquatic Environment. Springer-Verlag, New York.

Förstner, U. (1987). Changes in metal mobilities in aquatic and terrestrial cycles. In: Patterson, J.W. and Passino, R. (Editors) (1987). *Metals Speciation, Separation and Recovery*, Lewis, Chelsea, MI, pp. 3–26.

Foster, D.A. and Gray, D.R. (2000). Evolution and structure of the Lachlan Fold Belt (Orogen) of eastern Australia. *Annual Review of Earth and Planetary Sciences*, **28:** 47-80.

Froelich, P.N., Klinkhammer, G.P., Bender, M.L., Luedtke, N.A., Heath, G.R., Cullen, D., Dauphin, P., Hammond, D., Hartman, B. and Maynard, V. (1979). Early oxidation of organic matter in pelagic sediments of the eastern equatorial Atlantic: suboxic diagenesis. *Geochimica et Cosmochimica Acta*, **43** (7): 1075-1090.

Frost, M. T., Grey, I. E., Harrowfield, I. R. and Mason, K. (1983). The dependence of alumina and silica contents on the extent of alteration of weathered ilmenites from Western Australia. *Mineralogical Magazine*, **47**: 201-208.

Gambrell, R.P., Wiesepape, J.B., Patrick, W.H., Jr., and Duff, M.C. (1991). The effects of pH, redox, and salinity on metal release from a contaminated sediment. *Water, Air, and Soil Pollution*, **57-58**: 359-367.

García, D., Ravenne, C., Maréchal, B. and Moutte, J. (2004). Geochemical variability induced by entrainment sorting: quantified signals for provenance analysis. *Sedimentary Geology*, **171**: 113–128.

Gibbs, S.K. (1978). A survey of erosion and siltation within the catchment of Merimbula Lake. Soil Conservation of NSW.

Gingele, F., De Deckker, P. and Norman, M. (2007). Late Pleistocene and Holocene climate of SE Australia reconstructed from dust and river loads deposited offshore the River Murray mouth. *Earth and Planetary Science Letters*, **255**: 257–272.

Gray, D. R. and Foster, D. A. (2004). Tectonic evolution of the Lachlan Orogen, southeast Australia: historical review, data synthesis and modern perspectives. *Australian Journal of Earth Sciences*, **51**: 773-817.

Goldberg, E.D. (1963). Mineralogy and chemistry of marine sedimentation. *In:* SubMar. Geol. (ed. F.P. Shepard). Harper and Row, New York, pp. 436-466.

Gouveia, M. A., Araujo, M. F. D. and Dias, J. M. A. (1993). Rare earth element distribution in sediments from the Minho River and estuary (Portugal). A preliminary study. *Chemical Geology*, **107**: 379–383.

Green-Ruiz, C. and Páez-Osuna, F. (2001). Heavy metal anomalies in lagoon sediments related to intensive agriculture in Altata-Ensenada del Pabellón coastal system (SE Gulf of California). *Environment International*, **26** (4): 265 – 273.

Grey, I.E. and Reid, A.F. (1975). The Structure of Pseudorutile and its role in the natural alteration of ilmenite. *American Mineralogist*, **60**: 898-906.

Grey, I. E., Macrae, C. M. and Nicholson, T. (1999). Alteration of ilmenite in the Murray Basin–implications for processing. *Proceedings Murray Basin Mineral Sands, pp 129–134. Australian Institute of Geoscientists Bulletin,* **26**.

Guggenheim, S., Brown, R., Daniels, E., Peacor, D.R., Stanjek, H. and Stucki, J. (2009). The Clay Minerals Society Glossary for Clay Science Project, 2008/2009. http://www.clays.org/GLOSSARY/ClayTerms%20April%202009.doc

Guggenheim, S. and Koster van Groos, A.F. (2001). Baseline Studies of the Clay Minerals Society Source Clays: Thermal Analysis. *Clays and Clay Minerals,* **49**: 433-443.

Gulson, B.L. (1996). Nails: concern over their use in lead exposure assessment. *The Science of the Total Environment*, **177**: 323-327.

Gulson, B., Mizon, K., Korch, M. and Taylor, A. (2006). Changes in the lead isotopic composition of blood, diet and air in Australia over a decade: globalization and implications for future isotopic studies. *Environmental Research,* **100** (1): 130–138.

Gupta, S.K., Rajakumar, V. and Grieveson, P. (1991). Phase transformations during heating of llmenite concentrates. *Metallurgical and Materials Transactions B*, **22** (5): 711-716.

Hall, L.R. (1969). XI Geomorphology. *Australian Journal of Earth Sciences*, **16** (1): 559 — 580.

Hancock, G. and Caitcheon, G. (2010). Sediment sources and transport to the Logan-Albert River estuary during the January 2008 flood even. CSIRO: Water for a Healthy Country, National Research Flagship.

Harrington, J.M., Fendorf, S. and Rosenzweig, R.F. (1998). Biotic generation of As(III) in metal(loid) contaminated freshwater lake sediments. *Environmental Science and Technology,* **32** (16): 2425–2430.

Harris, P. T., Heap, A. D., Bryce, S. M., Porter-Smith, R., Ryan, D. A. and Heggie, D. T. (2002). Classification of Australian clastic coastal depositional environments based on a quantitative analysis of wave, tide and river power. *Journal of Sedimentary Research,* **72** (6):858-870.

Helfferich, F.G. (1962). Ion Exchange. McGraw-Hill, New York, 624 pp.

Hendershot, W. H., Courchesne, F. and Jeffries, D. S. (1996). Aluminium geochemistry at the catchment scale in watersheds influenced by acidic precipitation. The Environmental Chemistry of Aluminium (Sposito, G., ed.), 419–449, Lewis Publishers.

Herut, B., Hornung, H., Krom, M.D., Kress, N. and Cohen, Y. (1993). Trace metals in shallow sediments from the Mediterranean coastal region of Israel. *Marine Pollution Bulletin*, **26** (12): 675-682.

Hirst, D.M. (1962). The geochemistry of modern sediments from the Gulf of Paria—II The location and distribution of trace elements. *Geochimica et Cosmochimica Acta*, **26** (11): 1147-1187.

Hodell, D.A., Mueller, P.A., McKenzie, J.A. and Mead, G.A. (1989). Strontium isotope stratigraphy and geochemistry of the late Neogene ocean. *Earth and Planetary Science Letters*, **92**: 165–178.

Hough D.J. (1983). The influence of parent rock on the nature of surficial materials in the Eden region. MSC Thesis, The Australian National University, 208 pp.

Ip, C.C.M., Li, X.D., Zhang, G., Farmer, J.G. Wai, O.W.H. and Li, Y.S. (2004). Over one hundred years of trace metal fluxes in the sediments of the Pearl River Estuary, South China. *Environmental Pollution*, **132** (1): 157-172.

Ip, C.C.M., Li, X.D., Zhang, G., Wai, O.W.H. and Li, Y.S. (2007). Trace metal distribution in sediments of the Pearl River Estuary and the surrounding coastal area, South China. *Environmental Pollution,* **147**: 311–323.

Jones, B, and Turki, A. (1997). Distribution and Speciation of heavy metals in surficial sediments from the Tees Estuary, North-east England. *Marine Pollution Bulletin,* **34**: 768– 79.

Jones, B.G., Killian, H.E., Chenhall. B.E. and Sloss, C.R. (2003). Anthropogenic Effects in a Coastal Lagoon: Geochemical Characterization of Burrill Lake, NSW, Australia. *Journal of Coastal Research*, **19** (3): 621-632.

Kasten, S., Zabel, M., Heuer, V. and Hensen, C. (2003). Processes and Signals of Nonsteady-State Diagenesis in Deep-Sea Sediments and their Pore Waters. *In* Wefer, G. Mulitza, S. and V. Ratmeyer (Eds.), The South Atlantic in the Late Quaternary: Reconstruction of Material Budgets and Current Systems. Springer-Verlag, Berlin, pp. 431-459.

Kearey, P (Ed.) 1993. The Encyclopaedia of the Solid Earth Sciences, Blackwell Science, Oxford. Pp. 736.

Kehoe, R.A. (1965). Contaminated and natural lead environments of man. *Archives of Environmental Health*, **11** (5): 736–739.

Keith, D.A. and Saunders, J.M. (1990). Vegetation of the Eden region, south-eastern Australia: species composition, diversity and structure. *Journal of Vegetation Science,* **1**: 203-232.

Keller, W. D., "Diagenesis in clay minerals-A review," in Clays and Clay Minerals, Proceedings of the 11th National Conference, Monograph 13, Earth Science Series (New York: Pergamon Press, 1963), pp. 136-157.

Kemp, A.L. and Thomas, R.L. (1976). Cultural Impact on the geochemistry of the sediments of Lakes Ontario, Erie and Huron. *Geoscience Canada,* **3** (3): 191-207.

Kemp, A.L.W. (1976). Cultural impacts on the geochemistry of sediments. *In* Lake Erie, J. Fish. Res. Board Can. 33 (1976), pp. 440–462.

Kersten, M. (1988). Geochemistry of priority pollutants in anoxic sludges: Cadmium, arsenic, methyl mercury, and chlorinated organics. *In* Salomons, W., and Forstner, U., eds., Chemistry and biology of solid waste: Berlin, Springer-Verlag, p. 170-213.

Kober, B., Wessels, M., Bollhöfer, A. and Mangani, A. (1999). Pb isotopes in sediments of Lake Constance, Central Europe constrain the heavy metal pathways and the pollution history of the catchment, the lake and the regional atmosphere. *Geochemica et Cosmochimica Acta*, **63** (9): 1293-1303.

Krauskopf, K.B. (1967). Introduction to Geochemistry. McGraw-Hill Book Company, USA.

Kretzschmar, R. and Schäfer, T. (2005). Metal Retention and Transport on Colloidal Particles in the Environment. *Elements*, **1** (4): 205-210.

Lambeck, K. and Chappell, J. (2001). Sea Level Change Through the Last Glacial Cycle. *Science,* **292**: 679-686.

Langmuir, D. (1978). Uranium solution mineral equilibria at low temperatures with applications to sedimentary ore deposits. *Geochimica et Cosmochimica Acta*, **42** (60): 547-569.

Lawrence, M.G., Jupiter, S.D. and Kamber, B.S. (2006). Aquatic geochemistry of the rare earth elements and yttrium in the Pioneer River catchment, Australia. *Marine and Freshwater Research*, **57** (7): 725-736.

Leblanc, M., Morales, J.A., Borrego, J. and Elbaz-Poulichet, E. (2000). 4,500-years-old mining pollution in southwestern Spain: long-term implications for modern mining pollution. *Economic Geology*, **95**: 655–662.

Lee, S.V. and Cundy, A.B. (2001). Heavy Metal Contamination and Mixing Processes in Sediments from the Humber Estuary, Eastern England. *Estuarine, Coastal and Shelf Science*, **53** (5): 619-636.

Léonard, A. (1991), Arsenic, in Merian, E. (ed.), Metals and Their Compounds in the Environment: Weinheim, Germany, VCH, p. 751-774.

Lewis, P.C., Glen, R.A., Pratt, G.W. and Clarke, I. (1994). Bega - Mallacoota 1:250,000 geological sheet explanatory notes. Geological Survey of New South Wales, Sydney.

Lewis, S. E., Wüst, R. A. J., Webster, J. M. and Shields, G. A. (2008), Mid-late Holocene sea-level variability in eastern Australia. *Terra Nova*, **20**: 74–81.

Li, Y.-H. and Schoonmaker, J.E. (2003). Chemical Composition and Mineralogy of marine Sediments. Pp 1-35. *In*: Sediments, Diagenesis, and Sedimentary Rocks Mackenzie, F.T (ed.) Vol. 7 Treatise on Geochemistry, Holland, H.D. and Turekian, K.K. (Exec Eds) (2005). Elsevier –Pergamon, Oxford.

Liaghati, T., Preda, M. and Cox, M. (2004). Heavy metal distribution and controlling factors within coastal plain sediments, Bells Creek catchment, southeast Queensland, Australia. *Environment International*, **29** (7): 935-948.

Liaghati, T., Preda, M. and Cox, M.E. (2003). Heavy metal distribution and controlling factors within coastal plain sediments, Bells Creek catchment, southeast Queensland, Australia. *Environment International*, **29**: 935-948.

López-González, N., Borrego, F., Ruiz, F., Carro, B., Lozano-Soria, O. and Abad, M. (2006). Geochemical variations in estuarine sediments: provenance and environmental changes (Southern Spain). *Estuarine Coastal and Shelf Science*, **67**: 313–320.

Loring, D.H. (1990). Lithium—a new approach for the granulometric normalization of trace metal data. *Marine Chemistry*, **29**: 155– 68.

Loring, D.H. (1991). Normalization of heavy-metal data from estuarine and coastal sediments. *Journal of Marine Science,* **48**: 101– 15.

Loring, D.H. and Rantala, R.T.T. (1992). Manual for the geochemical analyses of marine sediments and suspended particulate matter. *Earth Science Reviews*, **32**: 235-283.

Machado, W., Luis-Silva, W., Sanders, C.J. and Patchineelam, S.R. (2008). Coupled anthropogenic anomalies of radionuclides and major elements in estuarine sediments. *Journal of Environmental Radioactivity*, **99** (8): 1329-1334.

Marchand, C., Lallier-Vergès, E., Baltzer, F., Albéric, P., Cossa, D. and Baillif, P. (2006). Heavy metals distribution in mangrove sediments along the mobile coastline of French Guiana. *Marine Chemistry*, **98** (1): 1-17.

Mackenzie, F.T. and Garrels, R.M. (1965). Silicates: Reactivity with Sea Water. *Science*, **150** (3692): 57-58.

Marins, R.V., Lacerda, L.D., Gonçalves, G.O. and de Paiva, E.C. (1997). Effect of Root Metabolism on the Post-Depositional Mobilization of Mercury in Salt Marsh Soils. *Bulletin of Environmental Contamination and Toxicology*, **58**: 733-738.

Martin, J.M. and Meybeck, M. (1979). Elemental mass Balance of Material Carried by Major World Rivers. *Marine Chemistry*, **7**: 173-206.

Martin, J.M. and Whitfield, M. (1983). The significance of river inputs into the ocean. *In :* Wong, C.H., Boyle, E., Bruland, K.W., Burton, J.D. and Goldberg, E.D. (Editors). Trace Metals in Seawater, Plenum, New York.

Mathew, P. K. and Rao, S. N. (1997). Effects of exchangeable cations on the geotechnical properties of a marine clay. *Marine Georesources & Geotechnology*, **15** (2): 83-93.

McCulloch, M.T. and Woodhead, J.D. (1993). Lead isotopic evidence for deep crustal-scale fluid transport during granite petrogenesis. *Geochimica et Cosmochimica Acta*. **57**: 659-674.

Taylor, S.R. and McLennan, S.M. (1985). The Continental Crust: Its Composition and Evolution. Blackwell Scientific Publications. 312 pp.

McLennan, S. M., Taylor, S. R. and Hemming, S. R. (2006). Composition, differentiation, and evolution of continental crust: Constraints from sedimentary rocks and heat flow. *In*: M. Brown and T. Rushmer, eds. Evolution and Differentiation of the Continental Crust. Cambridge Univ. Press, pp. 92-134.

McLennan, S. M., (1995). Sediments and soils: Chemistry and abundances, in: A Handbook of Physical Constants: Rock Physics and Phase Relations, AGU Ref. Shelf Ser., vol. 3, edited by T. J. Ahrens, pp. 8 – 19, AGU, Washington, D. C.).

Merimbula Information Centre, Image Gallery webpage, http://www.merimbula.com.au/pages/image-gallery/, accessed 07/02/2011.

Miao, S. Y., DeLaune, R. D., & Jugsujinda, A. (2006). Influence of sediment redox conditions on release/solubility of metals and nutrients in a Louisiana Mississippi River deltaic plain freshwater lake. *Science of the Total Environment*, **371**: 334–343.

Millward, G.E. and Moore, R.M. (1982). The adsorption of Cu, Mn and Zn by iron oxyhydroxide in model estuarine solutions. *Water Research*, **16** (6): 981-985.

Mkadam, K.M., Yonaha, T., Ali, V.S. and Tukuyama, A. (2006). Dissolved aluminium and silica release on the interaction of Okinawan subtropical red soil and seawater at different salinities: Experimental and field observations. *Geochemical Journal*, **40**: 333-343.

Moore, D.M., and Reynolds, R.C. (1997) X-ray diffraction and the identification and analysis of clay minerals, 2nd ed, *Oxford University Press*.

Moore, J. N., Brook, Edward J. and Johns, C. (1989). Grain size partitioning of metals in contaminated, coarse-grained river floodplain sediment: Clark Fork River, Montana, U.S.A. *Environmental Geology*, **14** (2): 107 – 115.

Morford, J.L. and Emerson, S. (1999). The geochemistry of redox sensitive trace metals in sediments. *Geochimica et Cosmochimica Acta*, **63**: 1735–1750.

Munksgaard, N.C., Batterham, G.J. and Parry, D.L. (1998). Lead isotope ratios determined by ICP-MS: Investigation of anthropogenic lead in seawater and sediment from the Gulf of Carpentaria, Australia. *Marine Pollution Bulletin*, **36** (7): 527-534.

Munksgaard, N.C., Lim, K. and Parry, D.L. (2003). Rare earth elements as provenance indicators in North Australian estuarine and coastal marine sediments. *Estuarine, Coastal and Shelf Science,* **57:** 399-409.

Négrel, P., Grosbois, C. and Kloppmann, W. (2000). The labile fraction of suspended matter in the Loire River (France): multi-element chemistry and isotopic (Rb–Sr and C–O) systematics. *Chemical Geology*, **166**: 271–285.

Nelson, C.H and Lamothe, P.J. (1993). Heavy Metal Anomalies in the Tinto and Odiel River and Estuary System, Spain. *Estuaries*, **16**: 496 – 511.

Nguyen, B., Liu, Y. and Withers, R. L. (2007). The local crystal chemistry and dielectric properties of the cubic pyrochlore phase in the Bi2O3-M2þO-Nb2O5 (M2þ ¼ Ni2þ and Mg2þ) systems. *Journal of Solid State Chemistry*, **180:** 549–557.

Norrish, K. and Pickering, J.G. (1983) Clay minerals. In 'Soils: an Australian viewpoint'. Division of Soils, CSIRO, pp. 281–308. (CSIRO: Melbourne/Academic Press: London).

Nowack, B., Kari, F.G., and Kruger, H.G. (2001) The remobilization of metals from iron oxides and sediments by metal-EDTA complexes. *Water, Air and Soil Pollution*, **125**: 243–257.

NSW Government, (2006/7). Estuarine Vegetation and Habitat Map. NSW Fisheries, Department of Planning's Comprehensive Coastal Assessment Program, (Department of Primary Industries, Department of Lands, Department of Planning, Department of Natural Resources).

OzCoasts (2005). Image. Department of Environment and Climate Change, NSW (Coastal and Floodplain Programs), Accessed 17/12/2005.

OzCoasts (2007). National Land and Water Resource Audit Merimbula Lake condition assessment report, ESTUARY ASSESSMENT FRAMEWORK FOR NON-PRISTINE ESTUARIES, Estuary 75, (MERIMBULA LAKE). http://dbforms.ga.gov.au/www/npm.ozcoast2.showmm?pBlobNo=9351. Accessed 22/07/2007.

OzCoasts, (2010). Climatic regions Of Australia, http://www.ozcoasts.org.au/conceptual_mods/class/climate_regions.jsp#sec; http://www.ozcoasts.org.au/conceptual_mods/typology.jsp Accessed 11/08/2010.

Palmer, M.R., Edmond, J.M. (1989). The strontium isotope budget of the modern ocean. *Earth and Planetary Science Letters*, **92**: 11–26.

Pearce, N. J. G., Perkins, W. T., Westgate, J. A., Gorton, M. J., Jackson, S. E., Neal, C. R. and Chenery, S. P. (1997). A compilation of new and published major and trace element data for NIST SRM 610 and NIST SRM 612 glass reference materials. *Geostand. News.*, **21**: 115–144.

Phillips, J.D. and Slattery, M.C. (2006). Sediment storage, sea level and sediment delivery to the ocean by coastal plain rivers. *Progress in Physical Geography*, **30** (4): 513-530.

Postma, D. and Jakobsen, R. (1996). Redox zonation: Equilibrium constraints on the Fe(III)/SO^{4-}reduction interface. *Geochimica et Cosmochimica Acta*, **60** (17): 3169-3175.

Pownceby, M.I. (2010). Alteration and associated impurity element enrichment in detrital ilmenites from the Murray Basin, southeast Australia: a product of multistage alteration. *Australian Journal of Earth Sciences*, **57** (2): 243-258.

Prasad, M.B.K. and Ramanathan, A.L. (2008). Distribution of Rare Earth Elements in the Pichavaram Mangrove sediments of Southeast Coast of India. *Journal of Coastal Research*, **24** (1): 126-134.

Pye, K. (1987). Aeolian Dust and Dust Deposits. Academic Press, London. Pp. 334.

Rachold, V., Eisenhauer, A., Hubberton, H.W., Hansen, B. and Meyer, H. (1997). Sr isotopic composition of suspended particulate matter (SPM) of east Siberian rivers: sediment transport to the Arctic Ocean. *Arctic and Alpine Research*, **29**: 422–429.

Renberg, I., Bränvall, M.L., Bindler, R. and Emteryd, O. (2002). Stable lead isotopes and lake sediments - a useful combination for the study of atmospheric lead pollution history. *The Science of the Total Environment*, **292**: 45–54.

Ridgway, J. and Shimmield, G. (2002). Estuaries as repositories of historical contamination and their impact on shelf seas. *Estuarine, Coastal and Shelf Science,* **55** (6): 903-928.

Rodríguez-Barroso, M. R., Benhamou, Y., El Moumni, B., El Hatimi, I. and García-Morales, J. L. (2009). Evaluation of metal contamination in sediments from north of Morocco: geochemical and statistical approaches. *Environmental Monitoring and Assessment*, **159** (1-4): 169-181.

Romov, A.B. (1983). The Earth's Sedimentary Shell: Quantitative Patterns of its Structure, Compositions and Evolution. American Geological Institute Reprint Series. 80pp.

Roy, P.S. and Thom, B.G. (1981). Late Quaternary marine deposition in New South Wales and southern Queensland - an evolutionary model. *Journal of the Geological Society of Australia*, **28**: 471-489.

Roy, P. S., Williams, R. J., Jones, A. R., Yassini, R., Gibbs, P. J., Coates, B., West, R. J., Scanes, P. R., Hudson, J. P., and Nichol, S., (2001). Structure and function of south-east Australian estuaries. *Estuarine, Coastal and Shelf Science*, **53**: 351-384.

Russell, K.L. (1970). Geochemistry and halmyrolysis of clay minerals, Rio Ameca, Mexico. *Geochimica et Cosmochimica Acta,* **34** (8): 893-907.

Rutland, R.W.R. (1976). Orogenic evolution of Australia. *Earth Science Reviews*, **12**: 161-196.

Sageman, B. B. and Lyons, T.W. (2005). Geochemistry of fine-grained sediments and sedimentary rocks. In: Sediments, Diagenesis, and Sedimentary Rocks Mackenzie, F.T (ed.) Vol. 7 Treatise on Geochemistry, Holland, H.D. and Turekian, K.K. (Exec Eds) 2005. Elsevier –Pergamon, Oxford.

Saint-Laurent, D., St-Laurent, J., Hähni, M., Ghaleb, B. and Chapados, C. (2010). Using Lead Concentrations and Stable Lead Isotope Ratios to Identify Contamination Events in Alluvial Soils. *Applied and Environmental Soil Science*, vol. 2010, Article ID 235210, 12 pages. doi:10.1155/2010/235210

Salomons, W. (1980). Adsorption processes and hydrodynamic conditions in estuaries. *Environmental Technology*, **1** (8): 356 — 365.

Salomons, W. & Förstner, U. (1984). Trace metals in the Hydrocycle. Springer Verlag, Berlin, 349 pp.

Sarkar, S.K., Frančišković-Bilinski, S., Bhattacharya, A., Saha, M. and Bilinski, H. (2004). Levels of elements in the surficial estuarine sediments of the Hugli River, northeast India and their environmental implications. *Environment International*, **30** (8): 1089-1098.

Sayles, F. L. and Mangelsdorf, P.C. Jr. (1977). The equilibration of clay minerals with seawater: exchange reactions. *Geochimica et Cosmochimica Acta*, **41**: 951–960.

Sayles F.L. and Mangelsdorf P.C. (1979). Cation exchange characteristics of Amazon River suspended sediment and its reaction with seawater. *Geochimica et Cosmochimica Acta*, **43**: 767-779.

Scheibner, E. (1978). Tasman Fold Belt System or Orogenic System—Introduction. *Tectonophysics*, **48**: 153–157.

Scheibner, E. (1987). Paleozoic tectonic development of eastern Australia in relation to the Pacific region, Circum-Pacific Orogenic Belts and Evolution of the Pacific Ocean Basin. *In*: J.W.H. Monger and J. Francheteau, Editors, Am. Geophys. Un. Geodyn. Ser. 18, pp. 133–165.

Schiff, K. C. and Weisberg, S. (1999). Iron as a reference element for determining trace metal enrichment in California coastal shelf sediments. *Marine Environmental Research*, **48**: 161–179.

Schuchert C. (1916). The problem of continental fracturing and diastrophism in Oceania. *American Journal of Science*, **42:** 91–105.

Schulz, H.D and Zabel M. (eds) (2006). Marine Geochemistry. Springer-Verlag, Berlin Heidelberg, 2nd Revised, updated and extended edition, pp 574.

Scoullos, M.J. (2003). Impact of anthropogenic activities in the coastal region of the Mediterranean Sea. International Conference on Sustainable Development of the Mediterranean and Black sea Environment. Online: http://www.iasonnet.gr/past_conf/program/program.html.

Shannon, R. D. (1969). Revised effective ionic radii and systematic studies of interatomic distances in halides and chalcogenides. *Acta Crystallographica,* **B25**: 925-946.

Shannon, R. D. and Prewitt C. T. (1970). Effective ionic radii in oxides and fluorides. *Acta Crystallographica,* **B26**: 1046-1048

Shannon, R. D. and Prewitt C. T. (1976). Revised values of effective ionic radii. *Acta Crystallographica,* **A32**: 751-767.

Sharman, P., Borole, D.V. and Zigde, M.D. (1984). ^{210}Pb based trace element fluxes in the nearshore and estuarine sediments of Bombay, India. *Marine Chemistry*, **47**: 227-241.

Sholkovitz, E. R. (1976). Flocculation of dissolved organic and inorganic matter during the mixing of river water and seawater. *Geochimica et Cosmochimica Acta*, **40**: 831–845.

Siegel, F.R. (2002). Environmental Geochemistry of Potentially Toxic Metals. Springer-Verlag. Washington. 223 pp.

Singer, P.C. (1977). Influence of dissolved organics on the distribution, transport, and fate of heavy metals in aquatic systems. Pages 155-182 *in* I. H. Suffet (ed.), Fate of pollutants in the air and water environment, part I. John Wiley and Sons, New York.

Singh, A.K., Hasnain, S.I. and Banerjee, D.K. (1999). Grain size and geochemical partitioning of heavy metals in sediments of the Damodar River – a tributary of the lower Ganga, India. *Environmental Geology*, **39** (1): 90-98.

Singh, S.K. and France-Lanord, C. (2002). Tracing the distribution of erosion in the Brahmaputra watershed from isotopic compositions of stream sediments. *Earth and Planetary Science Letters*, **202**: 645–662.

Sircombe, K.N. (1999). Tracing provenance through the isotope ages of littoral and sedimentary detrital zircon, eastern Australia. *Sedimentary Geology*, **124**: 47-67.

Sloss, C.R., Murray-Wallace, C.V. and Jones, B.G. (2006). Aminostratigraphy of two Holocene wave-dominated barrier estuaries in southeastern Australia. *Journal of Coastal Research*, **22** (1): 113–136.

Smith, J.P., Bullen, T.D., Brabander, D.J. and Olsen, C.R. (2009). Strontium isotope record of seasonal scale variations in sediment sources and accumulation in low-energy, subtidal areas of the lower Hudson River estuary. *Chemical Geology*, **264**: 375–384.

Southern Rivers and Catchment Management Authority (SRCMA) (2010). Far South Coast Catchment, http://www.southern.cma.nsw.gov.au/our_catchment-far_south_coast.php, accessed 30/6/2010

Southgate, T. Slinn, D.J and Eastham, J.F. (1983). Mine-derived metal pollution in the Isle of Man. *Marine Pollution Bulletin*, **14** (4): 137-140.

Spandler, C. J., Hermann, J., Arculus, R.J. and Mavrogenes, J.A. (2003). Redistribution of trace elements during prograde metamorphism from lawsonite blueschist to eclogite facies; implications for deep subduction-zone processes. *Contributions to Mineralogy and Petrology*, **146:** 205–222.

Sparks, D.L. (2003). Environmental Soil Chemistry, Second Edition. Elsevier Science, Academic Press, USA. 352 pp.

Standring, W.J.F., Oughton, D.H. and Salbu, B. (2002). Remobilisation of Cd, Zn and Mn from freshwater-labelled rover sediments when mixed with seawater. *Environment International*, **28**: 185–195.

Steiger, R.H. and Jäger, E. (1977). Subcommission on geochronology: convention on the use of decay constants in geo- and cosmochronology. *Earth and Planetary Science Letters,* **36**: 359 - 362.

Sugimura, Y., Suzuki, Y. and Miyake, Y. (1978). The dissolved organic iron in seawater. *Deep-Sea Research*, **25**: 309-314.

Tam, N.F.Y. and Yao, M.W.Y. (1998). Normalization and heavy metal contamination in mangrove sediments. *Science of the Total Environment*, **216**: 33–39.

Taylor, G. and Mayer, W. (1990). Depositional environments and palaeogeography of the Worange Point Formation, New South Wales. *Australian Journal of Earth Sciences*, **37** (2): 227 – 239.

Taylor, S.R and McLennan, S.M. (1985). The Continental Crust: its Composition and Evolution. An Examination of the Geochemical Record Preserved in Sedimentary Rocks. Blackwell Scientific Publications. Pp. 312.

Taylor, S.R. and McLennan, S.M. (1995). The geochemical evolution of the continental crust. *Reviews of Geophysics*, **33** (2): 241–265.

Taylor S. R. and McLennan S. M. (2009). Planetary Crusts: Their Composition and Evolution. Cambridge University Press, Cambridge. 378 pp.

Taylor, R. M., McKenzie. R. M., Fordham. A. W. & Gillman, G. P. (1983). Oxide minerals. *In* Soils: An Australian Viewpoint. Division of Soils, CSIRO pp. 309-334. (CSIRO: Melbourne/Academic Press: London).

Temple, A. K. (1966). Alteration of ilmenite. *Economic Geology*, **61**: 695-714.

Tessier, A., Rapin, F. and Carignan, R. (1985). Trace metals in oxic lake sediments: possible adsorption onto iron oxyhydroxides. *Geochimica et Cosmochimica Acta,* **49**: 183–194.

Thorne, L.T. and Nickless, G. (1981). The relationship between heavy metals and particle size fractions within the Severn Estuary (U.K.) inter-tidal sediments. *The Science of the Total Environment,* **19**: 207-213.

Townsend, A.T. and Snape, I. (2008). Multiple Pb sources in marine sediments near the Australian Antarctic Station, Casey. *Science of the Total Environment,* **389** (2-3): 466-474.

Trimble, C.A. and Hoenstine, R.W. (1997). Baseline investigation of estuarine sediment metals for the Steinhatchee River area of the Florida Big Bend. *Environmental Geoscience*, **4** (2): 95–103.

Tulau, M. (1997) Soil Landscapes of the Bega-Goalen Point 1:100000 Sheet Report. Department of Land and Water Conservation, Sydney

Turekian, K.K. (1976). Oceans. 2nd edition. Prentice-Hall, 149 pp.

Turner, L., Tracey, D., Tilden, J. and Dennison, W. (2006). Where River Meets Sea: Exploring Australia's Estuaries. CSIRO Publishing, 288pp

Ulrich, G.A., Krumholz, L.R. and Suflita, J.M. (1997). A rapid and simple method for estimating sulfate reduction activity and quantifying inorganic sulfides. *Applied Environmental Microbiology*, **63**: 1627–1630.

Uncles, R.J. (2002). Estuarine Physical Processes Research: Some Recent Studies and Progress. *Estuarine, Coastal and Shelf Science*, **55:** 829–856.

United States Environmental Protection Agency (EPA) (2010). Major Contaminants. Accessed: 6/6/2010. http://water.epa.gov/polwaste/sediments/cs/contaminants.cfm

Vaithiyanathan, P., Ramanathan, A. and Subramanian, V. (1992). Sediment transport in the Cauvery River basin: sediment characteristics and controlling factors. *Journal of Hydrology*, **139** (1–4): 197–210.

Valdez Domingos, F.X., Azevedo, M., Silva, M.D., Randi, M.A.F., Freire, C.A., Silva de Assis, H.C. and Oliveira Ribeiro, C.A. (2007). Multibiomarker assessment of three Brazilian estuaries using oysters as bioindicators. *Environmental Research*, **105** (3): 350-363.

Valsami Jones, E. (2000). Section 3: Minerals in contaminated environments. Pp 201 – 205. *In*: Environmental Mineralogy: Microbial Interactions, Anthropogenic Influences, Contaminated Land and Waste Management (J.D. Cotter-Howells, L.S. Campbell, E. Valsami-Jones and M Batchelder, editors). Mineralogical Series, 9. Mineralogical Society, London.

van der Land, C., Furu Mienis, F., de Haas, H., de Stigter, H.C., Swennen, R., Reijmer, J.J.G. and van Weering, T.C.E. (2011). Paleo-redox fronts and their formation in carbonate mound sediments from the Rockall Trough. *Marine Geology*, **284** (1-4): 86-95.

Vdovic, N., Billon, G., Gabelle, C., Potdevin, J.L. (2006). Remobilization of metals from slag and polluted sediments (Case Study: The canal of the Deule River, northern France). *Environmental Pollution*, **141**: 359–369.

Veizer, J. (1983). Trace elements and isotopes oin sedimentary carbonates. In, Carbonates: mineralogy and chemistry, (R.J. Reeder, ed.) *Reviews in Mineralogy*, Volume 11, Chapter 8, Min. Soc. America.

Veizer, J. (1989). Strontium isotopes in seawater through time. *Annual Reviews of Earth and Planetary Sciences*, **17**: 141-67.

Waeles, M., Tanguy, V., Lespes, G., and Riso, R.D. (2008). Behaviour of colloidal trace metals (Cu, Pb and Cd) in estuarine waters: An approach using frontal ultrafiltration (UF) and stripping chronopotentiometric methods (SCP). *Estuarine, Coastal and Shelf Science*, **80**: 538–544.

Walther, D., Prebha, S., Selvapathy, P. and Beck, D. (2003). Heavy Metals from the River Adayar, India: Infiltration into the Adjacent Groundwater Aquifer. *Ambio*, **32** (2): 153-157.

Wasserman, J.C., Figueiredo, A.M.G., Pellegatti, F. and Silva-Filho, E.V. (2001). Elemental composition of sediment cores from a mangrove environment using neutron activation analysis. *Journal of Geochemical Exploration*, **72** (2): 129-146.

Weaver, C.E. (1967). Potassium, illite and the ocean. *Geochimica et Cosmochimica Acta*, **31**: 2181–2196.

Weisberg, S.B., Wilson, H.T., Heimbuch, D.G., Windom, H.L. and Summers, J.K. (2000). Comparison of sediment metal: aluminum relationships between the eastern and gulf coasts of the United States. *Environmental Monitoring and Assessment*, **61** (3): 373-385.

Whitney, D. L. and Bozkurt, E. (2002). Metamorphic history of the southern Menderes massif, western Turkey. *Geological Society of America Bulletin*, **114** (7): 829–838.

Wilson, C.A., Bacon, J.R., Cresser, M.S. and Davidson, D.A. (2006). Lead isotope ratios as a means of sourcing anthropogenic lead in archaeological soils: a pilot study of an abandoned shetland croft. *Archaeometry*, **24** (3): 501-509.

Windom H.L., Schropp S.J., Calder F.D., Ryan J.D., Smith R.G., Burney L.C., Lewis F.G. and Rawlinson C.H. (1989). Natural trace metal concentrations in estuarine and coastal marine sediments of the southern United States. *Environmental Science and Technology*, **23** (3): 314 – 20.

Wiseman, S. (2009). Aquaculture production report 2008–2009. Aquaculture Unit, Port Stephens Fisheries Institute, State of New South Wales through Industry & Investment NSW 2009. Published by Industry & Investment NSW, ISSN 1444-840

Wyborn, L.A.I. and Chappell, B.W. (1983). Chemistry of the Ordovician and Silurian greywackes of the Snowy Mountains, southeastern Australia: an example of chemical evolution with time. *Chemical Geology*, **39**: 81-92.

Xu, Y. and Marcantonio, F. (2007). Strontium isotope variations in the lower Mississippi River and its estuarine mixing zone. *Marine Chemistry*, **105**: 118-128.

Xu, H., Zhang, J., Ren, J.L. and Liu, C.L. (2002). Aluminium in the macrotidal Yalujiang Estuary: Partitioning of Al along the estuarine gradients and flux. *Estuaries*, **25** (4A): 606-621.

Young, G.C. (2007). Devonian formations, vertebrate faunas, and age control on the far south coast of New South Wales and adjacent Victoria. *Australian Journal of Earth Sciences*, **54**: 991-1008.

Zann, L.P. (1995). State of the Marine Environment Report (SOMER), 1995. Chapter 7: The state of Australia's marine environment and the major issues. Great Barrier Reef Marine Park Authority, Townsville Queensland, Department of the Environment, Sport and Territories, Canberra, Department of the Environment, Water, Heritage and the Arts. www.environment.gov.au/coasts/publications/somer/chapter7.html

Appendix 1

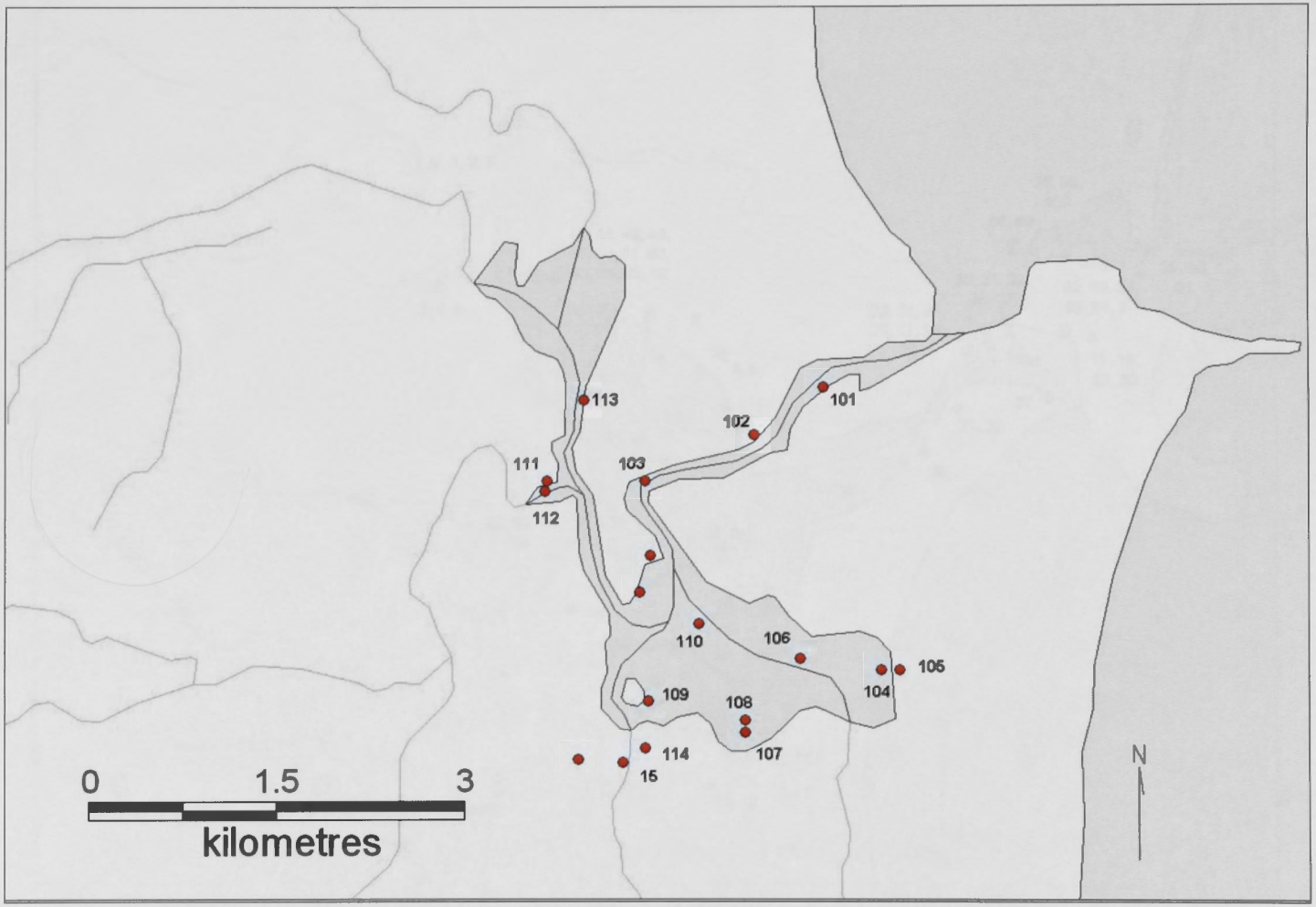

Localities of sampling sites at Pambula Lake and freshwater sites.

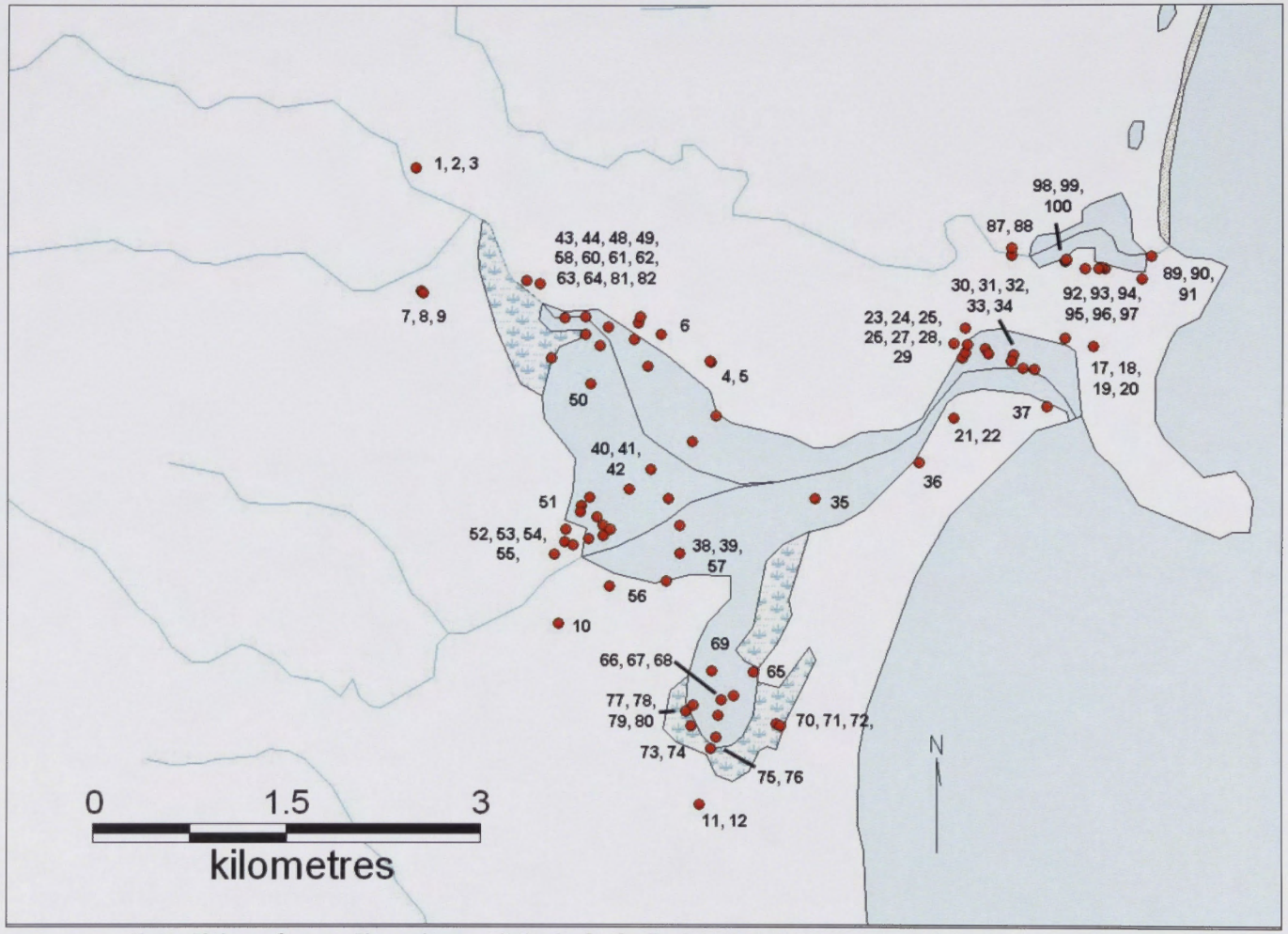

Localities of sampling sites at Merimbula Lake, Back Lagoon and freshwater sites.

Appendix 2

Freshwater sediment samples								
Sample	**1**	**2**	**3**	**4**	**5**	**6**	**7**	**8**
SiO_2	73.82	81.46	93.51	76.4	95.93	75.6	56.82	81.76
Al_2O_3	14.79	10.14	3.19	15.3	2.09	16.27	10.29	8.3
CaO	0.36	0.4	0.09	0.36	0.2	0.33	1.34	1.05
MgO	0.98	0.62	0.15	0.53	0.19	0.62	0.91	0.95
MnO	0.03	0.02	0.01	0.01	0	0.01	0.28	0.09
Na_2O	0.91	1.18	0.38	0.18	0.25	0.21	1.05	0.9
K_2O	2.94	2.36	1.08	2.31	0.54	2.16	1.43	1.5
TiO_2	1.09	0.73	0.2	0.7	0.19	0.84	1.27	0.81
P_2O5	0.09	0.06	0.02	0.09	0.02	0.1	1.01	0.1
SO_3	0	0	0	0.23	0	0.15	0.74	0.03
Fe_2O_3	5.01	3.03	1.38	3.89	0.65	3.72	24.86	4.52
Cl	155	177	476	136	45	93	408	2570
Be	2.86	2.43	1.12	1.98	0.63	2.07	1.48	1.4
Sc	16.08	11.24	4.57	13.71	3.39	14	12.05	11.19
V	140.96	113.29	82.67	134.58	77.94	138.77	146.73	136.46
Cr	68.04	53.32	28.12	91.65	39.8	110.04	76.72	69.14
Ni	14.96	10.07	6.02	12.36	6.79	19.12	23.28	21.23
Cu	65.59	10.31	5.56	43.83	4.3	11.25	59.59	9.73
Zn	46.65	31.29	7.37	23.55	4.9	20.09	35.49	28.19
Ga	18.02	12.21	3.74	15.26	2.38	15.69	8.3	8.21
Ge	7.02	7	6.6	6.43	5.83	6.64	5.29	5.75
As	5.04	3.21	3.23	5.52	1.63	5.23	17.23	3.98
Rb	138.8	101.89	40.65	117.65	22.39	120.06	53.2	57.08
Sr	63.93	65.4	20.09	44.45	22.58	57.63	70.22	70.61
Y	47.34	35.93	13.16	29.74	8.33	30.96	26.97	20.12
Zr	265.18	341.68	200.45	177.22	110.74	237.5	197.71	139.83
Nb	22.41	15.9	4.49	12.6	4.48	14.99	8.57	6.79
Mo	1.68	1.36	0.81	1.17	0.72	1.27	1.04	0.74
Ag	0.48	0.29	0.54	0.12	0.11	0.67	0.14	0.15
Cd	0.04	0.02	0.02	0.01	0.01	0.03	0.03	0.02
In	0.08	0.05	0.01	0.06	0.01	0.07	0.04	0.05
Sn	5.33	3.47	1.18	3.51	1.15	3.84	1.79	1.85
Sb	1.14	1.05	0.82	1.6	0.78	1.47	0.89	0.79
Cs	8.45	5.4	1.44	7.08	1.02	7.2	3.66	3.67
Ba	424.84	334.55	149.97	509.59	101.9	477.67	381.57	242.9

Table A.1: Elemental geochemistry of freshwater sediment samples. Major and minor elements are expressed in weight %; trace elements are expressed in ppm. 1: MC 030506-1a; 2: MC 030506-1b; 3: MC 030506-1c; 4: MLI 080307-01; 5: MLI 080307-02; 6: MLI 080307-03; 7: MLI 080307-04; 8: MLI 080307-05.

Freshwater sediment samples								
Sample	**1**	**2**	**3**	**4**	**5**	**6**	**7**	**8**
La	63.96	41.01	14.68	53.96	10.33	60.18	29.66	23.95
Ce	124.52	79.84	29.48	105.01	18.65	113.82	54.69	43.84
Pr	13.76	8.96	3.19	11.01	1.95	12.02	6.12	4.75
Nd	52.14	34.78	11.49	48.08	8.27	52.78	28.26	22.24
Sm	9.58	6.74	2.22	8.52	1.44	9.23	5.47	3.97
Eu	1.68	1.18	0.34	1.59	0.26	1.68	1.15	0.93
Gd	9.06	6.34	2.07	7.88	1.54	8.42	5.37	4.08
Tb	1.31	0.94	0.35	1.1	0.24	1.22	0.83	0.61
Dy	8.3	6.25	2.15	6.66	1.54	6.95	5.3	4.02
Ho	1.66	1.27	0.44	1.12	0.32	1.17	0.97	0.74
Er	4.87	3.78	1.44	3.05	0.93	3.1	2.7	2.11
Tm	0.74	0.55	0.22	0.44	0.12	0.47	0.42	0.3
Yb	4.85	3.98	1.45	2.94	0.93	3.1	2.74	2.12
Lu	0.7	0.6	0.2	0.42	0.12	0.47	0.38	0.28
Hf	7.45	9.5	6.61	5.41	6.61	6.7	5.34	4.53
Ta	2.16	1.51	0.45	1.08	0.39	1.26	0.73	0.6
Tl	0.38	0.31	0.29	0.52	0.07	0.44	0.19	0.06
Pb	19.64	14.52	8.04	20.37	4.52	19.92	8.84	8.07
Bi	0.34	0.21	0.08	0.23	0.04	0.26	0.11	0.09
Th	23.27	16.42	5.74	14.88	3.43	16.29	8.13	6.38
U	5.09	4.01	1.25	2.54	0.8	3.19	1.61	1.4

Table A.1 (continued): Elemental geochemistry of freshwater sediment samples. Major and minor elements are expressed in weight %; trace elements are expressed in ppm. 1: MC 030506-1a; 2: MC 030506-1b; 3: MC 030506-1c; 4: MLI 080307-01; 5: MLI 080307-02; 6: MLI 080307-03; 7: MLI 080307-04; 8: MLI 080307-05.

Freshwater sediment samples								
Sample	**9**	**10**	**11**	**12**	**13**	**14**	**15**	**16**
SiO_2	72.1	74.48	96.27	80.29	53.5	85.76	64.95	65.13
Al_2O_3	13.79	15.84	1.76	10.32	11.5	7.75	11.62	18.14
CaO	0.63	0.63	0.13	0.43	0.69	0.91	0.24	0.02
MgO	0.72	0.78	0.12	0.47	0.52	0.13	0.68	0.6
MnO	0.06	0.05	0	0.01	0.04	0.01	0.03	0
Na_2O	0.88	0.54	0.3	0.32	1.34	1.65	0.21	0.21
K_2O	1.3	1.81	0.5	0.84	2.06	2.28	1.91	3.74
TiO_2	1.72	1.07	0.16	0.91	0.64	0.03	0.58	0.78
P_2O5	0.06	0.3	0.04	0.3	0.43	0.02	0.13	0.03
SO_3	0	0.42	0.23	2.95	0.4	0	0.29	0
Fe_2O_3	8.77	4.09	0.47	3.16	4.62	0.62	2.94	3.87
Cl	87	313	48	326	315	215	295	223
Be	2.29	2	0.58	1.52	2.71	1.25	2.89	2.55
Sc	23.21	12.3	2.36	8.71	11.19	4.93	11.74	22.74
V	220.94	132.34	87.53	117.79	65.84	27.21	73.98	137.55
Cr	128.31	85.22	23.24	73.2	40.05	38.6	86.7	145.91
Ni	33.78	24.57	25.63	23.01	18.55	50.94	31.06	11.25
Cu	14.03	8.81	95.83	22.04	31.81	90.59	13.79	4.09
Zn	30.46	34.18	7.19	48.92	84.15	7.9	57.46	13.04
Ga	14.27	12.9	1.93	10.62	13.18	6.36	14.84	22.87
Ge	6.24	5.78	6.81	5.95	2.15	1.62	1.54	2.98
As	6.83	4.2	1.75	5.39	6.15	0.92	3.09	7.67
Rb	64.84	93.76	20.18	55.83	116.45	87.18	117.13	207.9
Sr	70.2	55.12	20.13	33.5	80.89	99.93	34.3	41.92
Y	48.91	33.44	5.49	26.66	37.08	4.78	49.05	40.27
Zr	241.94	213.68	86.78	322.19	299.53	31.01	235.46	219.04
Nb	11.23	12.16	3.01	15.17	13.27	1.31	12.94	17.11
Mo	1.1	1.76	2.27	3.07	1.17	1.09	2.24	0.68
Ag	0.12	0.27	0.35	0.25	0.14	0.21	0.62	0.21
Cd	0.04	0.09	0.04	0.1	0.27	0.04	0.29	0
In	0.08	0.06	0.02	0.06	0.05	0.03	0.06	0.13
Sn	2.28	2.24	1.07	2.9	2.63	0.7	1.36	4.85
Sb	1.08	1.07	0.85	1.05	2.66	3.32	1.63	5.28
Cs	4.64	6.22	0.75	4.56	4.9	1.77	8.34	13.93
Ba	254.88	349.52	99.11	165.48	409.2	397.23	336.03	796.03

Table A.1 (continued): Elemental geochemistry of freshwater sediment samples. Major and minor elements are expressed in weight %; trace elements are expressed in ppm. 9: MLI 080307-06; 10: MLI 080307-09; 11: MLI 080307-10; 12: MLI 080307-11; 13: 111107-13; 14: 111107-14; 15: 141107-02; 16: Merimbula Group.

Freshwater sediment samples								
Sample	**9**	**10**	**11**	**12**	**13**	**14**	**15**	**16**
La	44.51	48.81	5.59	32.6	45.41	6.02	52.6	45
Ce	82.35	92.74	9.31	58.03	83.3	9.33	101.55	85.05
Pr	10.07	9.81	0.99	6.09	8.95	0.94	10.26	8.9
Nd	47.66	44.2	4.38	26	39	4.17	44.81	40.34
Sm	9.59	7.93	0.68	4.66	7.1	0.77	8.02	7.48
Eu	2.49	1.52	0.16	0.88	1.21	0.43	1.62	1.42
Gd	10.64	7.78	0.94	4.76	6.82	0.8	9.09	7.04
Tb	1.66	1.12	0.15	0.78	1.1	0.15	1.43	1.1
Dy	10	6.86	1.01	5.21	7.43	0.74	9.2	6.6
Ho	1.76	1.21	0.21	0.94	1.28	0.16	1.72	1.25
Er	4.8	3.28	0.53	2.73	3.82	0.48	4.29	3.79
Tm	0.68	0.5	0.1	0.41	0.61	0.08	0.66	0.66
Yb	4.34	3.31	0.58	2.98	3.74	0.48	4.12	4.12
Lu	0.65	0.46	0.1	0.43	0.57	0.09	0.58	0.62
Hf	6.73	6.6	4.17	8.7	7.9	8.35	6.57	6.17
Ta	0.91	1.03	0.24	1.28	1.4	0.21	1.27	1.61
Tl	0.36	0.43	0.1	0.34	0.23	0.24	0.26	0.59
Pb	12.02	20.07	5.23	15.74	16.15	7.84	26.15	20.49
Bi	0.13	0.17	0.07	0.18	0.12	0.1	0.21	0.32
Th	9.6	12.44	2.28	10.67	15	2.06	13.59	21.26
U	2.08	3.07	0.61	2.89	5.81	0.58	3.8	2.8

Table A.1 (continued): Elemental geochemistry of freshwater sediment samples. Major and minor elements are expressed in weight %; trace elements are expressed in ppm. 9: MLI 080307-06; 10: MLI 080307-09; 11: MLI 080307-10; 12: MLI 080307-11; 13: 111107-13; 14: 111107-14; 15: 141107-02; 16: Merimbula Group.

Merimbula Front Lake sediment samples								
Sample	**17**	**18**	**19**	**20**	**21**	**22**	**23**	**24**
SiO_2	92.27	96.83	94.87	95.18	95.83	94.29	88.09	94.73
Al_2O_3	1.27	0.98	1.36	1.49	1.71	1.9	4.53	2.49
CaO	4.27	0.97	1.69	1.3	0.38	1.64	0.58	0.15
MgO	0.37	0.15	0.22	0.2	0.21	0.19	0.65	0.2
MnO	0	0	0	0	0	0	0.01	0
Na_2O	0.75	0.35	0.78	0.61	0.64	0.5	2.13	0.77
K_2O	0.61	0.48	0.63	0.67	0.72	0.75	1.26	0.97
TiO_2	0.06	0.04	0.06	0.06	0.09	0.12	0.3	0.1
P_2O5	0.02	0.02	0.02	0.02	0.02	0.02	0.12	0.02
SO_3	0.14	0	0.12	0.18	0.03	0.15	0.68	0.15
Fe_2O_3	0.24	0.18	0.25	0.29	0.36	0.44	1.65	0.41
Cl	5129	1401	5471	3668	3650	1597	15217	4281
Be	0.4	0.38	0.6	0.45	0.57	0.62	0.96	0.58
Sc	2.05	1.85	2.21	2.32	2.45	2.83	4.91	2.79
V	48.54	45.8	52.18	51.36	58.5	53.99	70.48	46.27
Cr	16.67	16.54	15.15	18.21	26.75	23.91	54.29	14.85
Ni	29.12	9.75	5.37	7.05	9.48	8.05	9.68	5.18
Cu	10.53	10.38	9.36	7.83	8.89	12.8	20.18	9.64
Zn	5.61	8.48	7.9	8.5	15.8	17.29	54.27	21.06
Ga	1.11	0.83	1.22	1.35	1.82	1.87	4.79	2.4
Ge	4.01	4.33	4.97	4.55	5.24	5.44	4.7	4.6
As	2.26	2.6	2.66	2.54	2.89	4.11	11.4	3.09
Rb	21.49	18.57	23.06	23.6	27.37	29.11	44.02	33.73
Sr	224.2	60.73	91.11	72.94	38.26	70.49	58.73	25.36
Y	3.82	3.12	3.83	4.18	4.56	6.03	12.28	5.87
Zr	31.12	22.07	30.67	34.41	58.01	87.37	144.8	126.6
Nb	0.79	0.67	1.05	1.26	2.18	2.07	6.01	2.01
Mo	1.07	0.87	0.95	1.48	0.96	1.2	2.24	1.28
Ag	0.48	0.61	0.42	0.56	0.84	0.29	0.57	0.43
Cd	0.08	0.06	0.15	0.11	0.22	0.33	0.11	0.04
In	0.02	0.03	0.03	0.02	0.03	0.03	0.03	0.02
Sn	0.71	0.56	0.72	0.71	0.66	0.74	1.02	0.63
Sb	0.6	0.6	0.76	0.72	0.55	0.77	1.18	0.9
Cs	0.42	0.38	0.56	0.6	0.64	0.77	1.91	1.08
Ba	91.88	78.46	103.3	109.5	115.3	117.6	171.5	122.8

Table A.2: Elemental geochemistry of Merimbula Front Lake sediment samples. Major and minor elements are expressed in weight %; trace elements are expressed in ppm. 17: ML 181006-03a; 18: ML 181006-03b; 19: ML 181006-04a; 20: ML 181006-04b; 21: ML 181006-06a; 22: ML 181006-06b; 23: BST. A1; 24: BST. A2.

Merimbula Front Lake sediment samples								
Sample	**17**	**18**	**19**	**20**	**21**	**22**	**23**	**24**
La	4.02	2.84	4.2	4.67	5.65	6.02	13	4.96
Ce	6.71	4.6	7.26	8.32	10.11	11.06	24.93	8.89
Pr	0.78	0.49	0.82	0.93	1.09	1.15	2.79	0.97
Nd	3.02	1.76	3.24	3.63	4.52	4.37	10.8	3.88
Sm	0.67	0.45	0.67	0.74	0.65	0.91	2.09	0.81
Eu	0.14	0.06	0.11	0.14	0.18	0.22	0.42	0.14
Gd	0.62	0.43	0.61	0.75	0.7	0.98	1.99	0.66
Tb	0.1	0.07	0.08	0.1	0.12	0.14	0.33	0.13
Dy	0.72	0.56	0.65	0.7	0.81	0.92	2.12	0.95
Ho	0.12	0.12	0.11	0.15	0.2	0.24	0.44	0.22
Er	0.4	0.35	0.42	0.46	0.43	0.66	1.49	0.64
Tm	0.05	0.05	0.07	0.08	0.08	0.1	0.21	0.11
Yb	0.38	0.33	0.36	0.39	0.61	0.76	1.52	0.76
Lu	0.07	0.04	0.07	0.07	0.06	0.11	0.23	0.1
Hf	1.88	3.4	3.28	4.39	4.49	3.35	4.68	5.12
Ta	0.08	0.1	0.13	0.17	0.24	0.22	0.57	0.23
Tl	0.02	0.05	0.02	0.01	0.02	0.08	0	0.08
Pb	7.49	7.27	8.08	8.05	11.67	16.63	28.25	10.64
Bi	0.11	0.11	0.06	0.13	0.15	0.22	0.16	0.09
Th	1.35	1.06	1.73	1.68	2.23	2.16	5.61	2.72
U	0.45	0.28	0.36	0.49	0.52	0.76	1.46	0.78

Table A.2 (continued): Elemental geochemistry of Merimbula Front Lake sediment samples. Major and minor elements are expressed in weight %; trace elements are expressed in ppm. 17: ML 181006-03a; 18: ML 181006-03b; 19: ML 181006-04a; 20: ML 181006-04b; 21: ML 181006-06a; 22: ML 181006-06b; 23: BST. A1; 24: BST. A2.

Merimbula Front Lake sediment samples								
Sample	**25**	**26**	**27**	**28**	**29**	**30**	**31**	**32**
SiO_2	95.98	95.65	95.88	95.6	96.34	95.76	92.84	95.93
Al_2O_3	1.78	1.7	1.76	1.68	1.65	1.43	1.7	1.5
CaO	0.13	0.46	0.35	0.22	0.11	1.06	2.81	0.76
MgO	0.15	0.17	0.14	0.18	0.14	0.18	0.25	0.16
MnO	0	0	0	0	0	0	0	0
Na_2O	0.61	0.68	0.63	0.89	0.57	0.5	1.01	0.57
K_2O	0.87	0.88	0.9	0.83	0.8	0.68	0.77	0.76
TiO_2	0.05	0.04	0.03	0.03	0.03	0.06	0.07	0.05
P_2O5	0.02	0.02	0.02	0.03	0.02	0.03	0.02	0.02
SO_3	0.03	0.12	0.09	0.07	0.04	0.06	0.23	0.05
Fe_2O_3	0.37	0.28	0.21	0.48	0.29	0.25	0.29	0.2
Cl	3305	4572	3242	6024	2791	2416	7893	3272
Be	0.57	0.46	0.46	0.48	0.46	0.69	0.56	0.47
Sc	2.22	4.32	4.21	4.16	4.25	3.87	3.95	4.08
V	53.89	21.94	22.12	24.54	24.68	22.21	24.12	22.36
Cr	20.19	21.92	27.58	21.56	19.36	41.02	34.71	28.76
Ni	57.15	25.12	35.11	22.07	15.3	33.06	41.16	35.72
Cu	21.62	18.59	10.67	7.29	90.61	9.46	11.32	8.43
Zn	15.9	49.73	61.21	9.98	20.51	95.79	44.06	8.35
Ga	1.61	1.66	1.8	1.55	1.56	1.57	1.68	1.47
Ge	4.89	1.61	1.71	1.51	1.69	1.77	2.05	6.19
As	3.77	3.1	2.93	4.29	3.07	3.41	3.12	2.64
Rb	33.52	28.95	30.55	24.7	25.57	21.94	26.41	25
Sr	29.29	27.15	22.44	21.32	15.87	50.3	107.9	41.5
Y	3.84	4.46	2.86	3.87	3.78	4.2	4.25	3.52
Zr	28.37	31.62	26.89	27.03	33.21	42.48	45.97	39.83
Nb	1.39	1.03	1.02	1.26	1.3	1.53	1.96	1.62
Mo	1.63	1.27	1.66	1.31	1.34	0.89	2.21	1.15
Ag	1.32	0.37	0.68	0.55	0.36	0.4	0.47	0.38
Cd	0.23	0.51	1.87	0.04	0.58	1.14	1.01	0.38
In	0.02	0.05	0.05	0.02	0.03	0.01	0.03	0.01
Sn	1.17	0.75	0.72	0.78	0.61	0.81	1.27	0.78
Sb	0.71	3.48	4.08	3.43	3.62	3.95	3.93	3.75
Cs	0.69	0.67	0.78	0.64	1.23	0.58	0.71	0.68
Ba	144.4	114.2	111.4	114.9	107.2	93.82	103.0	104.5

Table A.2 (continued): Elemental geochemistry of Merimbula Front Lake sediment samples. Major and minor elements are expressed in weight %; trace elements are expressed in ppm. 25: Merimbula B; 26: 101107-01; 27: 101107-02; 28: 101107-03; 29: 101107-04; 30: 101107-05; 31: 101107-06; 32: 101107-07.

Merimbula Front Lake sediment samples								
Sample	**25**	**26**	**27**	**28**	**29**	**30**	**31**	**32**
La	3.85	3.52	2.68	3.46	3.36	4.42	4.31	3.88
Ce	6.91	6.76	5.08	6.66	6.43	8.04	8.08	7.33
Pr	0.72	0.66	0.54	0.64	0.59	0.8	0.91	0.77
Nd	2.88	2.92	2.34	2.61	2.81	3.95	3.42	3.47
Sm	0.51	0.52	0.28	0.57	0.4	0.57	0.91	0.61
Eu	0.14	0.12	0.13	0.14	0.1	0.12	0.17	0.11
Gd	0.55	0.72	0.54	0.57	0.45	0.61	0.71	0.59
Tb	0.09	0.11	0.09	0.08	0.07	0.15	0.11	0.14
Dy	0.54	0.85	0.41	0.72	0.59	0.78	0.94	0.52
Ho	0.14	0.18	0.1	0.14	0.14	0.13	0.15	0.15
Er	0.41	0.4	0.38	0.31	0.31	0.47	0.47	0.35
Tm	0.07	0.58	0.05	0.07	0.07	0.06	0.1	0.04
Yb	0.44	0.51	0.32	0.47	0.32	0.42	0.51	0.36
Lu	0.06	0.06	0.04	0.04	0.07	0.06	0.08	0.04
Hf	4.56	0.87	0.75	10.34	1	1.16	1.3	6.41
Ta	0.14	0.2	0.12	0.2	0.31	0.17	0.48	0.19
Tl	0.07	0.05	0.1	0.04	0.03	0.01	0.05	0.04
Pb	15.68	6.53	8.66	7.89	7.6	4.14	4.85	4.99
Bi	0.13	0.07	0.17	0.06	0.07	0.05	0.08	0.16
Th	1.33	1.48	1.07	1.42	1.29	1.44	1.48	1.56
U	0.37	0.38	0.5	0.29	0.35	0.4	0.77	0.36

Table A.2 (continued): Elemental geochemistry of Merimbula Front Lake sediment samples. Major and minor elements are expressed in weight %; trace elements are expressed in ppm. 25: Merimbula B; 26: 101107-01; 27: 101107-02; 28: 101107-03; 29: 101107-04; 30: 101107-05; 31: 101107-06; 32: 101107-07.

Merimbula Front Lake sediment samples					
Sample	**33**	**34**	**35**	**36**	**37**
SiO_2	93.36	93.2	95.98	94.82	97.19
Al_2O_3	1.35	1.45	1.56	2.28	0.78
CaO	3.08	3.12	0.43	0.22	1.16
MgO	0.27	0.23	0.16	0.22	0.13
MnO	0	0	0	0	0
Na_2O	0.85	0.8	0.77	0.81	0.17
K_2O	0.65	0.71	0.84	1	0.33
TiO_2	0.05	0.05	0.04	0.12	0.06
P_2O5	0.03	0.02	0.02	0.02	0.02
SO_3	0.14	0.16	0.05	0.18	-0.04
Fe_2O_3	0.22	0.25	0.15	0.33	0.2
Cl	5827	5588	5105	5186	117
Be	0.43	0.39	0.46	0.57	0.41
Sc	3.72	3.77	3.94	4.14	3.33
V	22.69	23.18	20.99	25.61	21.36
Cr	20.77	26.06	24.53	35.7	14.38
Ni	44.68	32.03	31.34	38.79	10.42
Cu	10.91	15.56	16.05	98.35	6.12
Zn	44.71	23.76	12.85	16.33	14.83
Ga	1.43	1.62	1.45	2.19	0.94
Ge	1.8	2.14	13.98	2.11	2.01
As	2.41	3.37	2.59	3.2	2.62
Rb	22.39	23.66	27.58	33.69	11.65
Sr	144.2	127.2	26.49	25.78	70.34
Y	3.42	3.07	2.62	5.06	3.45
Zr	32.35	36.29	35.22	70.5	27.71
Nb	1.39	1.16	1.24	2.32	1.13
Mo	1.19	1.88	1.1	1.89	0.77
Ag	0.67	0.34	0.92	0.45	0.3
Cd	1.46	1.37	0.71	0.7	0.57
In	0.03	0.02	0.04	0.08	0.01
Sn	0.81	0.78	5.35	4.48	0.54
Sb	4.11	4.6	3.86	3.87	3.88
Cs	0.62	0.6	0.57	0.92	0.35
Ba	84.85	93.99	106.1	137.2	54.92

Table A.2 (continued): Elemental geochemistry of Merimbula Front Lake sediment samples. Major and minor elements are expressed in weight %; trace elements are expressed in ppm. 33: 101107-08; 34: 101107-09; 35: 101107-10; 36: 101107-12; 37: sand filter.

Merimbula Front Lake sediment samples					
Sample	**33**	**34**	**35**	**36**	**37**
La	4.28	3.36	2.86	5.68	3.17
Ce	8.39	6.53	5.7	10.46	5.83
Pr	0.91	0.63	0.55	1.07	0.63
Nd	3.66	2.89	2.58	4.46	2.43
Sm	0.6	0.54	0.37	0.73	0.58
Eu	0.12	0.11	0.1	0.17	0.07
Gd	0.63	0.54	0.29	0.86	0.26
Tb	0.13	0.13	0.09	0.15	0.12
Dy	0.62	0.61	0.45	0.91	0.65
Ho	0.13	0.11	0.09	0.22	0.13
Er	0.35	0.32	0.32	0.54	0.35
Tm	0.05	0.06	0.03	0.1	0.06
Yb	0.44	0.4	0.35	0.59	0.33
Lu	0.1	0.07	0.05	0.12	0.06
Hf	0.87	0.76	7	1.96	0.87
Ta	0.14	0.21	0.19	0.23	0.23
Tl	0.04	0.04	0.04	0.07	0.01
Pb	5.33	6.07	5.29	6.68	5.19
Bi	0.09	0.1	0.11	0.07	0.04
Th	1.35	1.16	1.11	1.93	1.09
U	0.48	0.54	0.3	0.92	0.3

Table A.2 (continued): Elemental geochemistry of Merimbula Front Lake sediment samples. Major and minor elements are expressed in weight %; trace elements are expressed in ppm. 33: 101107-08; 34: 101107-09; 35: 101107-10; 36: 101107-12; 37: sand filter.

Merimbula Top Lake sediment samples									
Sample	**38**	**39**	**40**	**41**	**42**	**43**	**44**	**45**	**46**
SiO_2	67.82	96.34	57.54	76.76	54.64	61.74	70.65	58.95	89.91
Al_2O_3	10.57	1.1	14.92	4.67	15.27	14.62	12.01	15.7	4.29
CaO	4.05	0.88	4.01	11.71	4.6	3.64	0.9	1.25	0.58
MgO	1.82	0.17	2.52	0.94	2.7	2.12	1.63	2.19	0.4
MnO	0.02	0	0.02	0.02	0.02	0.02	0.02	0.02	0.02
Na_2O	4.56	0.47	5.29	1.55	6.75	4.01	3.33	6.65	0.53
K_2O	1.93	0.45	2.35	1.11	2.61	2.56	2.32	2.61	0.79
TiO_2	0.69	0.07	1.15	0.31	0.96	1.04	0.99	0.97	0.41
P_2O5	0.2	0.02	0.25	0.11	0.3	0.22	0.14	0.21	0.07
SO_3	4.33	0.17	5.57	0.74	6.03	4.22	3.31	6.07	0
Fe_2O_3	4.02	0.32	6.36	2.07	6.11	5.8	4.71	5.39	3
Cl	32143	4205	36017	10708	48303	26705	21196	42869	1063
Be	1.71	0.68	2.1	0.82	2.09	2.29	2.25	1.85	1.11
Sc	10.37	3.07	14.7	5.55	13.52	14.43	13.02	12.92	6.96
V	133.45	84.37	159.84	99.01	160.49	156.98	138.23	146.56	106.21
Cr	80.44	23.63	111.17	42.87	99.64	100.36	90.07	83.91	48.2
Ni	21.93	9.1	28.22	10.86	26.85	25.65	21.53	21.65	38.15
Cu	18.42	9.53	166.92	104.92	247.88	69.58	36.14	30.03	6.27
Zn	42.65	7.75	55.64	15.99	59.78	53.13	42.12	50.87	9.43
Ga	9.18	1.22	12.69	4.27	12.61	13.07	11.58	13.45	4.8
Ge	6.88	7.77	6.69	6.8	5.71	6.85	7.55	6.19	5.73
As	17.74	5.21	16.66	10.37	16.84	14.8	10.33	9.69	11.08
Rb	69.99	16.23	87.71	37.13	91.54	101.06	92.71	91.52	33.26
Sr	169.78	42.98	197.68	499.01	219.2	164.8	85.55	104.03	56.75
Y	20.28	3.63	28	12.44	26.2	30.73	34.3	25.74	17.78
Zr	130	33.97	172.56	75	133.33	191.2	279.72	160.8	153.46
Nb	8.23	1.35	11.44	3.83	10.54	12.4	13.32	11.65	4.86
Mo	5.89	1.26	5.6	1.27	5.86	4.02	2.59	7.63	9.53
Ag	1.05	1.21	0.55	0.74	0.82	1.03	0.88	0.72	0.3
Cd	0.16	-0.02	0.22	0.04	0.14	0.06	0.07	0.15	0.01
In	0.06	0.02	0.06	0.02	0.05	0.06	0.04	0.06	0.03
Sn	2.48	0.7	2.58	1.07	2.65	2.76	2.47	2.93	1.37
Sb	0.89	0.65	1.11	0.78	0.97	1	0.96	0.95	0.78
Cs	4.29	0.64	6.05	2.05	5.44	6.45	5.57	5.39	2.06
Ba	216.2	67.7	248.82	136.22	265.11	284.35	259.59	262.34	103.49

Table A.3: Elemental geochemistry of Merimbula Top Lake sediment samples. Major and minor elements are expressed in weight %; trace elements are expressed in ppm. 38: ML 130406-01 (14); 39: ML 130406-02 (15); 40: ML 130406-03 (16); 41: ML 130406-04 (17); 42: ML 130406-05 (18); 43: ML 130406-06 (19); 44: ML 130406-07 (20); 45: CB 030506-1d; 46: MLI 080307-12.

Merimbula Top Lake sediment samples									
Sample	**38**	**39**	**40**	**41**	**42**	**43**	**44**	**45**	**46**
La	25.11	3.63	33.67	18.09	33.38	39.49	41.26	37.15	18.76
Ce	50.19	7.76	68.15	36.46	66.76	79.3	82.93	71.73	37.67
Pr	5.83	0.81	7.85	4.28	7.5	9.06	9.33	7.94	3.94
Nd	23.19	3	31.61	17.67	29.32	35.76	37.33	30.49	17.39
Sm	4.7	0.59	6.36	3.36	6.2	6.95	7.26	5.81	3.25
Eu	0.95	0.13	1.27	0.63	1.25	1.39	1.36	1.15	0.69
Gd	4.5	0.54	5.74	2.83	5.5	6.64	6.79	5.3	3.56
Tb	0.63	0.1	0.9	0.4	0.85	0.96	0.99	0.81	0.57
Dy	4.02	0.46	5.53	2.47	5.21	6.01	6.55	5.04	3.47
Ho	0.8	0.16	1.09	0.51	1.04	1.17	1.27	0.98	0.64
Er	2.23	0.46	3.01	1.36	2.76	3.46	3.66	2.81	1.81
Tm	0.32	0.04	0.43	0.2	0.38	0.47	0.53	0.4	0.27
Yb	2.23	0.42	3.01	1.15	2.68	3.22	3.53	2.78	1.93
Lu	0.33	0.08	0.42	0.2	0.42	0.48	0.53	0.39	0.26
Hf	4.34	5.19	4.87	2.73	4.02	5.36	7.95	4.69	8.1
Ta	0.71	0.13	0.99	0.36	0.89	1.1	1.1	1.1	0.45
Tl	0	0.03	0.03	0.05	0	0	0.02	0.01	0.09
Pb	17.31	8.09	18.84	8.95	22.3	20.58	22.67	21.13	5.61
Bi	0.27	0.19	0.17	0.08	0.17	0.16	0.25	0.2	0.1
Th	9.82	1.29	12.79	5.51	13.05	14.49	14.23	14.21	4.9
U	3.23	0.39	4.03	1.38	3.53	3.52	3.29	3.89	3.6

Table A.3 (continued): Elemental geochemistry of Merimbula Top Lake sediment samples. Major and minor elements are expressed in weight %; trace elements are expressed in ppm. 38: ML 130406-01 (14); 39: ML 130406-02 (15); 40: ML 130406-03 (16); 41: ML 130406-04 (17); 42: ML 130406-05 (18); 43: ML 130406-06 (19); 44: ML 130406-07 (20); 45: CB 030506-1d; 46: MLI 080307-12.

Merimbula Top Lake sediment samples									
Sample	**47**	**48**	**49**	**50**	**51**	**52**	**53**	**54**	**55**
SiO_2	60.44	80.63	94.76	63.7	67.59	65.52	88.27	93.32	76.93
Al_2O_3	14.93	7.4	2.42	12.72	9.29	12.43	4.7	2.97	8.19
CaO	2.74	1.76	0.14	3.68	3.53	2.48	1.02	0.56	0.97
MgO	1.92	1.15	0.3	2.18	1.81	1.98	0.51	0.33	1.17
MnO	0.02	0.01	0	0.02	0.02	0.03	0.01	0.01	0.02
Na_2O	5.2	2.16	0.65	4.83	4.75	3.88	1.66	0.58	2.67
K_2O	2.54	1.44	0.79	2.26	1.67	1.87	0.96	0.77	1.5
TiO_2	0.95	0.63	0.15	0.89	0.76	1.26	0.54	0.23	0.67
P_2O5	0.18	0.13	0.02	0.25	0.25	0.19	0.04	0.02	0.12
SO_3	5.95	1.65	0.1	4.41	6.18	4.56	0.83	0.25	4.21
Fe_2O_3	5.13	3.05	0.67	5.06	4.16	5.82	1.46	0.96	3.56
Cl	37580	15922	5815	34894	34632	23631	7714	3073	17363
Be	1.86	1.41	0.69	1.76	1.29	1.87	0.83	0.71	1.28
Sc	12.26	8.47	3.5	11.59	9.26	14.19	6.87	4.77	9.28
V	134.18	110.69	77.48	134.83	119.98	146.78	98.09	82.1	115.43
Cr	92.26	72.48	36.08	98.83	76.16	106.77	43.48	30.46	64.72
Ni	43.83	21.56	27.15	35.93	26.37	36.2	9.66	9.05	18.31
Cu	17.34	17.3	5.07	229.43	15.43	19.42	7.27	4.07	13.19
Zn	44.83	25.52	7.06	41.23	32.02	42.4	15.69	7.44	31.25
Ga	12.04	7	2.71	10.09	7.04	10.56	4.05	3.12	7.27
Ge	5.73	5.93	6.08	5.57	5.47	5.87	5.86	5.6	5.35
As	9.86	13.3	3.17	22.18	16.04	18.48	5.77	2.82	10.02
Rb	91.46	60.1	30.1	83.02	56	74.03	32.94	27.47	55.32
Sr	140.82	96.58	17.18	162.04	146.01	153.46	83.48	46.12	84.19
Y	25.3	21.85	8.5	24.93	19.69	27.7	13.61	8.76	19.83
Zr	165.9	181.15	65.14	161.14	151.04	226.55	195.4	117.5	169.01
Nb	11.44	8.41	2.8	9.62	7.1	10.94	5.48	3.08	7.24
Mo	5.72	1.9	1.18	5.95	11.63	3.42	2.28	1.15	7.47
Ag	0.44	0.42	0.42	0.36	0.32	0.3	0.35	0.3	0.37
Cd	0.11	0.06	0	0.15	0.36	0.12	0.08	0.03	0.09
In	0.06	0.03	0.02	0.07	0.03	0.05	0.02	0.02	0.03
Sn	2.98	2	1.27	2.91	1.61	2.52	1.25	0.97	1.93
Sb	0.94	0.94	0.66	1.05	0.83	1.06	0.87	0.68	0.94
Cs	5.58	3.65	1.2	5.45	3.72	5.46	1.59	1.33	3.55
Ba	247.75	176.52	97.58	215.9	163.84	208.35	138.79	102.93	166.51

Table A.3 (continued): Elemental geochemistry of Merimbula Top Lake sediment samples. Major and minor elements are expressed in weight %; trace elements are expressed in ppm. 47: MLI 080307-13; 48: ML 090307-01; 49: ML 090307-02; 50: ML 090307-03; 51: ML 090307-04; 52: ML 090307-05; 53: ML 090307-06; 54: ML 090307-07; 55: ML 090307-08.

Merimbula Top Lake sediment samples									
Sample	**47**	**48**	**49**	**50**	**51**	**52**	**53**	**54**	**55**
La	40.22	30.24	11.63	33.62	23.99	33.3	14.76	10.86	24.7
Ce	71.59	56.54	21.57	63.56	45.09	63.84	27.83	18.93	45.73
Pr	7.58	6.15	2.12	6.9	4.95	7.01	2.97	2	4.91
Nd	32.54	27	9.58	30.94	22.59	31.47	13.65	8.65	21.68
Sm	5.84	4.77	1.5	5.54	4.27	5.82	2.52	1.62	4.06
Eu	1.1	0.92	0.3	1.12	0.89	1.27	0.51	0.36	0.83
Gd	5.66	4.68	1.5	5.65	4.51	6.18	2.54	1.62	4.16
Tb	0.83	0.72	0.25	0.86	0.68	0.9	0.42	0.24	0.66
Dy	5.05	4.43	1.66	5.16	4.11	5.72	2.73	1.6	4.03
Ho	0.91	0.79	0.33	0.93	0.73	1.05	0.5	0.28	0.75
Er	2.63	2.17	0.88	2.62	2.01	2.9	1.46	0.91	2.01
Tm	0.39	0.34	0.13	0.38	0.3	0.43	0.23	0.14	0.32
Yb	2.67	2.25	0.98	2.65	2.03	2.95	1.59	1.07	2.15
Lu	0.37	0.32	0.13	0.38	0.29	0.44	0.24	0.17	0.31
Hf	4.76	5.76	2.86	4.65	5.31	6.61	7.09	6.14	5.79
Ta	0.99	0.72	0.27	0.82	0.57	0.89	0.48	0.35	0.66
Tl	0	0.02	0.02	0.02	0.02	0.02	0.02	0.04	0.02
Pb	19.26	11.59	4.86	15.14	10.69	13.63	6.45	3.97	11.25
Bi	0.2	0.16	0.09	0.28	0.1	0.16	0.08	0.07	0.14
Th	13.09	8.67	3.37	11.15	7.69	10.5	4.88	3.43	7.76
U	3.28	2.09	0.69	2.94	4.15	3.4	1.84	1.2	3.24

Table A.3 (continued): Elemental geochemistry of Merimbula Top Lake sediment samples. Major and minor elements are expressed in weight %; trace elements are expressed in ppm. 47: MLI 080307-13; 48: ML 090307-01; 49: ML 090307-02; 50: ML 090307-03; 51: ML 090307-04; 52: ML 090307-05; 53: ML 090307-06; 54: ML 090307-07; 55: ML 090307-08.

Merimbula Top Lake sediment samples									
Sample	**56**	**57**	**58**	**59**	**60**	**61**	**62**	**63**	**64**
SiO_2	63.53	89.98	84.34	88.51	89.54	78.37	84.45	89.92	92.73
Al_2O_3	11.69	3.73	6.26	5.83	3.65	7.82	5.9	3.99	3.23
CaO	2.1	0.99	0.37	0.27	0.81	0.98	0.37	0.33	0.18
MgO	2.04	0.59	0.84	0.56	0.54	1.26	0.9	0.6	0.39
MnO	0.02	0	0.01	0	0.01	0.01	0.01	0.01	0
Na_2O	4.9	1.31	1.9	1.59	1.35	2.95	2.25	1.48	0.83
K_2O	1.87	0.92	1.49	0.99	0.96	1.71	1.5	1.09	0.98
TiO_2	1.02	0.24	0.47	0.48	0.3	0.71	0.49	0.27	0.17
P_2O5	0.28	0.08	0.07	0.05	0.06	0.12	0.07	0.05	0.03
SO_3	6.91	0.85	1.82	0.56	1.49	2.77	1.86	0.81	0.24
Fe_2O_3	5.64	1.3	2.44	1.17	1.3	3.31	2.2	1.45	1.22
Cl	33264	9738	13827	11611	10092	20825	18686	11960	6914
Be	1.65	0.78	1.34	1.67	0.89	1.51	1.3	0.95	0.88
Sc	11.89	4.56	8.31	8.11	6.25	10.02	8.19	6.6	5.66
V	137.59	88.03	56.79	60.88	39.58	66.16	51.46	42.37	36.92
Cr	93.63	39.74	68.46	94.32	48.71	67.21	59.67	57.77	45.32
Ni	23.36	10.4	28.29	78.94	24.74	18.67	19.88	49.07	43.09
Cu	18.13	7.2	17.18	13.46	11.78	76.96	83.57	33.43	8.45
Zn	48.63	13.85	37.55	14.95	18.05	36.32	30.31	20.14	16.05
Ga	9.22	3.46	6.8	5.9	3.91	7.93	6.41	4.57	3.95
Ge	5.05	5.47	1.9	1.93	2	2.13	2.53	2.33	1.77
As	20.94	9.46	5.25	6.45	8.15	11.15	5.34	3.54	3.34
Rb	67.13	33.72	60.49	47.15	39.14	68.76	61.45	44.96	40.42
Sr	126.45	58.11	41.04	35.92	45.09	77.98	44.29	32.66	20.56
Y	23.7	9.5	21.62	24.36	13.45	27.6	20.18	13.59	9.95
Zr	183.96	69.98	202.06	214.97	147.01	252.88	194.94	112.78	73.14
Nb	9.42	3.55	7.47	7.34	5.16	9.96	7.77	4.93	3.3
Mo	6.41	1.96	4.12	14.02	4.78	3.38	2.35	1.66	1.03
Ag	0.32	0.32	0.35	0.36	0.32	0.24	0.26	0.43	0.56
Cd	0.3	0.07	0.29	0.29	0.42	0.16	0.4	0.36	0.37
In	0.05	0.01	0.05	0.04	0.03	0.03	0.03	0.02	0.04
Sn	2.26	1.22	2.22	1.41	1.15	1.44	1.62	1.18	1.08
Sb	0.98	0.72	3.85	3.83	3.37	2.84	3.39	3.44	3.64
Cs	4.71	1.83	2.97	2.95	1.92	3.88	3.24	2.3	1.71
Ba	193.77	121.92	161.38	113.5	112.92	184.86	160.27	127.83	119.88

Table A.3 (continued): Elemental geochemistry of Merimbula Top Lake sediment samples. Major and minor elements are expressed in weight %; trace elements are expressed in ppm; 56: ML 090307-09; 57: ML 090307-10; 58: 111107-15; 59: 161107-01; 60: 150408-01; 61: 150408-02; 62: 150408-03; 63: 150408-04; 64: 150408-05.

Merimbula Top Lake sediment samples									
Sample	**56**	**57**	**58**	**59**	**60**	**61**	**62**	**63**	**64**
La	28.54	12.15	24.03	30.51	16.46	34	24.93	17.08	12.65
Ce	54.27	22.7	46.14	57.58	31.58	64.05	46.35	31.26	22.97
Pr	5.99	2.41	4.97	5.74	3.35	6.93	4.95	3.33	2.38
Nd	27.24	10.98	21.76	25.26	14.61	31.06	22.21	14.89	10.58
Sm	5.17	1.85	3.98	4.73	2.73	5.75	3.76	2.33	1.66
Eu	1.05	0.39	0.72	0.91	0.51	1.09	0.8	0.47	0.26
Gd	5.28	2.08	4.18	5.05	2.85	5.88	3.97	2.46	1.86
Tb	0.79	0.31	0.65	0.75	0.4	0.84	0.6	0.38	0.23
Dy	4.89	2.03	3.99	4.29	2.75	5.37	4.08	2.79	2.03
Ho	0.86	0.35	0.69	0.8	0.45	0.98	0.71	0.45	0.34
Er	2.52	1.09	2.17	2.55	1.35	2.81	2.21	1.44	1.19
Tm	0.38	0.15	0.33	0.29	0.22	0.39	0.31	0.18	0.15
Yb	2.47	1.04	2.13	2.17	1.45	2.69	2.25	1.28	1.12
Lu	0.37	0.15	0.33	0.36	0.24	0.43	0.3	0.23	0.11
Hf	5.42	3.55	5.13	6.95	3.83	6.82	5	3.06	2.12
Ta	0.81	0.33	0.71	0.74	0.6	0.92	0.75	0.48	0.39
Tl	0.01	0.02	0.01	0	0.04	0	0.02	0	0
Pb	15.02	7.06	9.81	7.68	5.91	10.13	8.45	6.08	5.4
Bi	0.14	0.12	0.14	0.12	0.12	0.13	0.15	0.15	0.17
Th	9.71	3.79	7.91	7.42	5.29	10.32	7.87	5.39	4.06
U	3.29	1.28	2.7	21.31	2.04	2.68	1.99	1.35	1.02

Table A.3 (continued): Elemental geochemistry of Merimbula Top Lake sediment samples. Major and minor elements are expressed in weight %; trace elements are expressed in ppm; 56: ML 090307-09; 57: ML 090307-10; 58: 111107-15; 59: 161107-01; 60: 150408-01; 61: 150408-02; 62: 150408-03; 63: 150408-04; 64: 150408-05.

Merimbula Golf Lake sediment samples							
Sample	**65**	**66**	**67**	**68**	**69**	**70**	**71**
SiO_2	88.06	81.55	83.52	77.3	82.9	91.65	92.9
Al_2O_3	4.07	5.64	5.97	7.48	4.84	4.79	3.72
CaO	1.64	4.59	1.5	1.26	4.58	0.06	0.13
MgO	0.61	0.84	0.91	1.44	0.82	0.26	0.34
MnO	0	0.01	0.01	0.01	0	0	0
Na_2O	1.89	2.12	2.45	4.82	2.37	0.77	1.22
K_2O	1.11	1.27	1.32	1.51	1.13	0.36	0.41
TiO_2	0.21	0.3	0.38	0.45	0.28	0.29	0.25
P_2O5	0.09	0.12	0.13	0.17	0.12	0.02	0.05
SO_3	1.27	1.88	2	3.13	1.65	0.26	0.28
Fe_2O_3	1.04	1.67	1.82	2.42	1.31	1.52	0.71
Cl	13655	15134	17814	38495	18445	6511	10597
Be	0.76	0.87	1.04	0.94	0.85	0.6	0.52
Sc	4.2	5.34	5.9	6.64	4.55	5.13	4.33
V	65.16	71.85	73.06	79.78	69.27	82.52	73.12
Cr	33.45	48.85	65.77	74.78	44.09	45.66	32.39
Ni	8.71	10.61	12.21	32.78	9.86	9.99	8.97
Cu	10.23	120.5	12.29	26.69	14.38	10.29	5.78
Zn	13.39	17.23	18.12	29	16.18	8.89	9.38
Ga	3.87	5.21	5.71	6.69	4.32	5.08	3.84
Ge	4.66	4.32	4.56	4.32	4.48	4.47	5.26
As	10.86	11.02	12.26	16	12.8	9.29	1.75
Rb	38.7	46.61	49.57	54.3	39.73	19.52	17.64
Sr	69.36	148.49	75.53	80.24	141.92	11.62	18.72
Y	7.49	10.18	13.23	13.98	7.89	6.7	7.41
Zr	72.93	88.87	194.78	164.17	77.54	126.85	100.42
Nb	3.42	4.99	6.11	6.99	3.9	5.08	4.32
Mo	4.87	2.64	2.85	3.47	6.22	5.28	2.19
Ag	0.68	0.5	0.63	0.85	0.44	0.38	0.5
Cd	0.14	0.16	0.12	0.26	0.05	0.19	0.13
In	0.02	0.03	0.03	0.04	0.02	0.03	0.04
Sn	0.61	0.68	0.73	0.81	0.64	0.61	0.6
Sb	0.72	0.74	0.76	0.88	0.65	1.09	0.63
Cs	1.77	2.38	2.65	2.95	1.98	1.67	1.25
Ba	147.16	159.89	173.4	180.81	141.76	49.89	54.39

Table A.4: Elemental geochemistry of Merimbula Golf Lake sediment samples. Major and minor elements are expressed in weight %; trace elements are expressed in ppm. 65: GL 161006-01; 66: GL 161006-02; 67: GL 161006-03; 68: GL 161006-04; 69: GL 161006-05; 70: 08-19-10-05; 71: 13-19-10-05.

Merimbula Golf Lake sediment samples							
Sample	**65**	**66**	**67**	**68**	**69**	**70**	**71**
La	8.6	13.1	13.92	16.01	10.13	6.59	6.91
Ce	16.44	25	27.31	31.19	18.87	12.03	12.89
Pr	1.82	2.75	3.02	3.49	2.17	1.22	1.4
Nd	7.33	10.72	11.6	13.3	8.52	4.85	5.24
Sm	1.4	2.08	2.4	2.55	1.66	1.01	0.96
Eu	0.23	0.38	0.43	0.49	0.31	0.16	0.19
Gd	1.37	1.93	2.2	2.4	1.44	0.95	0.99
Tb	0.18	0.27	0.37	0.4	0.23	0.17	0.18
Dy	1.28	1.84	2.31	2.5	1.46	1.2	1.25
Ho	0.29	0.41	0.47	0.56	0.27	0.23	0.25
Er	0.8	1.11	1.45	1.65	0.92	0.75	0.84
Tm	0.12	0.16	0.21	0.23	0.12	0.11	0.13
Yb	0.78	1.15	1.62	1.61	0.87	0.86	0.87
Lu	0.13	0.17	0.24	0.22	0.15	0.12	0.13
Hf	3.21	3.22	5.71	5.42	3.34	4.47	3.72
Ta	0.35	0.44	0.57	0.64	0.36	0.47	0.49
Tl	0.04	0.02	0.03	0	0.02	0.04	0.01
Pb	9.21	10.36	11.47	17.57	8.89	6.31	6.57
Bi	0.11	0.1	0.12	0.17	0.1	0.17	0.12
Th	3.73	5.25	6.01	7.23	4.36	5.37	3.82
U	1.86	1.74	1.99	2.27	2.29	1.58	2.3

Table A.4 (continued): Elemental geochemistry of Merimbula Golf Lake sediment samples. Major and minor elements are expressed in weight %; trace elements are expressed in ppm. 65: GL 161006-01; 66: GL 161006-02; 67: GL 161006-03; 68: GL 161006-04; 69: GL 161006-05; 70: 08-19-10-05; 71: 13-19-10-05.

Merimbula Golf Lake sediment samples							
Sample	**72**	**73**	**74**	**75**	**76**	**77**	**78**
SiO_2	89.93	94.06	94.69	91.37	97.02	95.13	92.09
Al_2O_3	3.22	1.25	1.72	1.82	1.26	1.9	1.51
CaO	0.2	0.14	0.1	0.33	0.08	0.15	3.7
MgO	0.52	0.33	0.27	0.55	0.17	0.27	0.26
MnO	0	0	0	0	0	0	0
Na_2O	2.19	1.44	0.86	2.18	0.54	1.03	0.78
K_2O	0.51	0.59	0.46	0.5	0.42	0.87	0.4
TiO_2	0.19	0.08	0.17	0.15	0.12	0.08	0.17
P_2O5	0.14	0.02	0.02	0.09	0.02	0.03	0.02
SO_3	0.4	1.5	1.06	0.6	0.06	0.31	0.58
Fe_2O_3	2.69	0.59	0.64	2.41	0.31	0.22	0.48
Cl	18455	12052	7129	18162	3965	7130	5709
Be	0.63	0.4	0.71	0.79	0.55	0.46	0.61
Sc	3.73	2.13	3.04	2.77	2.62	2.53	2.8
V	74.19	55.83	65.38	69.39	63.73	57.45	64.19
Cr	30.78	20.24	36.09	34.99	30.71	20.24	37.88
Ni	9.52	6.02	8.32	8.56	7.48	6.75	6.99
Cu	9.96	11.06	11.07	5.57	6.51	5.28	74.77
Zn	7.92	11.39	11.63	6.74	5.8	9.06	7.31
Ga	3.36	1.08	1.95	1.79	1.44	1.67	1.72
Ge	4.46	5.06	5.8	4.31	4.91	5.12	6.06
As	10.18	11.11	8.52	18.62	3.57	1.72	5.23
Rb	17.69	16.4	17.87	13.25	14.05	24.95	14.63
Sr	28.85	20.49	16.04	33.03	12.9	23.03	134.49
Y	8.84	3.58	7.79	11.68	7.62	4.33	7.57
Zr	87.73	51.61	149.59	130.27	111.46	71.07	200.87
Nb	3.44	1.45	4.21	2.73	2.35	1.96	3.33
Mo	7.41	12.95	8.94	7.09	2.67	1.15	6.12
Ag	0.46	0.43	0.57	0.37	0.45	0.63	0.24
Cd	0.04	0.31	0.26	0.12	0.06	0.31	0.14
In	0.02	0.02	0.02	0.01	0.02	0.01	0.01
Sn	0.42	0.38	0.53	0.35	0.34	0.47	0.41
Sb	0.66	0.75	1.09	0.69	0.68	0.76	0.87
Cs	0.97	0.45	0.85	0.58	0.52	0.68	0.71
Ba	60.39	78.6	69.85	59.35	64.47	116.61	62.37

Table A.4 (continued): Elemental geochemistry of Merimbula Golf Lake sediment samples. Major and minor elements are expressed in weight %; trace elements are expressed in ppm. 72: 16-19-10-05; 73: 36-19-10-05; 74: 37-19-10-05; 75: 46-19-10-05; 76: 47-19-10-05; 77: 02-20-10-05; 78: 11-20-10-05.

Merimbula Golf Lake sediment samples							
Sample	**72**	**73**	**74**	**75**	**76**	**77**	**78**
La	14.07	4.46	11.06	20.27	7.89	4.82	9.29
Ce	23.63	7.84	18.49	33.82	17.62	8.54	17.15
Pr	2.28	0.86	1.95	3.08	1.85	0.91	1.99
Nd	8.42	3.02	7.88	10.96	7.18	3.77	7.38
Sm	1.41	0.64	1.45	1.72	1.15	0.59	1.51
Eu	0.24	0.11	0.25	0.32	0.21	0.16	0.21
Gd	1.54	0.5	1.3	1.68	1.28	0.72	1.24
Tb	0.22	0.09	0.2	0.25	0.2	0.12	0.21
Dy	1.4	0.61	1.26	1.59	1.3	0.72	1.34
Ho	0.29	0.11	0.28	0.34	0.28	0.17	0.28
Er	0.89	0.37	0.78	0.9	0.79	0.45	0.83
Tm	0.13	0.07	0.11	0.16	0.11	0.08	0.12
Yb	0.81	0.41	0.75	0.89	0.78	0.44	0.93
Lu	0.12	0.05	0.12	0.15	0.11	0.07	0.12
Hf	3.7	3.02	6.01	6.83	8.25	3.01	6.75
Ta	0.32	0.19	0.53	0.29	0.33	0.26	0.34
Tl	0.01	0.02	0.03	0.03	0.06	0.03	0.02
Pb	7.73	5.15	6.5	7.86	6.15	6.02	4.71
Bi	0.1	0.06	0.09	0.08	0.1	0.08	0.07
Th	3.21	1.34	2.58	2.46	1.95	1.65	2.96
U	3.49	4.22	2.27	2.6	3.24	2.25	1.78

Table A.4 (continued): Elemental geochemistry of Merimbula Golf Lake sediment samples. Major and minor elements are expressed in weight %; trace elements are expressed in ppm. 72: 16-19-10-05; 73: 36-19-10-05; 74: 37-19-10-05; 75: 46-19-10-05; 76: 47-19-10-05; 77: 02-20-10-05; 78: 11-20-10-05.

Merimbula Golf Lake sediment samples								
Sample	**79**	**80**	**81**	**82**	**83**	**84**	**85**	**86**
SiO_2	93.34	62.31	94.57	93.46	94.09	84.75	88.14	82.43
Al_2O_3	2.94	4.3	2.43	2.74	2.61	6.5	5.61	8.37
CaO	0.18	1.87	0.23	0.53	0.23	0.41	0.39	0.53
MgO	0.41	3.38	0.33	0.36	0.35	0.57	0.57	0.95
MnO	0	0	0	0	0	0.01	0.01	0.03
Na_2O	1.32	14.93	0.66	0.65	0.65	1.58	0.95	1.88
K_2O	0.75	1.26	0.75	0.78	0.78	1.79	1.55	1.88
TiO_2	0.19	0.25	0.15	0.18	0.16	0.37	0.36	0.52
P_2O5	0.05	0.47	0.03	0.02	0.02	0.07	0.09	0.14
SO_3	0.3	4.3	0.12	0.42	0.33	1.63	0.07	0.21
Fe_2O_3	0.51	6.92	0.73	0.84	0.77	2.31	2.27	3.06
Cl	10535	92043	5108	4640	4781	8939	5220	9798
Be	0.72	0.68	0.72	0.9	0.76	1.61	1.61	2.01
Sc	3.92	3.28	4.13	4.43	4.08	6.61	6.57	8.78
V	68.33	98.79	63.21	66.92	62.72	89.58	85.57	100.07
Cr	38.39	29.1	24.69	30.04	23.49	40.13	44.03	54.98
Ni	8.78	9.91	10.32	7.71	7.69	10.69	10.41	23.57
Cu	9.9	6.93	13.59	70.43	10.55	47.85	6.39	8.86
Zn	9.63	8.41	10.59	11.74	11.91	18.49	19.13	27.69
Ga	2.91	2.99	2.97	3.24	3.09	7.83	7.63	9.77
Ge	5.3	2.88	5	5.25	5.26	5.06	4.55	4.93
As	3.13	16.21	3.46	3.93	2.97	14.65	14.41	13.9
Rb	28.94	16.09	30.51	32.58	32.22	71.26	67.22	80.37
Sr	25.68	124.94	21.93	31.18	21.05	58.43	44.14	66.54
Y	8.64	14.21	9.32	11.27	10.02	24.52	24.07	29.35
Zr	134.42	70.78	74.12	114.88	89.47	198.8	179.13	208.71
Nb	3.54	2.75	2.85	3.34	2.77	9.32	9	11.73
Mo	1.27	6.44	2.09	1.54	2.18	6.13	1.29	3.21
Ag	0.29	0.59	0.39	0.29	0.2	0.37	0.34	0.43
Cd	0.15	0.05	0.02	0.02	0.01	0.09	0.03	0.03
In	0.02	0.01	0.01	0.02	0.02	0.04	0.05	0.07
Sn	0.48	0.14	0.45	0.53	0.47	0.73	0.8	0.95
Sb	0.74	0.41	0.64	0.85	0.8	1.29	1.47	1.53
Cs	1.43	0.81	1.24	1.41	1.38	3.08	2.98	4.09
Ba	100.12	52.85	100.07	103.29	102.57	186.55	146.96	190.55

Table A.4 (continued): Elemental geochemistry of Merimbula Golf Lake sediment samples. Major and minor elements are expressed in weight %; trace elements are expressed in ppm. 79: 27-20-10-05; 80: 29-20-10-05; 81: 2-22-10-05; 82: 3-22-10-05; 83: 5-22-10-05; 84: 10-22-10-05; 85: 24-22-10-05; 86: 25-22-10-05.

Merimbula Golf Lake sediment samples								
Sample	**79**	**80**	**81**	**82**	**83**	**84**	**85**	**86**
La	10.87	25.33	11.37	13.53	12.14	23.44	22.7	30.16
Ce	21.07	44.79	21.8	25.96	23.21	43.49	44.67	54.67
Pr	2.37	4.88	2.38	2.92	2.58	5.33	5.21	6.81
Nd	9.11	18.92	8.86	11.38	10.14	20.59	20.08	26.22
Sm	1.88	3.23	1.59	2.26	1.91	4.29	4.02	5.29
Eu	0.29	0.62	0.28	0.36	0.32	0.6	0.64	0.81
Gd	1.6	2.93	1.65	2.02	1.81	3.99	3.98	5.2
Tb	0.25	0.4	0.25	0.32	0.26	0.65	0.62	0.81
Dy	1.46	2.45	1.62	1.9	1.69	4.3	4.31	5.25
Ho	0.32	0.47	0.31	0.4	0.35	0.89	0.87	1.08
Er	1	1.33	0.95	1.2	0.97	2.75	2.7	3.2
Tm	0.14	0.18	0.14	0.17	0.13	0.4	0.39	0.48
Yb	0.97	1.21	0.87	1.14	1.03	2.73	2.83	3.17
Lu	0.13	0.18	0.13	0.18	0.16	0.41	0.41	0.46
Hf	4.27	3.01	4.03	5.17	4.79	7.08	6.22	6.79
Ta	0.36	0.28	0.34	0.38	0.31	0.93	0.93	1.09
Tl	0.04	0.01	0.06	0.06	0.04	0.03	0.05	0.03
Pb	7.54	9.64	6.34	5.68	5.4	9.02	8.52	11.06
Bi	0.08	0.04	0.1	0.09	0.07	0.13	0.16	0.25
Th	3.33	2.9	3.68	4.02	3.83	9.64	9.21	11.6
U	1.16	6.44	0.71	1.39	1.15	3.88	2.32	3.87

Table A.4 (continued): Elemental geochemistry of Merimbula Golf Lake sediment samples. Major and minor elements are expressed in weight %; trace elements are expressed in ppm. 79: 27-20-10-05; 80: 29-20-10-05; 81: 2-22-10-05; 82: 3-22-10-05; 83: 5-22-10-05; 84: 10-22-10-05; 85: 24-22-10-05; 86: 25-22-10-05.

Merimbula Back Lagoon sediment samples							
Sample	**87**	**88**	**89**	**90**	**91**	**92**	**93**
SiO_2	80.74	85.78	91.88	98.45	98.56	93.78	97.06
Al_2O_3	8.27	6.78	4.35	0.44	0.46	3.16	1.39
CaO	0.45	0.36	0.13	0.29	0.27	0.12	0.04
MgO	0.91	0.59	0.42	0.11	0.09	0.32	0.15
MnO	0.01	0.01	0	0.00	0.00	0	0
Na_2O	1.76	1.17	0.69	0.27	0.16	0.6	0.39
K_2O	1.95	1.7	1.17	0.25	0.24	0.87	0.52
TiO_2	0.42	0.3	0.27	0.02	0.03	0.2	0.07
P_2O5	0.11	0.06	0.03	0.01	0.01	0.03	0.01
SO_3	2.69	1.35	0.26	0.00	0.00	0.15	0.11
Fe_2O_3	2.68	1.89	0.79	0.15	0.17	0.77	0.26
Cl	10196	5079	3873	1874	761	3497	2450
Be	1.52	1.34	1.16	0.29	0.3	0.87	0.45
Sc	7.48	6.31	5.51	1.56	1.75	4.07	2.47
V	78.03	71.3	102.25	75.07	76.84	87.71	77.88
Cr	48.29	44.44	35.27	15.41	13.51	29.63	21.47
Ni	12.83	11.86	8.66	8.51	12.51	18.92	13.26
Cu	24.86	15.52	5.54	3.23	77.35	11.59	5.17
Zn	48.62	31.95	13.89	2.04	2.14	11.12	4.2
Ga	8.49	7.06	4.93	0.42	0.43	3.3	1.54
Ge	4.64	4.7	6.09	6.08	5.82	6.76	6.01
As	5.01	5.07	2.7	3.43	5.65	2.76	1.69
Rb	78.75	70.89	51.75	7.57	7.52	35.57	19.86
Sr	63.93	52.29	27.75	16.15	15.04	19.95	9.35
Y	22.83	17.46	16.58	1.7	1.71	11.15	4.59
Zr	177.77	149.9	164.15	14.5	15.27	121.39	51.45
Nb	7.64	5.91	5.77	0.43	0.43	3.97	1.69
Mo	4.34	2.81	1.07	1.04	0.88	1.49	1.61
Ag	0.5	0.6	0.25	0.31	0.8	0.34	0.39
Cd	0.22	0.18	0	0.03	0.03	0.02	0.04
In	0.04	0.03	0.02	0	0	0.01	0.01
Sn	0.85	0.87	1.6	0.66	0.69	1.31	0.81
Sb	0.87	0.84	0.89	0.59	0.73	0.66	0.66
Cs	4.45	3.44	2.77	0.29	0.23	1.9	0.77
Ba	262.4	229.55	165.7	37.41	37.79	118.19	71.24

Table A.5: Elemental geochemistry of Merimbula Back Lagoon sediment samples. Major and minor elements are expressed in weight %; trace elements are expressed in ppm. 87: BL 181006-01; 88: BL 181006-02; 89: BL Short Point; 90: BL 070307-01; 91: BL 070307-02; 92: BL 070307-03; 93: BL 070307-04.

Merimbula Back Lagoon sediment samples							
Sample	**87**	**88**	**89**	**90**	**91**	**92**	**93**
La	29.43	22.93	22.66	2.11	1.78	15.3	6.03
Ce	58.26	44.66	41.46	2.98	2.8	27.91	10.87
Pr	6.56	5	4.38	0.32	0.3	2.95	1.11
Nd	25.31	19.22	19.12	1.33	1.22	12.82	4.67
Sm	4.87	3.81	3.25	0.28	0.18	2.17	0.85
Eu	0.88	0.72	0.54	0.01	0.05	0.35	0.14
Gd	4.31	3.42	3.48	0.26	0.27	2.22	0.85
Tb	0.64	0.49	0.51	0.03	0.06	0.33	0.14
Dy	4.03	2.99	3.3	0.28	0.32	2.27	0.71
Ho	0.82	0.63	0.58	0.07	0.05	0.38	0.17
Er	2.36	1.94	1.71	0.16	0.16	1.14	0.46
Tm	0.35	0.27	0.27	0.02	0.02	0.18	0.08
Yb	2.21	1.78	1.73	0.2	0.14	1.12	0.55
Lu	0.35	0.28	0.27	0.02	0.03	0.17	0.07
Hf	5.6	5.49	6.87	4.6	3.69	5.68	4.72
Ta	0.72	0.64	0.53	0.08	0.05	0.41	0.25
Tl	0.05	0.07	0.04	0.01	0.03	0.02	0.02
Pb	24.71	14.88	8.44	2.19	2.67	6.33	3.34
Bi	0.18	0.15	0.11	0.04	0.04	0.09	0.08
Th	9.99	7.46	6.76	0.74	0.64	4.98	2
U	3.18	2.07	1.94	0.15	0.17	1.21	0.55

Table A.5 (continued): Elemental geochemistry of Merimbula Back Lagoon sediment samples. Major and minor elements are expressed in weight %; trace elements are expressed in ppm. 87: BL 181006-01; 88: BL 181006-02; 89: BL Short Point; 90: BL 070307-01; 91: BL 070307-02; 92: BL 070307-03; 93: BL 070307-04.

Merimbula Back Lagoon sediment samples							
Sample	**94**	**95**	**96**	**97**	**98**	**99**	**100**
SiO_2	88.46	67.62	70.76	92.87	86.53	88.99	84.6
Al_2O_3	5.25	13.92	13.88	3.97	6.84	5.45	7.48
CaO	0.3	0.41	0.49	0.09	0.16	0.24	0.29
MgO	0.61	2.17	1.54	0.32	0.7	0.5	0.71
MnO	0	0.01	0.01	0	0	0	0.01
Na_2O	1.14	6.34	4.34	0.58	1.79	1.42	1.06
K_2O	1.33	2.97	2.93	1.19	1.9	1.74	2.07
TiO_2	0.31	0.78	0.74	0.18	0.4	0.3	0.48
P_2O5	0.07	0.13	0.15	0.03	0.04	0.04	0.05
SO_3	0.57	2.72	1.82	0.17	0.3	0.16	0.89
Fe_2O_3	1.96	2.93	3.33	0.6	1.34	1.16	2.35
Cl	8043	50755	31812	3278	13696	9895	4696
Be	1.25	2.1	2.21	1.1	1.32	1.12	1.53
Sc	5.72	11.27	11.22	4.29	6.88	5.51	7.47
V	99.77	127.28	124.62	88.27	104.58	90.15	99.32
Cr	37.13	66.31	67.21	27.49	50.41	47.59	55.81
Ni	14.96	16.66	17.56	8.26	9.76	11.87	11.34
Cu	7.34	14.74	14.92	6.34	7.41	8.05	7.09
Zn	21.07	29.65	34.07	10.35	19.48	14.77	23.21
Ga	5.41	12.07	11.93	4	6.79	5.45	7.39
Ge	5.8	5.8	5.89	5.88	5.81	5.61	5.54
As	8.2	5.12	5.52	1.66	3.36	3.65	7.31
Rb	54.58	106.71	108.57	48.48	74.1	64.06	79.67
Sr	45.33	64.51	68.1	23.06	37.34	33.31	46.82
Y	17.38	33.84	33.12	12.95	23.16	16.9	25.49
Zr	143.87	228.35	223.44	89.16	245.37	210.53	294.18
Nb	5.74	12.42	12.18	3.5	7.83	6.26	9.25
Mo	2.29	5.34	6.51	1.49	1.59	1.37	1.79
Ag	0.48	0.47	0.58	0.39	0.38	0.28	0.29
Cd	0	0.02	0.03	0.01	0	0.01	0.03
In	0.03	0.05	0.05	0.02	0.03	0.02	0.03
Sn	1.85	3.37	3.02	1.46	2.08	1.78	2.26
Sb	0.83	0.96	0.8	0.61	0.87	0.74	0.92
Cs	3.11	6.61	6.66	2.37	3.86	2.95	4.29
Ba	178.18	307.85	311.21	162.24	241.32	216.82	255.03

Table A.5 (continued): Elemental geochemistry of Merimbula Back Lagoon sediment samples. Major and minor elements are expressed in weight %; trace elements are expressed in ppm. 94: BL 070307-05; 95: BL 070307-06; 96: BL 070307-07; 97: BL 070307-08; 98: BL 070307-10; 99: 070307-11; 100: BL 070307-12.

Merimbula Back Lagoon sediment samples							
Sample	**94**	**95**	**96**	**97**	**98**	**99**	**100**
La	25.07	47.93	46.96	17.16	30.49	23.84	35.47
Ce	45.19	89.28	87.17	30.36	56.12	43.55	65.03
Pr	4.84	9.65	9.45	3.14	6	4.59	6.91
Nd	20.95	42.1	41.52	13.28	26.05	19.63	30.21
Sm	3.65	7.56	6.96	2.3	4.56	3.31	5.25
Eu	0.68	1.36	1.31	0.41	0.83	0.57	0.91
Gd	3.8	7.44	7.28	2.56	4.43	3.23	5.42
Tb	0.57	1.06	1.03	0.4	0.71	0.51	0.8
Dy	3.49	6.44	6.61	2.52	4.43	3.06	5.07
Ho	0.65	1.24	1.2	0.41	0.86	0.59	0.89
Er	1.86	3.37	3.35	1.34	2.42	1.68	2.75
Tm	0.29	0.5	0.53	0.21	0.36	0.27	0.39
Yb	1.81	3.41	3.26	1.24	2.45	1.85	2.83
Lu	0.27	0.51	0.48	0.18	0.35	0.27	0.4
Hf	5.6	6.26	6.58	4.87	7.85	8.46	9.91
Ta	0.56	1.18	1.12	0.35	0.76	0.66	0.9
Tl	0.05	0.01	0.01	0.08	0.02	0.02	0.04
Pb	11.51	20.48	20.92	6.92	11.71	8.66	11.49
Bi	0.12	0.21	0.22	0.09	0.13	0.04	0.15
Th	7.48	15.84	15.78	4.96	9.37	7.48	10.59
U	1.63	5.07	5.26	1.81	2.51	1.72	2.44

Table A.5 (continued): Elemental geochemistry of Merimbula Back Lagoon sediment samples. Major and minor elements are expressed in weight %; trace elements are expressed in ppm. 94: BL 070307-05; 95: BL 070307-06; 96: BL 070307-07; 97: BL 070307-08; 98: BL 070307-10; 99: 070307-11; 100: BL 070307-12.

Pambula Lake sediment samples							
Sample	**101**	**102**	**103**	**104**	**105**	**106**	**107**
SiO_2	99.07	60.36	80.95	70.51	97.46	69.06	83.03
Al_2O_3	0.37	2.89	1.7	14.28	1.24	13.3	7.2
CaO	0.14	29.5	14.05	0.83	0.13	4.06	1.8
MgO	0.05	2.02	0.77	1.71	0.11	1.57	0.87
MnO	0	0.01	0	0.02	0	0.02	0.01
Na_2O	0.09	2.01	0.96	2.97	0.28	3.04	1.74
K_2O	0.13	0.83	0.68	2.24	0.23	2.25	1.24
TiO_2	0.03	0.2	0.07	1.01	0.04	1.04	0.63
P_2O5	0.01	0.12	0.06	0.19	0.03	0.17	0.1
SO_3	0	1.12	0.34	0.72	0.01	0.56	0.61
Fe_2O_3	0.12	0.96	0.42	5.52	0.46	4.93	2.77
Cl	617	11171	5576	15765	2520	15071	10133
Be	0.63	0.78	0.57	2.76	0.79	2.56	1.6
Sc	2.94	3.29	2.87	14.11	3.46	13.25	8.93
V	78.07	82.2	79.75	146.09	71.76	138.02	110.91
Cr	21.23	34.56	22.01	95.65	13.21	94.52	63.86
Ni	20.51	7.75	6.66	28.58	7.01	27.76	14.86
Cu	21.49	7.97	8.43	20.34	10.78	191.61	29.4
Zn	3.25	8.75	7.03	52.83	4.96	46.68	66.01
Ga	0.64	2.84	1.93	14.81	2.05	13.57	8.1
Ge	5.13	6.52	5.23	6.65	6.5	7.27	7.01
As	0.92	3.25	2.89	12.58	5.04	11.48	10.17
Rb	4.54	22.46	22.91	97.13	12.54	92.91	53.78
Sr	8.71	1,223.88	591.53	84.58	7.86	229.17	104.54
Y	2.18	12.62	6.11	38.34	10.13	35.84	25.49
Zr	16.34	94.58	39.96	262.81	65.2	288.52	270.02
Nb	0.76	3.12	1.72	18.38	3.44	18.9	12.23
Mo	0.8	3.84	1.05	1.93	1.05	1.47	1.48
Ag	0.61	0.5	0.78	0.65	1.07	0.53	0.78
Cd	0.07	0.17	0.18	0.02	0	0.06	0
In	0.01	0.04	0.01	0.07	0.04	0.05	0.05
Sn	0.72	1.05	0.81	3.65	1.78	3.64	3.2
Sb	0.08	0.38	0.62	1.34	0.79	1.26	1.16
Cs	0.28	0.96	0.62	6.3	0.77	5.72	3.4
Ba	21.94	97.45	85.73	226.93	18.46	244.18	151.35

Table A.6: Elemental geochemistry of Pambula Lake sediment samples. Major and minor elements are expressed in weight %; trace elements are expressed in ppm. 101: PR 120406-01; 102: PR 120406-02; 103: PR 120406-03; 104: PR 120406-04; 105: PR 120406-05; 106: PR 120406-06; 107: PR 120406-07.

Pambula Lake sediment samples							
Sample	**101**	**102**	**103**	**104**	**105**	**106**	**107**
La	2.07	15.74	7.77	47.53	5.26	44.81	30.3
Ce	3.78	28.82	14.79	96.66	10.88	86.68	60.63
Pr	0.37	3.56	1.82	11.27	1.14	10.33	7.13
Nd	1.43	14.26	7.22	43.57	4.55	40.88	27.15
Sm	0.24	2.83	1.38	8.72	0.97	8.47	5.66
Eu	0.07	0.49	0.22	1.37	0.08	1.32	0.91
Gd	0.29	2.68	1.32	7.97	1.07	7.08	4.9
Tb	0.06	0.37	0.23	1.19	0.22	1.11	0.76
Dy	0.4	2.28	1.22	7.37	1.74	7.03	5.03
Ho	0.08	0.39	0.2	1.43	0.37	1.39	0.96
Er	0.23	1.26	0.68	4.14	1.16	3.92	2.87
Tm	0.02	0.16	0.12	0.61	0.16	0.59	0.43
Yb	0.2	1.25	0.53	4.06	1.37	3.95	2.89
Lu	0.05	0.18	0.09	0.58	0.19	0.55	0.42
Hf	6.01	3.15	4.85	7.03	6.16	7.63	8.07
Ta	0.13	0.26	0.17	1.51	0.35	1.55	1.04
Tl	0.12	0.02	0.03	0.01	0.07	0.05	0.06
Pb	2.68	4.98	5.44	17.64	3.95	16.52	16.17
Bi	0.07	0.11	0.1	0.3	0.11	0.24	0.14
Th	0.78	4.08	1.91	17.01	4.03	15.6	10.67
U	0.27	1.94	0.69	3.92	1.16	3.47	2.6

Table A.6 (continued): Elemental geochemistry of Pambula Lake sediment samples. Major and minor elements are expressed in weight %; trace elements are expressed in ppm. 101: PR 120406-01; 102: PR 120406-02; 103: PR 120406-03; 104: PR 120406-04; 105: PR 120406-05; 106: PR 120406-06; 107: PR 120406-07.

Pambula Lake sediment samples							
Sample	**108**	**109**	**110**	**111**	**112**	**113**	**114**
SiO_2	77.49	86.77	74.79	89.58	87.28	84.98	83.9
Al_2O_3	9.33	6.36	4.16	5.39	6.25	7.63	7.13
CaO	3.16	0.43	15.22	0.27	0.38	0.55	0.38
MgO	1.08	0.62	1.04	0.42	0.57	0.4	0.82
MnO	0.02	0.01	0.01	0.01	0.01	0.01	0.01
Na_2O	2.35	1.06	1.46	0.85	1.06	1.65	1.42
K_2O	1.73	1.69	1.35	1.59	1.6	2.83	1.36
TiO_2	0.9	0.44	0.23	0.25	0.5	0.24	0.55
P_2O5	0.12	0.08	0.09	0.04	0.06	0.05	0.11
SO_3	0.47	0.12	0.38	0.1	0.29	0.1	1.23
Fe_2O_3	3.38	2.41	1.27	1.5	1.99	1.57	3.11
Cl	10586	4883	7537	6167	5139	5556	9091
Be	2.13	1.86	0.95	1.48	1.95	1.4	1.65
Sc	10.87	7.29	4.08	5.65	7.25	5.59	8.99
V	119.12	102.89	84.75	92.82	100.71	92.87	66.7
Cr	75.64	43.27	29.12	26.52	45.49	28.03	65.51
Ni	16.1	10.51	9.03	8.07	10.95	7.85	22.19
Cu	21.67	11.15	9.82	9.69	10.66	16.1	15.84
Zn	40.51	21.87	10.93	16.25	20.54	13.8	35.92
Ga	9.8	7.67	4.01	7.11	7.84	6.31	8.04
Ge	7.21	6.91	6	5.38	6.91	6.93	2.33
As	9.12	11.76	6.69	6.92	9.02	6.83	14.57
Rb	69.42	69.94	37.45	67.8	67.86	83.66	64.11
Sr	179.66	48.46	673.82	34.17	47.25	96.5	49.21
Y	31.98	24.88	12.93	20.83	28.24	11.89	26.29
Zr	411.72	192.87	99.38	124.01	255.65	88.85	232.62
Nb	16.46	10.22	4.5	8.04	11.18	6.65	11.21
Mo	1.21	1.15	0.84	1.17	1.35	1.06	2.55
Ag	0.42	0.38	0.49	0.58	0.66	0.58	0.39
Cd	0.02	0	0	0.1	0	0	0.16
In	0.06	0.05	0.01	0.04	0.04	0.04	0.05
Sn	3.22	2.65	1.54	2.89	2.8	1.64	2.51
Sb	1.06	1.19	0.75	1.2	1.34	0.76	3.99
Cs	3.93	3.12	1.25	2.98	3.32	2.31	3.94
Ba	208.55	166.24	158.15	135.52	154.08	362.79	158.27

Table A.6 (continued): Elemental geochemistry of Pambula Lake sediment samples. Major and minor elements are expressed in weight %; trace elements are expressed in ppm. 108: PR 120406-08; 109: PR 120406-09; 110: PR 120406-10; 111: PR 120406-11; 112: PR 120406-12; 113: PR 120406-13; 114: P141107-03.

Pambula Lake sediment samples							
Sample	**108**	**109**	**110**	**111**	**112**	**113**	**114**
La	36.7	24.93	18.03	18.35	27.01	14.23	32.18
Ce	70.9	48.07	32.13	33.96	51.22	25.08	61.28
Pr	8.33	5.71	4.24	4	6.18	3.03	6.67
Nd	33.02	22.32	16.13	15.13	23.61	11.71	29.89
Sm	6.34	4.85	2.96	3.34	4.73	2.2	5.5
Eu	1.03	0.62	0.54	0.45	0.69	0.51	0.89
Gd	5.91	4.14	2.9	3.08	4.74	2.15	5.46
Tb	0.91	0.67	0.39	0.57	0.71	0.3	0.84
Dy	5.88	4.51	2.34	3.54	4.99	2.23	5.37
Ho	1.16	0.96	0.49	0.72	1.08	0.4	1.04
Er	3.45	2.72	1.41	2.4	2.9	1.28	2.77
Tm	0.52	0.41	0.19	0.39	0.48	0.19	0.46
Yb	3.67	2.77	1.26	2.44	3.28	1.19	2.71
Lu	0.53	0.4	0.17	0.37	0.49	0.22	0.38
Hf	11.6	7.82	4.13	5.29	8.06	4.42	8.46
Ta	1.42	0.98	0.39	0.78	1.03	0.77	1.08
Tl	0.01	0.04	0	0.05	0.07	0.03	0.01
Pb	13.34	8.56	7.84	7.25	8.56	8.43	12.51
Bi	0.16	0.11	0.08	0.12	0.14	0.14	0.15
Th	13.25	9.47	4.6	8.19	9.85	6.21	10.45
U	3.02	2.27	1.17	2.02	2.74	1.45	2.6

Table A.6 (continued): Elemental geochemistry of Pambula Lake sediment samples. Major and minor elements are expressed in weight %; trace elements are expressed in ppm. 108: PR 120406-08; 109: PR 120406-09; 110: PR 120406-10; 111: PR 120406-11; 112: PR 120406-12; 113: PR 120406-13; 114: P141107-03.

Sample	Core 1 - 0cm	Core 1 - 20cm	Core 1 - 30cm	Core 1 - 59cm	Core 2 - 0cm	Core 2 - 40cm	Core 2 - 68cm
SiO_2	94.65	94.64	73.17	91.11	86.53	80.01	74.71
Al_2O_3	2.71	1.85	1.32	2.11	5.03	9.68	13.05
CaO	0.34	1.46	23.69	4.31	1.43	0.89	0.48
MgO	0.14	0.13	0.18	0.22	0.61	0.56	0.70
MnO	0.00	0.00	0.00	0.00	0.01	0.02	0.02
Na_2O	0.55	0.46	0.71	0.66	1.81	1.48	1.35
K_2O	1.10	0.80	0.67	1.00	1.10	1.54	1.65
TiO_2	0.06	0.07	0.04	0.07	0.52	1.50	1.22
P_2O5	0.02	0.02	0.02	0.02	0.05	0.07	0.04
SO_3	0.02	0.20	0.03	0.21	0.90	0.41	0.07
Fe_2O_3	0.42	0.35	0.17	0.30	2.00	3.84	6.72
Cl	732	1742	2627	3411	11583	5005	5191
Be	0.67	0.45	0.30	0.42	0.80	1.60	2.96
Sc	4.52	4.02	2.20	3.45	9.26	15.51	20.57
V	23.84	24.04	19.14	20.25	59.43	110.93	138.22
Cr	15.69	20.98	13.95	20.61	49.79	92.68	109.38
Ni	7.32	13.96	12.59	17.40	13.39	18.25	35.42
Cu	18.84	7.87	4.06	49.35	8.88	41.78	46.31
Zn	11.33	11.25	3.81	4.05	17.45	18.70	28.64
Ga	3.28	1.82	1.19	1.74	5.39	10.50	15.12
Ge	2.29	1.41	1.59	1.83	1.99	2.28	2.96
As	2.56	3.18	1.09	4.96	4.56	3.76	6.93
Rb	41.01	28.30	17.76	28.45	39.12	90.88	89.89
Sr	32.45	49.87	643.16	119.76	99.10	96.00	67.50
Y	6.77	4.50	2.31	3.63	14.76	31.34	53.13
Zr	43.56	56.29	29.66	30.30	204.02	345.43	234.63
Nb	2.71	1.78	0.74	1.23	5.89	16.66	11.77
Mo	1.01	2.23	0.62	1.42	5.45	1.44	1.50
Ag	0.21	0.40	0.28	0.17	0.35	0.14	0.18
Cd	0.02	0.18	0.43	0.07	0.18	0.11	0
In	0.02	0.00	0.02	0.00	0.03	0.06	0.07
Sn	1.46	1.07	0.41	0.65	1.28	2.53	2.60
Sb	3.84	3.45	3.33	3.17	3.84	4.39	4.03
Cs	1.12	0.76	0.42	0.72	2.05	5.19	6.81
Ba	153.78	113.85	83.89	118.68	140.32	214.19	399.76

Table A.7: Elemental geochemistry of cores 1 and 2. Major and minor oxides are expressed in weight %; trace elements are expressed in ppm.

Sample	Core 1 - 0cm	Core 1 - 20cm	Core 1 - 30cm	Core 1 - 59cm	Core 2 - 0cm	Core 2 - 40cm	Core 2 - 68cm
La	6.07	4.76	3.36	3.62	15.62	38.52	52.26
Ce	11.67	8.42	5.81	6.71	29.06	71.96	94.28
Pr	1.19	0.86	0.65	0.74	3.09	7.51	11.64
Nd	5.49	3.74	2.82	3.28	13.73	33.82	53.32
Sm	0.90	0.77	0.40	0.58	3.01	6.30	10.40
Eu	0.12	0.12	0.09	0.18	0.62	1.26	2.30
Gd	0.97	0.66	0.42	0.52	2.97	5.72	11.73
Tb	0.13	0.13	0.09	0.08	0.42	1.00	1.70
Dy	1.22	0.74	0.40	0.78	2.77	5.99	10.57
Ho	0.27	0.17	0.06	0.12	0.58	1.10	1.86
Er	0.67	0.40	0.24	0.35	1.53	3.38	5.27
Tm	0.14	0.06	0.03	0.04	0.22	0.51	0.81
Yb	0.70	0.47	0.24	0.36	1.74	3.46	4.66
Lu	0.16	0.04	0.06	0.06	0.26	0.56	0.66
Hf	5.86	6.50	1.47	3.88	12.98	9.52	6.42
Ta	0.29	0.19	0.06	0.14	0.57	1.40	1.08
Tl	0.10	0.05	0.03	0.02	0.01	0.07	0.07
Pb	9.93	9.66	3.52	3.49	12.30	12.60	14.14
Bi	0.10	0.11	0.08	0.04	0.06	0.16	0.13
Th	3.03	1.81	0.85	1.35	5.11	14.30	10.49
U	0.86	0.93	0.50	1.20	4.19	6.94	2.58

Table A.7 (continued): Elemental geochemistry of cores 1 and 2. Major and minor oxides are expressed in weight %; trace elements are expressed in ppm.

Sample	1H – 3cm	1H - 43cm	1H - 63cm	1H - 70cm	2H – 3cm	2H - 30cm	2H - 45cm
SiO_2	94.48	90.54	85.37	83.43	94.82	90.49	85.27
Al_2O_3	1.49	1.68	1.87	1.84	1.36	1.91	1.70
CaO	2.02	5.06	9.21	11.58	1.88	4.19	9.77
MgO	0.20	0.31	0.59	0.58	0.16	0.31	0.31
MnO	0.00	0.00	0.00	0.00	0.00	0.00	0.00
Na_2O	0.57	0.73	0.95	1.06	0.66	1.02	0.96
K_2O	0.75	0.71	0.85	0.84	0.76	0.86	0.76
TiO_2	0.06	0.10	0.11	0.09	0.04	0.08	0.06
P_2O5	0.03	0.02	0.03	0.03	0.02	0.03	0.03
SO_3	0.16	0.46	0.59	0.26	0.16	0.68	0.71
Fe_2O_3	0.23	0.38	0.43	0.29	0.15	0.43	0.43
Sc	4.48	4.49	3.42	5.93	3.89	5.15	4.28
V	30.11	30.26	47.95	28.43	19.41	42.57	42.25
Cr	27.79	21.33	30.69	20.87	12.68	24.19	20.09
Ni	15.99	9.88	10.34	7.43	8.91	15.91	11.60
Cu	8.36	644.43	8.67	1.97	24.21	9.49	4.48
Zn	21.29	14.55	14.90	13.37	13.62	6.47	10.26
Ga	0	0	0	0	0	0	2.16
Ge	1.44	0	4.96	3.40	1.96	5.26	2.45
As	3.90	5.51	6.85	2.09	2.63	10.52	10.47
Rb	27.08	28.84	26.80	21.77	21.25	23.61	22.91
Sr	98.46	202.88	415.80	474.62	68.36	159.99	285.60
Y	3.69	4.89	4.83	4.76	1.81	4.38	3.49
Zr	35.65	63.34	52.27	56.35	19.68	64.06	49.92
Nb	1.73	1.98	1.60	1.72	0.57	1.54	1.03
Mo	2.91	2.43	2.64	1.26	2.34	7.21	5.50
Ag	0.74	0.34	1.28	0.56	0.05	1.12	0.91
Cd	1.42	0.87	3.89	0	1.67	1.99	2.49
In	0.26	0.08	-0.08	0.04	0.25	0.04	0.10
Sn	2.39	2.07	2.35	1.78	1.23	1.57	3.02
Sb	1.41	0.95	1.13	0	0.10	0.95	0.84
Cs	0.26	0.50	-0.01	0.30	0.39	0.64	0.53
Ba	110.34	101.20	122.46	121.68	85.62	119.76	99.15

Table A.8: Elemental geochemistry of cores 1H and 2H. Major and minor oxides are expressed in weight %; trace elements are expressed in ppm.

Sample	1H – 3cm	1H - 43cm	1H - 63cm	1H - 70cm	2H – 3cm	2H - 30cm	2H - 45cm
La	3.97	5.28	5.35	6.19	2.40	5.34	3.36
Ce	7.83	11.59	10.59	12.31	3.34	10.78	8.46
Pr	0.73	1.11	1.09	1.69	0.35	1.40	1.22
Nd	3.36	4.48	4.40	4.75	1.26	5.19	3.45
Sm	0	0	1.88	0.55	0.13	0.47	0.00
Eu	0.21	0.13	0.09	0.11	0.12	0.21	0.29
Gd	0.44	0.69	1.64	1.07	0.01	0.81	0.14
Tb	0.12	0.19	0.15	0.07	0.04	0.11	0
Dy	0.61	0.94	0.42	0.71	0.12	0.74	0.33
Ho	0.10	0.20	0.13	0.10	0.08	0.10	0.16
Er	0.42	0.38	0.26	0.29	0.46	0.14	0.39
Tm	0.16	0.06	0.07	0.07	0	0.01	0
Yb	0.53	0	1.39	0.49	0.18	0.54	0.34
Lu	0	0.14	0.00	0.13	0.02	0.09	0.04
Hf	0.78	1.87	1.49	1.36	0.55	2.34	2.29
Ta	0.30	0.09	0.05	0.22	0.18	0.16	0.09
Tl	0.31	0.14	0.25	0.12	0.12	0.27	0.33
Pb	21.36	8.50	9.08	7.47	10.38	7.10	9.13
Bi	0.83	0.03	0.81	0.59	0.27	0.63	0.89
Th	1.41	1.98	1.42	1.67	0.50	1.81	1.34
U	0.81	1.02	0.87	1.00	0.44	1.75	2.12

Table A.8 (continued): Elemental geochemistry of cores 1H and 2H. Major and minor oxides are expressed in weight %; trace elements are expressed in ppm.

Sample	3H - 17cm	3H - 41cm	3H - 69cm	4H - 3cm	4H - 28cm	4H - 53cm	4H - 69cm
SiO_2	96.78	96.55	96.40	95.42	89.49	89.18	91.04
Al_2O_3	1.50	1.51	1.51	1.36	1.52	1.73	1.56
CaO	0.15	0.35	0.17	1.57	6.75	6.12	4.80
MgO	0.11	0.13	0.15	0.17	0.29	0.38	0.35
MnO	0.00	0.00	0.00	0.00	0.00	0.00	0.00
Na_2O	0.42	0.40	0.66	0.43	0.61	0.75	0.74
K_2O	0.79	0.79	0.80	0.69	0.68	0.81	0.78
TiO_2	0.03	0.03	0.03	0.05	0.07	0.07	0.05
P_2O5	0.01	0.01	0.01	0.02	0.02	0.02	0.02
SO_3	0.05	0.08	0.10	0.11	0.27	0.55	0.36
Fe_2O_3	0.13	0.14	0.16	0.17	0.28	0.39	0.29
Sc	0.92	3.21	2.19	5.11	4.42	4.40	5.49
V	6.43	17.45	15.28	29.88	28.48	29.31	30.59
Cr	4.93	13.19	17.97	37.96	19.68	17.34	35.76
Ni	26.36	0.02	6.96	27.40	24.74	1.49	6.08
Cu	1.89	0	0	11.61	348.63	4.44	12.46
Zn	3.39	12.53	9.53	23.33	22.41	11.88	15.60
Ga	0.56	1.47	0.51	0.72	0	2.42	0
Ge	0.34	0.53	0	0.25	0.06	3.95	0.21
As	1.45	2.83	1.77	5.88	6.21	7.79	7.18
Rb	8.42	23.71	16.53	37.91	26.42	25.30	29.93
Sr	6.54	13.79	9.54	65.55	249.23	275.28	235.45
Y	0.56	1.45	1.14	2.88	3.62	4.44	3.02
Zr	5.20	11.44	9.57	29.43	41.75	61.24	35.53
Nb	0.20	0.42	0.55	1.13	1.59	1.57	1.00
Mo	0.48	1.44	1.22	2.97	3.02	4.06	4.62
Ag	0.42	0.91	0.25	2.74	0.55	0.74	1.07
Cd	0.45	1.43	1.34	2.45	3.67	1.03	1.97
In	0.04	0.07	0	0.28	0	0.23	0.01
Sn	0.41	1.01	0.87	3.39	1.21	1.21	1.86
Sb	0.12	0.35	0.23	1.03	0.26	0	0.63
Cs	0.18	0.49	0.32	0.85	0.46	0.80	0.82
Ba	24.37	65.24	65.18	108.05	98.97	115.74	112.18

Table A.8 (continued): Elemental geochemistry of cores 3H and 4H. Major and minor oxides are expressed in weight %; trace elements are expressed in ppm.

Sample	3H - 17cm	3H - 41cm	3H - 69cm	4H - 3cm	4H - 28cm	4H - 53cm	4H - 69cm
La	0.64	1.42	1.46	3.07	4.84	4.39	3.51
Ce	1.33	2.89	2.69	6.41	8.95	8.80	6.59
Pr	0.12	0.33	0.24	0.57	0.98	1.26	0.75
Nd	0.49	1.13	1.20	2.90	3.24	3.69	3.88
Sm	0.12	0.28	0.22	0.91	0.19	0.48	0
Eu	0.04	0.08	0.16	0.24	0.22	0.39	0.00
Gd	0.13	0.38	0.14	0.54	0.46	1.39	0.77
Tb	0.03	0.08	0.02	0.03	0.11	0.12	0.20
Dy	0.15	0.12	0.19	0.61	0.24	0.60	0.97
Ho	0.01	0.08	0.06	0.07	0.09	0.08	0.13
Er	0.01	0.21	0.09	0.35	0.40	0.25	0.72
Tm	0.01	0.06	0.05	0.06	0.00	0.11	0.02
Yb	0.13	0.22	0.11	0.29	0.95	0.00	0.12
Lu	0.02	0.01	0.04	0.05	0.10	-0.12	0.10
Hf	0.24	0.36	0.14	0.56	0.70	1.74	0.65
Ta	0.04	0.10	0.21	0.28	0.14	0.34	0.24
Tl	0.05	0.25	0.05	0.28	0.28	0.05	0
Pb	2.77	8.08	5.20	12.50	14.42	7.75	9.74
Bi	0.23	0.51	0.06	1.30	0.13	0.33	0.75
Th	0.23	0.50	0.60	1.18	1.47	2.19	1.48
U	0.14	0.30	0.11	0.48	0.62	1.05	1.12

Table A.8 (continued): Elemental geochemistry of cores 3H and 4H. Major and minor oxides are expressed in weight %; trace elements are expressed in ppm.

Sample	1	1^1	1^5	2	2^1	2^5	3	3^1	3^5
SiO_2	54.33	53.73	52.19	76.36	70.95	72.31	3.88	4.43	4.13
Al_2O_3	42.39	41.86	40.97	16.74	15.62	15.99	0.22	0.22	0.23
CaO	0.34	0.12	0.2	1.78	0.72	0.38	0.04	0.06	0.1
MgO	0.27	0.47	0.73	3.66	4.21	4.21	0.17	0.23	0.32
MnO	0	0	0	0.01	0.01	0.01	0.34	0.34	0.34
Na_2O	0.09	1.05	2.86	0.39	6.26	5.18	0.12	0.31	0.91
K_2O	0.32	0.39	0.4	0.1	0.43	0.42	0.02	0.03	0.05
TiO_2	1.69	1.66	1.63	0.25	0.25	0.25	0	0	0
P_2O_5	0.04	0.04	0.04	0.03	0.04	0.03	0.1	0.09	0.1
SO_3	0	0.09	0.43	0	0.83	0.53	0	0.03	0.15
Fe_2O_3	0.58	0.59	0.55	0.71	0.68	0.68	95.14	94.25	93.69
Cl	120	7106	23247	295	47339	34313	310	2355	7066
Be	1.33	1.25	1.11	1.79	1.64	1.56	1.27	1.28	1.15
Sc	16.74	15.83	14.64	6.14	5.46	5.53	9.25	9.24	8.52
V	83.03	82.53	78.6	19.96	20.33	20.36	28.14	29.17	28.1
Cr	84.25	89.5	83.54	9.8	12.23	12.5	8.44	9.52	11.8
Ni	32.24	33.77	35.51	8.06	9.75	14.63	12.52	12.99	17.02
Cu	19.04	24.32	18.81	1.86	121.12	20.09	23.38	24.52	23.39
Zn	24.43	49.45	23.16	35.83	92.55	41.11	21.43	40.75	24.46
Ga	40.92	40.87	38.09	16.59	15.4	15.92	0.15	0.19	0.18
Ge	2.12	2.4	2.21	1.6	1.74	1.45	1.44	1.62	1.56
As	0.71	0.81	1.04	1.09	0.85	1.01	4.07	4.2	4.14
Rb	8.22	9.11	7.53	3.38	4.28	4.77	0.53	0.54	0.62
Sr	25.34	29.95	37.4	90.52	58.57	40.81	4.71	7.5	11.49
Y	13.38	16.02	11.48	42.53	37.56	33.9	13.97	14.29	13.39
Zr	325.47	330.29	310.05	170.12	156.74	144.07	3.14	4.31	4.42
Nb	27.92	29.13	26.57	13.69	12.72	12.44	0.04	0.06	0.1
Mo	1.03	1.17	1.19	1.23	1.2	1.62	0.66	0.84	1.07
Ag	0.12	0.31	0.35	0.19	0.34	0.39	0.22	0.16	0.33
Cd	0.24	0.33	0.09	0	0.07	0.11	0	0.09	0.17
In	0.18	0.17	0.13	0.05	0.07	0.05	0.48	0.53	0.5
Sn	4.02	6.07	3.69	3.43	3.28	5.16	0.08	0.57	0.11
Sb	3.27	3.02	3.04	3.75	3.71	3.84	4.97	4.99	4.68
Cs	0.2	0.32	0.23	0.6	0.55	0.62	0.04	0.05	0.04
Ba	71.79	73.21	69.16	44.89	46.38	39.82	156.78	153.24	142.22

Table A.9: Trace element compositions of sediment samples. Concentration units of major element oxides are in wt%; concentration units of trace elements are ppm element. '0' indicates concentrations below detection limits. 1: Kaol + Chl +Ill; 1^1: Kaol + Chl +Ill (1 month); 1^5: Kaol + Chl +Ill (5 months); 2: Ca-Montmorillonite; 2^1: Ca-Montmorillonite (1 month); 2^5: Ca-Montmorillonite (5 months); 3: Goethite; 3^1: Goethite (1 month); 3^5: Goethite (5 months).

Sample	1	1^1	1^5	2	2^1	2^5	3	3^1	3^5
La	21.65	21.6	18.13	64.11	55.89	51.05	1.62	1.62	1.55
Ce	43.3	43.63	37.77	102.87	92.81	90.67	3.25	3.39	3.21
Pr	5.44	5.65	4.76	13.57	12.02	11.15	0.36	0.39	0.36
Nd	27.53	26.93	22.26	59.34	50.29	47.36	2.44	2.31	2.13
Sm	5.12	4.5	3.83	10	8.78	7.83	0.85	0.84	0.82
Eu	0.74	0.78	0.66	1.34	1.13	1.00	0.28	0.28	0.28
Gd	3.11	3.25	2.67	9.33	8.22	7.93	2.11	2.08	2.16
Tb	0.42	0.48	0.35	1.38	1.29	1.18	0.35	0.4	0.33
Dy	2.99	3.23	2.49	8.56	7.62	7.34	2.38	2.35	2.42
Ho	0.52	0.57	0.43	1.63	1.38	1.24	0.46	0.45	0.45
Er	1.66	1.72	1.4	4.32	4.01	3.74	1.22	1.3	1.2
Tm	0.24	0.29	0.19	0.72	0.6	0.57	0.19	0.18	0.16
Yb	1.83	1.97	1.46	4.71	4.27	3.75	1.15	1.13	1.18
Lu	0.30	0.28	0.24	0.65	0.6	0.54	0.19	0.18	0.18
Hf	8.84	8.93	8.55	5.79	5.31	4.98	0.10	0.18	0.19
Ta	2.29	2.3	2.01	1.27	1.13	1.06	0.03	0.04	0.04
Tl	0.06	0.05	0.02	0.15	0	0.01	0.05	0.02	0.01
Pb	15.11	14.89	13.38	4.62	6.31	5.72	0.59	1.23	0.79
Bi	0.38	0.42	0.33	0.23	0.22	0.3	0.04	0.02	0.03
Th	24.9	24.14	21.14	24.3	21.59	19.58	0.07	0.11	0.1

Table A.9 (continued): Trace element compositions of sediment samples. Concentration units of major element oxides are in wt%; concentration units of trace elements are ppm element. '0' indicates concentrations below detection limits. 1: Kaol + Chl +Ill; 1^1: Kaol + Chl +Ill (1 month); 1^5: Kaol + Chl +Ill (5 months); 2: Ca-Montmorillonite; 2^1: Ca-Montmorillonite (1 month); 2^5: Ca-Montmorillonite (5 months); 3: Goethite; 3^1: Goethite (1 month); 3^5: Goethite (5 months).

Sample	4	4^1	4^5	5	5^1	5^5
SiO_2	59.13	61.48	63.01	57.87	56.54	61.07
Al_2O_3	13.79	14.41	13.47	41.46	40.09	35.07
CaO	1.64	1.62	1.37	0.01	0.11	0.31
MgO	4.08	4.28	4.02	0	0.17	0.28
MnO	0.04	0.04	0.03	0	0	0
Na_2O	4.21	0.53	1.47	0.1	1.44	2.17
K_2O	6.15	6.59	6.24	0.02	0.11	0.19
TiO_2	0.52	0.56	0.52	0.09	0.09	0.07
P_2O_5	0.04	0.04	0.04	0.14	0.13	0.11
SO_3	0.5	0.05	0.16	0.01	0.22	0.39
Fe_2O_3	9.91	10.39	9.66	0.36	1.11	0.34
Cl	31837	3168	11663	553	13432	17170
Be	2.32	2.47	2.36	0.7	0.73	0.69
Sc	10.53	11.9	10.73	8.19	8.32	6.74
V	74.56	77.22	70.61	17.01	16.43	17.63
Cr	77.55	89	79.1	10.67	14.6	11.69
Ni	48.93	54.67	44.67	7.01	7.88	12.5
Cu	20.59	61.15	18.84	4.02	7.02	8.77
Zn	100.39	133.11	108.25	3.43	40.7	14.26
Ga	13.22	14.22	12.96	42.06	40.28	39.3
Ge	3.31	3.78	3.52	2.47	3.1	2.11
As	2.95	2.87	2.74	1.28	1.15	1.45
Rb	434.86	493.18	443.63	1.91	1.99	3.4
Sr	54.95	42.66	39.84	0.23	8.3	20.98
Y	24.26	25.43	21.75	32.63	34.76	25.36
Zr	166.17	181.75	165.22	98.71	114.62	82.57
Nb	6.47	6.79	6.31	32.44	32.76	28.51
Mo	1.73	1.08	1.38	2.6	2.85	2.41
Ag	0.4	0.19	0.21	0.32	0.39	0.37
Cd	0.21	0.23	0.07	0.11	0.11	0.5
In	0.08	0.06	0.06	0.15	0.13	0.15
Sn	2.36	3.31	2.09	16.22	13.21	12.58
Sb	3.48	3.24	3.48	4.12	3.75	3.99
Cs	8.78	11.17	9.52	0.87	0.83	0.79
Ba	48.41	49.67	53.8	0.85	3.48	17.95

Table A.9 (continued): Trace element compositions of sediment samples. Concentration units of major element oxides are in wt%; concentration units of trace elements are ppm element. '0' indicates concentrations below detection limits. 4: Illite; 4^1: Illite (1 month); 4^5: Illite (5 months); 5: Halloysite; 5^1: Halloysite (1 month); 5^5: Halloysite (5 months).

Sample	4	4^1	4^5	5	5^1	5^5
La	45.37	47.25	43.64	5.78	6.16	4.86
Ce	81.99	86.05	80.58	21.36	22.57	18.89
Pr	10	10.61	9.68	2.54	2.78	2.21
Nd	47.3	49.45	44.23	12.45	12.52	9.7
Sm	8.54	8.36	7.18	3.74	4.17	2.85
Eu	1.52	1.63	1.54	0.03	0	0.04
Gd	7.36	7.16	6.72	4.33	4.62	3.11
Tb	0.98	1.02	0.92	0.87	0.93	0.72
Dy	5.52	5.39	5.22	6.26	6.58	5.11
Ho	0.85	0.97	0.78	1.27	1.29	1.08
Er	2.34	2.58	2.18	3.37	4.01	3.11
Tm	0.38	0.36	0.31	0.59	0.64	0.43
Yb	2.33	2.49	2.2	4.13	4.41	3.2
Lu	0.35	0.32	0.29	0.63	0.65	0.55
Hf	4.51	4.84	4.28	5.73	6.37	4.5
Ta	0.55	0.56	0.53	4.39	4.74	3.59
Tl	0.01	0.08	0.02	0.04	0.02	0.02
Pb	8.86	10.28	8	8.31	16.46	7.79
Bi	0.14	0.12	0.11	0.07	0.03	0.04
Th	10.77	11.03	9.98	32.61	34.87	26.98

Table A.9 (continued): Trace element compositions of sediment samples. Concentration units of major element oxides are in wt%; concentration units of trace elements are ppm element. '0' indicates concentrations below detection limits. 4: Illite; 4^1: Illite (1 month); 4^5: Illite (5 months); 5: Halloysite; 5^1: Halloysite (1 month); 5^5: Halloysite (5 months).

Sample	CaO (%)	MgO (%)	Na_2O (%)	K_2O (%)	SO_3 (%)	Cl (%)	Sr
PR 120406-01	0.00	0.01	0.05	0.00	0.01	0.06	0.26
PR 120406-02	0.03	0.12	0.83	0.03	0.13	1.13	4.72
PR 120406-03	0.02	0.06	0.42	0.01	0.06	0.57	2.37
PR 120406-04	0.05	0.17	1.16	0.04	0.18	1.59	6.63
PR 120406-05	0.01	0.03	0.19	0.01	0.03	0.26	1.07
PR 120406-06	0.04	0.16	1.11	0.04	0.17	1.52	6.34
PR 120406-07	0.03	0.11	0.75	0.02	0.12	1.03	4.29
PR 120406-08	0.03	0.12	0.79	0.03	0.12	1.07	4.48
PR 120406-09	0.01	0.05	0.36	0.01	0.06	0.50	2.08
PR 120406-10	0.02	0.08	0.56	0.02	0.09	0.77	3.20
PR 120406-11	0.02	0.07	0.46	0.01	0.07	0.63	2.62
PR 120406-12	0.02	0.06	0.38	0.01	0.06	0.52	2.18
PR 120406-13	0.02	0.06	0.41	0.01	0.06	0.57	2.36
ML 130406-01 (14)	0.09	0.34	2.34	0.08	0.36	3.19	13.30
ML 130406-02 (15)	0.01	0.05	0.31	0.01	0.05	0.43	1.79
ML 130406-03 (16)	0.10	0.38	2.61	0.08	0.40	3.56	14.85
ML 130406-04 (17)	0.03	0.12	0.79	0.03	0.12	1.08	4.53
ML 130406-05 (18)	0.14	0.51	3.46	0.11	0.54	4.71	19.68
ML 130406-06 (19)	0.08	0.29	1.95	0.06	0.30	2.66	11.11
ML 130406-07 (20)	0.06	0.23	1.56	0.05	0.24	2.12	8.87
CB 030506-1d	0.12	0.45	3.08	0.10	0.48	4.21	17.56
GL 161006-01	0.04	0.15	1.01	0.03	0.16	1.38	5.76
GL 161006-02	0.04	0.16	1.12	0.04	0.17	1.53	6.37
GL 161006-03	0.05	0.19	1.31	0.04	0.20	1.79	7.48
GL 161006-04	0.11	0.41	2.78	0.09	0.43	3.79	15.84
GL 161006-05	0.05	0.20	1.36	0.04	0.21	1.85	7.74
BL 181006-01	0.03	0.11	0.76	0.02	0.12	1.03	4.31
BL 181006-02	0.01	0.06	0.38	0.01	0.06	0.52	2.16
ML 181006-03a	0.02	0.06	0.38	0.01	0.06	0.52	2.18
ML 181006-03b	0.00	0.02	0.10	0.00	0.02	0.14	0.60
ML 181006-04a	0.02	0.06	0.41	0.01	0.06	0.56	2.32
ML 181006-04b	0.01	0.04	0.27	0.01	0.04	0.37	1.56
ML 181006-06a	0.01	0.04	0.27	0.01	0.04	0.37	1.55
ML 181006-06b	0.00	0.02	0.12	0.00	0.02	0.16	0.68
BST. A1	0.04	0.17	1.12	0.04	0.17	1.53	6.40
BST. A2	0.01	0.05	0.32	0.01	0.05	0.44	1.82
MERIMBULA B	0.01	0.04	0.25	0.01	0.04	0.34	1.41

Table A.10: Saltwater sediment samples.

Sample	CaO (%)	MgO (%)	Na_2O (%)	K_2O (%)	SO_3 (%)	Cl (%)	Sr
08-19-10-05	0.02	0.07	0.49	0.02	0.08	0.66	2.76
13-19-10-05	0.03	0.12	0.79	0.03	0.12	1.07	4.48
16-19-10-05	0.05	0.20	1.36	0.04	0.21	1.85	7.74
36-19-10-05	0.04	0.13	0.89	0.03	0.14	1.22	5.09
37-19-10-05	0.02	0.08	0.53	0.02	0.08	0.72	3.02
46-19-10-05	0.05	0.20	1.34	0.04	0.21	1.83	7.62
47-19-10-05	0.01	0.04	0.30	0.01	0.05	0.40	1.69
02-20-10-05	0.02	0.08	0.53	0.02	0.08	0.72	3.02
11-20-10-05	0.02	0.06	0.43	0.01	0.07	0.58	2.43
27-20-10-05	0.03	0.11	0.78	0.03	0.12	1.07	4.45
29-20-10-05	0.25	0.93	6.32	0.21	0.98	8.62	36.01
2-22-10-05	0.02	0.06	0.38	0.01	0.06	0.52	2.17
3-22-10-05	0.01	0.05	0.35	0.01	0.05	0.47	1.97
5-22-10-05	0.01	0.05	0.36	0.01	0.06	0.49	2.03
10-22-10-05	0.03	0.10	0.66	0.02	0.10	0.91	3.79
24-22-10-05	0.02	0.06	0.39	0.01	0.06	0.53	2.22
25-22-10-05	0.03	0.11	0.73	0.02	0.11	0.99	4.15
BL Short Point	0.01	0.04	0.29	0.01	0.04	0.39	1.65
BL 070307-01	0.01	0.02	0.14	0.00	0.02	0.19	0.80
BL 070307-02	0.00	0.01	0.06	0.00	0.01	0.08	0.32
BL 070307-03	0.01	0.04	0.26	0.01	0.04	0.36	1.49
BL 070307-04	0.01	0.03	0.18	0.01	0.03	0.25	1.04
BL 070307-05	0.02	0.09	0.60	0.02	0.09	0.82	3.41
BL 070307-06	0.14	0.53	3.62	0.12	0.56	4.94	20.64
BL 070307-07	0.09	0.34	2.31	0.08	0.36	3.15	13.17
BL 070307-08	0.01	0.04	0.25	0.01	0.04	0.33	1.40
BL 070307-10	0.04	0.15	1.01	0.03	0.16	1.38	5.77
BL 070307-11	0.03	0.11	0.74	0.02	0.11	1.00	4.19
BL 070307-12	0.01	0.05	0.35	0.01	0.05	0.48	2.00
MLI 080307-12	0.00	0.01	0.08	0.00	0.01	0.11	0.45
MLI 080307-13	0.11	0.40	2.72	0.09	0.42	3.71	15.47
ML 090307-01	0.05	0.17	1.18	0.04	0.18	1.60	6.70
ML 090307-02	0.02	0.06	0.43	0.01	0.07	0.59	2.47
ML 090307-03	0.10	0.37	2.53	0.08	0.39	3.45	14.40
ML 090307-04	0.10	0.37	2.51	0.08	0.39	3.42	14.30
ML 090307-05	0.07	0.25	1.73	0.06	0.27	2.36	9.86
ML 090307-06	0.02	0.08	0.57	0.02	0.09	0.78	3.27
ML 090307-07	0.01	0.03	0.23	0.01	0.04	0.31	1.31
ML 090307-08	0.05	0.19	1.28	0.04	0.20	1.75	7.29
ML 090307-09	0.10	0.35	2.42	0.08	0.37	3.29	13.75
ML 090307-10	0.03	0.11	0.72	0.02	0.11	0.99	4.12
H1	0.00	0.00	0.00	0.00	0.00	0.00	0.00
H2	0.00	0.00	0.00	0.00	0.00	0.00	0.00
H3	0.00	0.00	0.00	0.00	0.00	0.00	0.00
H4	0.00	0.00	0.00	0.00	0.00	0.00	0.00
H mud	0.00	0.00	0.00	0.00	0.00	0.00	0.00

Table A.10 (Continued): Saltwater sediment samples.

Sample	CaO (%)	MgO (%)	Na_2O (%)	K_2O (%)	SO_3 (%)	Cl (%)	Sr
ML 101107-01	0.01	0.05	0.34	0.01	0.05	0.47	1.94
ML 101107-02	0.01	0.04	0.24	0.01	0.04	0.33	1.38
ML 101107-03	0.02	0.07	0.45	0.01	0.07	0.61	2.56
ML 101107-04	0.01	0.03	0.21	0.01	0.03	0.28	1.19
ML 101107-05	0.01	0.03	0.18	0.01	0.03	0.25	1.03
ML 101107-06	0.02	0.09	0.59	0.02	0.09	0.80	3.35
ML 101107-07	0.01	0.04	0.24	0.01	0.04	0.33	1.39
ML 101107-08	0.02	0.06	0.43	0.01	0.07	0.59	2.47
ML 101107-09	0.02	0.06	0.42	0.01	0.06	0.57	2.37
ML 101107-10	0.02	0.06	0.38	0.01	0.06	0.52	2.17
ML 101107-12	0.02	0.06	0.39	0.01	0.06	0.53	2.20
ML 111107-15	0.04	0.15	1.02	0.03	0.16	1.40	5.83
P141107-03	0.03	0.10	0.68	0.02	0.10	0.92	3.85
ML 161107-01	0.03	0.13	0.86	0.03	0.13	1.17	4.90
ML 150408-01	0.03	0.11	0.75	0.02	0.12	1.02	4.27
ML 150408-02	0.06	0.22	1.53	0.05	0.24	2.09	8.72
ML 150408-03	0.05	0.20	1.38	0.04	0.21	1.88	7.84
ML 150408-04	0.04	0.13	0.89	0.03	0.14	1.21	5.05
ML 150408-05	0.02	0.08	0.52	0.02	0.08	0.70	2.93
C1-0	0.00	0.01	0.05	0.00	0.01	0.07	0.31
C1-20	0.01	0.02	0.13	0.00	0.02	0.18	0.74
C1-30	0.01	0.03	0.20	0.01	0.03	0.27	1.12
C1-59	0.01	0.04	0.26	0.01	0.04	0.35	1.45
C2-0	0.03	0.13	0.86	0.03	0.13	1.17	4.89
C2-40	0.01	0.05	0.37	0.01	0.06	0.51	2.13
C2-68	0.02	0.06	0.39	0.01	0.06	0.53	2.21
SAND FILTER	0.00	0.00	0.01	0.00	0.00	0.01	0.05

Table A.10 (Continued): Saltwater sediment samples.

Sample	CaO (%)	MgO (%)	Na_2O (%)	K_2O (%)	SO_3 (%)	Cl (%)	Sr
111107-13	0.00	0.00	0.02	0.00	0.00	0.03	0.13
111107-14	0.00	0.00	0.02	0.00	0.00	0.02	0.09
P141107-01	0.00	0.00	0.02	0.00	0.00	0.03	0.13
P141107-02	0.00	0.00	0.02	0.00	0.00	0.03	0.13
MLI 080307-01	0.00	0.00	0.01	0.00	0.00	0.01	0.06
MLI 080307-02	0.00	0.00	0.00	0.00	0.00	0.00	0.02
MLI 080307-03	0.00	0.00	0.01	0.00	0.00	0.01	0.04
MLI 080307-04	0.00	0.00	0.03	0.00	0.00	0.04	0.17
MLI 080307-05	0.01	0.03	0.19	0.01	0.03	0.26	1.10
MLI 080307-06	0.00	0.00	0.01	0.00	0.00	0.01	0.04
MLI 080307-09	0.00	0.00	0.02	0.00	0.00	0.03	0.13
MLI 080307-10	0.00	0.00	0.00	0.00	0.00	0.00	0.02
MLI 080307-11	0.00	0.00	0.02	0.00	0.00	0.03	0.14
MC 030506-1a	0.00	0.00	0.01	0.00	0.00	0.02	0.07
MC 030506-1b	0.00	0.00	0.01	0.00	0.00	0.02	0.08
MC 030506-1c	0.00	0.01	0.04	0.00	0.01	0.05	0.20
MERIMBULA GROUP	0.00	0.00	0.02	0.00	0.00	0.02	0.10

Table A.10 (Continued): Freshwater sediment samples.

Appendix 3

The following diagrams are of XRD scans undertaken on clay samples, 2: Ca-montmorillonite; 4: Illite; and. 5: Halloysite. The black scan indicates the original, freshwater clay; the red scan indicates the clay after a one month period; the blue scan indicates the clay after a five month period which has been treated with ethylene glycol; and, the green scan indicates the clay after a five month period which has been heated to 350°C.

Clay 2-O

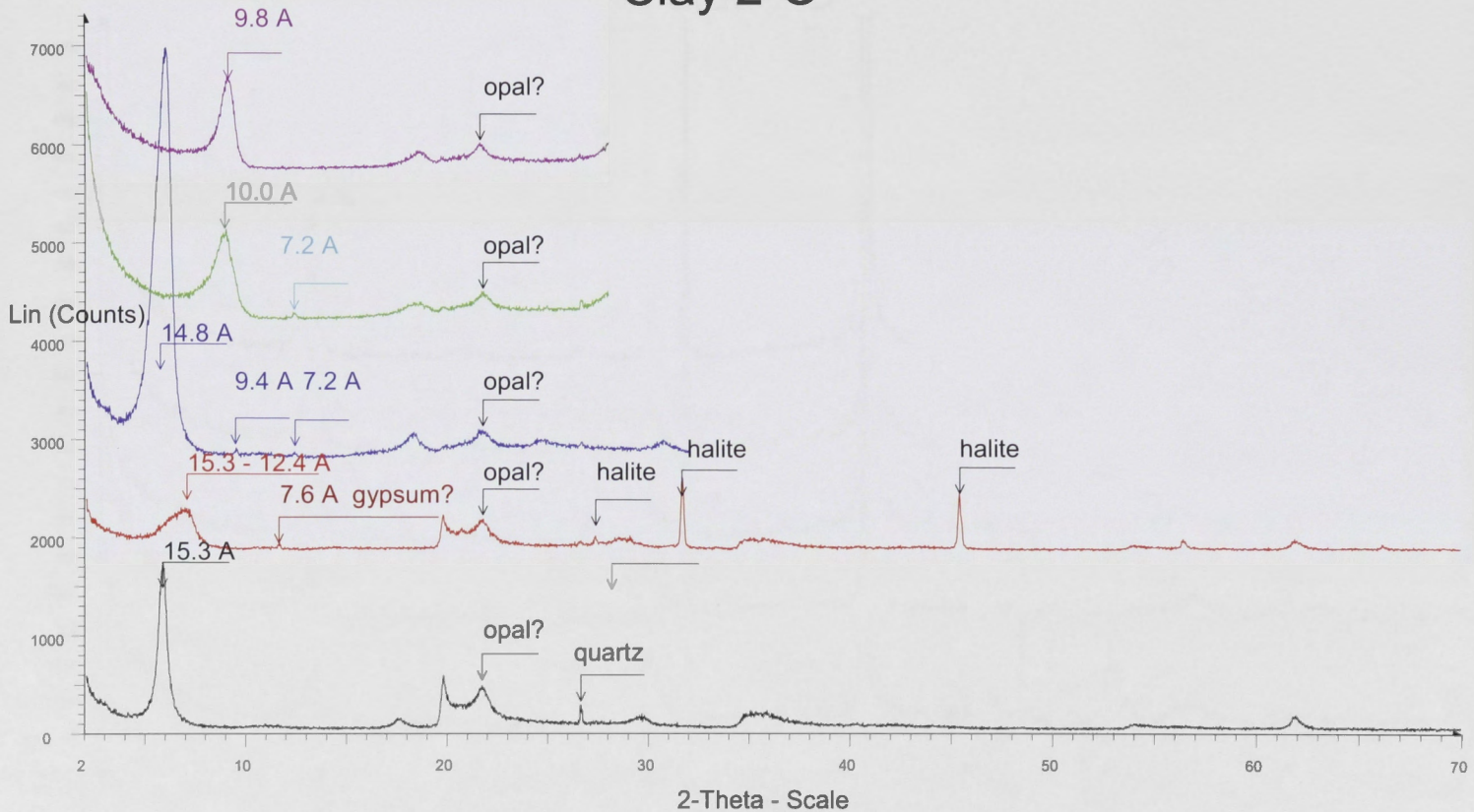

Clay 2-O - File: A22248.raw - Type: 2Th/Th locked - Start: 2.000 ° - End: 70.000 ° - Step: 0.020 ° - Step
Operations: Import

Clay 2 - 181207 - File: A22306.raw - Type: 2Th/Th locked - Start: 2.000 ° - End: 70.000 ° - Step: 0.020 ° -
Operations: Y Scale Add 1667 | Y Scale Add -167 | Y Scale Add 333 | Import

Clay 2b - last (ethylene glycol) - File: A22769.raw - Type: 2Th/Th locked - Start: 2.000 ° - End: 32.000 ° -
Operations: Y Scale Add -3250 | Y Scale Add 2833 | Y Scale Add 2833 | Y Scale Add -167 | Y Scale Add

Clay 2b - last - 350o - File: A22773.raw - Type: 2Th/Th locked - Start: 2.000 ° - End: 28.000 ° - Step: 0.02
Operations: Y Scale Add 3667 | Y Scale Add -167 | Y Scale Add 0 | Y Scale Add 667 | Import

Clay 2b - last - 550o - File: A22777.raw - Type: 2Th/Th locked - Start: 2.000 ° - End: 28.000 ° - Step: 0.02
Operations: Y Scale Add 5000 | Y Scale Add 208 | Y Scale Add 500 | Import

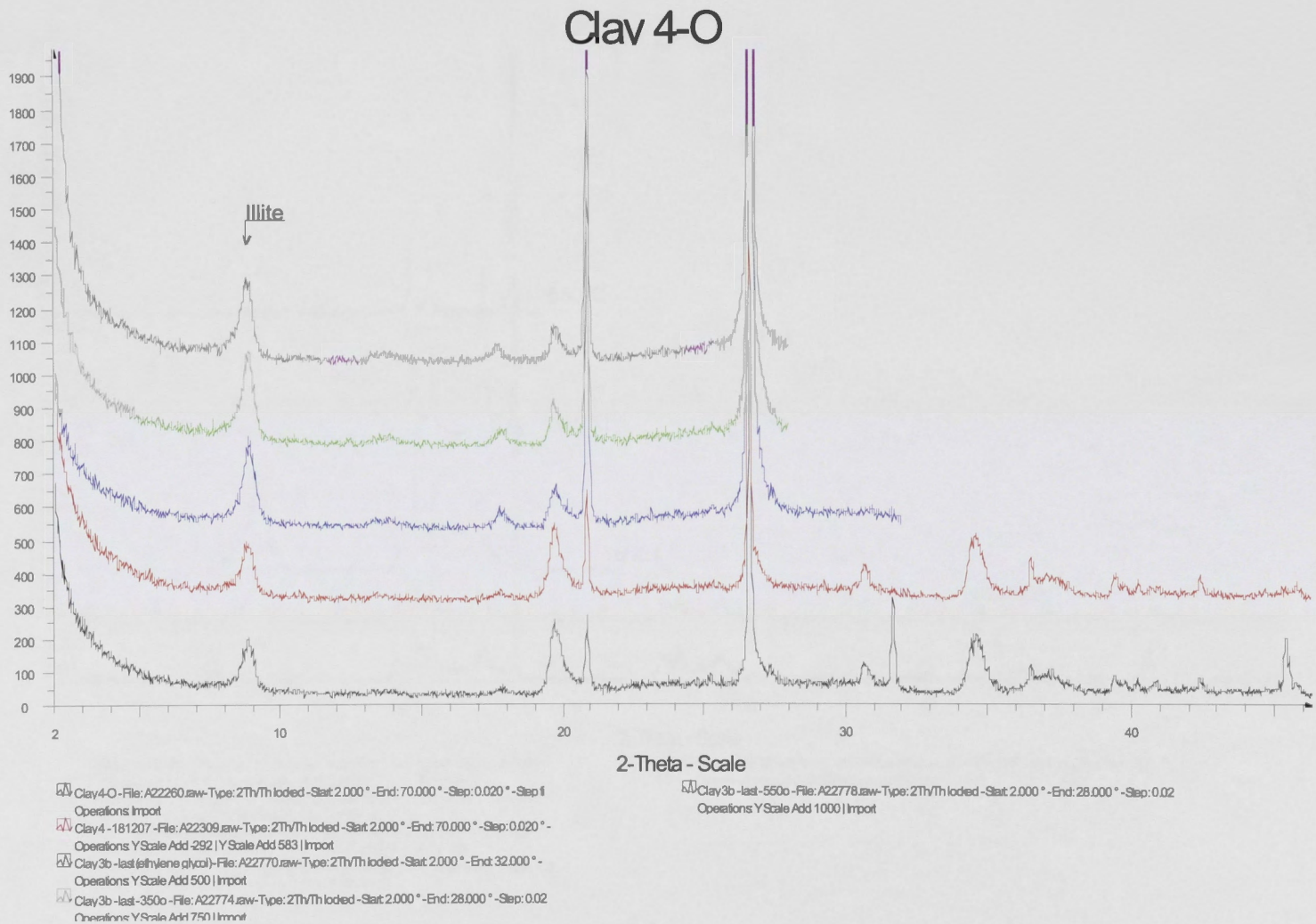
Clay 4-O
Illite
1900
1800
1700
1600
1500
1400
1300
1200
1100
1000
900
800
700
600
500
400
300
200
100
0
2
10
20
30
40
2-Theta - Scale
Clay4-O -File: A22260.raw -Type: 2Th/Th locked -Start: 2.000 ° -End: 70.000 ° -Step: 0.020 ° -Step ti
Operations: Import
Clay4 -181207 -File: A22309.raw -Type: 2Th/Th locked -Start: 2.000 ° -End: 70.000 ° -Step: 0.020 ° -
Operations: Y Scale Add -292 | Y Scale Add 583 | Import
Clay3b -last (ethylene glycol) -File: A22770.raw -Type: 2Th/Th locked -Start: 2.000 ° -End: 32.000 ° -
Operations: Y Scale Add 500 | Import
Clay3b -last -350o -File: A22774.raw -Type: 2Th/Th locked -Start: 2.000 ° -End: 28.000 ° -Step: 0.02
Operations: Y Scale Add 750 | Import
Clay3b -last -550o -File: A22778.raw -Type: 2Th/Th locked -Start: 2.000 ° -End: 28.000 ° -Step: 0.02
Operations: Y Scale Add 1000 | Import

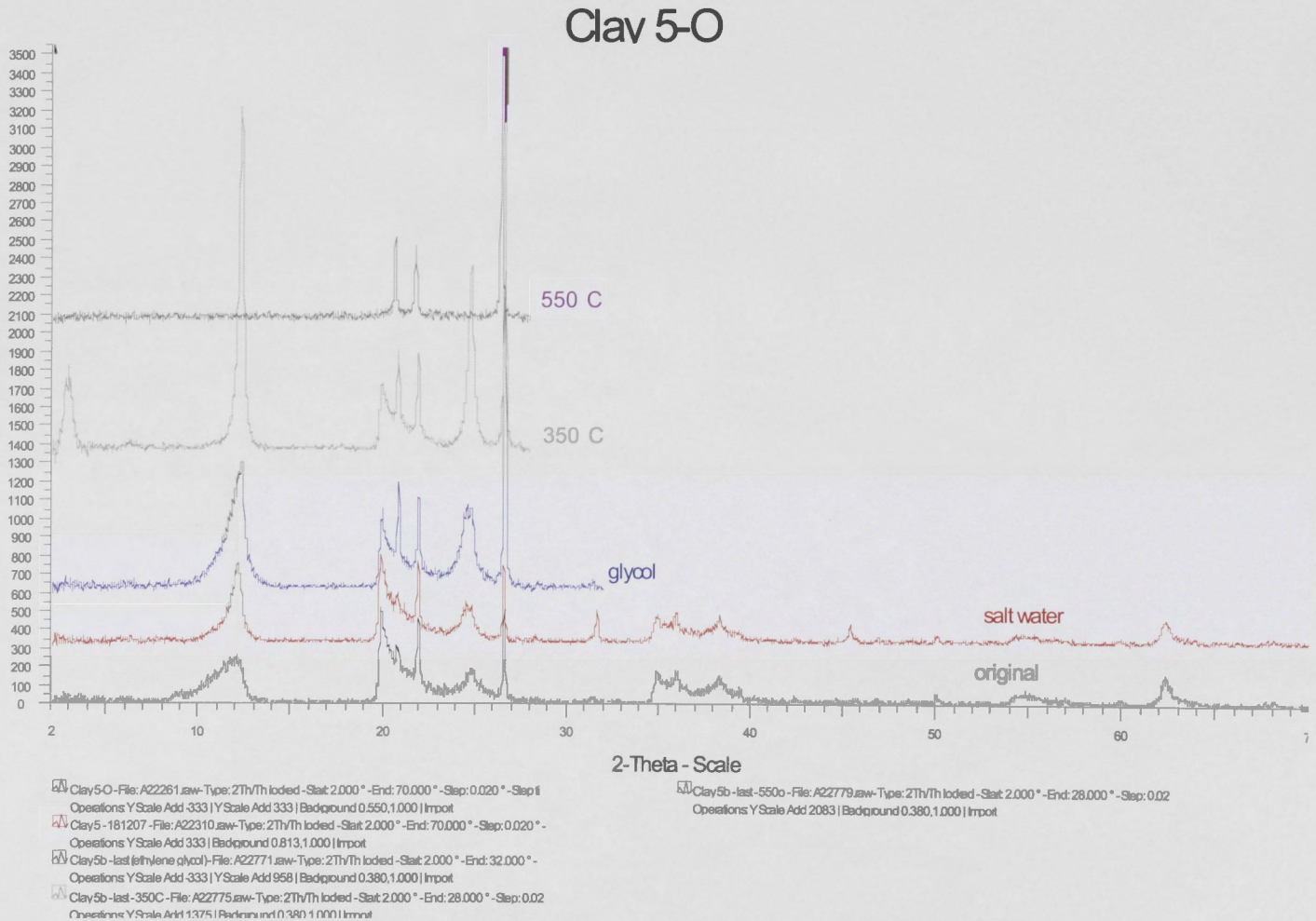
Clay 5-O
550 C
350 C
glycol
salt water
original
2-Theta - Scale
Clay 5-O - File: A22261.raw - Type: 2Th/Th locked - Start: 2.000 ° - End: 70.000 ° - Step: 0.020 ° - Step
Operations: Y Scale Add -333 | Y Scale Add 333 | Background 0.550,1.000 | Import
Clay 5 - 181207 - File: A22310.raw - Type: 2Th/Th locked - Start: 2.000 ° - End: 70.000 ° - Step: 0.020 ° -
Operations: Y Scale Add 333 | Background 0.813,1.000 | Import
Clay 5b - last (ethylene glycol) - File: A22771.raw - Type: 2Th/Th locked - Start: 2.000 ° - End: 32.000 ° -
Operations: Y Scale Add -333 | Y Scale Add 958 | Background 0.380,1.000 | Import
Clay 5b - last - 350C - File: A22775.raw - Type: 2Th/Th locked - Start: 2.000 ° - End: 28.000 ° - Step: 0.02
Operations: Y Scale Add 1.375 | Background 0.380,1.000 | Import
Clay 5b - last - 550c - File: A22779.raw - Type: 2Th/Th locked - Start: 2.000 ° - End: 28.000 ° - Step: 0.02
Operations: Y Scale Add 2083 | Background 0.380,1.000 | Import